

# NASA TECHNICAL MEMORANDUM

NASA TM X-64885

(NASA-TM-X-64885) WEATHER WATCH STUDIES  
BY MEANS OF AN OPTICAL TECHNIQUE (NASA)  
177 p HC \$12.00 CACL 04B

N74-35037  
THRU  
N74-35044  
Unclas

G3/20 50998

## WEATHER WATCH STUDIES BY MEANS OF AN OPTICAL TECHNIQUE

By Robert E. Turner, Editor  
Space Sciences Laboratory

October 1974

**NASA**

*George C. Marshall Space Flight Center  
Marshall Space Flight Center, Alabama*

TECHNICAL REPORT STANDARD TITLE PAGE

1. REPORT NO. <b>TMX-64885</b>		2. GOVERNMENT ACCESSION NO.		3. RECIPIENT'S CATALOG NO.	
4. TITLE AND SUBTITLE  <b>Weather Watch Studies By Means of an Optical Technique</b>				5. REPORT DATE <b>October 1974</b>	
				6. PERFORMING ORGANIZATION CODE	
7. AUTHOR(S) <b>Robert E. Turner, Editor</b>				8. PERFORMING ORGANIZATION REPORT #	
9. PERFORMING ORGANIZATION NAME AND ADDRESS  <b>George C. Marshall Space Flight Center Marshall Space Flight Center, Alabama 35812</b>				10. WORK UNIT NO.	
				11. CONTRACT OR GRANT NO.	
12. SPONSORING AGENCY NAME AND ADDRESS  <b>National Aeronautics and Space Administration Washington, D. C. 20546</b>				13. TYPE OF REPORT & PERIOD COVERED  <b>Technical Memorandum</b>	
				14. SPONSORING AGENCY CODE	
15. SUPPLEMENTARY NOTES <b>This document was prepared from a series of articles, which were the requirement of NASA Contract NAS8-21049, by various staff members of the Department of Civil Engineering, Colorado State University, for the Aerospace Environment Division, Space Sciences Laboratory, MSFC.</b>					
16. ABSTRACT <p>A series of articles is presented in this report on a passive, optical, cross beam system. The passive, optical, cross beam system was evaluated as a remote sensor of atmospheric conditions. The system employed the light scattered from natural aerosols to sense atmospheric mean and turbulent motion. A space-time correlation of the output of two optical sensors was used to evaluate the mean convective wind speed. In approximately 20% of the tests, signal-to-noise levels were sufficient to allow estimation of convective wind speeds. The feasibility of employing intersecting beams to evaluate the atmospheric turbulent motion was also investigated. The intersecting beams produced maximums in the space-time correlation curves for other than zero time delay. The non-zero time delay maximums indicate the cross beam system was detecting "aerosol layers" in the atmosphere, rather than information from the common intersecting volume.</p> <p>Evidence was obtained which indicates that aerosol layers could produce large correlations at heights not predicted from the beam geometry. These layers appear to dominate the correlations, thus limiting measurement to the layer only. When aerosol layers are found to exist, the cross beam system could serve as a means of remotely measuring their convective velocity.</p>					
17. KEY WORDS <b>Optical Techniques Cross Correlation Techniques Light Scattering Aerosols</b>			18. DISTRIBUTION STATEMENT  <b>UNCLASSIFIED-UNLIMITED</b>  <i>Robert E. Turner</i> <b>Robert E. Turner</b>		
19. SECURITY CLASSIF. (of this report)  <b>UNCLASSIFIED</b>		20. SECURITY CLASSIF. (of this page)  <b>UNCLASSIFIED</b>		21. NO. OF PAGES  <b>176</b>	22. PRICE  <b>NTIS</b>

## FOREWORD

This report is a series of articles, from research under NASA Contract NAS8-21049, by various staff members of Colorado State University. A number of approaches have been, and continue to be, followed in the conduct of remote sensing research. The results presented in this report represent only a portion of the total research efforts and techniques being conducted today.

Sincere appreciation is expressed to J. F. Nelson, W. W. Vaughan, and personnel of the Aerospace Environment Division for their review of this report and their helpful suggestions.

TABLE OF CONTENTS

<u>SECTION</u>	<u>TITLE</u>	<u>PAGE</u>
I. ✓	CROSS BEAM WEATHER WATCH STUDY	
	1.1 Summary-----	1
	1.2 Introduction-----	1
	1.3 Theoretical Considerations-----	2
	1.4 Optical Cross Beam Technique-----	6
	1.5 Atmospheric Measurement-----	10
	1.6 Analog and Digital Evaluation of Cross Beam Signals-----	12
	1.7 Conclusions-----	14
	1.8 References-----	15
II. ✓	EXPERIMENTAL PROBABILITY DENSITY DISTRIBUTIONS FOR OPTICAL AND INFRA-RED CROSS BEAM UNITS	
	2.1 Summary-----	30
	2.2 Introduction-----	30
	2.3 Method of Analysis-----	31
	2.4 Evaluation-----	31
	2.5 References-----	32
III. ✓	ANALOG COMPUTATION OF AUTO- AND CROSS-CORRELATION FUNCTIONS	
	3.1 Introduction-----	41
	3.2 Computation Procedure-----	42
	3.3 Equipment Used-----	44
IV. ✓	PRELIMINARY ANALYSIS OF CROSS BEAM DATA FROM THE GUN BARREL HILL SITE	
	4.1 Summary-----	47
	4.2 Introduction-----	47
	4.3 Experimental Measurements-----	48
	4.4 Analysis of Measurements-----	48
	4.5 Concluding Remarks-----	51
	4.6 References-----	52

TABLE OF CONTENTS (Cont'd)

<u>SECTION</u>	<u>TITLE</u>	<u>PAGE</u>
V. ✓	CHECK OUT OF REBUILT OPTICAL CROSS BEAM UNITS	
5.1	Summary-----	111
5.2	Introduction-----	111
5.3	Evaluation of Signals-----	112
5.4	Results-----	113
VI. ✓	OPTICAL CROSS BEAM FIELD TEST AT HSSA HASWELL FIELD SITE	
6.1	Summary-----	127
6.2	Introduction-----	127
6.3	Test Conditions-----	127
VII. ✓	ANALYSIS OF CROSS BEAM RUNS TAKEN AT HASWELL FIELD SITE	
7.1	Summary-----	138
7.2	Introduction-----	138
7.3	Evaluation of the Correlations-----	138
7.4	References-----	139

1774-35038

SECTION I.  
CROSS BEAM WEATHER WATCH STUDY

by

V. A. Sandborn

1.1 SUMMARY

A passive, optical, cross beam system was evaluated as a remote sensor of atmospheric conditions. The system employed the light scattered from natural aerosols to sense atmospheric mean and turbulent motion. A space-time correlation of the output of two optical sensors was used to evaluate the mean convective wind speed. In approximately 20% of the tests signal-to-noise levels were sufficient to allow estimation of convective wind speeds. The feasibility of employing intersecting beams to evaluate the atmospheric turbulent motion was also investigated. The intersecting beams produced maximums in the space-time correlation curves for other than zero time delay. The non-zero time delay maximums indicate the cross beam system was detecting "aerosol layers" in the atmosphere, rather than information from the common intersecting volume.

1.2 INTRODUCTION

An optical cross beam correlation method, ref. 1, has been proposed as a remote measuring system for atmospheric studies. Atmospheric measurements are limited due to the difficulty of placing measuring instruments at the desired location. Although meteorological towers and balloon flights are able to obtain wind data, they are greatly limited in their location. Thus, a real need exists for remote-sensing instrumentation in atmospheric measurements.

Several methods have been proposed to remotely sense atmospheric conditions, ref. 2. These methods include several types of microwave units, acoustic sounders, infrared sensors, optical sensors and related laser techniques. All of these techniques have proven of value in atmospheric probing.

The present report covers the evaluation of a simple visible optical technique as a possible remote measuring system. A feasibility study of field tests of the instrumentation at meteorological sites in Colorado is reported.

### 1.3 THEORETICAL CONSIDERATIONS

The optical cross beam correlation employs the scattering of light as a means of remotely sensing the motion in the atmosphere. A space-time correlation technique is employed to evaluate the light scattering signals. The instrument has been evaluated as a means of sensing wind speeds as a function of height. Also, possible measures of the local turbulent fluctuations have been considered. The present feasibility study was limited exclusively to a passive system wherein only available solar radiation was employed.

The cross beam system senses the fluctuation of light along a path defined by a narrow view telescope. The fluctuation in light is related mainly to light scattering due to aerosol particles. The original assumption, upon which possible remote sensing of atmospheric winds could be made, was that the aerosol particles are carried along at the speed of the mean wind. The cross beam technique employs a measure of the space-time correlation between two optical light beams to evaluate the transient time of the aerosols. By measuring the time required for

the tracer aerosols to travel a given path distance, the mean wind convective speed can be determined. Fisher and Krause, ref. 1, have demonstrated that it was possible to make such measurements in the laboratory.

a) Evaluation of wind velocities from correlation measurements.

The optical system employed two narrow view telescopes to sense the light scattering. These two telescopes view different optical paths. Figure 1 shows the general arrangement of the cross beam detection system. It is assumed that the aerosols are carried along by the mean wind. Thus, for the path denoted by  $\xi$  on Figure 1, the same aerosols will pass through the two light beams. For the present experiments the beams were always set in a direction normal to the mean wind. The majority of the tests were conducted such that the common streamline  $\xi$  for the two beams occurred at the top of the meteorological tower. For a uniform wind the only streamline that is common to both beams is the one denoted as  $\xi$  in Figure 1.

The common signal from the two telescopes is obtained by measuring the time-delayed correlation between the two signals. The output from the upstream telescope is delayed in time and then correlated with the output from the downstream telescope. Ideally, for a time delay just equal to the transient time for the aerosol particle to travel from the upstream to the downstream beam, a maximum in the correlation curve would be obtained. The paper by Sandborn and Pickelner, ref. 3, demonstrated that some degree of success was obtained in the original tests of the optical system.

Figure 2 shows a space-time, cross correlation curve for a case where the signal-to-noise level was large. The correlation curves,

computed both by analog and digital techniques, are compared with the first order probability density curve of the velocity measured by a cup anemometer. The second peak of the space-time correlation curve agrees with the peak of the cup anemometer curve.

b) Convective velocity indicated by space-time correlations.-

The time delay measured between the two light signals for maximum correlation must be related to the velocity at which identifiable disturbances are convected between the two beams. In a turbulent flow, such as that near the surface in the atmospheric boundary layer, disturbances do not travel in straight path lines. Any group of aerosol particles would be expected to travel in some sort of a random walk path line. Attempts to evaluate the random walk of particles in flows are reported by Patterson and Corrsin, ref. 4.

A recent experimental study by Cliff, ref. 5, in a large scale turbulent boundary layer has produced a new insight into the relation between the mean and convective velocities. It was found that for the outer region of the boundary layer, which is equivalent to the location of the cross beam measurements, the turbulent convective velocities are within 10% of the mean velocity. The relation between the convective velocity and the mean velocity was found to be a function of the size of the turbulence and also the time that the turbulent "eddy" was in the particular mean velocity field. Convective velocities can be greatly different from the mean velocity in flows with large shear gradients. Also, if the source of the turbulence, such as buildings or trees, is nearby, the convective velocity is likely to be different from the mean velocity.

c) Light scattering from aerosols employed as atmospheric tracers.- The present field experiments with the cross beam system employed optical wave lengths between approximately 0.45 and 0.65 microns. Light scattering as a function of altitude for this band of wave lengths was given by Sandborn and Pickelner, ref. 3. Details of scattered sunlight measurements are also discussed by Montgomery, ref. 2. In general it is assumed that aerosol particles are the main source of scattering. The field experiments demonstrated that light fluctuations were always present during the daylight hours. However, sufficient signal-to-noise level to produce measurable correlations between the two beams was not always present. Even the special case of the two beams looking directly at each other did not produce a measurable correlation. It was concluded that the light scattering quality of the aerosol-solar radiation did not remain constant from day to day.

It was assumed that any light fluctuation observed in the beam on a clear day was due to scattering from aerosol particles. Thus, a positive or negative signal appearing at the output of the beam sensor indicates that a particle has scattered light in or out of the beam. This requires that positive and negative signals can mean the same thing; that a particle has passed through the beam. In order that a correlation technique can be employed to eliminate background noise, the positive and negative parts of the signal must have different meaning. Apparently, only on specific days were the aerosol distributions able to produce the necessary consistent signals.

Figure 3, taken from reference 6 and attached as Appendix A, demonstrates the problem encountered in the correlation studies.

Figure 3 a) shows the output signal from one of the two optical beams. This run, H-11, was for the optical units looking directly at each other over a distance of 160 feet (48.8 meters). Figure 3 b) shows the correlation between the two beams at zero time delay. The correlation time trace, while not equally likely in positive and negative correlation, is closer to symmetry than desired. The actual probability density for this cross correlation time trace is shown in figure 4. The skewness ( $\overline{e^3}$ ) is proportional to the time mean amount of correlation that would be measured for this test. The bottom two traces are for a corresponding run made with infra-red cross beam units taken at the same time as run H-11. For the infra-red units a positive fluctuation indicates an increase in local temperature, and a negative fluctuation indicates a decrease in local temperature. Thus, for the infra-red units positive and negative signals have well defined different meanings. The cross correlation for the infra-red units is shown in figure 3 d). In the infra-red case the probability distribution shows a very definite skewness as might be expected.

#### 1.4 OPTICAL CROSS BEAM TECHNIQUE

The optical cross beam systems were supplied to the Colorado State University Meteorological field site by NASA, Marshall Space Flight Center. Details of the detection system were reported by Montgomery, ref. 2, and Sandborn and Pickelner, ref. 3. Briefly, the units consisted of telescope optics looking along a narrow field of view of approximately an angle of 30 minutes spread. The light sensors are silicon diodes. The incoming light was chopped to eliminate dc drift and 1/f noise of the photodiode. The output signals were recorded on FM tape recorders and analyzed either analog or digitally. The analog computer analysis

was done at CSU, and the digital analysis was done at the Marshall Space Flight Center. Appendix B gives a detailed outline of the analog computer setup used in the present study.

The present section covers the specific field test setups of the optical crossbeam units and the analog computer analysis of the outputs.

a) Field Tests. - Three specific field test sites were employed during the course of the present study. The initial studies of wind measurements, reported by Sandborn and Pickelner, ref. 3, were made at Colorado State University field site near Platteville, Colorado. Figure 5 shows the local terrain of this field site. The second set of tests were conducted at the Gun Barrel Hill test site of the Environmental Sciences Services Administration (ESSA) near Boulder, Colorado. Tests at the Gun Barrel Hill site were mainly concerned with the evaluation of atmospheric turbulence with the optical cross beam system. The third site was the ESSA field site near Haswell, Colorado. Figure 6 shows the general area of the meteorological tower at the Haswell, Colorado, field site.

The results of the wind measurements made at the Platteville, Colorado, field site have been reported in detail in references 3 and 7. Roughly 1/3 of the tests at Platteville gave a measurable peak in the space-time correlation curves. An error of  $\pm 20\%$  was indicated in the agreement between wind velocities measured with cup anemometers and the cross beam system. Details of special tests conducted at the Platteville, Colorado, field site were also reported by Sandborn in reference 2.

Details of the Gun Barrel Hill test site measurements were reported in references 8 and 9 (attached as Appendix C). Most of the runs made at

Gun Barrel were for intersecting light beams. The measurements did not produce maximum peaks in the space-time correlations curves at zero time delay. The original intent of these tests was to evaluate the cross beam system for measurement of atmospheric turbulence. As part of the initial study, a detailed set of hot wire turbulence measurements was made in the atmosphere. The hot wire turbulence measurements were evaluated and reported by Stankov, ref. 10, as part of the overall research program. It was apparent that the measured correlations were affected by information outside the intersection volume of the two beams, so no meaningful turbulence information was obtained.

Although the evaluation of the cross beam system as a turbulence sensor did not prove feasible, the information indicates that the system was responding to a specific layer of aerosols, rather than to light scattering from the common volume formed by the beam intersection. The results suggest that the optical cross beam system may be of value in both defining and studying aerosol layers in the atmosphere.

At the end of the Gun Barrel field tests, the electronics of the optical units were returned to IIT Research Laboratories to rebuild and upgrade. Reference 9 (attached as Appendix C) is a report of the checkout of the rebuilt units.

In September of 1969 the optical cross beam system was moved to the ESSA-Haswell, Colorado, field site. A large number of test runs were made over a short period of time at this field site. Reference 11 (attached as Appendix D) gives a detailed outline of the optical cross beam tests. The optical system was compared with an infra-red cross beam system during the course of these experiments. Analog evaluation of the Haswell test runs made at CSU is reported in reference 9 (attached

as Appendix A) and 12 (attached as Appendix E). The results of the Haswell measurements further confirm the fact that the optical system responds mainly to layers of aerosols. Further details of these tests will be discussed in the following sections of this report.

b) Analog analysis of cross beam data. - All of the cross beam runs made by CSU have been evaluated by analog techniques. Appendix B is a detailed outline of the analog computer setup. The basic instrument employed in the analysis is the Princeton time correlator. This single instrument is able to compute the complete time delay, cross correlation between the two optical signals in a matter of a few minutes.

In all cases the output signal from the two optical units was recorded on magnetic tape at a speed of 1 7/8 inches per second. For analysis the magnetic tape is replayed at a speed of up to 60 inches per second. The increased tape speed has the effect of compressing the actual time over which the run was made by a factor of 32 times. Thus, for one hour of actual data recorded the play back time is less than two minutes. This compression of time makes it possible to compute time averages over an hour of actual run time without modification of the analog computer averaging times. The higher speed play back also increases the frequency range of the signals to those better suited for analog analysis.

Although the time delay, cross correlations were the major interest of the current research program, other evaluations were also made. During the course of the study it became increasingly evident that the long time variations in the atmospheric flow pose a major problem in the analysis. The digital analysis made at the Marshall Space Flight Center attempted to develop criterion to specify when "time varying

mean flow" was a problem. The most sensitive criterion related to cross correlation evaluations proved to be the r.m.s. amplitude variation with time. The variation of the mean square rather than the r.m.s. was computed using a true r.m.s. voltmeter. The voltmeter had a special output directly proportional to the mean square of the input signal. Figure 7 shows a typical output trace of the mean square of optical unit no. 2 for Haswell run No. 20. A similar result, although in less detail, was obtained from the digital analysis, fig. 8. The maximum value of the cross correlation for the complete time period of run ii-20 (3200 seconds) was approximately 0.1. For the shorter periods where the average mean square is reasonably steady (80 to 1008 seconds) the peak correlation was found to be 0.4.

A comparison between the analog and digital evaluation of the optical cross correlation data was reported in ref. 7. Further comparison will be covered in the last section of the present report.

### 1.5 ATMOSPHERIC MEASUREMENTS

The specific objective of the present research program was the evaluation of a passive cross beam system as a remote atmospheric measurement tool. Three areas of application were investigated:

- a) Wind Measurements
- b) Turbulence Measurements
- c) Aerosol Layer Measurements

The results of these three areas of investigation are summarized in the present section.

a) Wind Measurements. - For ideal conditions of aerosol light scattering the passive, optical, cross beam system was shown to

indicate convective velocities. The feasibility study suggests that the present optical cross beam system is not practical as a passive remote sensor of wind. The logical improvement would be the use of light sources instead of available sky light. The present system does not appear to be selective in the height at which the measurement is made. Apparently the system is most sensitive to particular layers of aerosols, rather than the common intersection point. Use of external light sources would allow a better defined height to be measured.

b) Turbulence Measurements. - The feasibility study of the cross beam system for obtaining turbulent information was not successful. Failure to obtain a maximum in the cross correlation measurements at zero time delay for intersecting beams masks the direct turbulence measurements. Evaluation of the shape of the space-time correlation, as related to the turbulence, at other than the intersecting beam case was suggested to be invalid by Townsend, ref. 13.

c) Aerosol Layer Measurements. - Although not a specific part of the feasibility studies of the passive, optical cross beam systems, experiments indicate that the system responds to aerosol layers. Figure 9 shows a cross correlation measure made for Haswell run No. 20. For this run one optical unit was pointed straight up, and the second unit intersected it at a height of 128 ft (39 meters). A large peak value of correlation is obtained; however, the peak does not occur at zero time lag. This type of result was found for a great number of the Haswell tests. It is obvious that the correlation is affected by aerosol particles that are either above or below the point of intersection. Thus, the major information being correlated must come from a layer of aerosols, rather than from the volume of common intersection of the two beams.

## 1.6 ANALOG AND DIGITAL EVALUATION OF CROSS BEAM SIGNALS

Measurements from the optical cross beam signals have been evaluated both digitally and by analog techniques. Figure 2 is a typical comparison between the two techniques. The major difference in the calculations shown in figure 2 is due to the reduced frequency response, or data points employed in the digital analysis. For the detailed measurements of most of the Haswell tests the agreement between digital and analog values was found to be quite close.

Figure 10 is a comparison between the analog and digital evaluation for typical Haswell runs. Figure 10 a) compares the analog and digital evaluation of the cross correlation for run No. H-19. The comparison is found to be very good. In general it is found that the agreement between the analog and digital evaluation is good as long as the signals are well above the indicated noise levels. The original data for run No. H-19 was recorded for a frequency range of 0.01 to 3 hertz. The analog analysis reported by Huff and Sandborn, ref. 12 (attached as Appendix E), was also carried out for the frequency range of 0.01 to 3 hertz. The original digital analysis was based on a 50 second piece length, which corresponds to a frequency of 0.02 hertz. The correlation calculated by the digital computer corresponded to a frequency range of 0.02 to 3 hertz. The computed correlation is then corrected to account for the so-called "DC trends" which reflect the variation for the 0.01 to 0.02 hertz range of frequencies. The corrected correlation is termed the "modified accumulative correlation," and it is this correlation that is shown on figure 10 a). The good comparison suggests that the digital technique used to account for low sampling

rate is a useable approach. Figure 10 a) also compares the digital calculations of the modified accumulative correlations for run H-19, both with a 50 second and a 100 second sample piece. The longer sample rate reduces the lower frequency to 0.01 hertz. Figure 10 b) shows a similar comparison for Haswell run No. 20. In both the runs for which the 100 second sample piece length was employed the magnitude of the correlation was decreased. This decrease in correlation was not explained.

A criterion for selecting the best time over which to analyze the cross beam signals was found to be when the r.m.s. signal output is reasonably constant (fig. 8). This region of steady r.m.s. signal has been evaluated both for runs H-19 and H-20. Figure 11 shows the digital evaluation of the r.m.s. amplitude of run H-19 for the 50 second piece lengths. The piece number should be multiplied by 50 to evaluate the run time in seconds. Similar curves to those of figure 11 were computed by the analog technique. Figure 12 is an error curve obtained from the digital analysis for the modified accumulative cross correlation calculations. The Chi Squared confidence levels are also noted on fig. 13. At approximately the 30th piece the error approaches the limits. The number 1 optical unit shows a major rise in the r.m.s. at the same time. Thus, for analysis it would be indicated that the first 30 pieces or 1500 seconds be employed. Figure 13 shows the cross correlation obtained both by analog and digital means for the first 1200 seconds of run No. H-19. A maximum correlation of the order of .6 was obtained from the analog computer. A value of .26 was obtained by the digital computer.

Figure 14 compares the cross correlation obtained on the digital computer for time of 1200, 1450, 1500, 1650 and 1700 seconds. A definite drop in the correlation is noted between the 1500 and 1650 time periods. This drop in maximum value of the correlation appears to be directly related to the unsteady r.m.s. variation of the light signal. Thus, it can be concluded that for optimum operation of the cross beam system a steady value of the r.m.s. light fluctuations is desired.

### 1.7 CONCLUSIONS

For ideal light scattering conditions the passive, optical, cross beam system was shown to measure mean convective velocities in the atmosphere. Useable results were obtained from approximately 20% of the total tests. A fundamental difficulty appears to exist in many of the tests, in whether a particle scatters light in an identifiable way. If the scattering is not consistent between the two beams, the net mean correlation is zero, even though the instantaneous values of the correlations are large. Evidence of this apparent inconsistent scattering was observed for the beams looking directly at each other.

Evidence was obtained which indicates that aerosol layers could produce large correlations at heights not predicted from the beam geometry. These layers appear to dominate the correlations, thus limiting measurement to the layer only. When aerosol layers are found to exist, the cross beam system could serve as a means of remotely measuring their convective velocity.

## 1.8 REFERENCES

1. Fisher, M. J., and Krause, F. R., The Crossed Beam Correlation Method. Jour. Fluid Mech., Vol. 28, p. 705, 1967.
2. Atmospheric Exploration by Remote Probes, Vol. 2, Proceedings of the Scientific Meeting of the Panel on Remote Atmospheric Probing. National Research Council, 1969.
3. Sandborn, V. A., and Pickelner, D. J., Measurements of Wind Speeds With an Optical Cross Beam System. IEEE Transactions on Geoscience Electronics, Vol. GE-7, No. 4, pp. 244-249, 1969.
4. Patterson, G. S., and Corrsin, S., Computer Experiments on Random Walks With Both Eulerian and Lagrangian Statistics. Dynamics of Fluids and Plasmas, Academic Press, Inc., New York, 1966.
5. Cliff, W. C., Convective Velocities in the Turbulent Boundary Layer. Ph.D. Dissertation, Colorado State University, 1972.
6. Huff, L. L., and Sandborn, V. A., Experimental Probability Density Distributions for Optical and Infra-Red Cross-Beam Units. Research Memorandum 20, Colorado State University.
7. Hablutzel, B. C., Cross Beam Wind Measuring Techniques. Masters Thesis, Colorado State University, 1970.
8. Sandborn, V. A., Bice, A. R., Cliff, W. C., and Hablutzel, B. C., Preliminary Analysis of Cross-Beam Data from the Gun Barrel Hill Site, Colorado State University, College of Engineering Research Memorandum No. 15, 1969.
9. Huff, L. L., Sandborn, V. A., and Cary, K. E., Check Out of Rebuilt Optical Cross-Beam Units. Colorado State University, College of Engineering Research Memorandum No. 17, 1969.
10. Stankov, Borislava, Some Characteristics of Turbulence in the Lower 200 Feet of the Atmosphere. Masters Thesis, Colorado State University, 1970.
11. Sandborn, V. A., Optical Cross Beam Field Tests at ESSA-Haswell Field Site, October 1969. Colorado State University, College of Engineering Research Memorandum No. 18, 1969.
12. Huff, L. L., and Sandborn, V. A., Analysis of Cross Beam Runs Taken at Haswell Field Site, October 1969. Colorado State University, College of Engineering Research Memorandum No. 19, 1969.
13. Townsend, A. A., Entrainment and the Structure of Turbulent Flow, Vol. 41, p. 13, 1970.

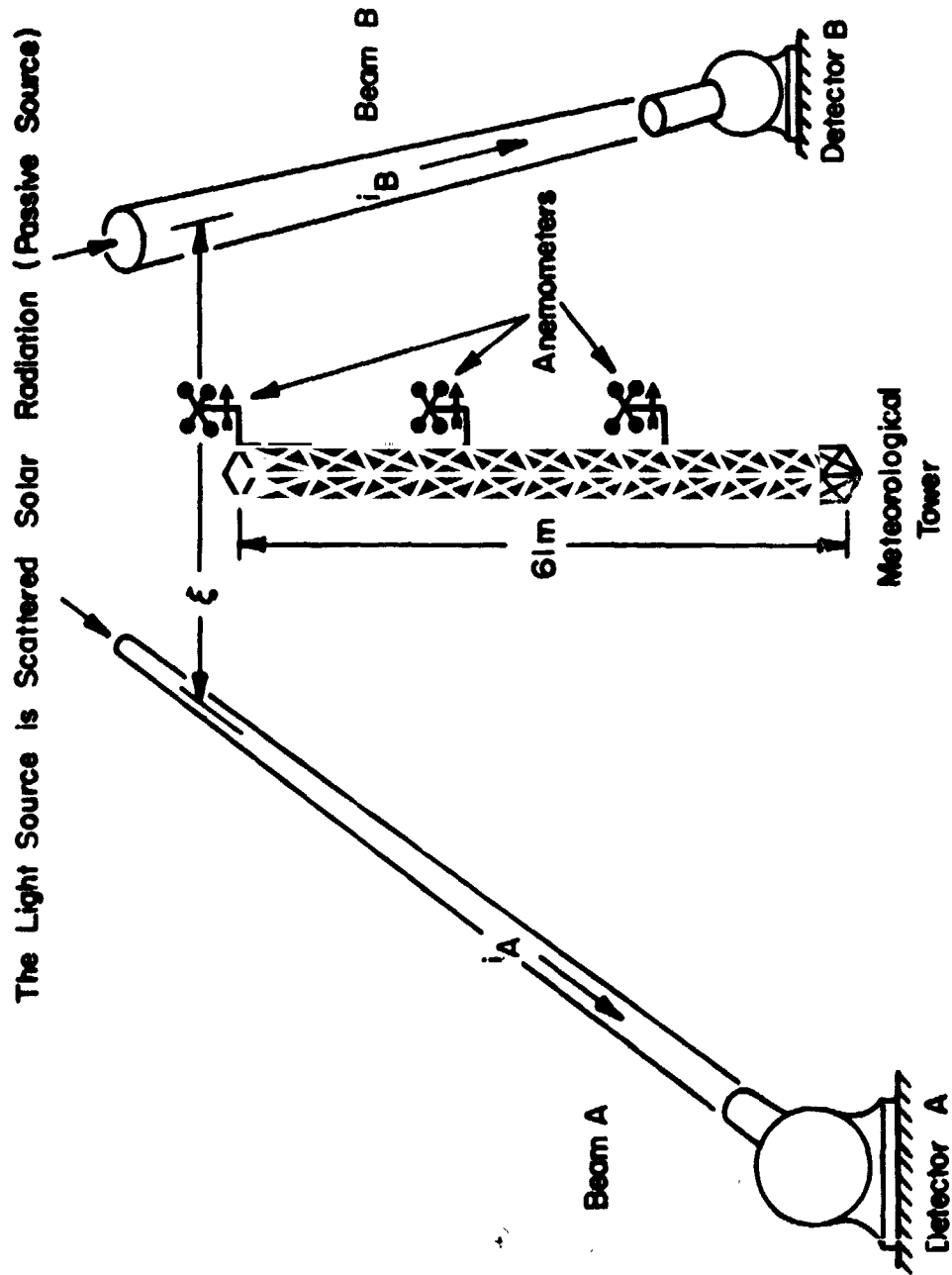


Fig.1 Cross Beam System

(%) First Order Probability Density of Velocity as Measured by an Anemometer

$$R_{12}(\tau) = \frac{R_{12}(\tau)}{\sqrt{R_1(0)R_2(0)}}$$

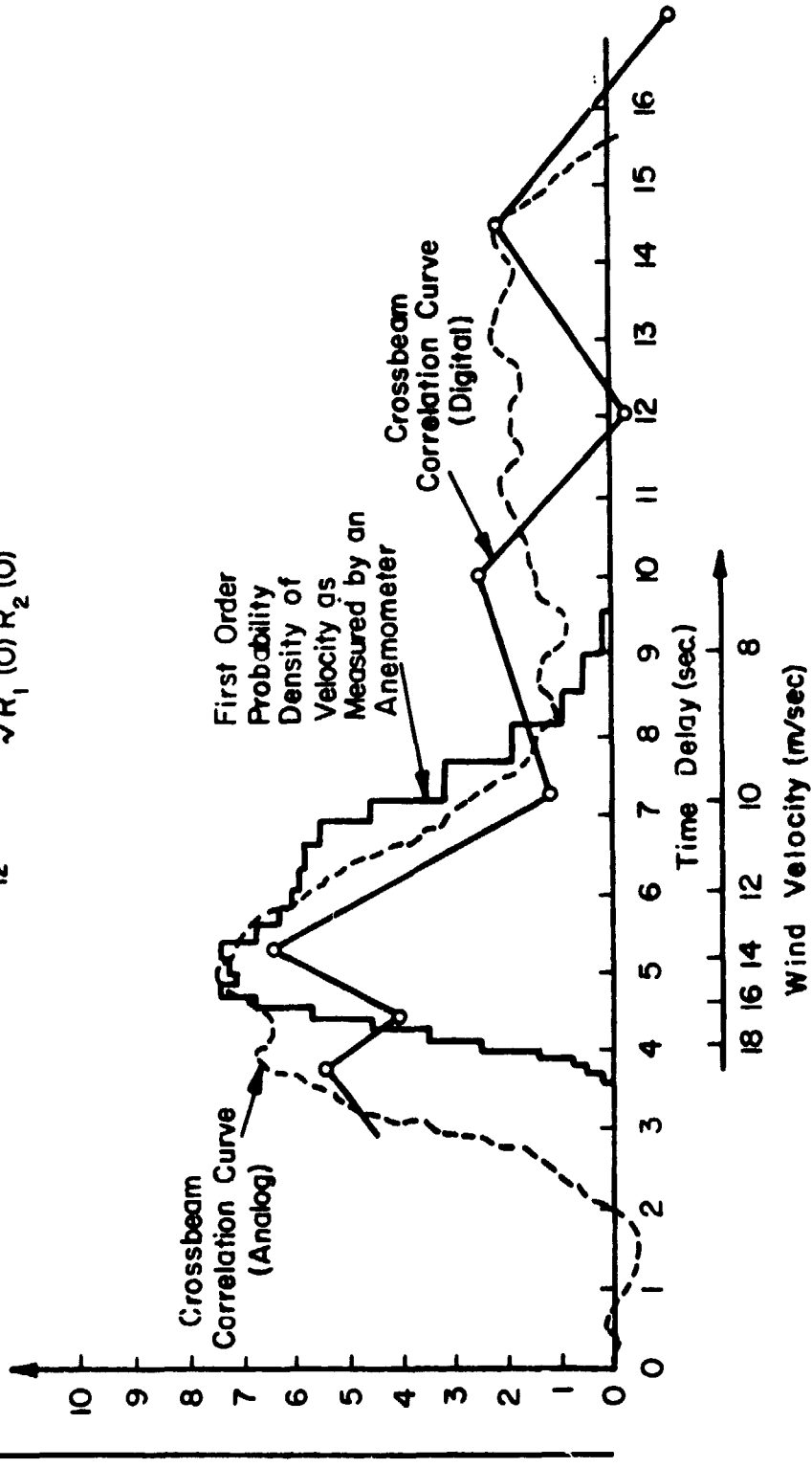
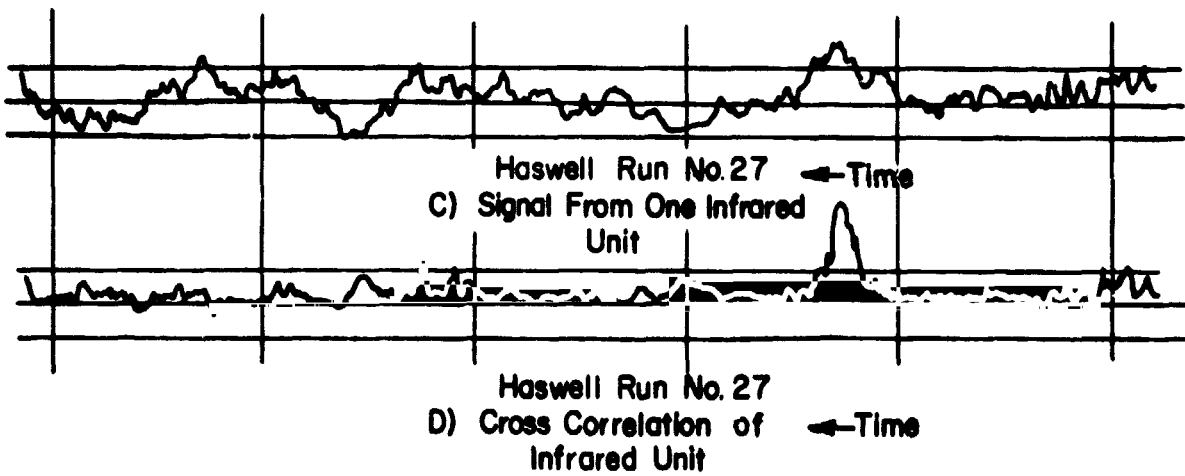
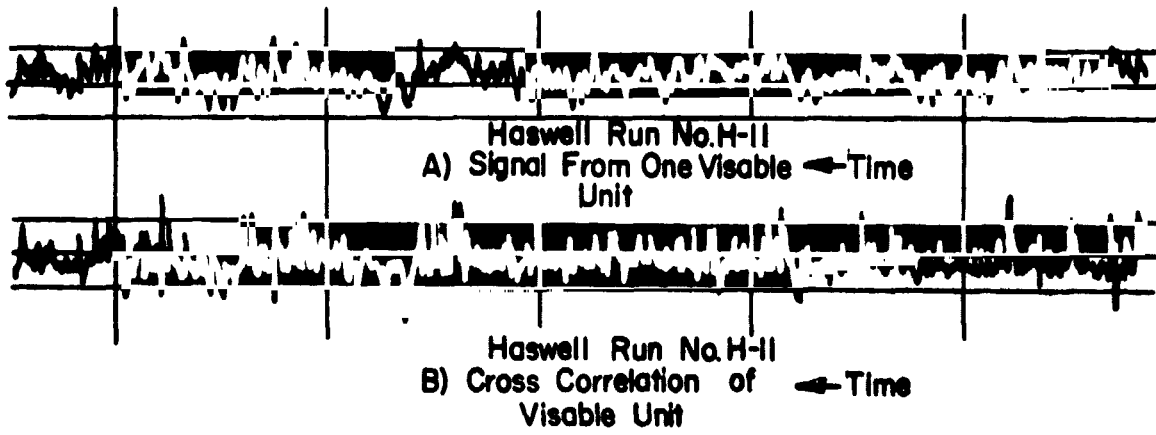


Fig. 2 Space Time Correlation Measurements for a High Wind



**Fig.3 Time Variation of Cross Beam Signals and Their Cross Correlations for Zero Time Delay**

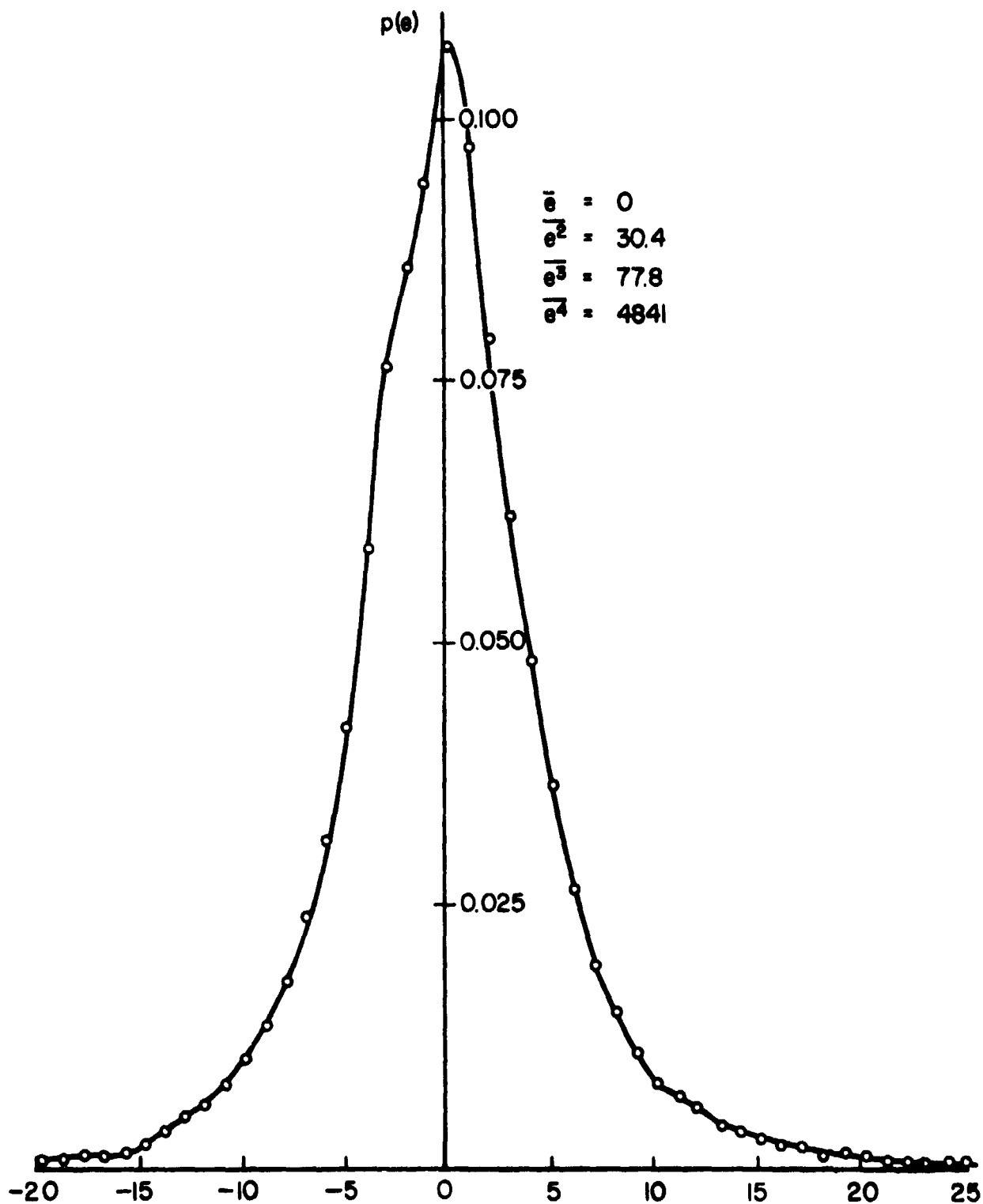


Fig.4 Probability Density of Cross-Correlation for Run H-II

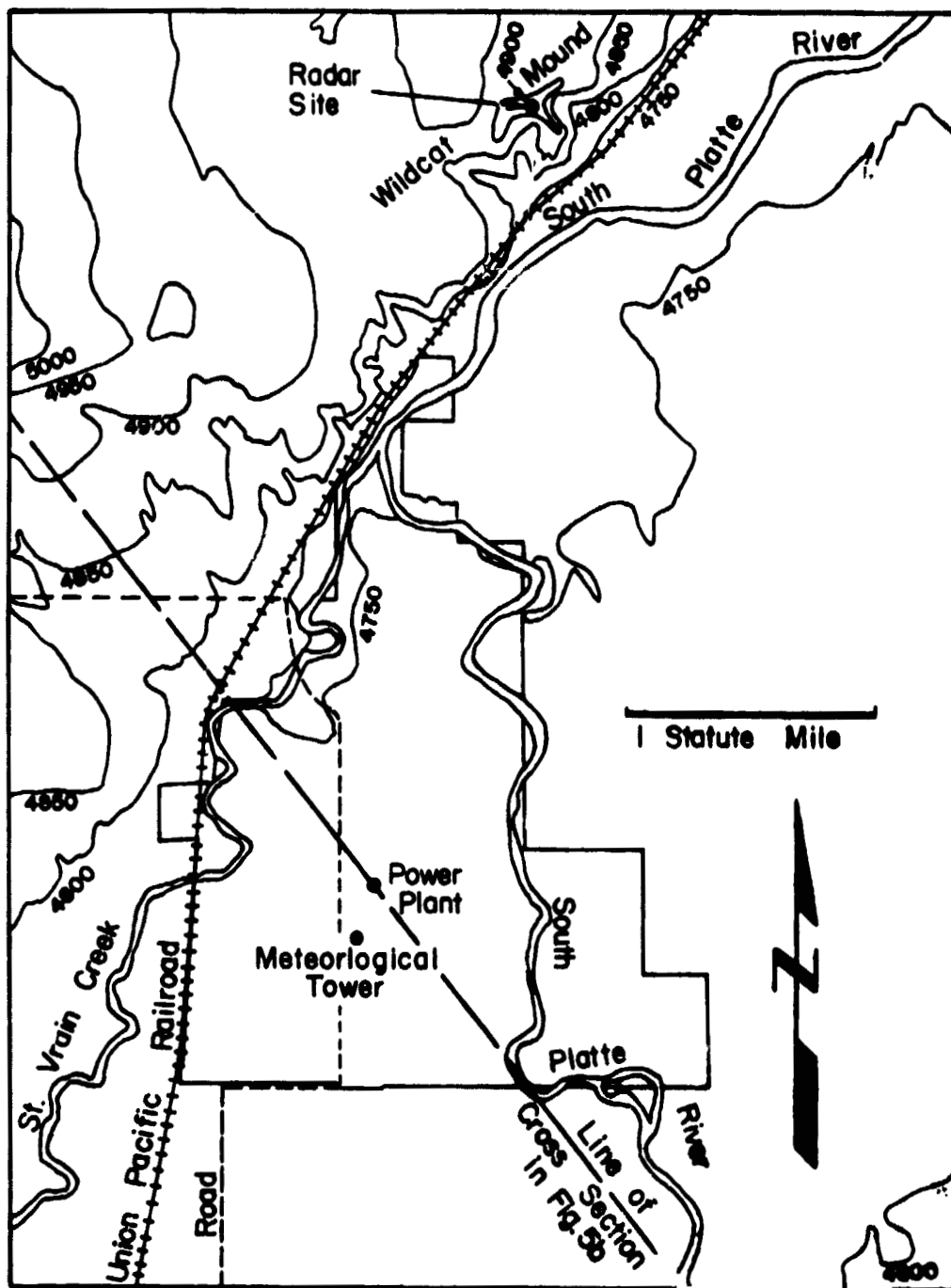


Fig. 5a. Detailed Map of the Meteorological Tower. Height Contours are Given in Feet. The Straight Line Indicates the Plane of the Cross Section in Fig. 5b. (Reiter, 1967, Meteorological Conditions at the Fort St. Vrain Nuclear Generating Station).

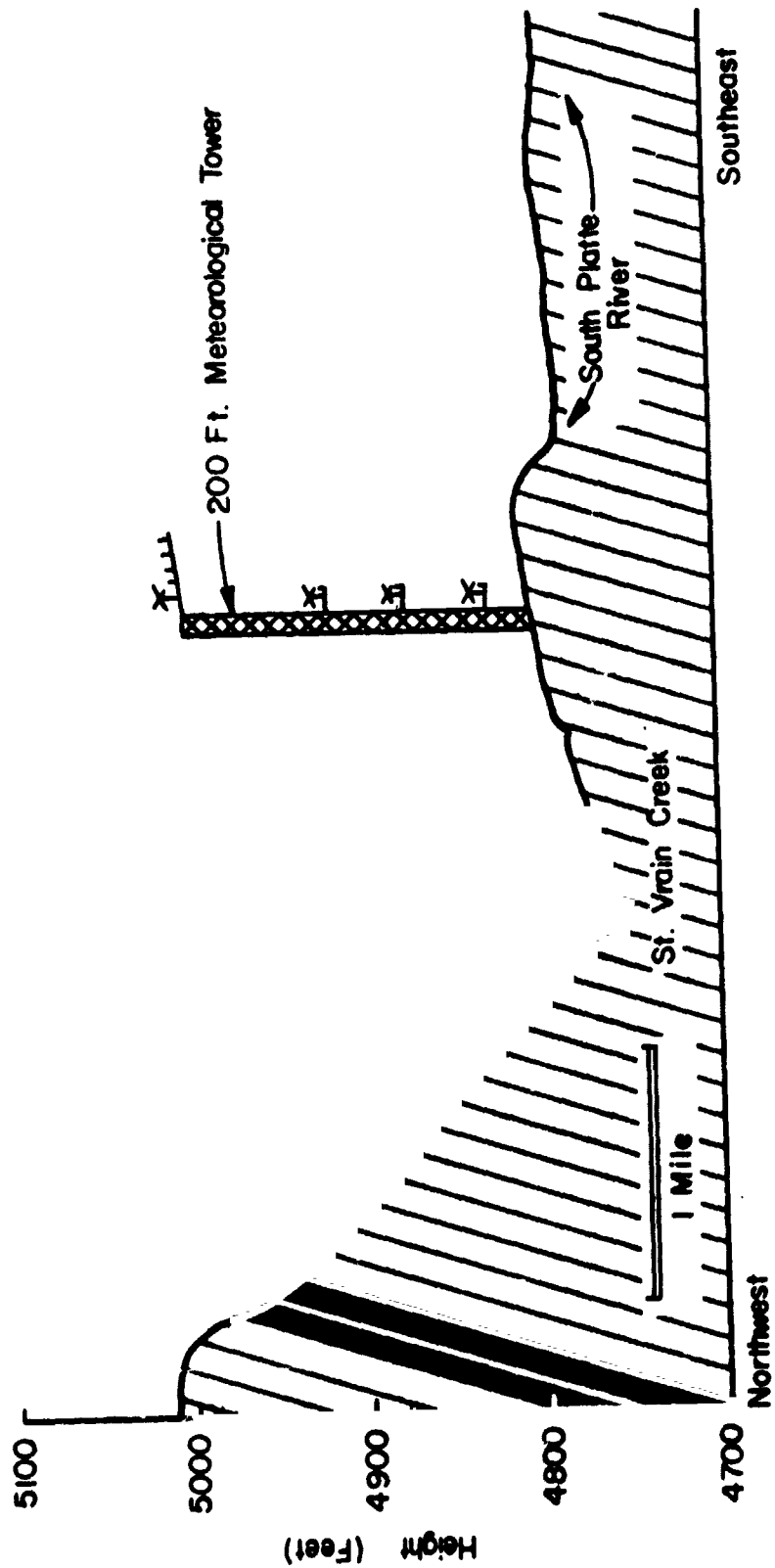


Fig. 5b Terrain Cross Section as Indicated in Fig. 5a, with Meteorological Tower and the Position of Hot Wire and Cup Anemometer. (Reiter, 1967, Meteorological Conditions of the Fort St. Vrain Nuclear Generating Station.)

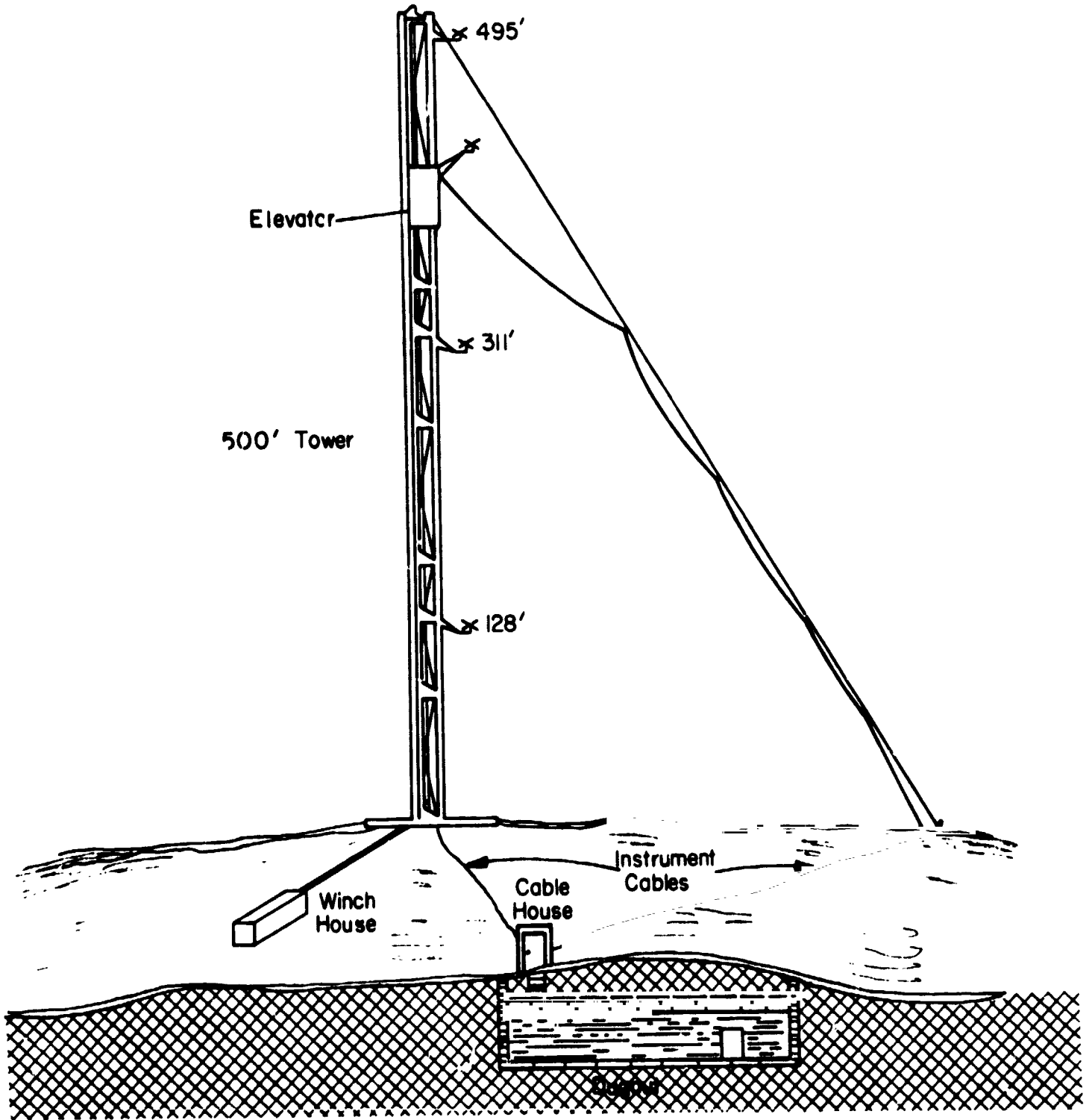


Fig 6 Haswell Meteorological Tower

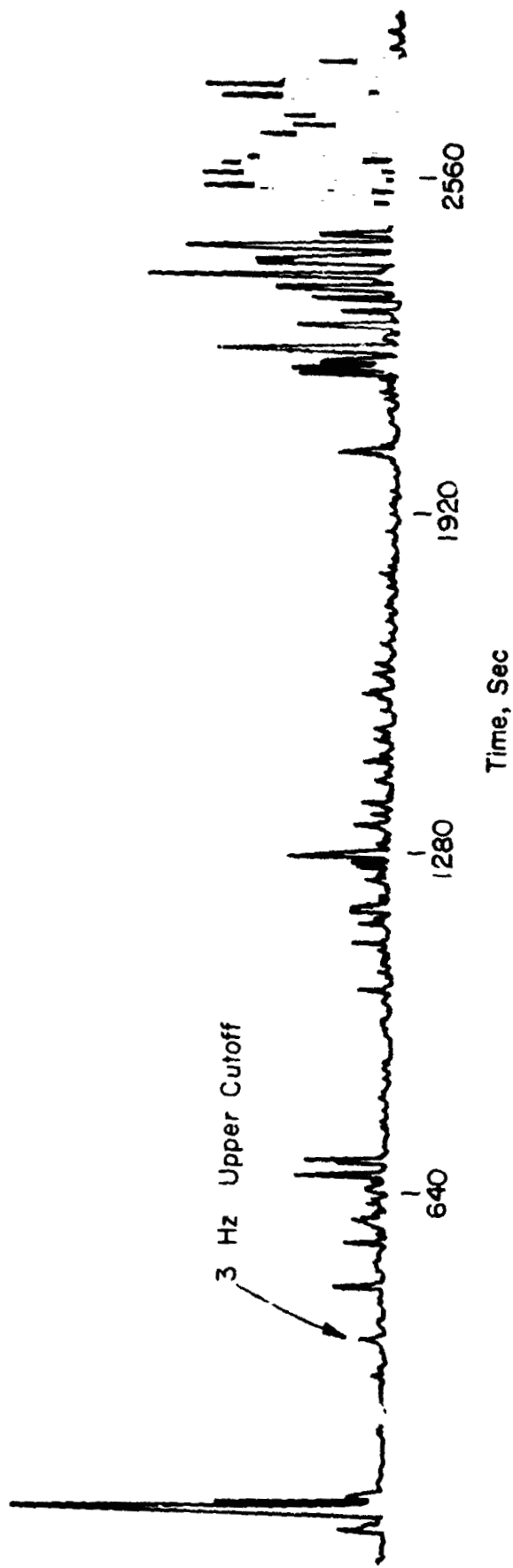


Fig. 7 Variation of the Mean Square Signal Measured by Analog Technique

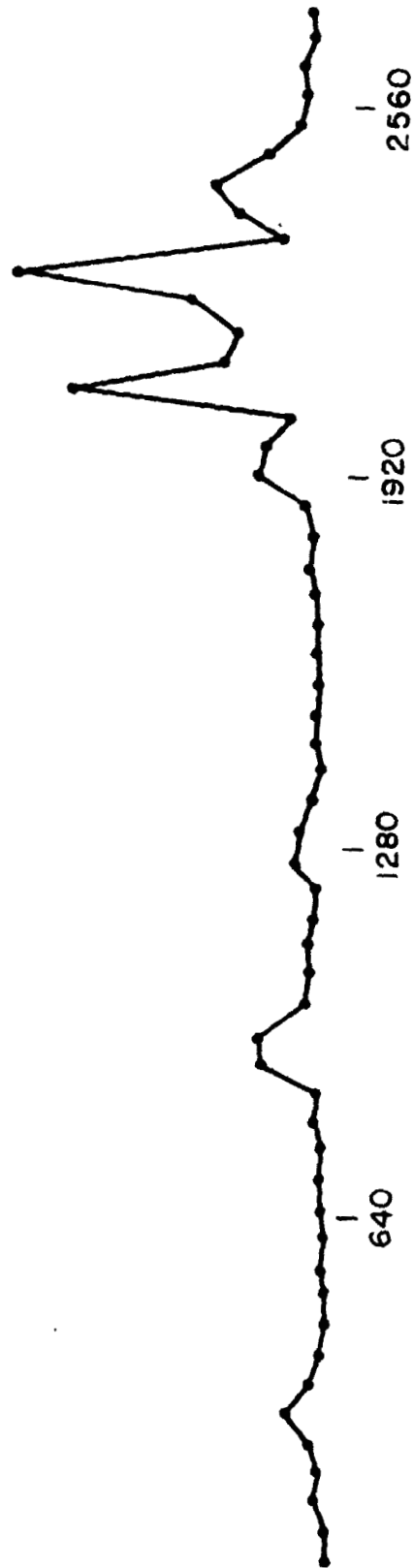


Fig. 8 Variation of R.M.S. Signal Computed on Digital Computer

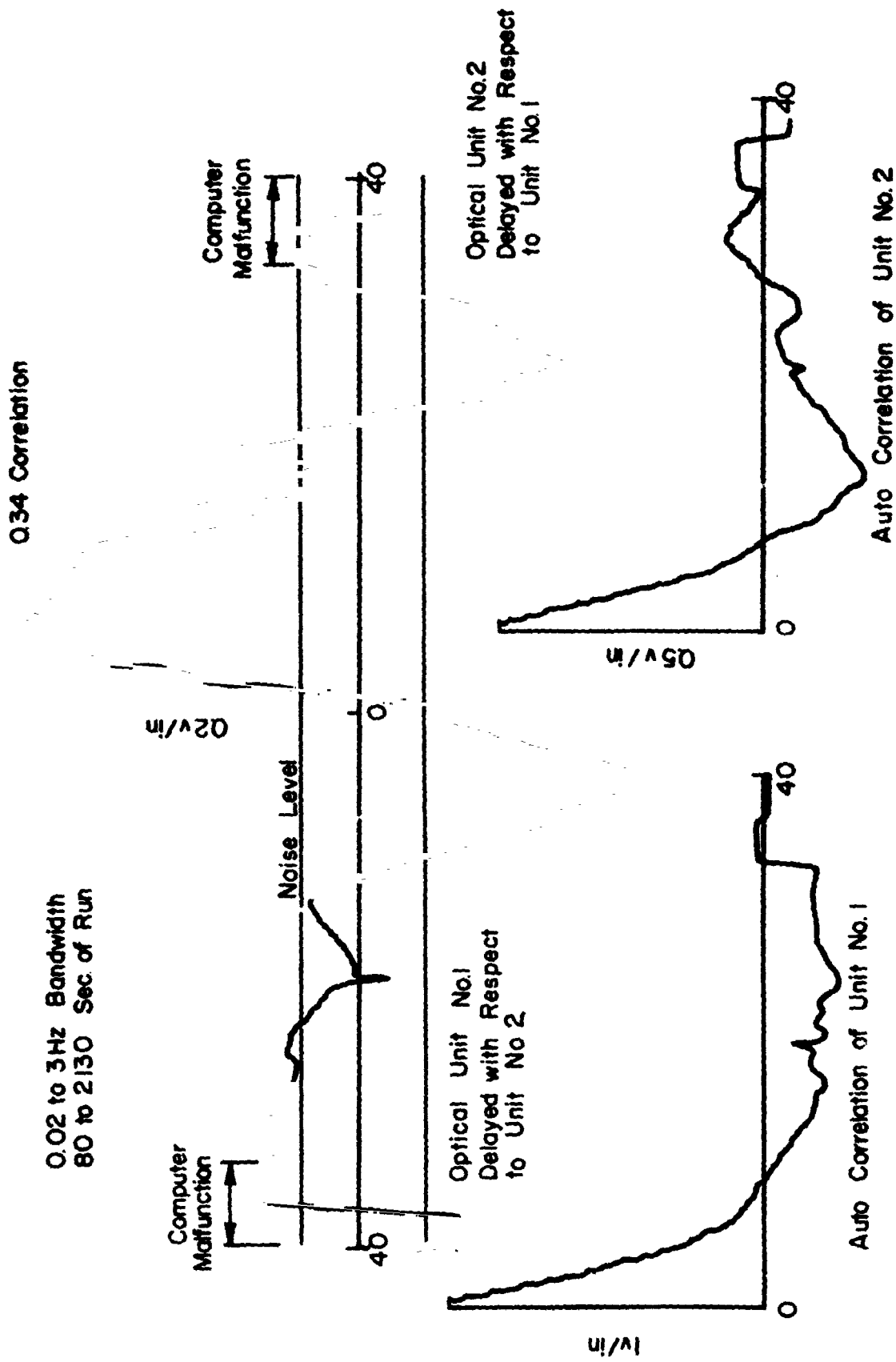


Fig. 9 Space-Time and Autocorrelation Measurement for Beams Intersecting at 39 Meters (128 Feet)

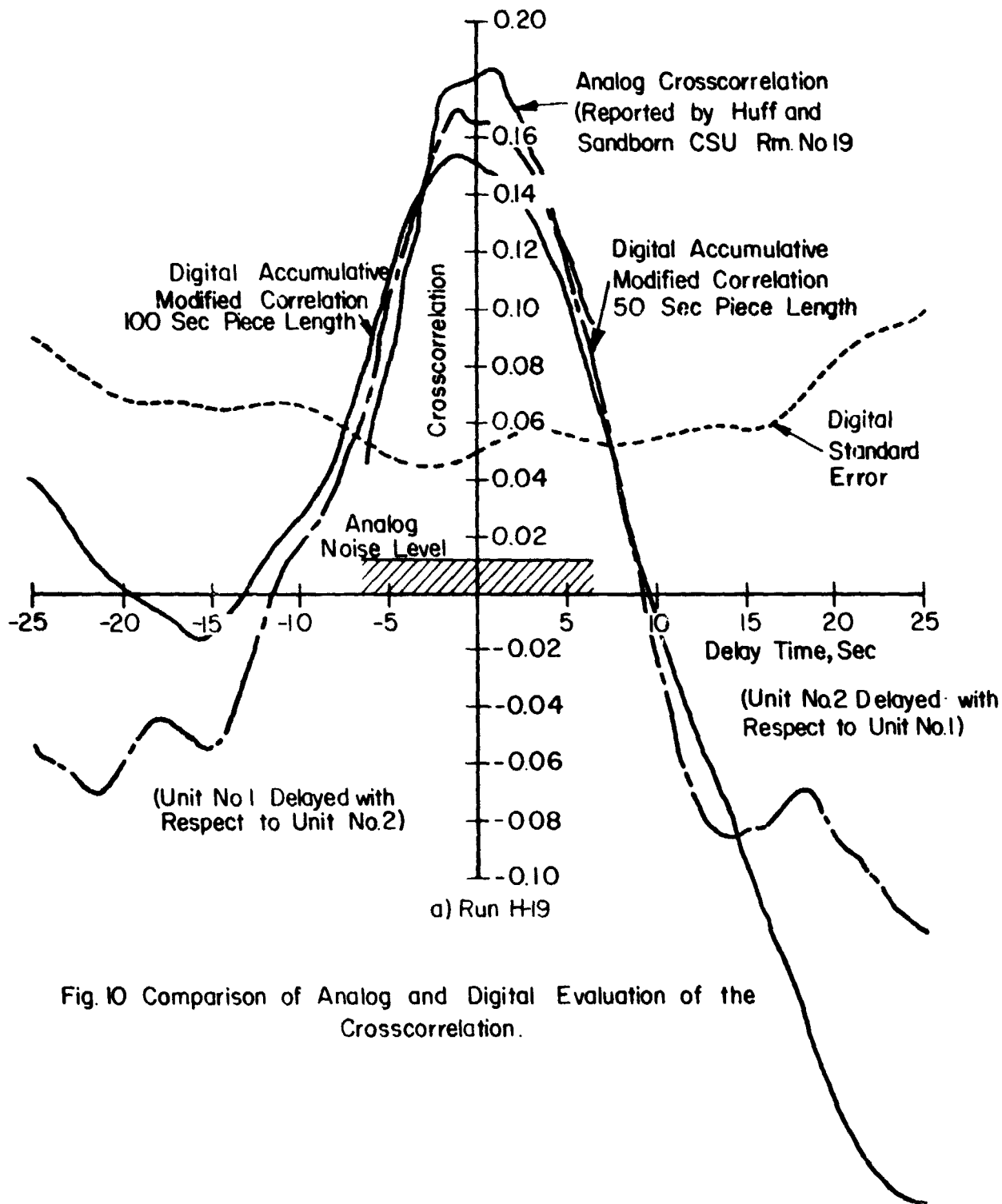
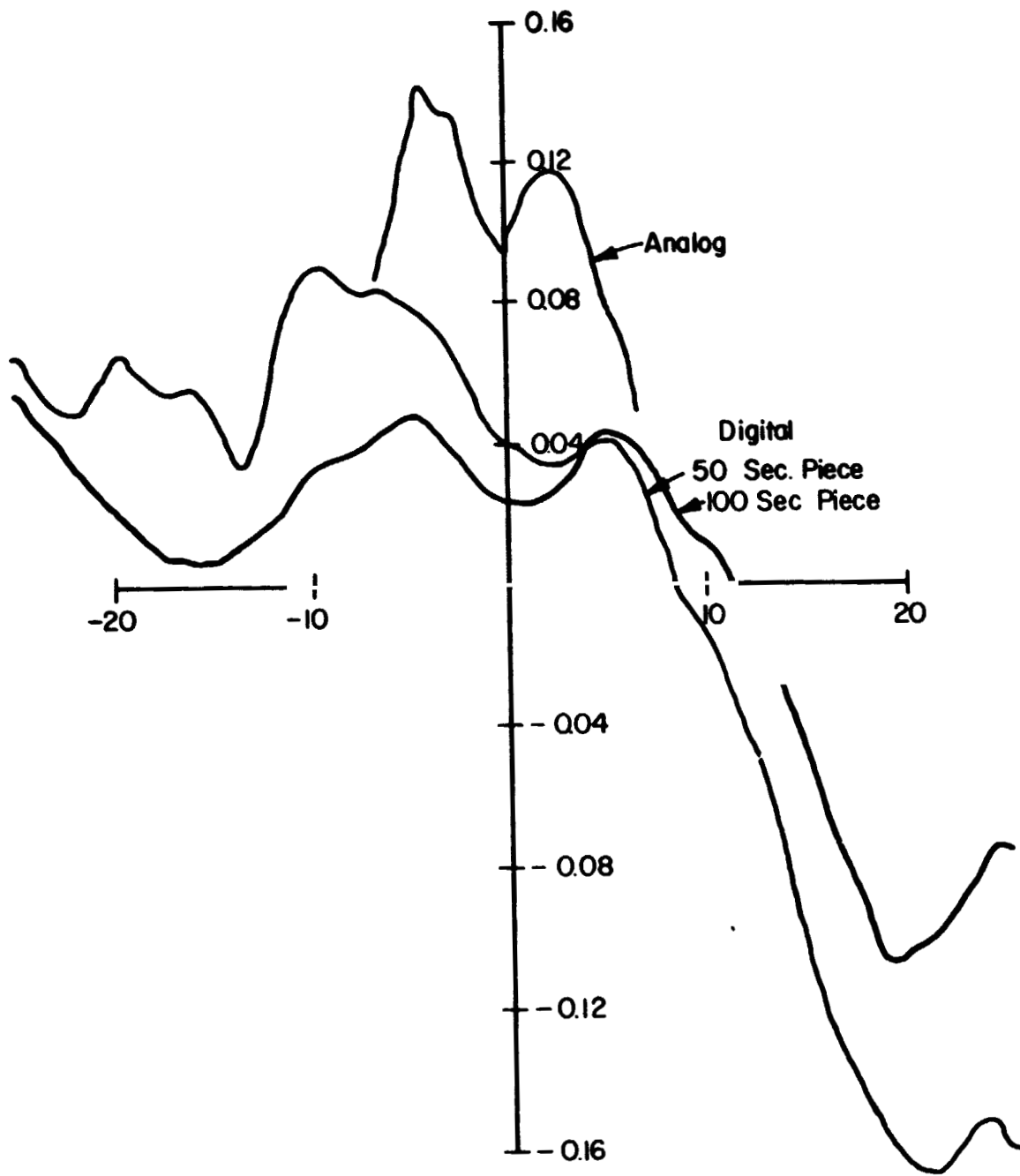


Fig. 10 Comparison of Analog and Digital Evaluation of the Crosscorrelation.



b) Run H-20

Fig. 10 (Concluded)

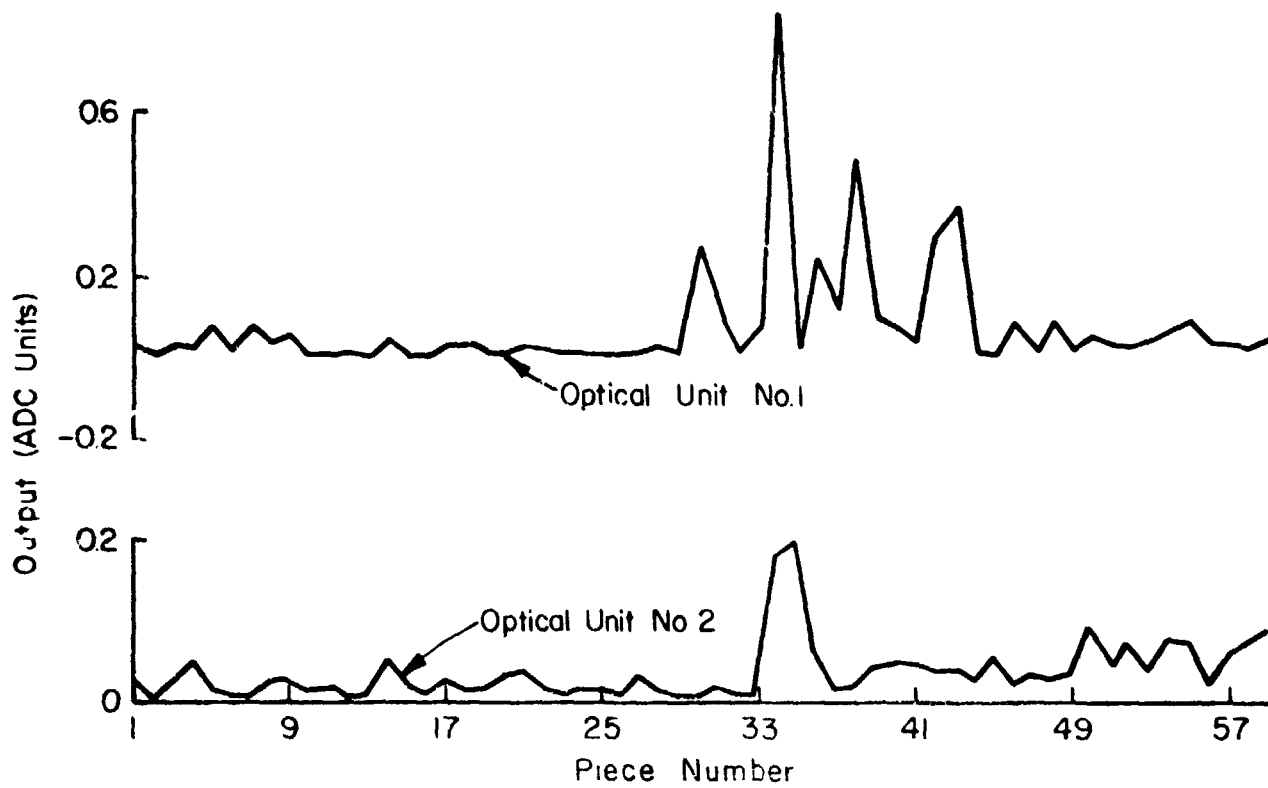


Fig. 11 RMS Amplitude Variation for Run H-19.

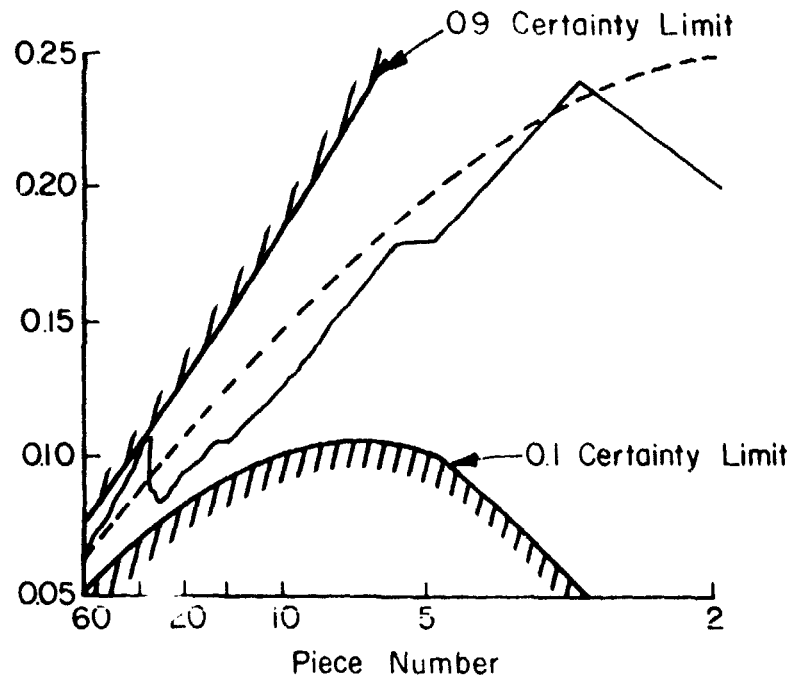


Fig 12 Error Curve for the Modified Accumulative Averages Crosscorrelation for Run H-19.

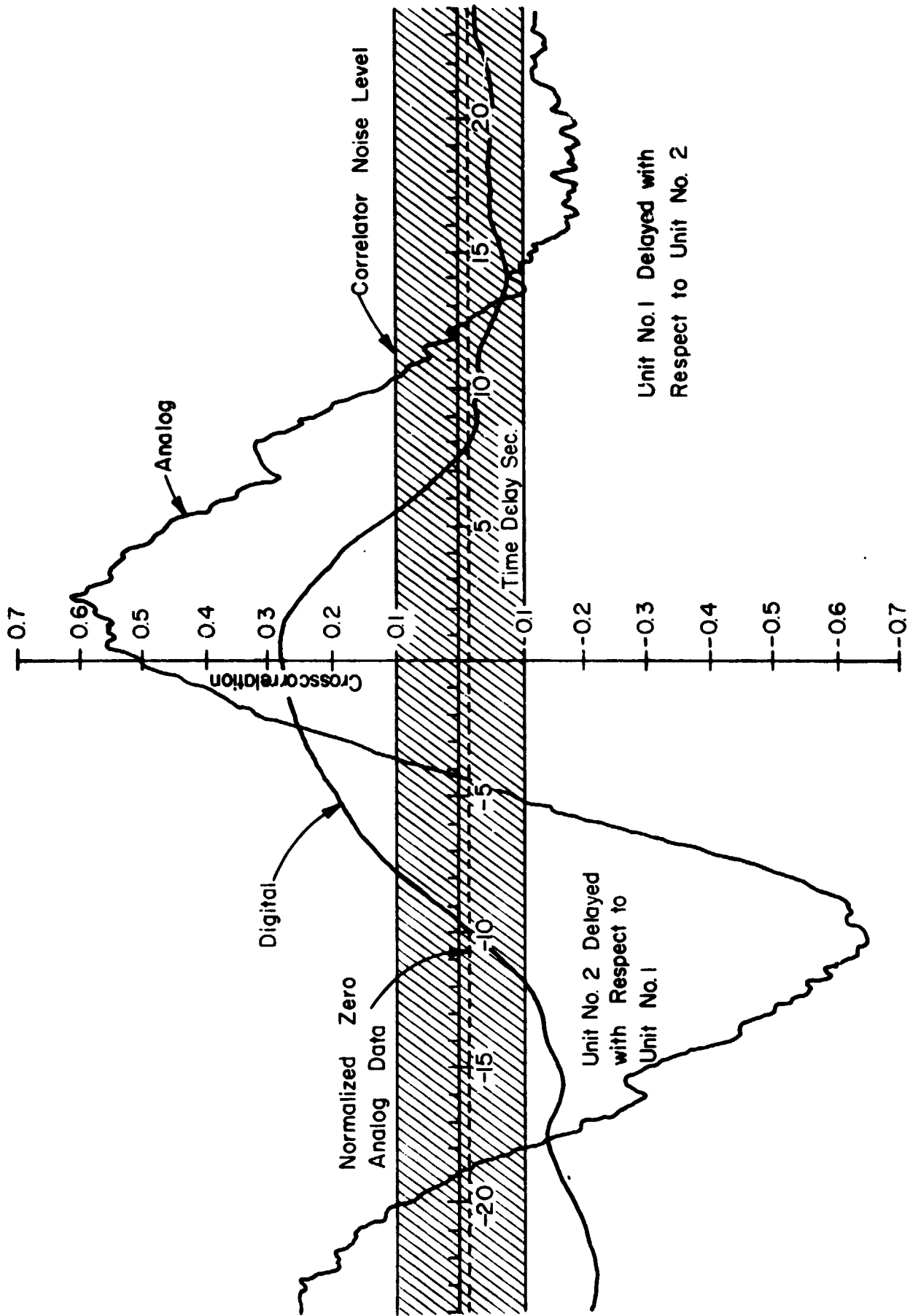


Fig.13 Crosscorrelation Measurement for Haswell Run No H-19. Average Over First 1200 Sec. of the Run. 0.02 to 3 Hz Frequency Band

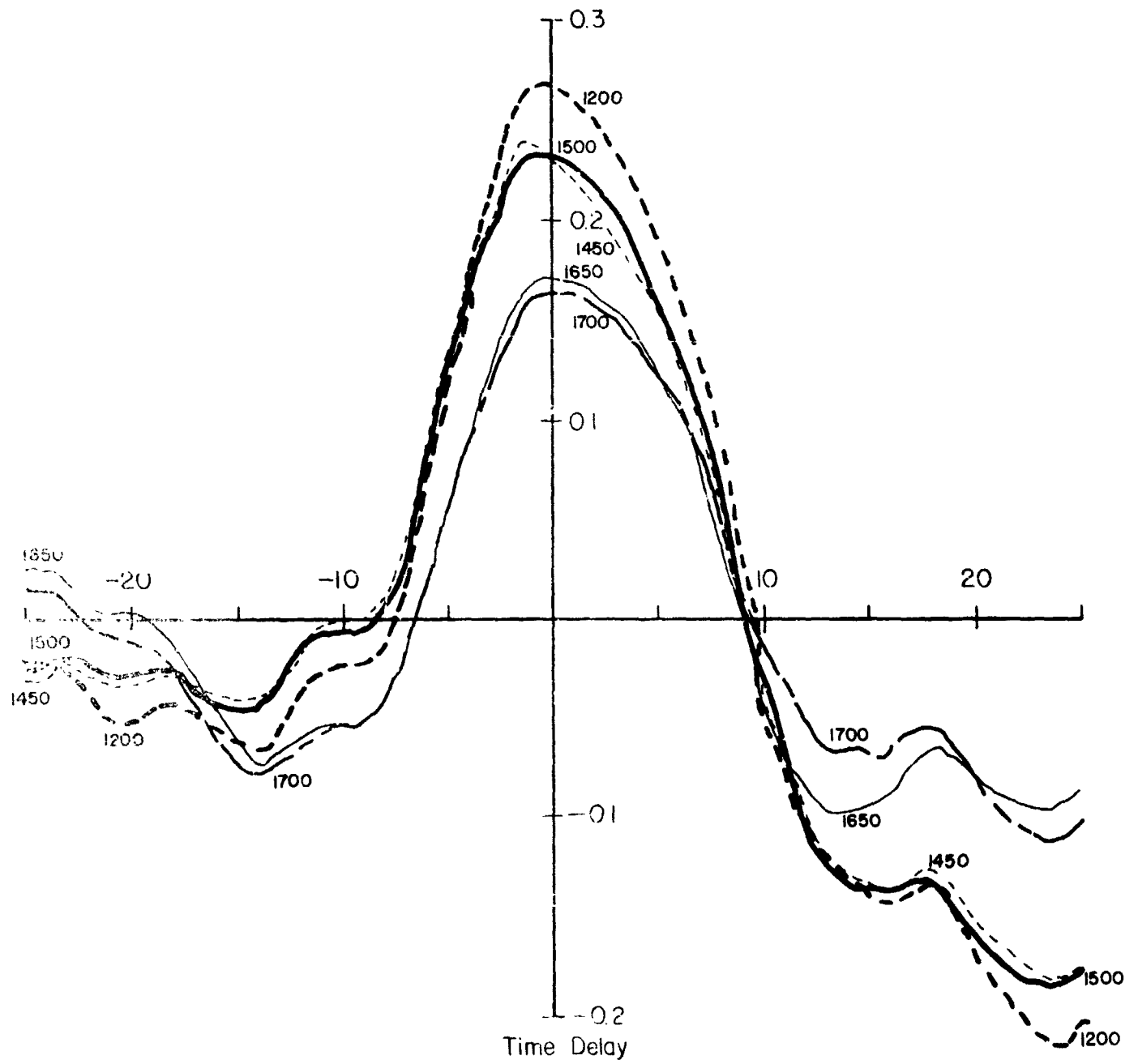


Fig 14 Cross Correlation for Run H-19 for Different Run Times

SECTION II.  
EXPERIMENTAL PROBABILITY DENSITY DISTRIBUTIONS  
FOR OPTICAL AND INFRA-RED CROSS-BEAM UNITS

by

L. L. Huff

and

V. A. Sandborn

2.1 SUMMARY

Approximate probability density distributions have been computed for selected optical and infra-red cross-beam data from the Haswell experiments. From this limited analysis it appears reasonable to assume that the signals from a single IR unit are log-normally distributed. This does not appear to be a reasonable assumption for either a single optical unit or for the instantaneous product of two signals. The experimental probability density distributions are presented as plots, and comparisons are made with fitted log-normal distributions.

2.2 INTRODUCTION

A series of cross-beam experiments was conducted at the ESSA field site at Haswell, Colorado, in October 1969. Both optical and infra-red units were operated on a comparison basis. Reference 1 reported the test configuration and experiment identification. A preliminary correlation analysis of the data was reported in Reference 2. The present report is a data report presenting an approximate analysis of the probability density distributions for the signals from both the optical units and the IR units. Two runs representing each of the two types of cross-beam units were selected for analysis. Probability density distributions are also presented for the instantaneous product of the signals for each of the runs.

### 2.3 METHOD OF ANALYSIS

Strip chart recorder traces of selected portions of the data were made from the magnetic tape recordings. Figure 8 shows a representative sample of each of these traces. As can be seen on Figure 8, one trace is the signal from a single cross-beam unit while the second trace is the product of the signals from both units. After establishing an arbitrary zero level for the signal traces, the number of crossings of the trace for a given voltage level was determined by a visual count, and the results were plotted versus voltage level. These curves were then normalized by scaling the ordinate so that the area under the resulting curve was equal to one. These curves are a reasonable approximation for the probability density distributions of the signals. No analysis was made for the single optical unit in Run li-10 because of the poor quality of the strip chart recorder trace.

Graphical methods were used to determine the first four moments of these distributions. The distributions were then replotted with a shifted abscissa to obtain a distribution with a zero first moment. These distributions are shown as Figures 1, 2, 3, 4, 5, 6 and 7 and the values of the second, third, and fourth moments about the mean are given on the figures.

A suggestion by Mr. Tony Weigandt of ITTRI to the effect that the distribution of the data should be log-normal was checked by attempting to fit a log-normal curve to the above data. The results are shown on Figures 2, 6 and 7.

### 2.4 EVALUATION

As can be seen from the figures, the distributions for the optical units as well as those for product of the signals of two units seem to be very strongly peaked near the mean. On the other hand, the distributions for the

signals from a single IR unit have a flattened appearance near the mean.

Figure 7 shows the result of attempting to fit a log-normal distribution to one of the peaked cases. Because of the poor fit in this case, no attempt was made to fit the other peaked distributions. Figures 2 and 6 show the result of fitting a log-normal in the flattened cases. The closeness of the fit is rather surprising considering the admittedly somewhat crude analysis of the data. It appears that it is reasonable to assume a log-normal distribution for the signal from a single infra-red unit. To date, no reasonable explanation has been proposed for the extremely peaked distributions.

#### 2.5 REFERENCES

1. Sandborn, V. A.: Optical Cross Beam Field Tests at ESSA Haswell Field Site, Research Memorandum No. 18, Colo. State Univ. Oct. 1969.
2. Huff, L. L. and Sandborn, V. A. : Analysis of Cross Beam Runs Taken At Haswell Field Site, Research Memorandum No. 19, Colo. State Univ. Oct. 1969.

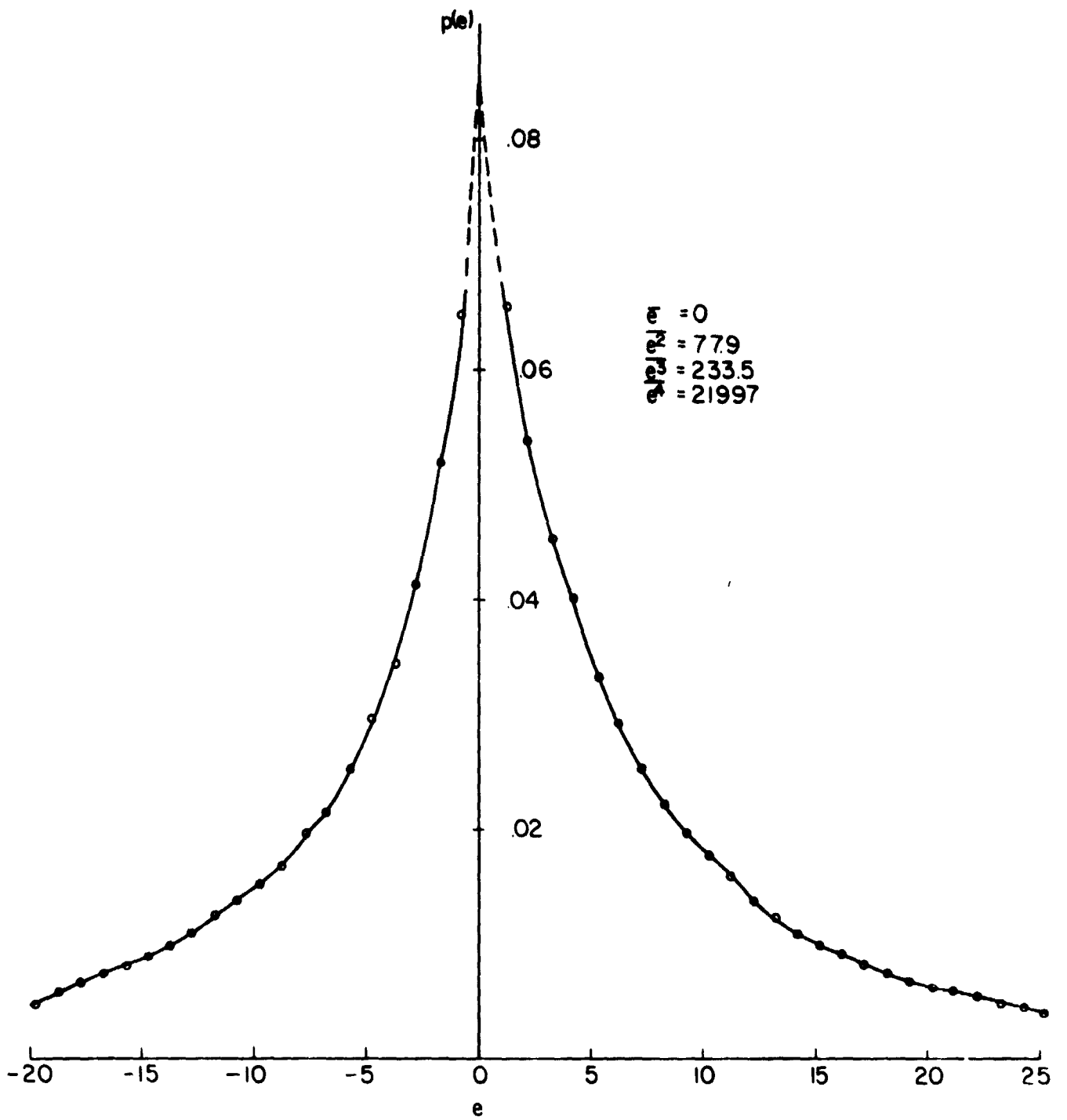


Fig. 1 Probability distribution of cross-correlation for optical units  
Run H-10

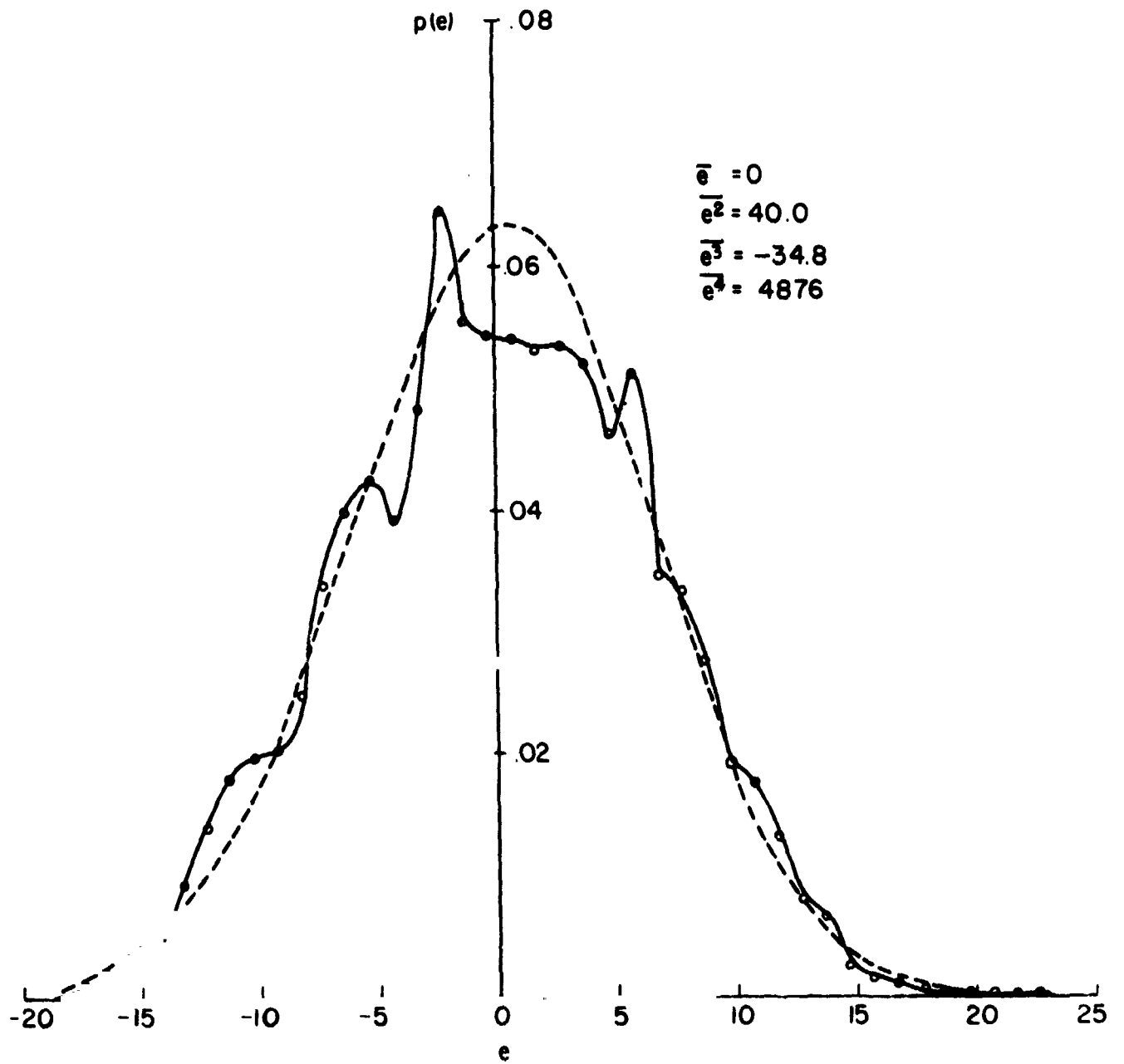


Fig. 2 Probability distribution for one IR unit  
 Fun No 25

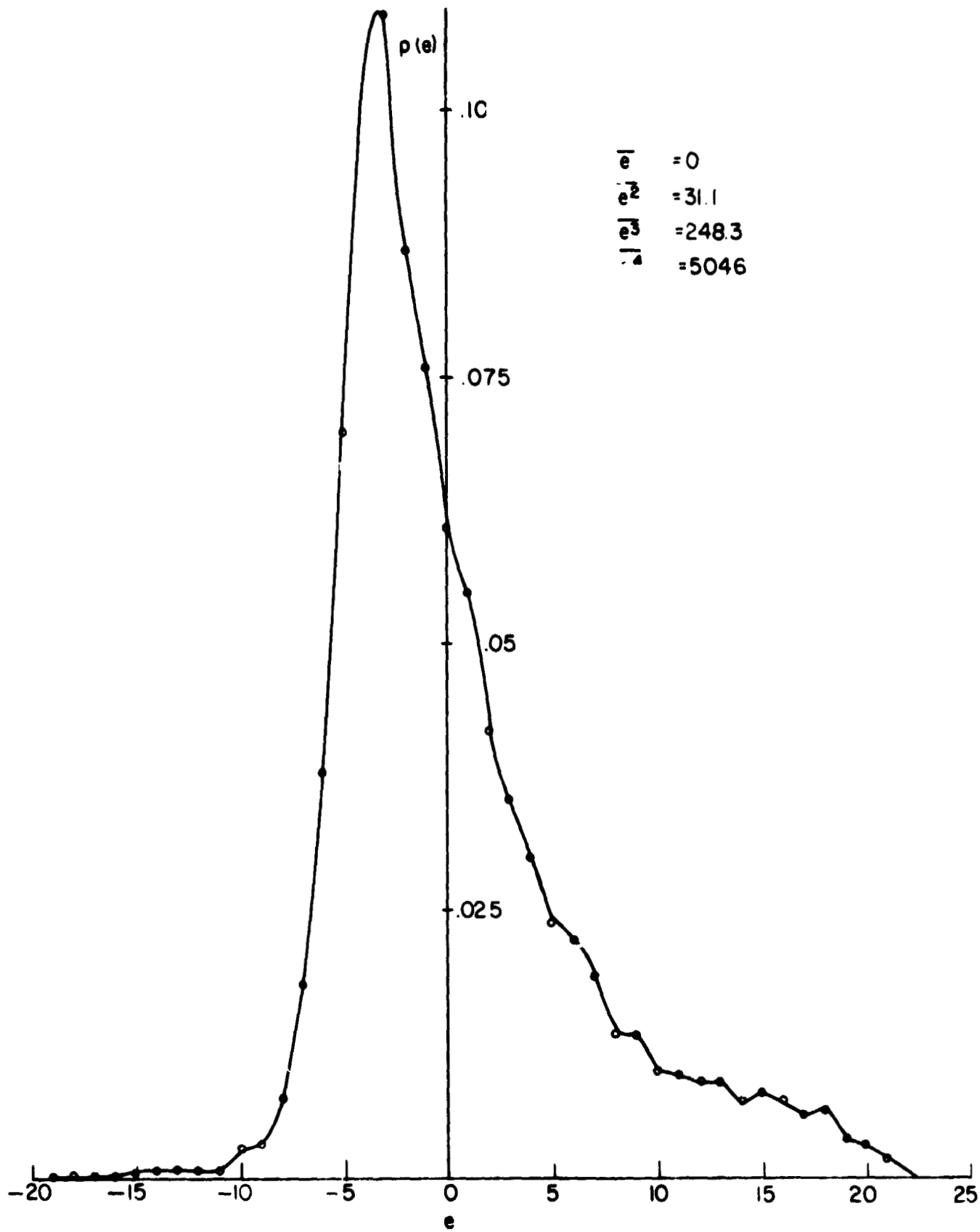


Fig. 3 Probability density of cross-correlation for IR units  
Run No 25

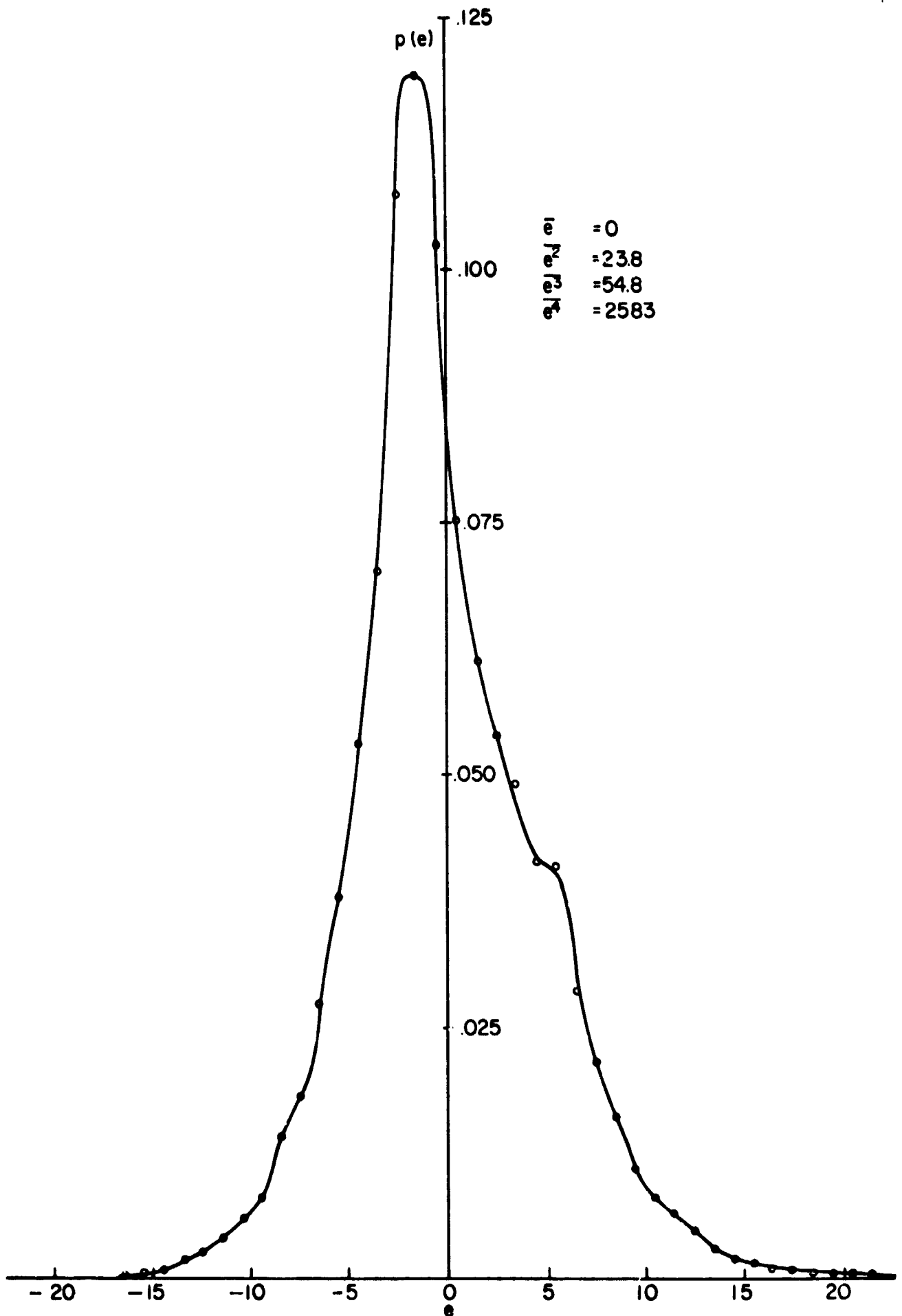


Fig. 4 Probability density of optical unit. Run H-11

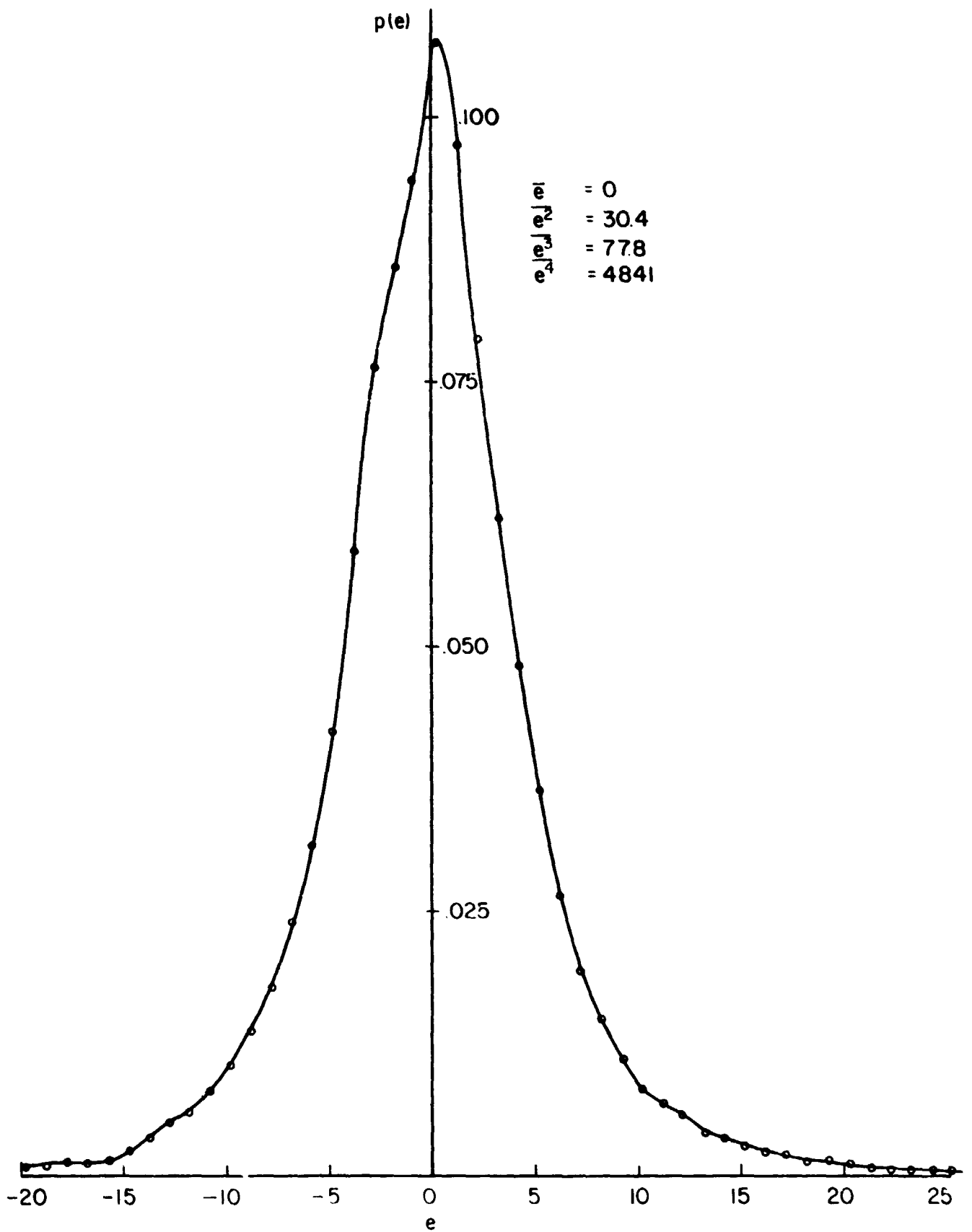


Fig 5 Probability density of cross-correlation for run H-11

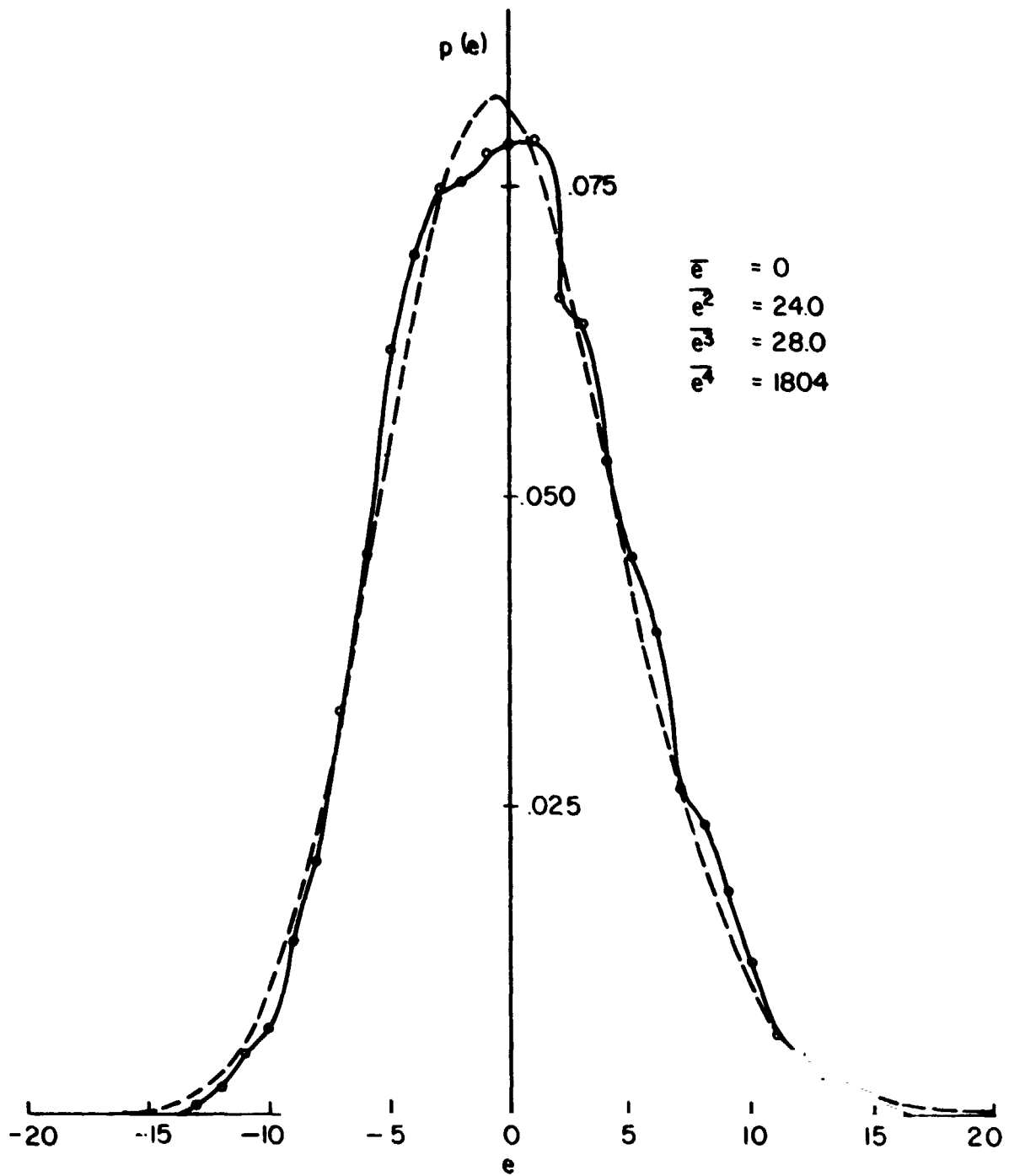


Fig. 6 Probability density of one IR unit for Run 27

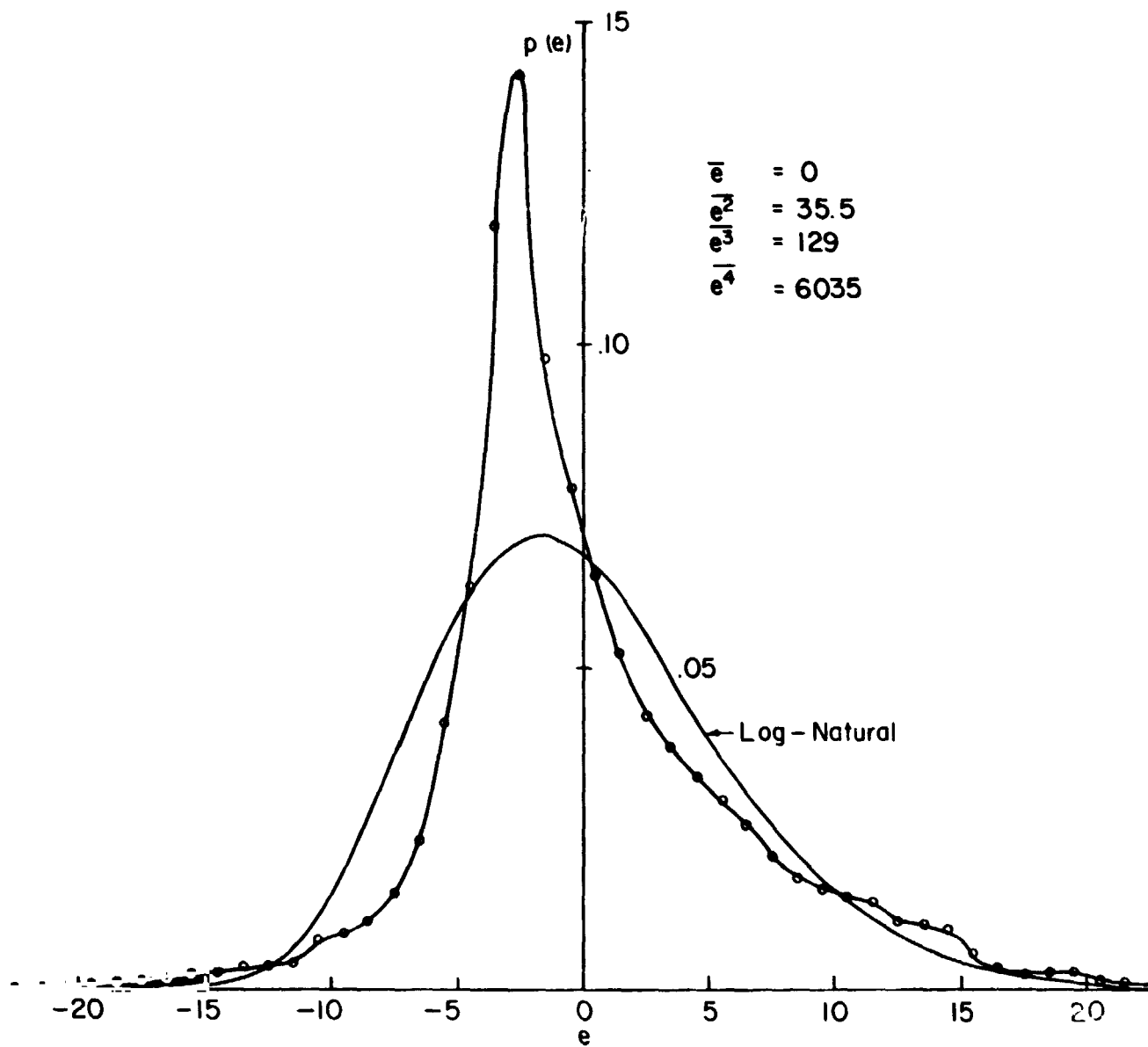
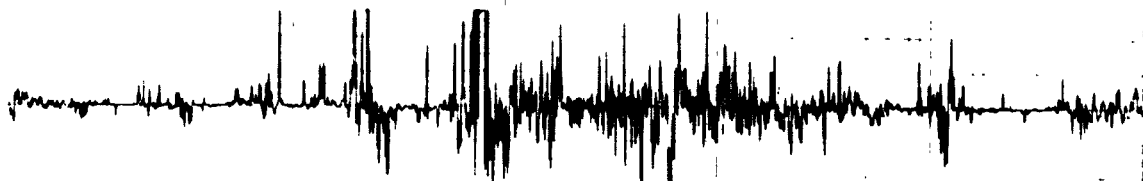


Fig. 7 Probability distribution of cross-correlation of IR units for Run 27.



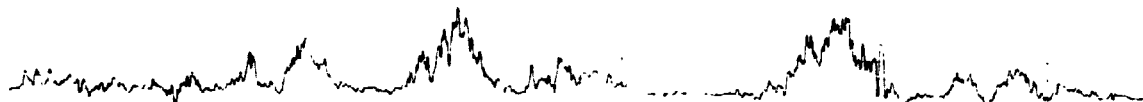
HASWELL RUN No. 10  
CROSS-CORRELATION OF VISIBLE UNITS



HASWELL RUN No. 21  
SIGNAL FROM ONE INFRARED UNIT



HASWELL RUN No. 25  
CROSS-CORRELATION OF INFRARED UNITS



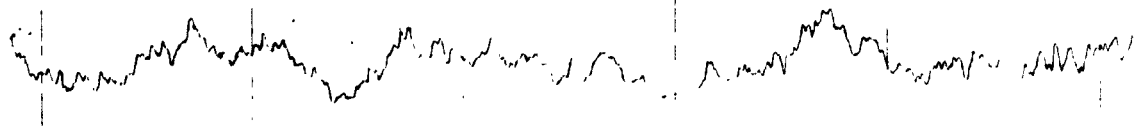
HASWELL RUN No. 11-11  
SIGNAL FROM ONE VISIBLE UNIT



HASWELL RUN No. 11-11  
CROSS-CORRELATION OF VISIBLE UNITS



HASWELL RUN No. 27  
SIGNAL FROM ONE INFRARED UNIT



HASWELL RUN No. 27  
CROSS-CORRELATION OF INFRARED UNITS

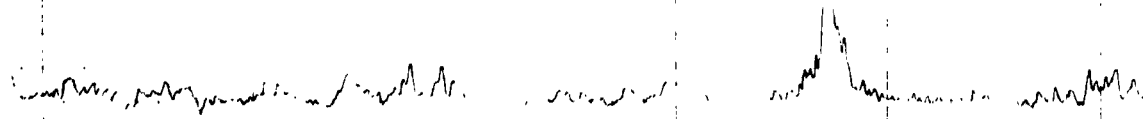


FIGURE 8

REPRODUCIBILITY OF THE  
ORIGINAL PAGE IS POOR

**SECTION III.**  
**ANALOG COMPUTATION OF AUTO- AND CROSS-CORRELATION FUNCTIONS**

**3.1 INTRODUCTION**

For analysis of the data obtained from the cross beam systems it was deemed desirable to compute the auto- and cross-correlation functions by both digital and analog methods to provide a cross-check of the analysis methods and an indication as to which of the two methods would be most suitable for routine use in the analysis of such data. It is the purpose of this appendix to provide a concise description of the equipment and procedures used for the electronic analog analysis of the cross beam data.

Figure A-1 is a block diagram showing the signal processing and computation set-up used for most of the analog data analysis. The data obtained at the field test sites were recorded on magnetic tape using wide-band FM recording techniques. The recording tape speed used was 1 7/8 IPS. The data as recorded were band-pass filtered by electronic signal processing in the data acquisition systems. The data was reproduced in the analog computation lab by play back of the magnetic tape on an AMPEX model FR 1300 tape recorder with the appropriate FM reproduce amplifiers. The tape speed used for play back was 60 IPS. This tape speed provided a real time to computation time compression ratio of 32 to 1 and produced a data frequency band which was compatible with the signal processing equipment available in the lab. Some short data records were played back at 30 IPS.

The data as reproduced by the tape recorder was then amplified by two Philbrick Model K2W operational amplifiers with variable gain

feed back systems and then bandpass filtered through two SKL Model 308A variable electronic filters. These filters were set to pass the frequency band covered by the recorded data and to reject frequencies outside this band, thereby minimizing the contribution of extraneous electronic noise to the signals of interest. The processed signals were then fed to a PAR Model 101 correlation function computer which computed the auto- and cross-correlation functions for the data. The computed correlation functions were then recorded by plotting on a Moseley Model 135 X-Y recorder. A typical correlation plot is shown on Figure A-2.

### 3.2 COMPUTATION PROCEDURE

The procedure for computing the correlation functions was as follows:

1. The tape recorder reproduce amplifiers were carefully calibrated following the procedure given in the AMPEX FR 1300 manual
2. The DC output levels of the Philbrick OP amps and the SKL filters were carefully nulled following the procedures recommended in the manufacturer's manuals, and the appropriate cut-off frequencies were set on the filters.
3. The system was connected and the gain of the OP amps was set to provide an appropriate signal level at the inputs of the correlation function computer. The gains were adjusted to provide very nearly equal peak values for the auto-correlation functions of the two signal inputs.

4. The computation of the cross-correlation and the two auto-correlations was performed using a 100 second (computation time) averaging time. The individual correlation functions were recorded on the X-Y plotter as shown in Figure A-2. (The PAR correlation function computer was equipped with a time constant of 18.8 seconds, which required a minimum of 94 seconds averaging time for computing the correlation functions. The time delay,  $T$ , on the correlator, was set in accordance with the requirement,  $T \leq 25/F_{\max}$ , where  $F_{\max}$  was taken to be the upper cut-off frequency set on the filters, in order to avoid aliasing effects.)
5. The data signals were visually monitored on the monitor scope during computation so that any malfunctions of equipment or obvious anomalies in the data could be detected and corrected.

This procedure produced satisfactory and repeatable results provided that the starting time and stopping time of the computation always occurred at the same points of the data record. Since it was not always possible to start the computation exactly at the beginning of a data record, the starting time was set by starting at a fixed number of seconds after visual observation of the beginning of the data signal on the monitor scope. The stopping time was then determined by carefully timing the duration of the computation.

A limited number of computations were performed using different tape speeds for play back of the data and utilizing narrower frequency pass bands but no consistent effect of the variation of these parameters were observed. However, there was ample evidence observed during these computations to indicate that the recorded data had non-stationary characteristics.

### 3.3 EQUIPMENT USED

Various types of signal processing equipment were used at one time or another in performing the analog computations. However, the vast majority of the computations were performed with the equipment, set-up, and procedures as outlined above. In summary, the items of equipment used were as follows:

1. Ampex Model FR 1300 tape recorder with appropriate FM reproduce amplifiers.
2. Philbrick Model K2W operational amplifiers with variable gain feed back networks. (1 for each data channel.)
3. Spencer-Kennedy laboratories Model 308A variable electronic filters. (1 for each data channel.)
4. Princeton Applied Research Model 101 correlation function computer (time constant = 18.8 seconds).
5. Moseley Model 135 X-Y recorder.
6. Tektronix type 502A Dual-Beam Oscilloscope. (Normally used only for visual monitoring of data signals.)

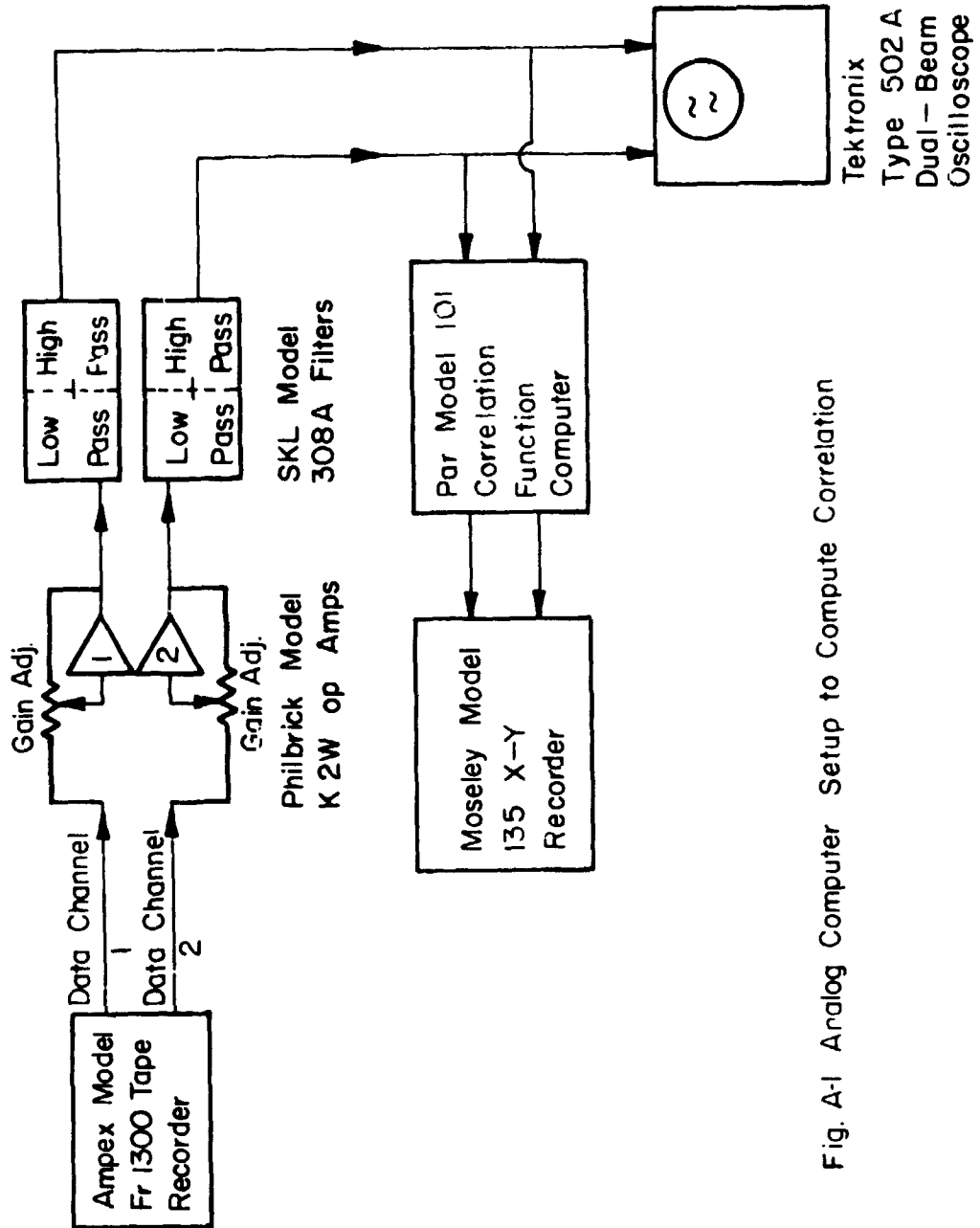


Fig. A-1 Analog Computer Setup to Compute Correlation

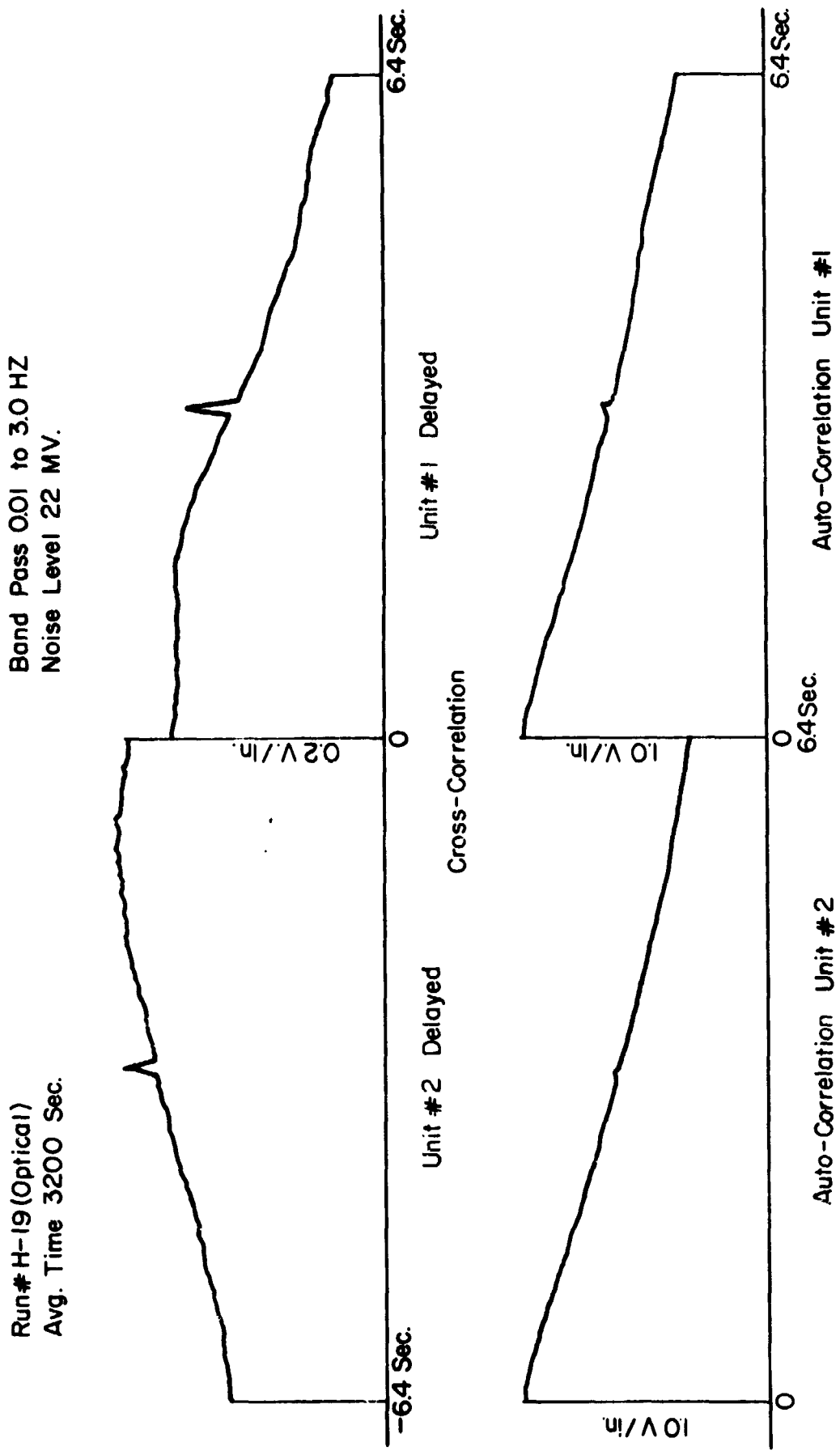


Fig. A-2 Typical Measured Cross and Auto Correlations

**SECTION IV.**  
**PRELIMINARY ANALYSIS OF CROSS BEAM DATA FROM THE**  
**GUN BARREL HILL SITE**

by  
 V. A. Sandborn  
 A. R. Bice  
 W. C. Cliff  
 B. C. Hablutzel

**4.1 SUMMARY**

Preliminary evaluation of cross beam data taken at the Gun Barrel Hill test site of ESSA is presented. The evaluation is made using the analog Princeton Time Correlator. A study of the frequency band width limitations of the Princeton Time Correlator is made. Based on the band width limitations, it is possible to demonstrate that nearly identical correlation is obtained for frequencies from .01 to 3.9 hertz. Difficulty is encountered in that maximums in the correlation curves do not occur at zero time lag for zero beam separations.

**4.2 INTRODUCTION**

The NASA cross beam system was set up at the Gun Barrel Hill meteorological test site of ESSA in June of 1968. A set of runs (No. 201, 202, 203 and 204) was recorded in June to check the equipment. Initial checks of these runs indicated the equipment was operational and no major problems had developed during the move from the Platteville meteorological test site. During July the cross beam electronics was installed in the ESSA field house, so the mobile unit could be returned to NASA. A set of cross beam measurements was made during August of zero separation beams at tower heights. Lack of a Princeton Time Correlator prevented an analog analysis of this data until recently. Of the measurements made, runs 209, 210 and 211 were sent to NASA-MSEC for evaluation and are not available at CSU for analog analysis. Space-time correlations of runs No. 204 through 208, and 212 through 215 are included in this Memo. These correlations are preliminary in that they are single samples without repeat runs. Data from a low level run (No. BC 100) is also analyzed with the present correlations. This BC100 run is a preliminary check out run for the evaluation of turbulence with hot wire anemometers and the cross beam system.

### 4.3 EXPERIMENTAL MEASUREMENTS

The cross beam experiments were made with the NASA optical units, ref. 1. The ESSA Gun Barrel Hill test site was employed for the present tests. Figure 1 a) shows the setup of the two optical units with respect to the meteorological tower. Figure 1 b) is an elevation drawing of the tower and the two optical units. For test runs 204 through 215, reported herein, a climet cup anemometer and wind direction unit was used to indicate winds at tower heights. All data was recorded on a 14 channel tape recorder at 4.76 cm per sec. The data is played back for analog analysis at 152.4 cm per sec. The output of the wind instruments and the optical units were also recorded on chart recorders.

### 4.4 ANALYSIS OF MEASUREMENTS

Time lag correlations for the two optical signals and their cross product have been measured. These runs were also supplied to NASA-MSFC in digital form from the ESSA data logger. Specific information about the runs is listed in Table I.

The chart recordings of wind speed and direction for the runs analyzed are shown in figure 2. The optical units' light fluctuations for the runs are shown in figure 3. These two sets of figures are reprints of the original data and have not been redrawn. In some cases it was necessary to divide the charts in sections in order to get a complete run on the page. These charts should be used instead of the approximate wind speeds and direction given in Table I for accurate evaluation of the data.

The cross-and auto- correlations for the two optical units were made with the Princeton Time Correlator. Figure 4 is the cross-correlation of an 0.02 Hz sine wave calibration signal that was recorded just before run no. 204. This calibration signal was treated just as the cross-correlation signals are obtained. The right side of the signal is the correlation between channels No. 1 delayed with respect to channel No. 5 of the tape recorder. This arrangement is identical to delaying the output of optical unit No. 1 with respect to optical unit No. 2 for

REPRODUCIBILITY OF THE  
ORIGINAL PAGE IS POOR

TABLE 1 CROSS-BEAM RUNS AT GUN BARREL HILL

Run No.	Sky Conditions	Wind Information	Beam Separation	Approximate Altitude of Sep.	Unit #1		Unit #2		Remarks
					Pointing Angles	Pointing Angles	Pointing Angles	Pointing Angles	
204	clear "After Front"	From East 2 to 3 m/sec	168.4 meters	48.2 meters	Az 355°55' El. 68°8.6'	Az. 208°59.5' El. 4°58.5'	sun in unit #2 at 10:30 a.m., Gain #2 decreased at 11:36 a.m.		
205	scattered clouds	From WSW 11m/sec	0	49 meters	Ax. 283°27' El. 36°19'	Az. 136°51.5' El. 24°16'	Attenuated signals chan. #7-AC unit #1 chan. #11-AC unit #2		
206	clear	From NNE 3.5m/sec	0	49 meters	Az. 283°27' El. 36°19'	Az. 136°51.5' El. 24°16'	two parts on tape as original start was aborted.		
207	clear over- head clouds on Horiz.	From NE 3m/sec	0	49 meters	Az. 283°27' El. 36°19'	Az. 136°51.5' El. 24°16'	Large light signals		
208	clear	From NE 3 to 4m/sec	0	49 meters	A. 283°27' El. 36°19'	Ax. 136°51.5' El. 24°16'	Wind shifted to SSE at end of run		
212	clear	From South variable 2m/sec	0	49 meters	Az. 283°27' El. 36°19'	Az. 136°51.5' El. 24°16'	Wind shifting from south to east		
213	clear overhead	From ENE 4m/sec	0	49 meters	Az. 283°27' El. 36°19'	Az. 136°51.5' El. 24°16'			
214	clear overhead	From south 5m/sec	0	49 meters	Az. 283°27' El. 36°19'	Az. 136°51.5' El. 24°16'			
215	clear	From ENE 1.5m/sec	0	49 meters	Az. 283°27' El. 36°19'	Az. 136°51.5' El. 24°16'	Sum giving problems for first 1/2 hour		

the light fluctuation signals. Figure 4 is a check of the accuracy of the speed of the two tape recorders used for recording and playing back the signal. It also demonstrates that no interchannel displacement errors are introduced in the record-playback operations. The slight mismatch of the two sides of the correlation curve at zero time lag is a characteristic of the time correlator. For all the data presented, the right-hand side of the correlation curve is consistent between the auto- and cross-correlations. The left-hand side of the cross-correlation curves should be scaled up to be equivalent to those of the right side.

Figures 5 show the measured cross- and auto-correlations for the runs listed in Table I. In several cases more than one curve of the correlations for a particular run is given. For these cases of more than one curve the time lag scale has usually been varied. For run 206 (figures 5 c-1 and 5 c-2) the correlation was repeated to determine reproducibility of the correlation measurement. Figure 6 is a replot of these two measurements. The results of figure 6 are that the correlation curves are uncertain within approximately  $\pm 0.01$  in the measured correlation. This uncertainty is not unreasonable within the accuracy of the correlator and the sampling time.

All plots shown in figure 5 were time averaged for 88 seconds in the Princeton Time Correlator. Since the signals were played back at a speed 32 times greater than recorded, the 88 seconds corresponds to a time average of 46.9 minutes in real time. Details of the time averaging of the correlator have not been specifically evaluated, so the 88 seconds is an approximation. A time count was recorded on channel No. 14 of each tape so the correlations are started at a specific time and ended at the predetermined 88 seconds. This insures that the cross- and auto-correlations correspond to the same time period of the recording.

Figure 7 is a comparison of cross-correlation curves obtained for different time delays. The original curves are presented in figures 5 b-1) through 5 b-5). The set of data was taken to determine the effect of frequency limitations imposed by the Princeton Time Correlator. As pointed out in a recent IIT monthly report, the band width of the correlator is limited by the delay time selected. The frequency range is given as

$$\frac{1}{\Delta\tau} < f < \frac{25}{\Delta\tau} \quad (1)$$

where  $\Delta\tau$  is the maximum delay time of a given correlation curve. For all time delays, employed the first peak was determined. The variation in magnitude between the different curves is no greater than the repeatability results obtained in figure 6. Adequate evaluation has not been completed to conclude whether the frequency restrictions given by equation (1) are valid. Figure 7 suggests that equation (1) is not a major restriction on the evaluations of cross correlations. The second possibility is that there is equal contribution to the correlation from all the frequency bands indicated on figure 7. Further evaluation of the band limited contributions to the cross-correlations is required.

The present analysis of zero beam separation correlations fails to produce a maximum in the correlation at zero time delay. The maximum in the correlation varies from side to side of the time delay scale. For example, the maximum correlation for run No. 205 occurs when unit No.1 is delayed with respect to unit No. 2. For run No. 206 the maximum correlation occurs when unit No.2 is delayed with respect to unit No. 1. These results are taken to indicate that the shift of the maximum correlation away from zero time lag is not caused by electronic problems within the units.

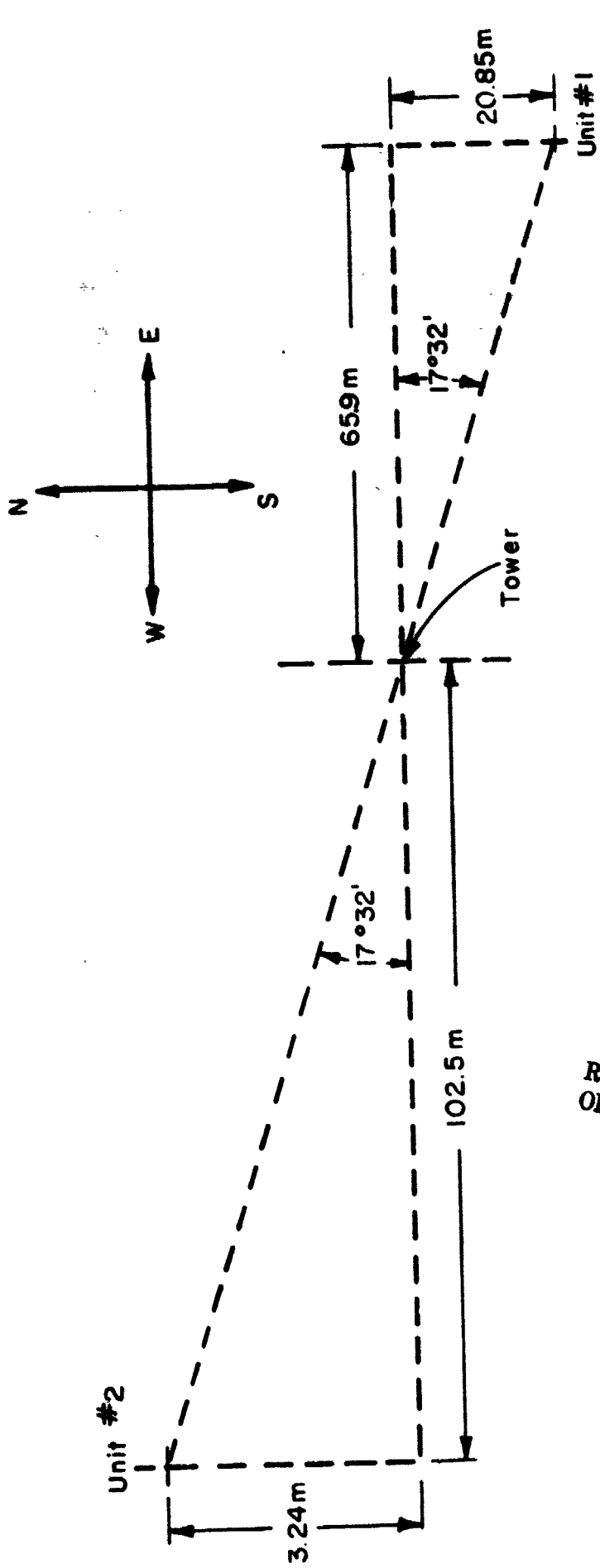
A very recent set of zero beam data was taken for the first level of the tower. This run was a preliminary set of hot wire and cross-beam data. The low level crossing of the beams has been evaluated and is shown in figure 8. The run, which is noted as run BC 100, was approximately 6 hours in length. The first two 46.9 minute sections of the data are evaluated in figure 8. The first set gives a maximum correlation at or near zero time lag. The correlation curve is "skewed" to the left side. Data on the wind velocity is not yet available to fully evaluate possible scales from this data. It appears that the correlation indicates scales much larger than are expected. The broad correlation curve may represent a smearing effect due to the extreme low level intersection.

#### 4.5 CONCLUDING REMARKS

The present memo gives a review of correlations measured for the initial runs made at the Gun Barrel Hill test site. The major problem is that the zero beam results do not produce maximum correlations at zero time lag. Some indication of maximums at zero time lag is observed for low level correlations.

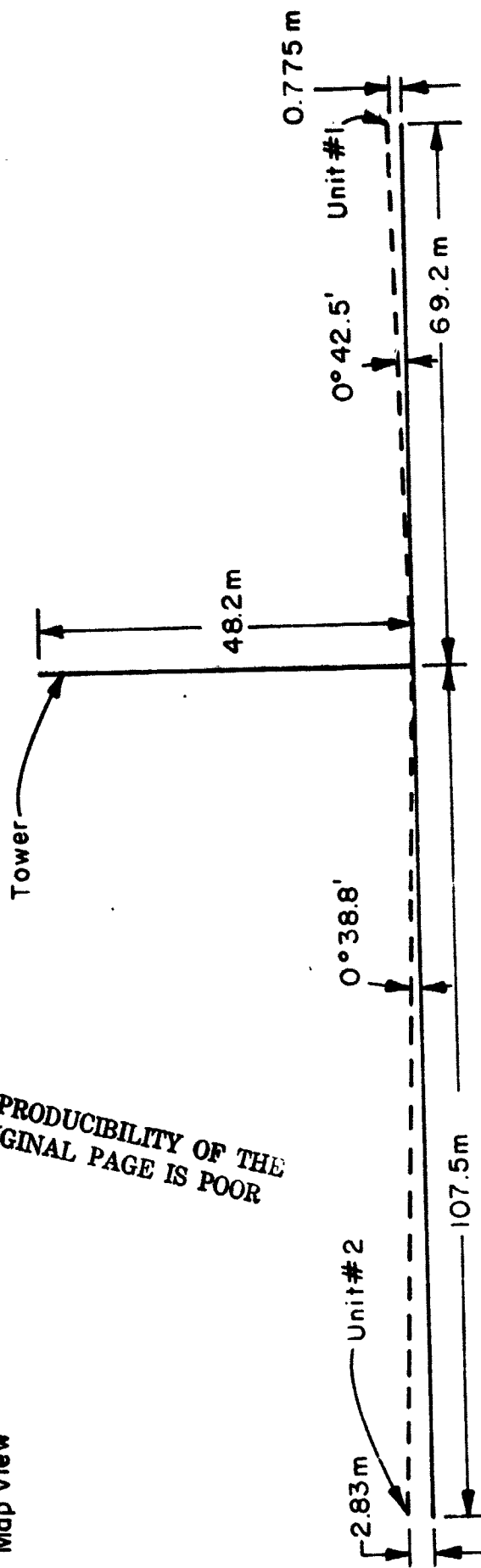
#### 4.6 REFERENCES

1. Montgomery, A. J., Remote Sensing of Winds and Atmospheric Turbulence by Cross-Correlation of Passive Optical Signals. Presented to the National Academy of Science - Committee for Atmospheric Sciences Panel on Remote Atmospheric Probing. Chicago, May 17, 1968.



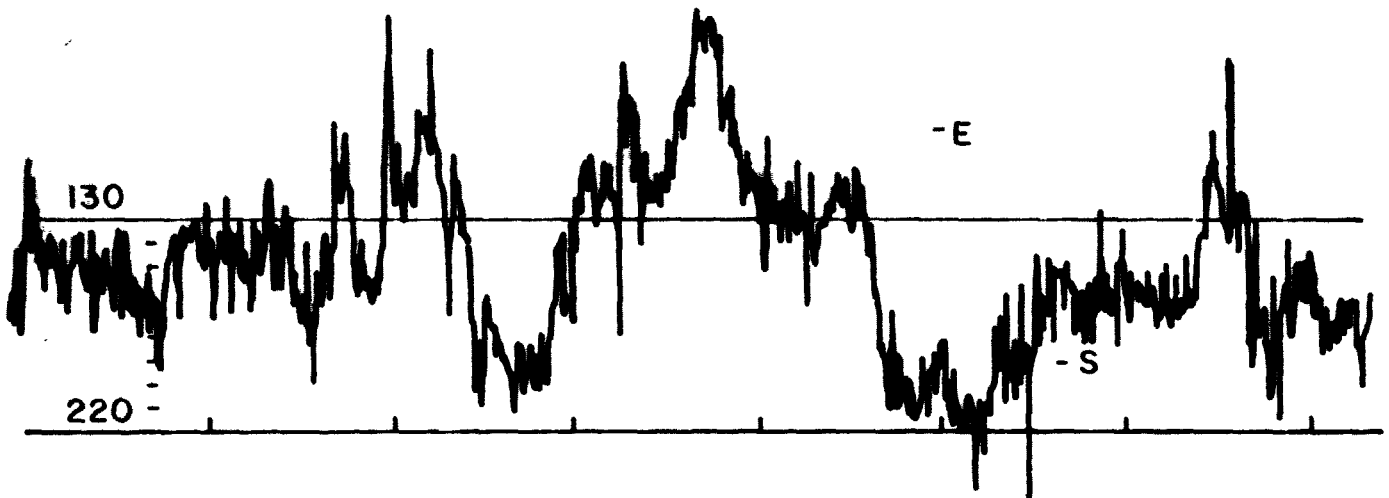
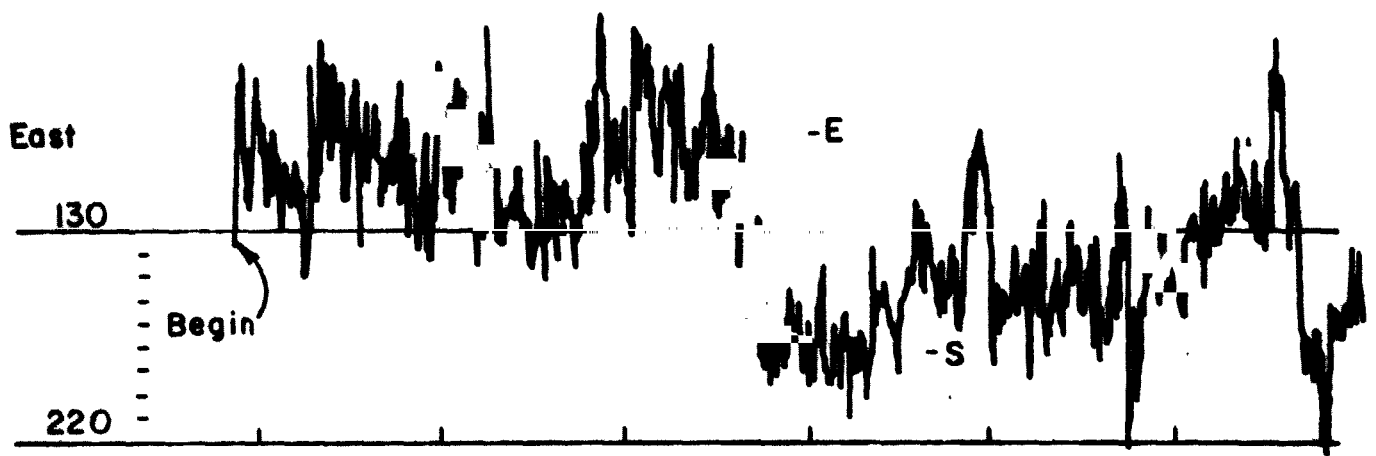
(a.) Map View

REPRODUCIBILITY OF THE ORIGINAL PAGE IS POOR

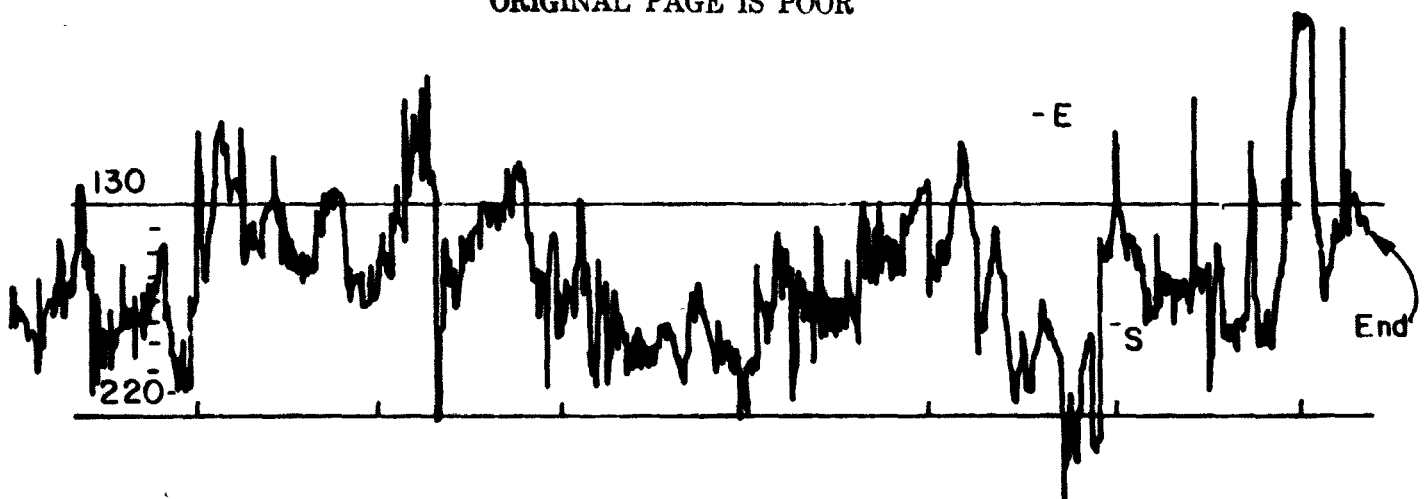


(b.) Elevation

Figure 1. Cun Barrel Test Site

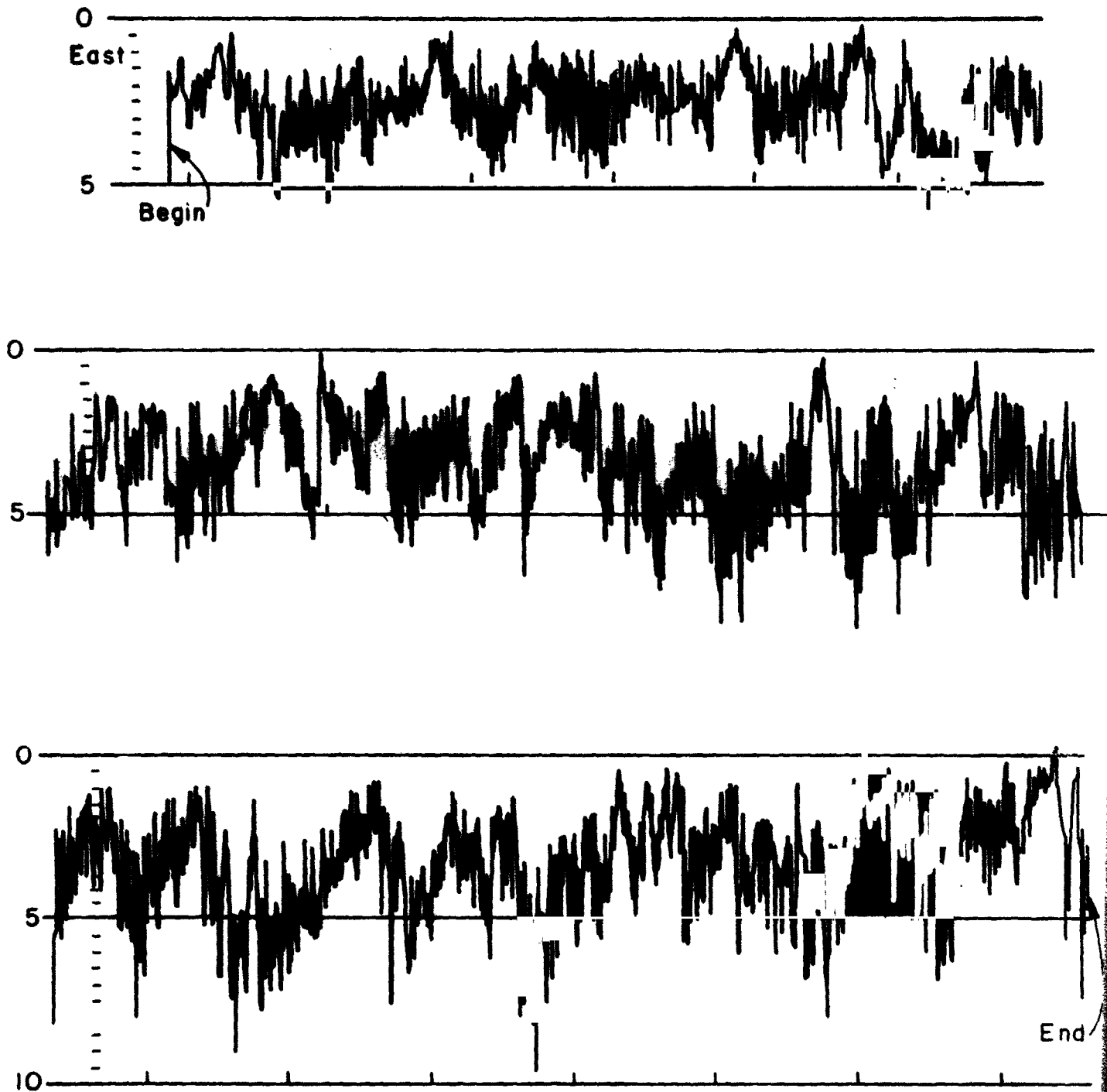


REPRODUCIBILITY OF THE ORIGINAL PAGE IS POOR



a-1) Run 204 - Direction

Figure 2. Time Variation of Wind Speed and Direction



a-2) Run 204 - Speed

Figure 2. Continued

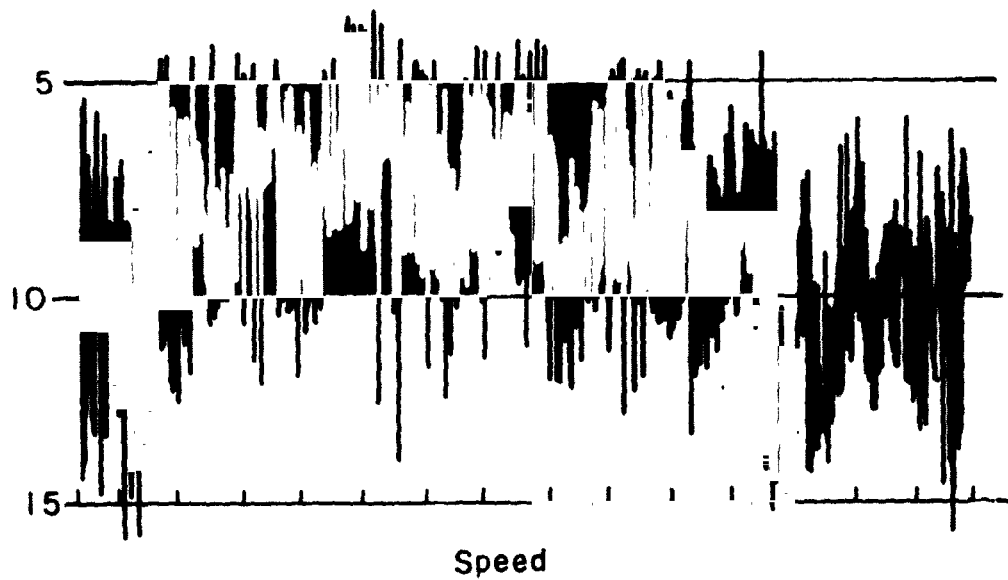
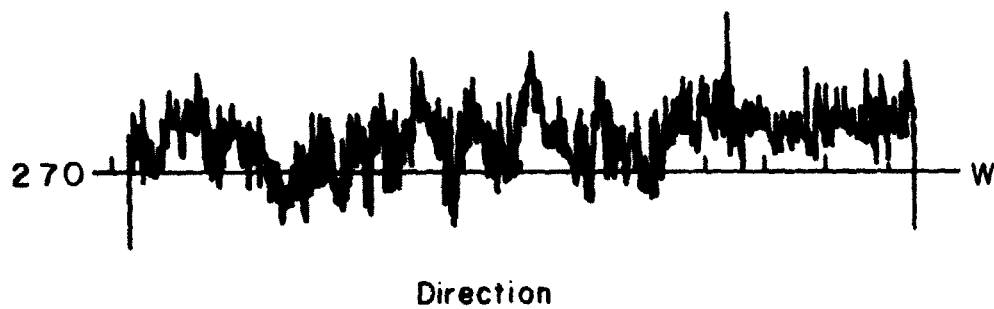
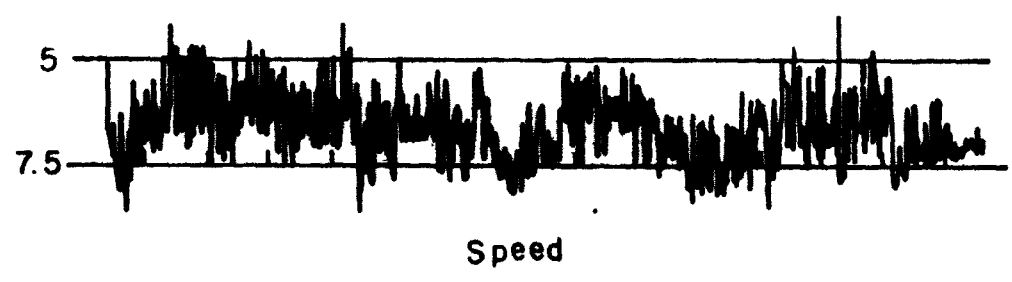
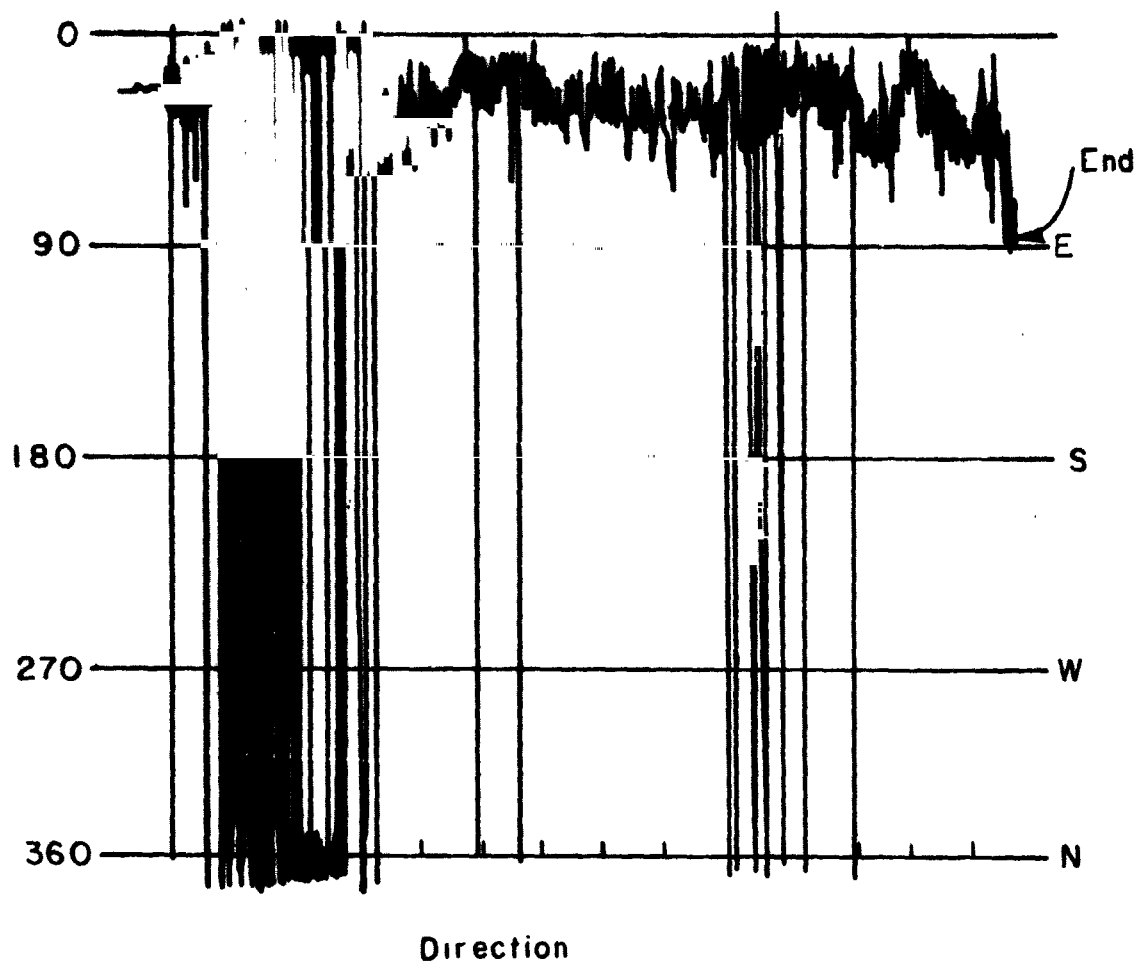


Figure 2. Continued

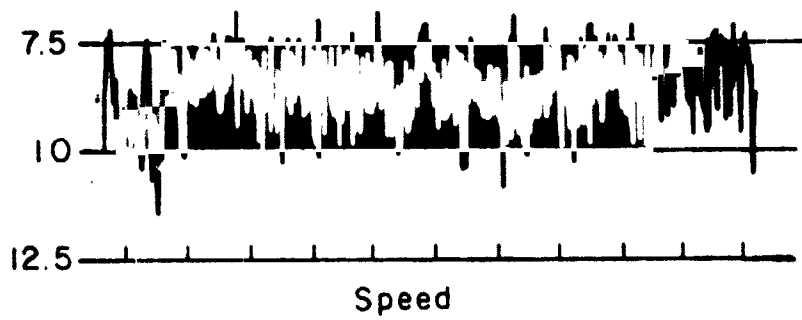
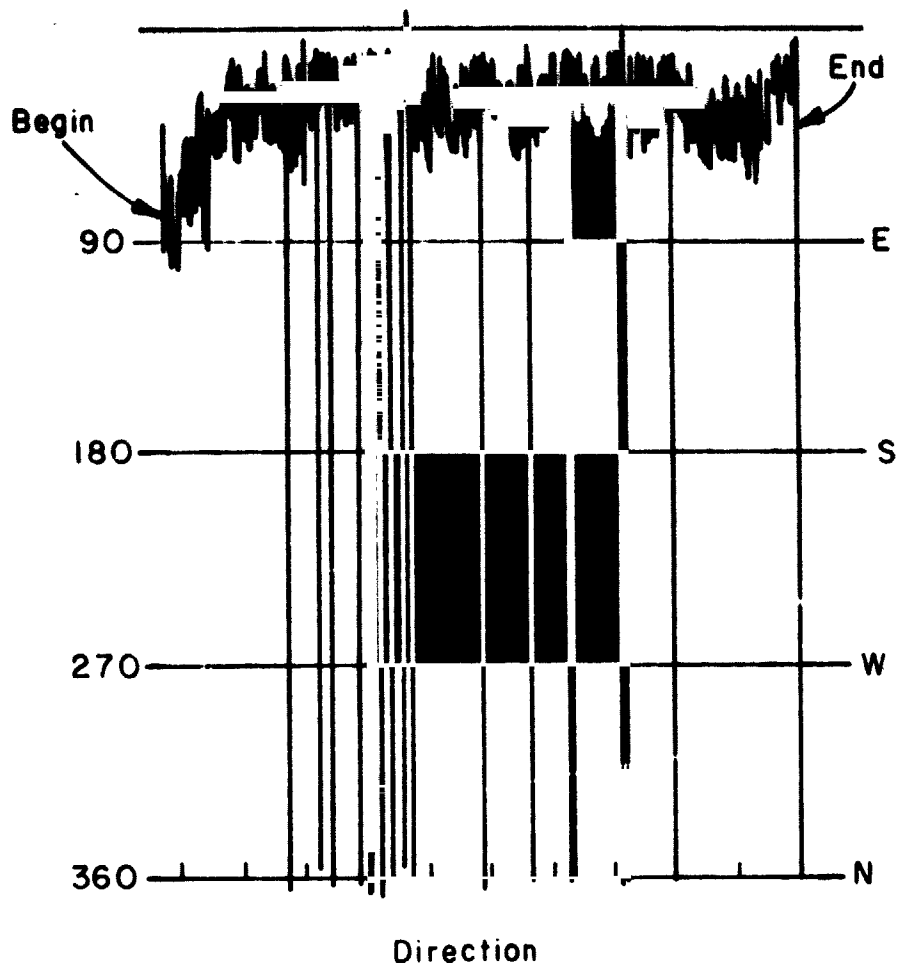
b) Run 205

REPRODUCIBILITY OF THE  
ORIGINAL PAGE IS POOR



c) Run 206

Figure 2. Continued



d) Run 207

Figure 2. Continued

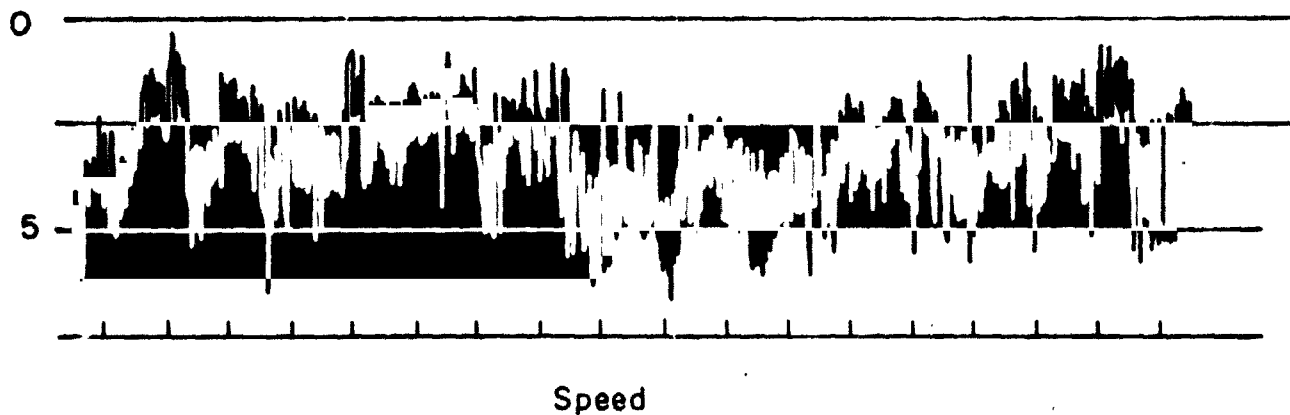
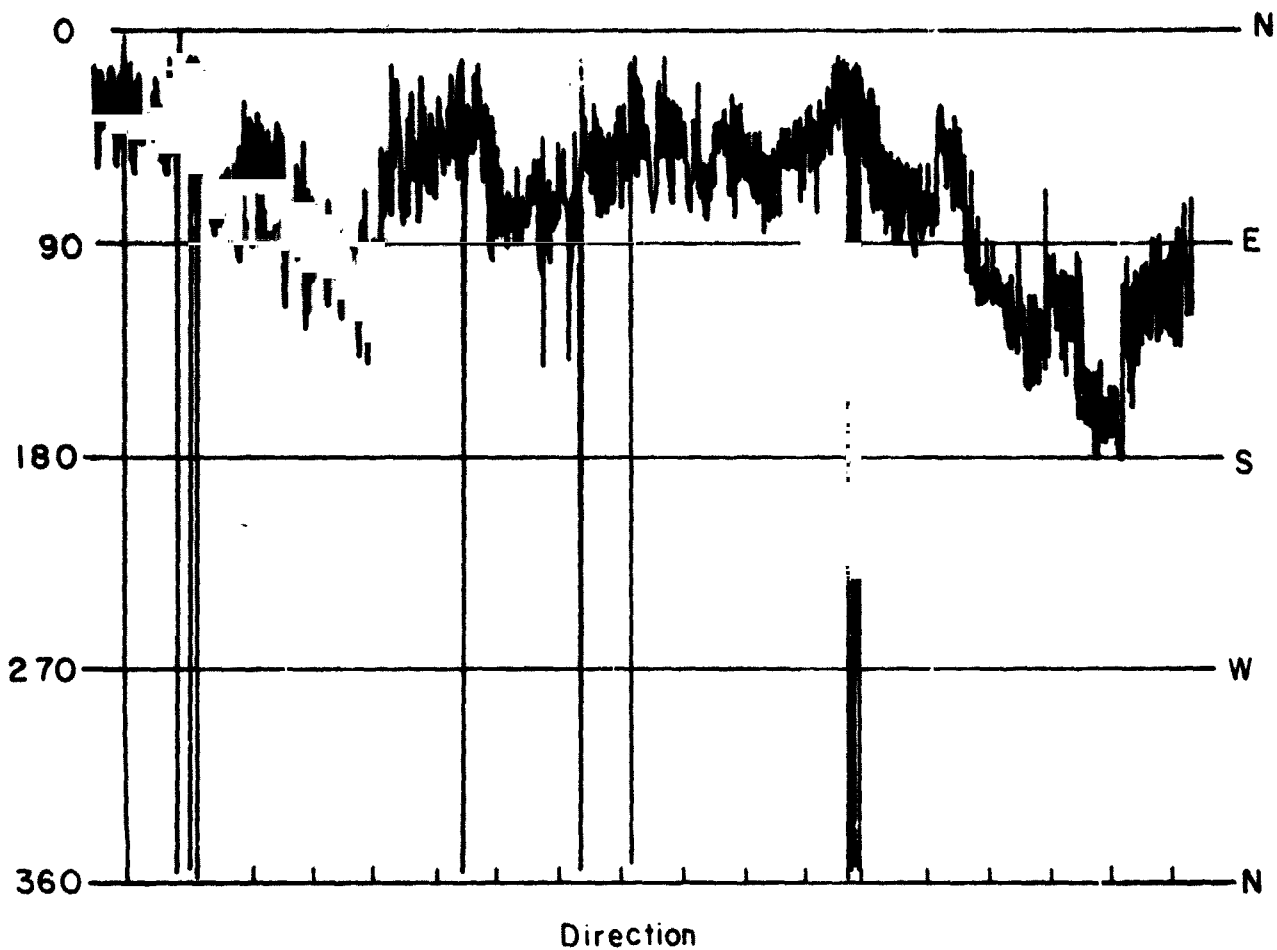
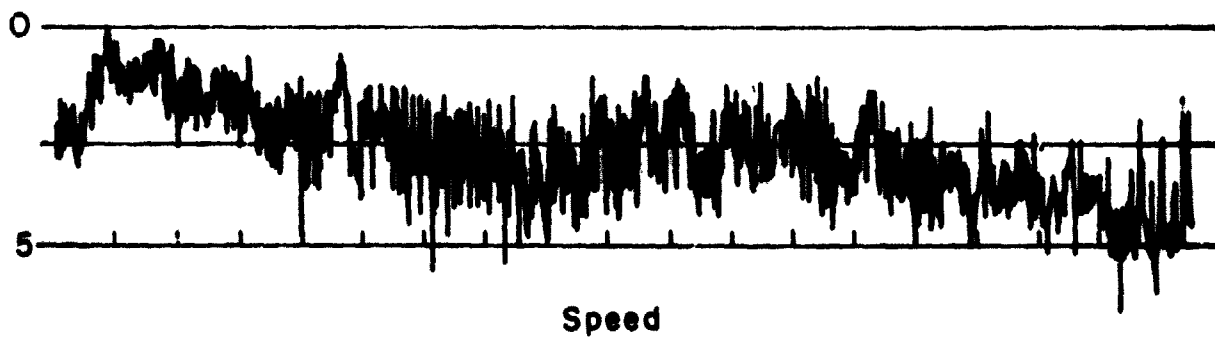
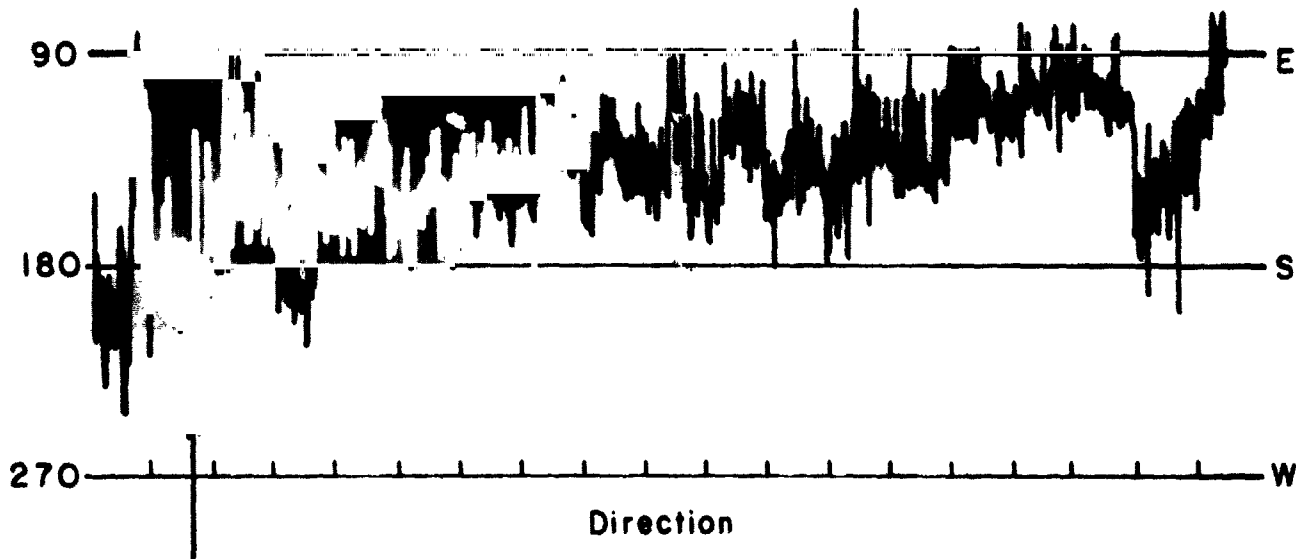


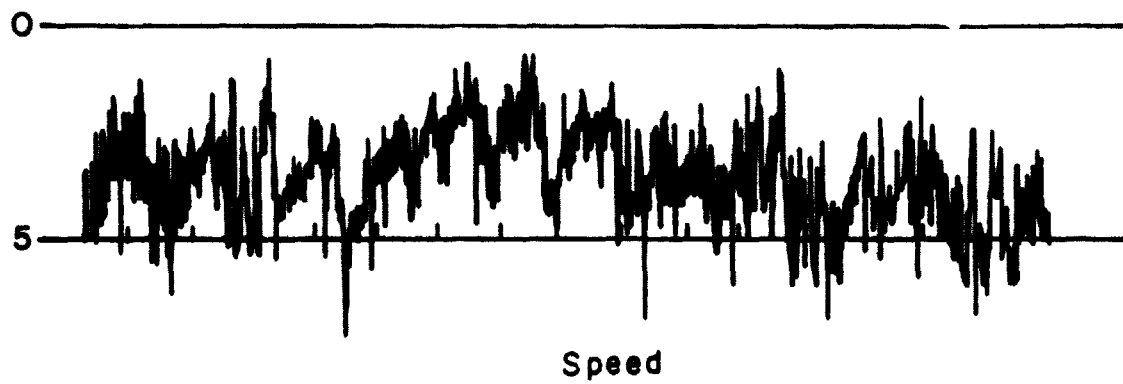
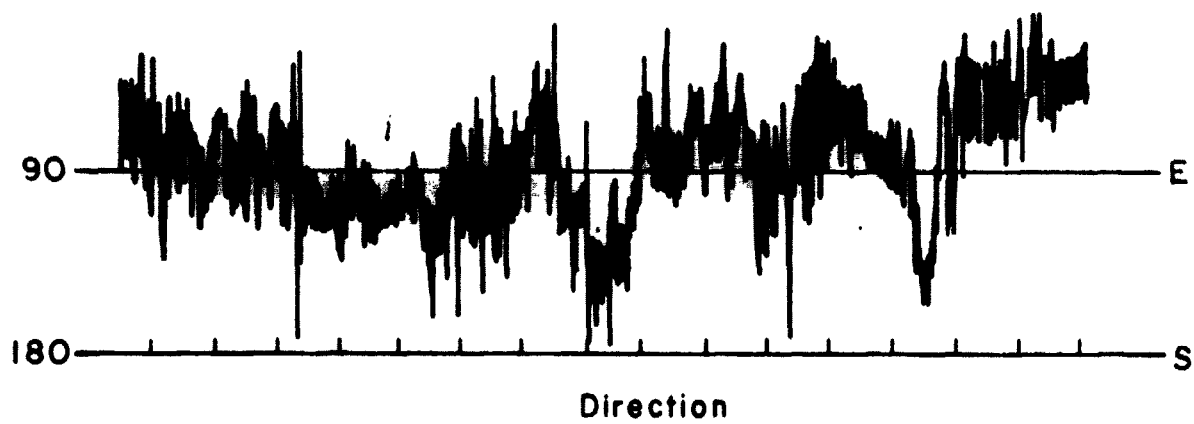
Figure 2. Continued

e) Run 208



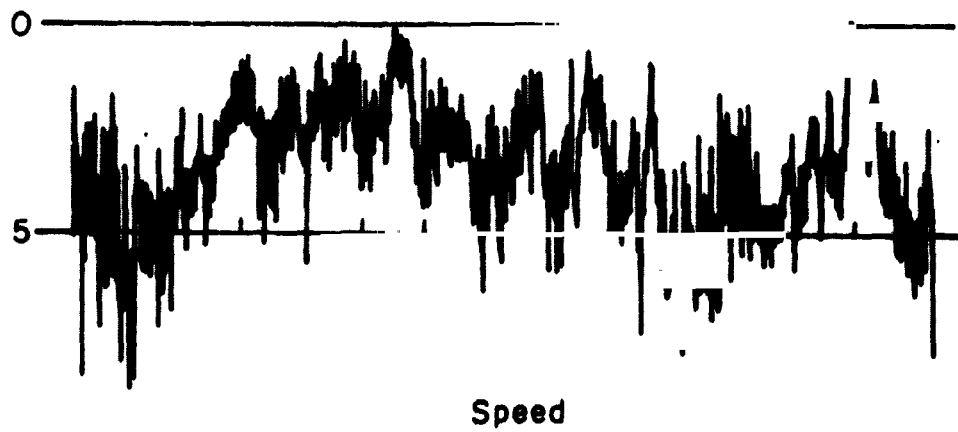
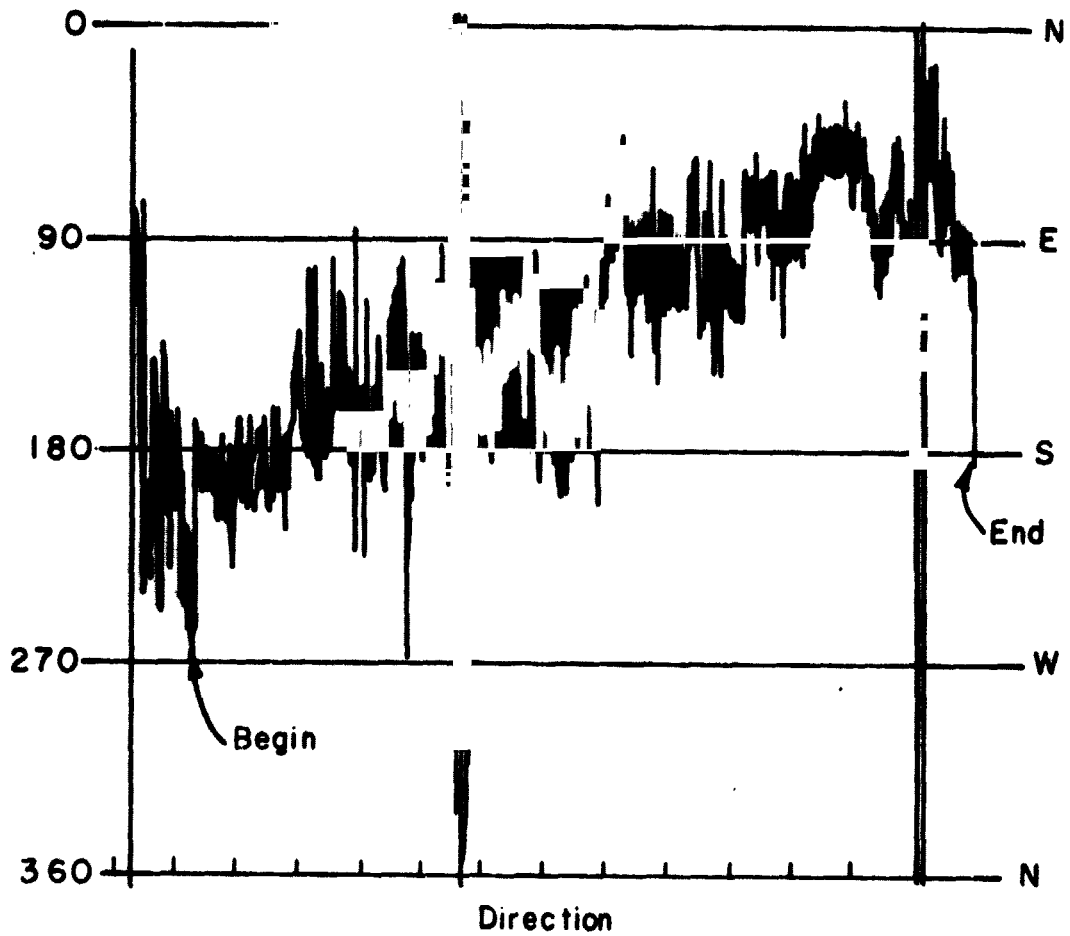
f) Run 212

Figure 2. Continued



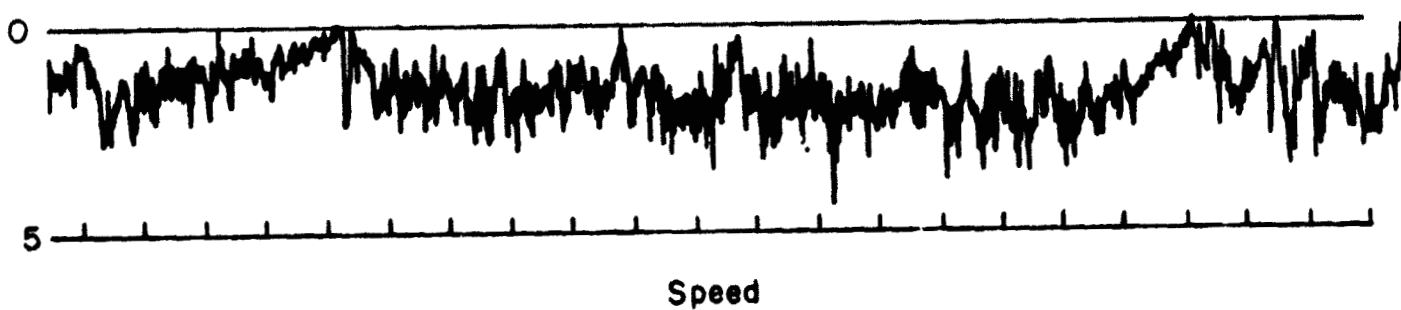
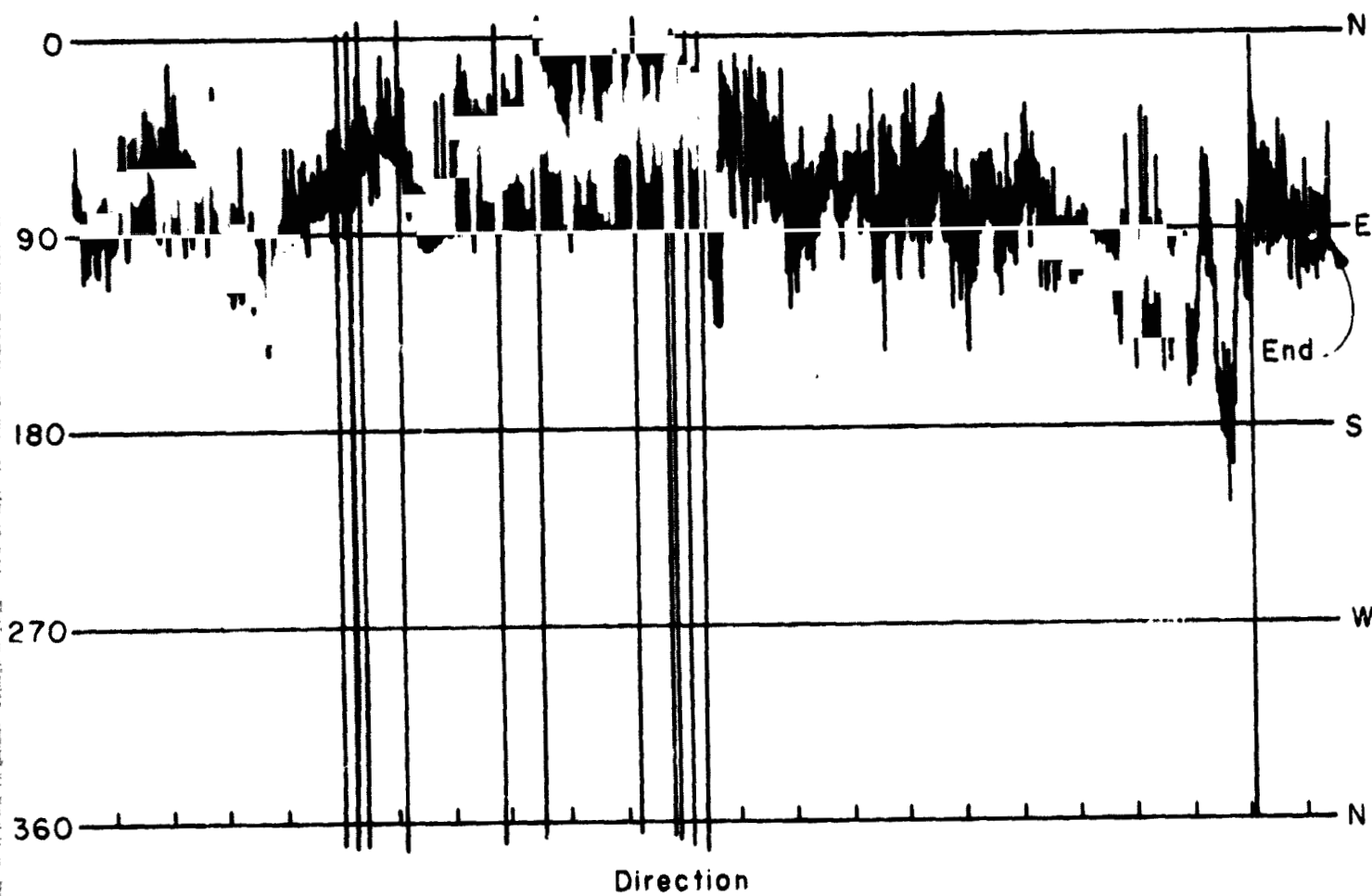
g) Run 213

Figure 2. Continued



h) Run 214

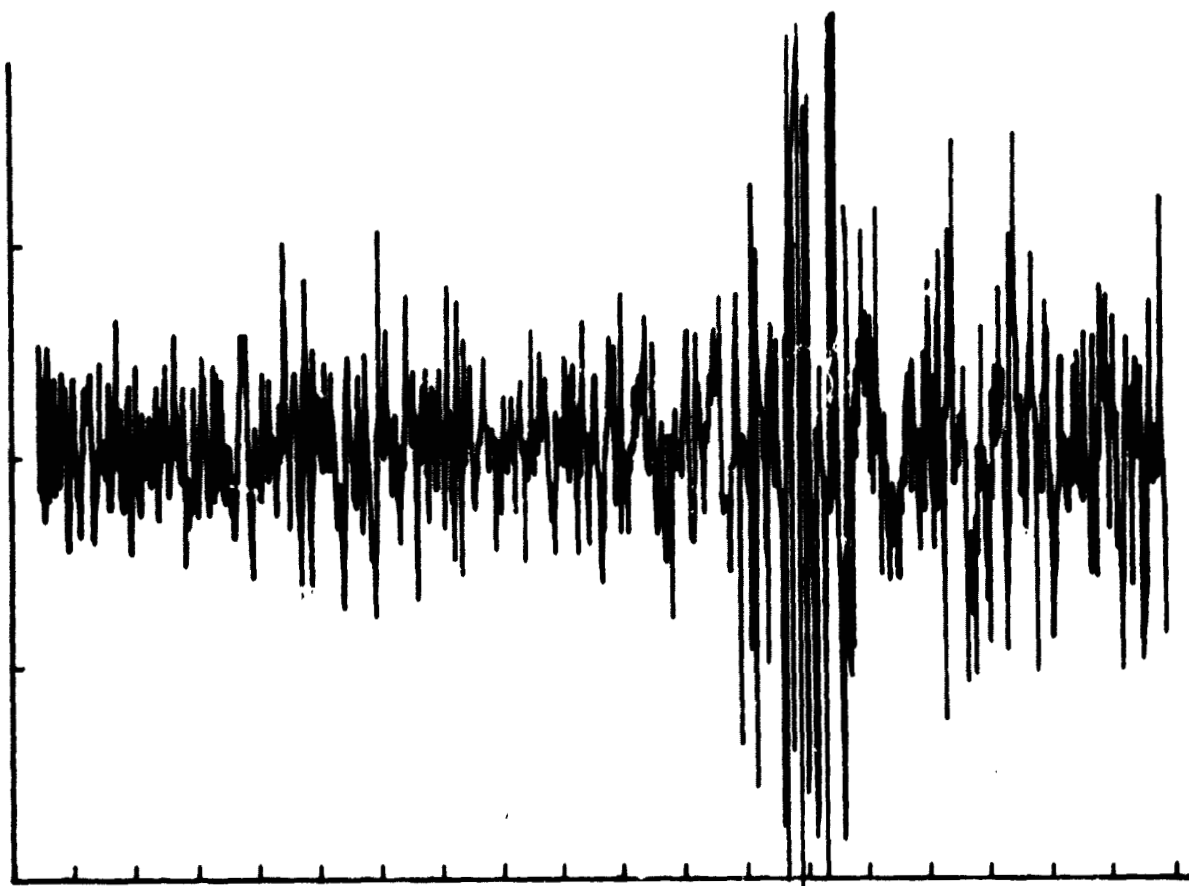
Figure 2. Continued



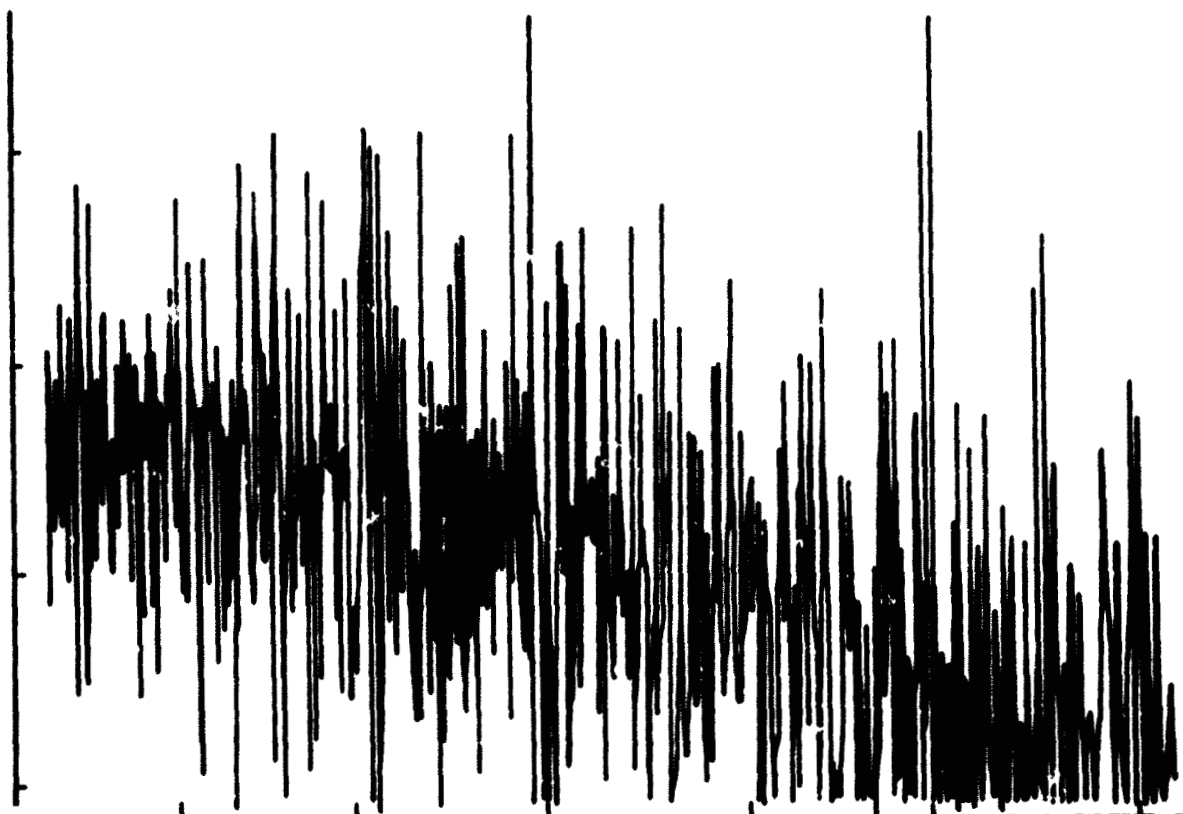
1) Run 215

Figure 2. Concluded

REPRODUCIBILITY OF THE ORIGINAL PAGE IS POOR



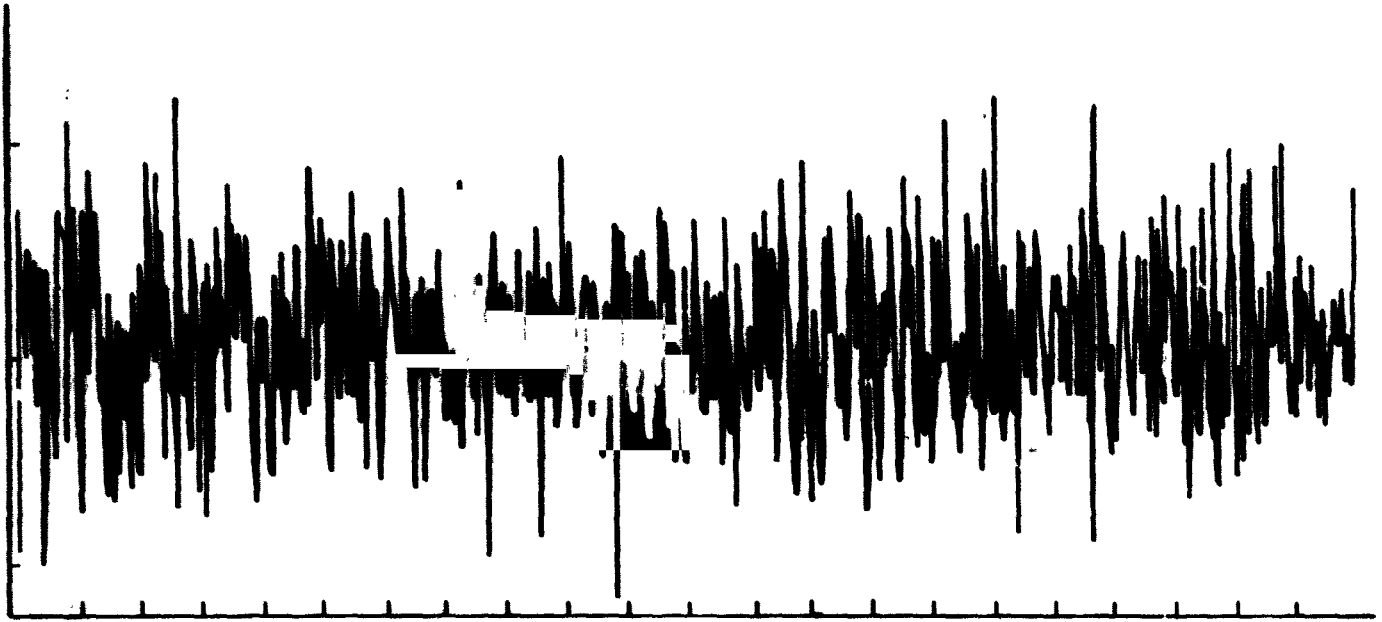
Unit 1



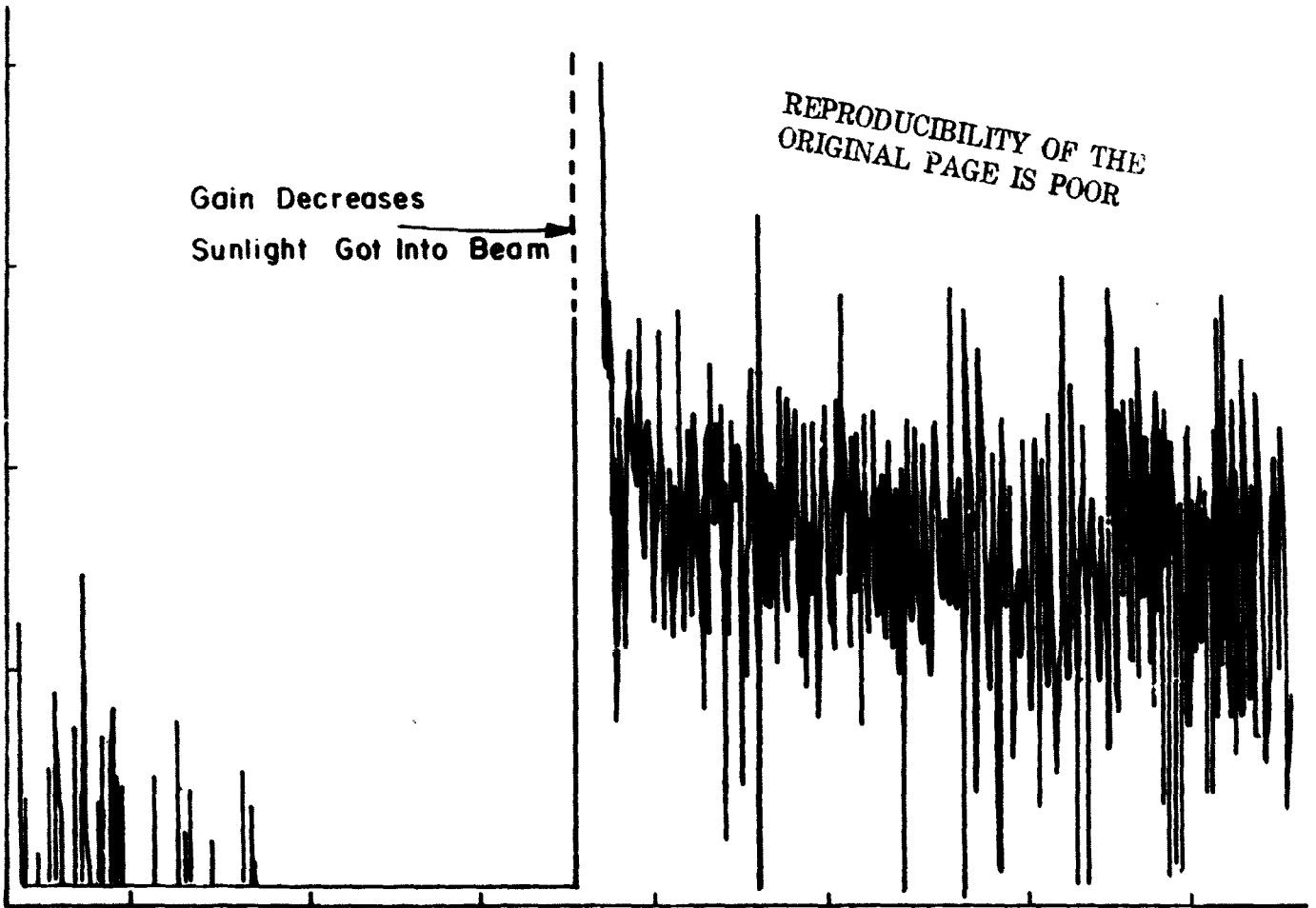
Unit 2

a-1) Run 204

Figure 3. Light Fluctuations 64



Unit 1



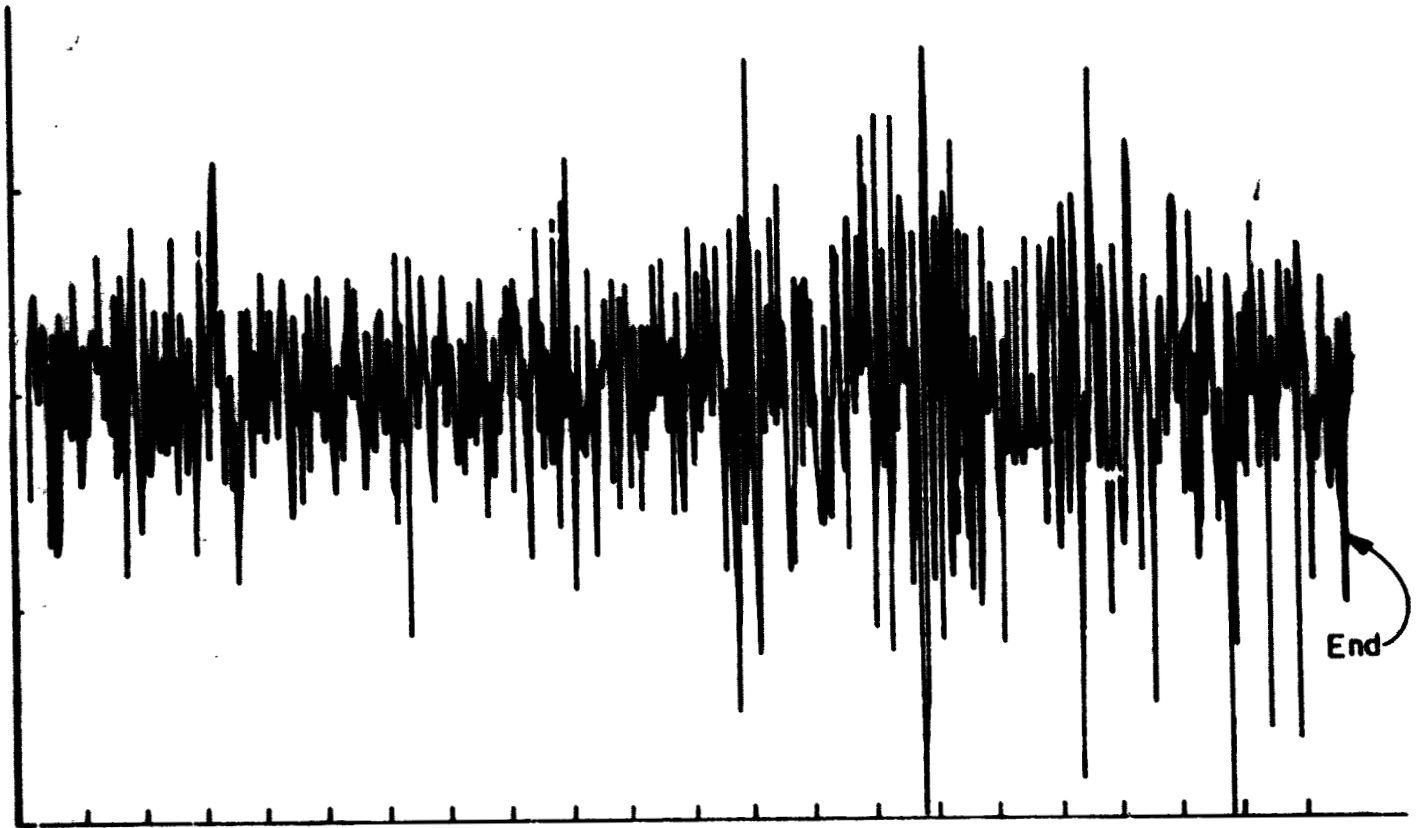
Gain Decreases  
 Sunlight Got Into Beam

REPRODUCIBILITY OF THE ORIGINAL PAGE IS POOR

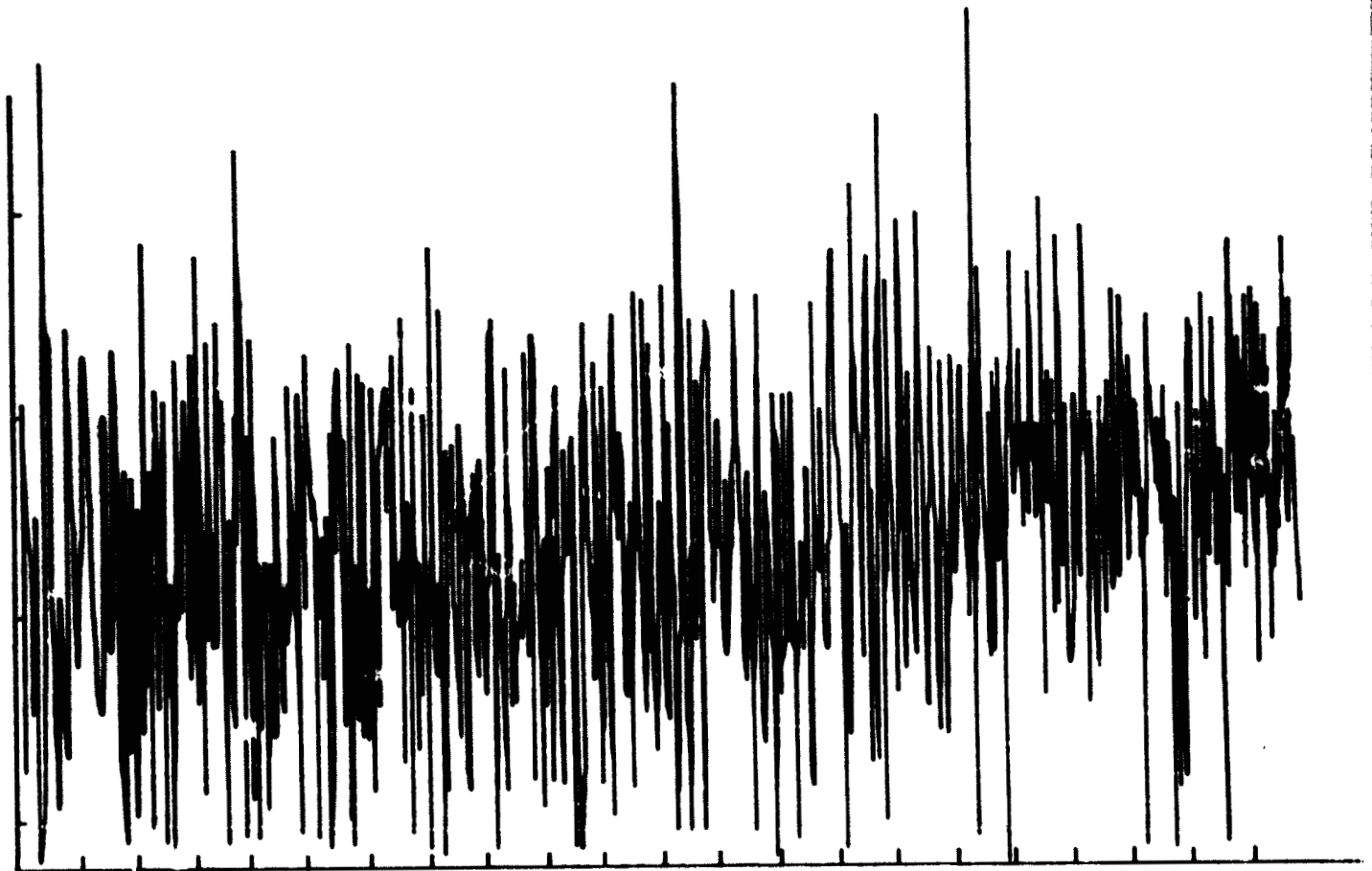
Unit 2

a-2) Run 204

Figure 3. Continued

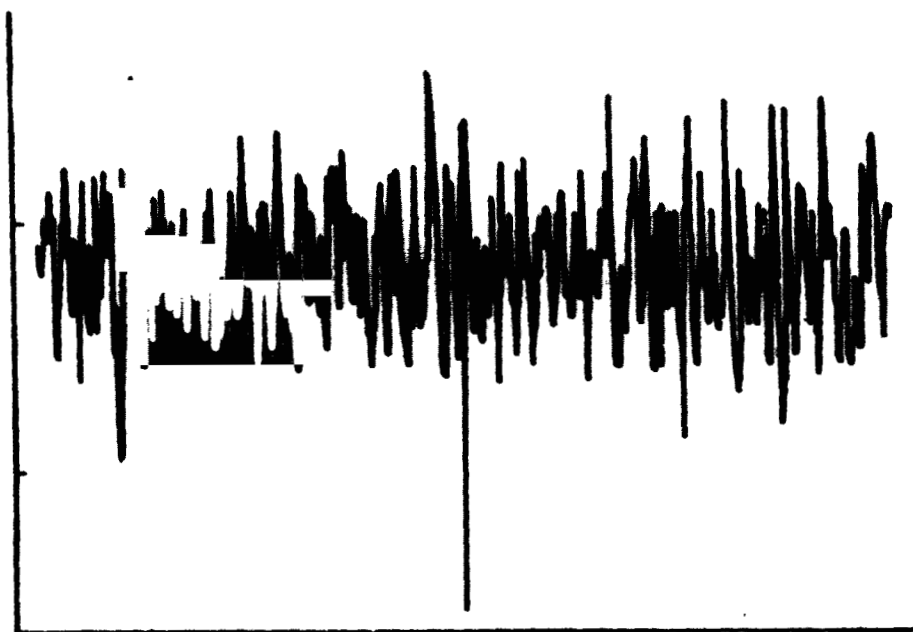


Unit 1

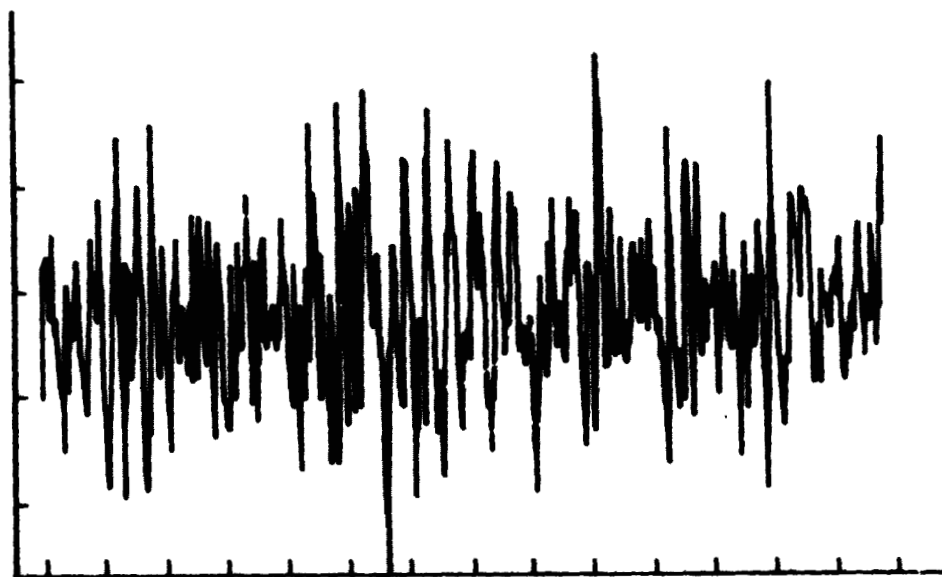


Unit 2  
a-3) Run 204

Figure 3. Continued



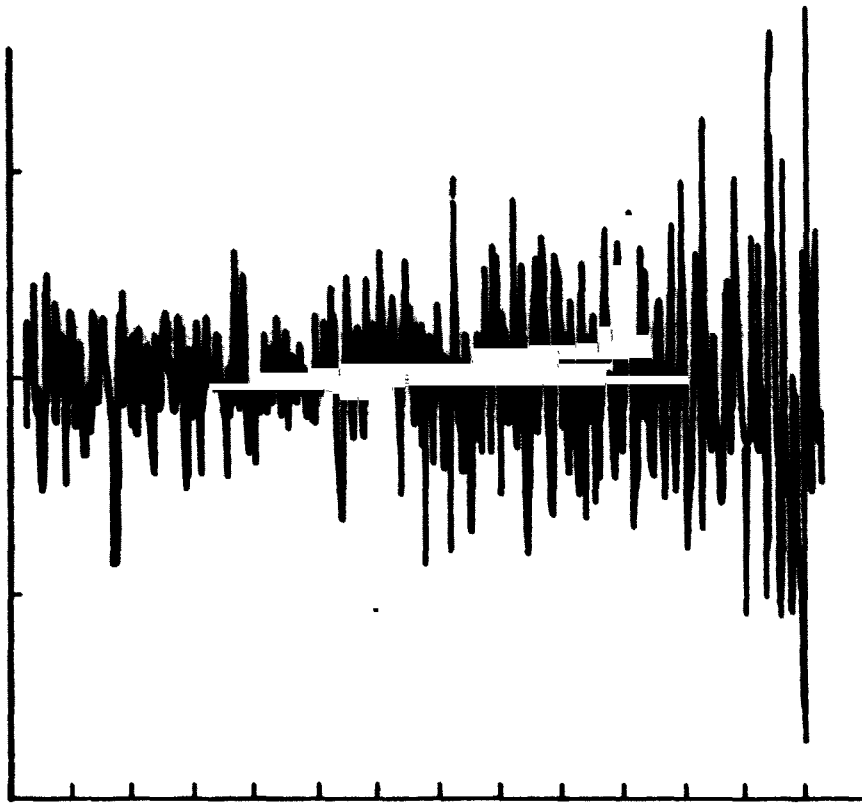
Unit 1



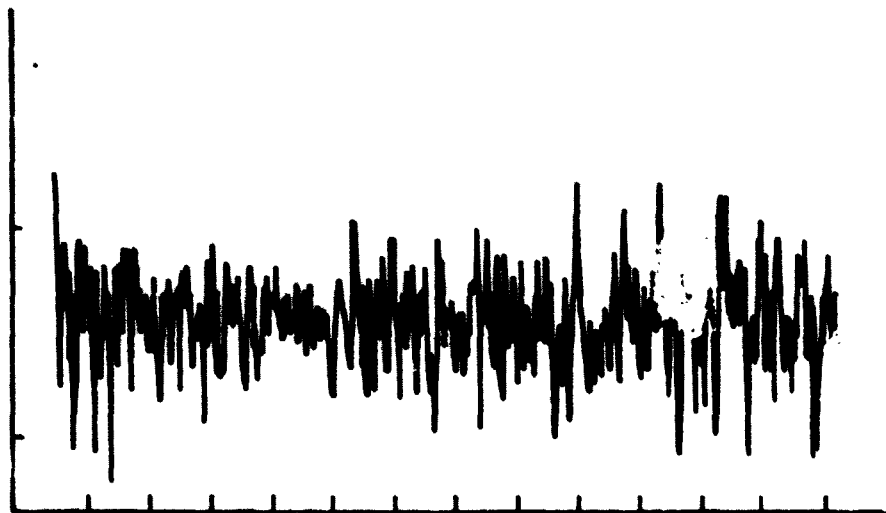
Unit 2

b) Run 205

Figure 3. Continued



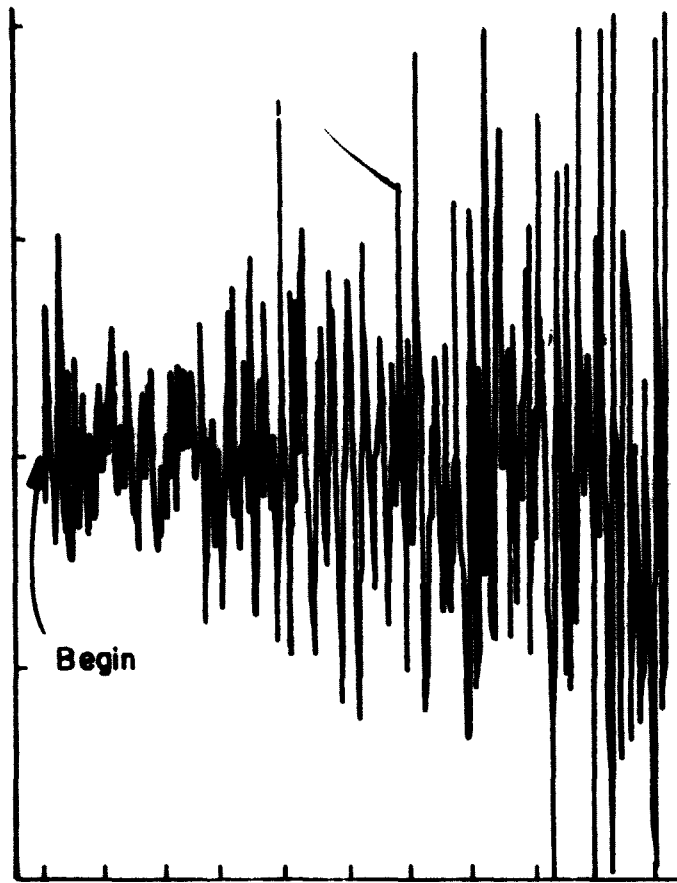
Unit 1



Unit 2

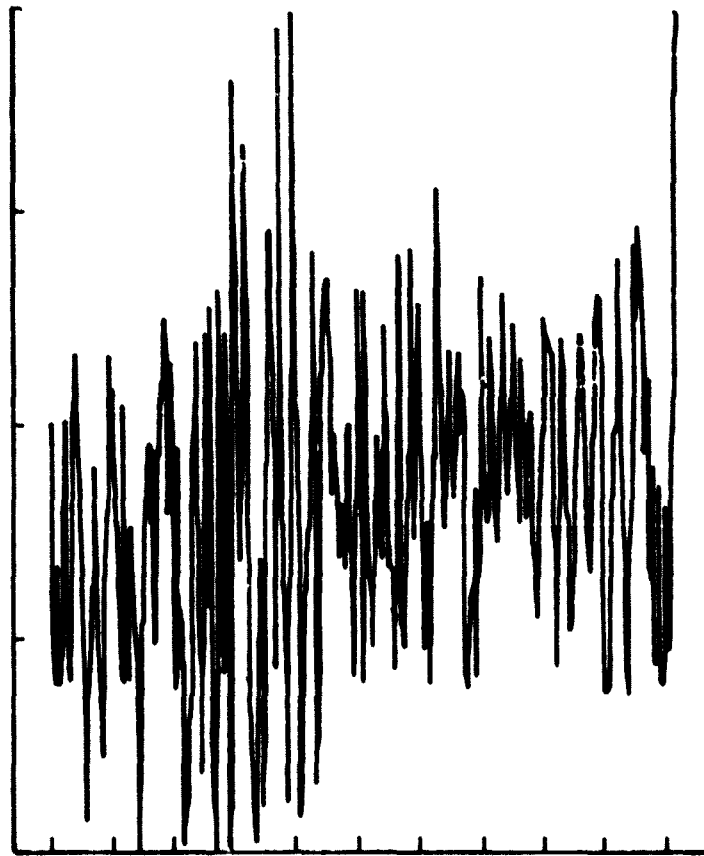
c) Run 206

Figure 3. Continued



Begin

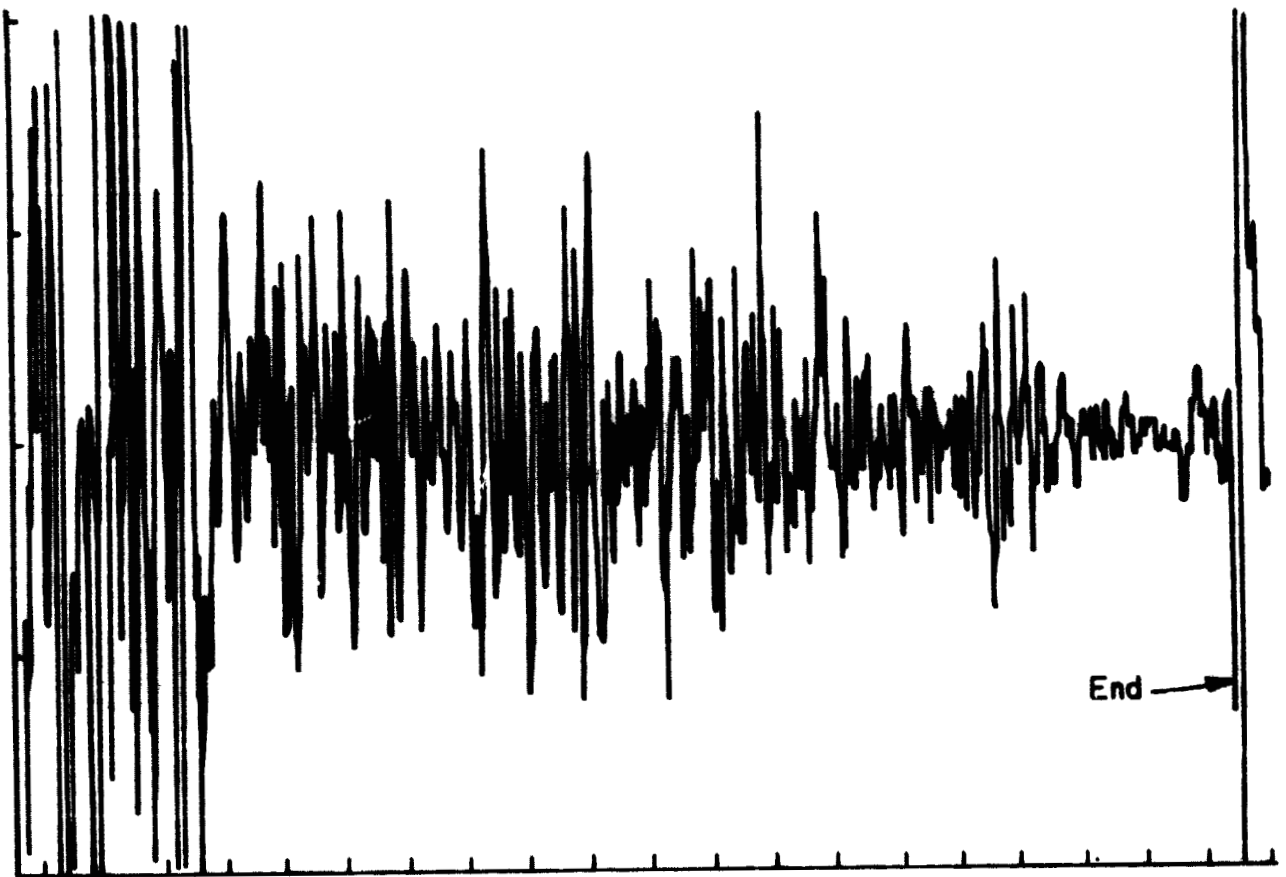
Unit 1



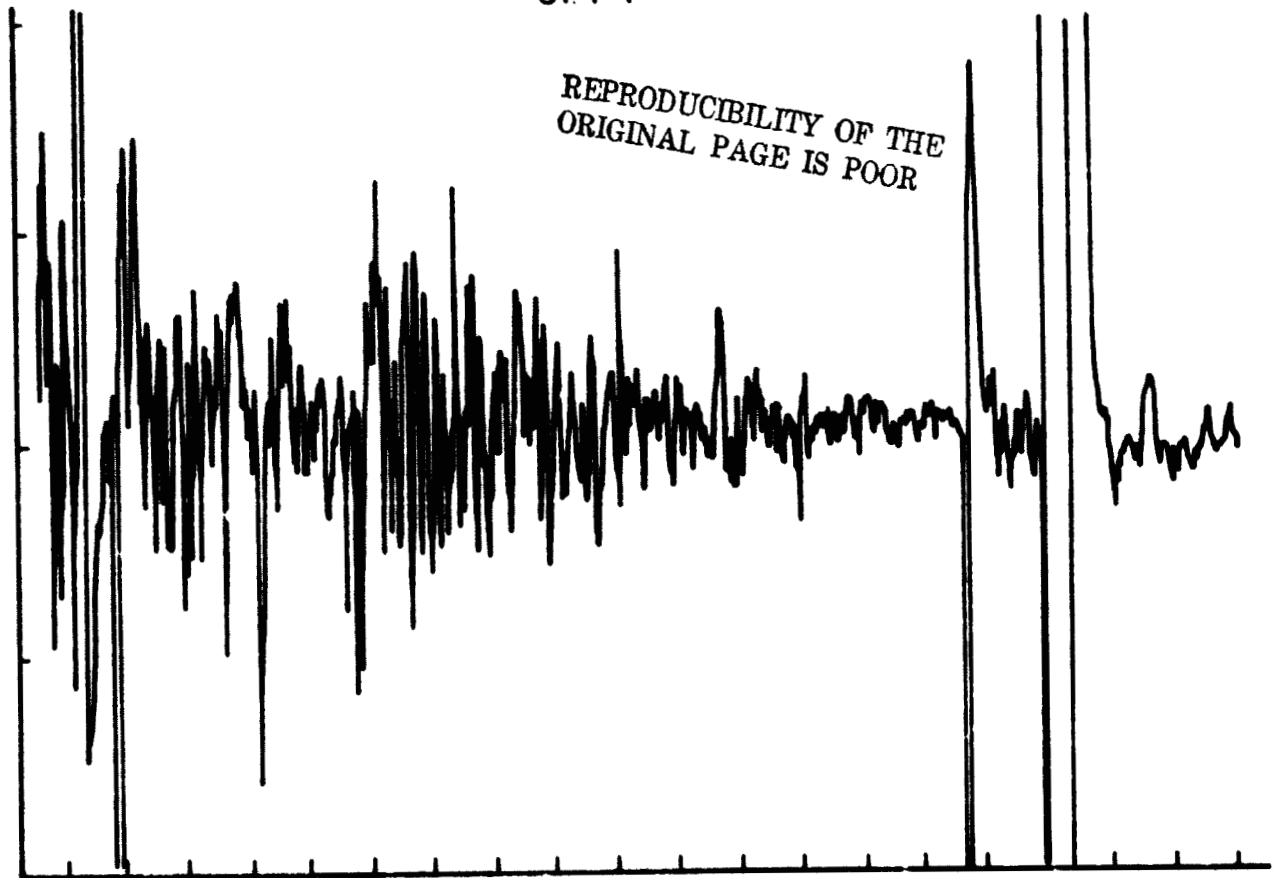
Unit 2

d) Run 207

Figure 3. Continued



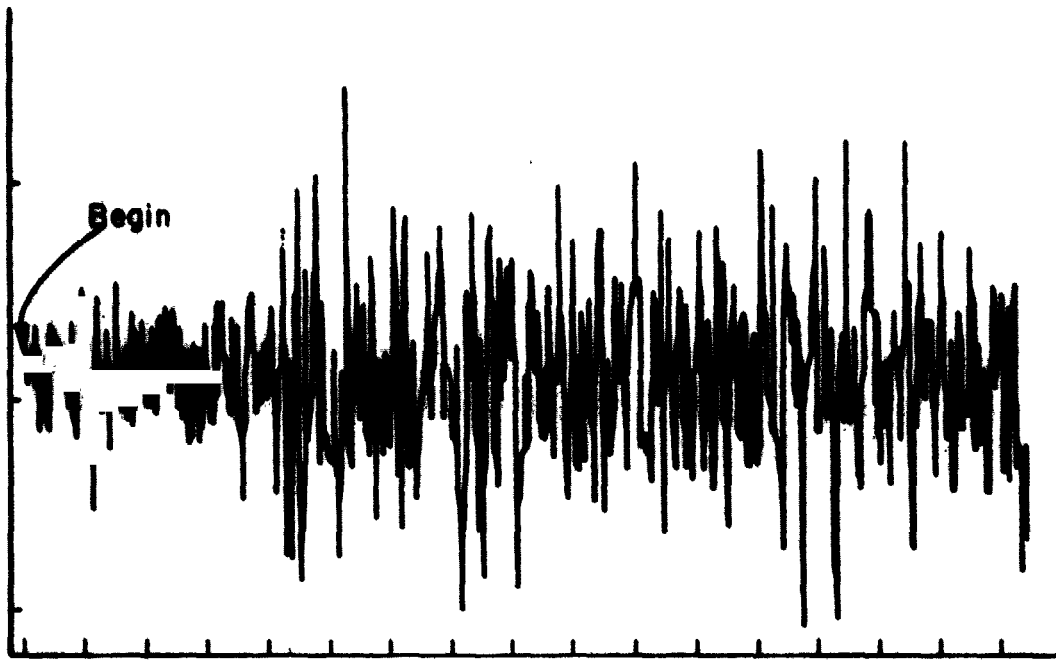
Unit 1



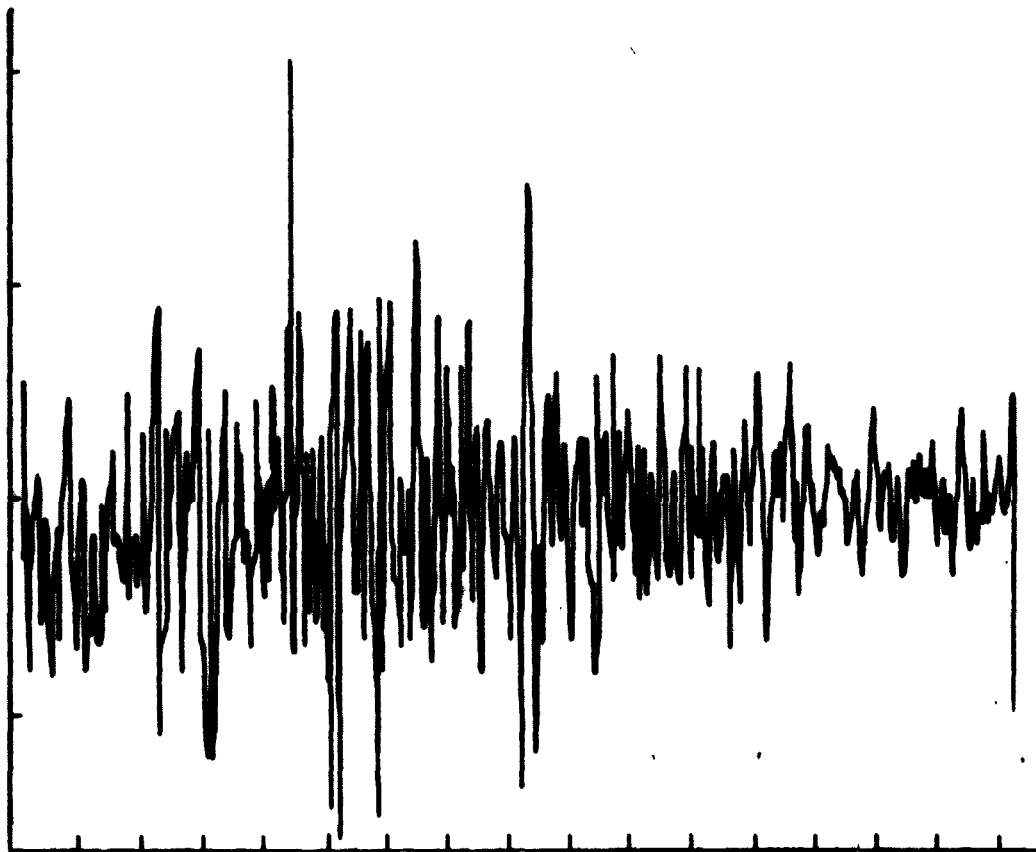
REPRODUCIBILITY OF THE ORIGINAL PAGE IS POOR

Unit 2  
e) Run 208

Figure 3. Continued



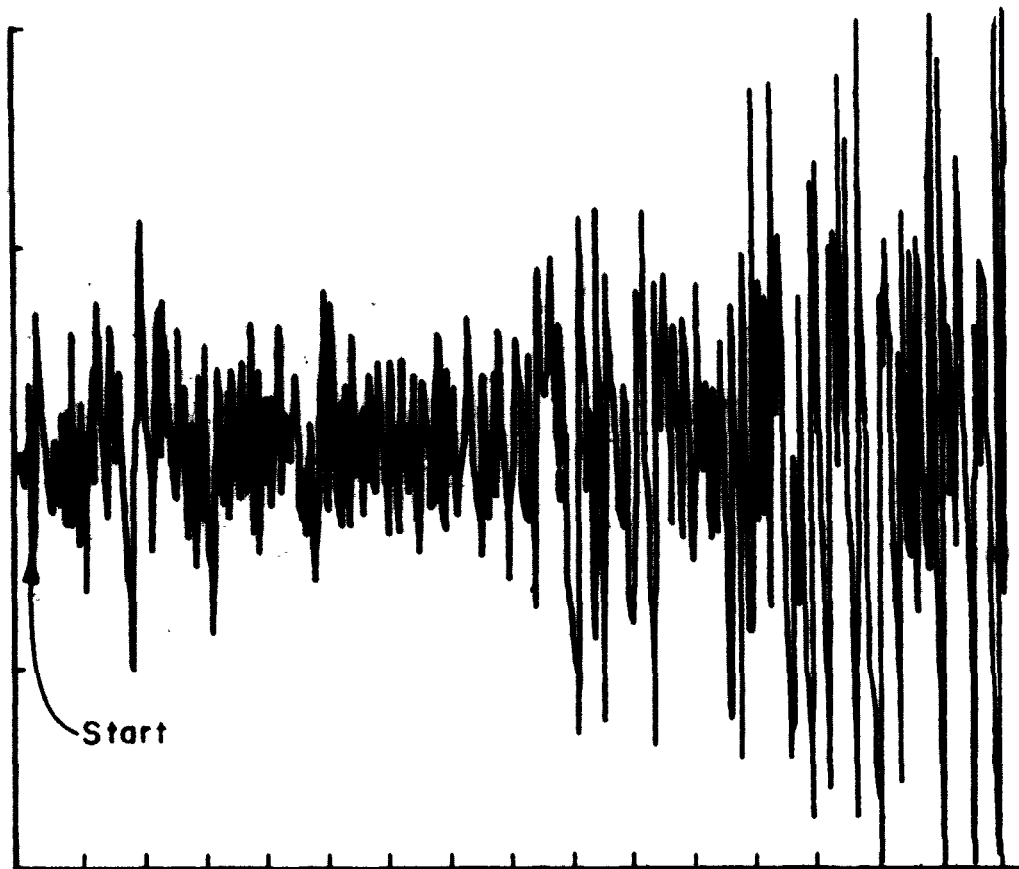
Unit 1



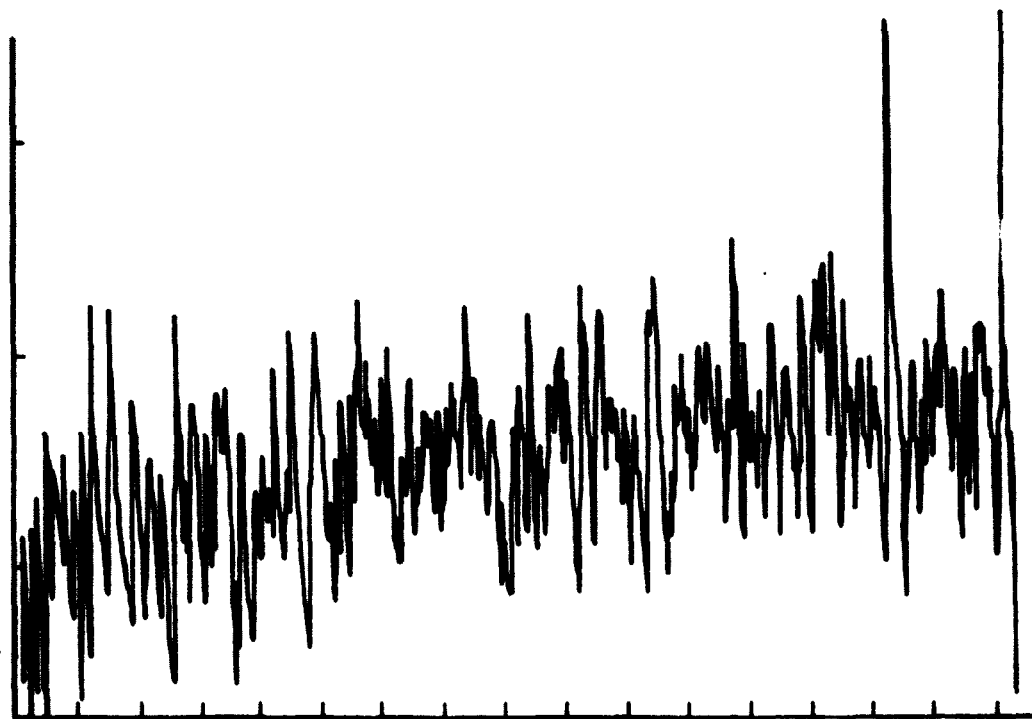
Unit 2

f) Run 212

Figure 3. Continued



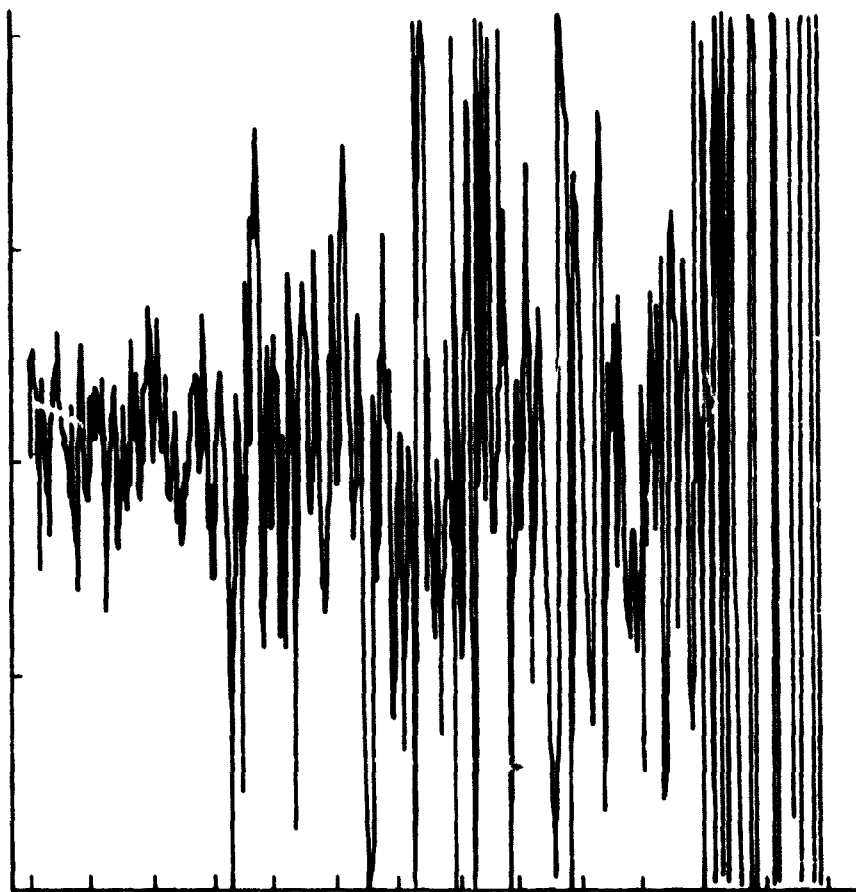
Unit 1



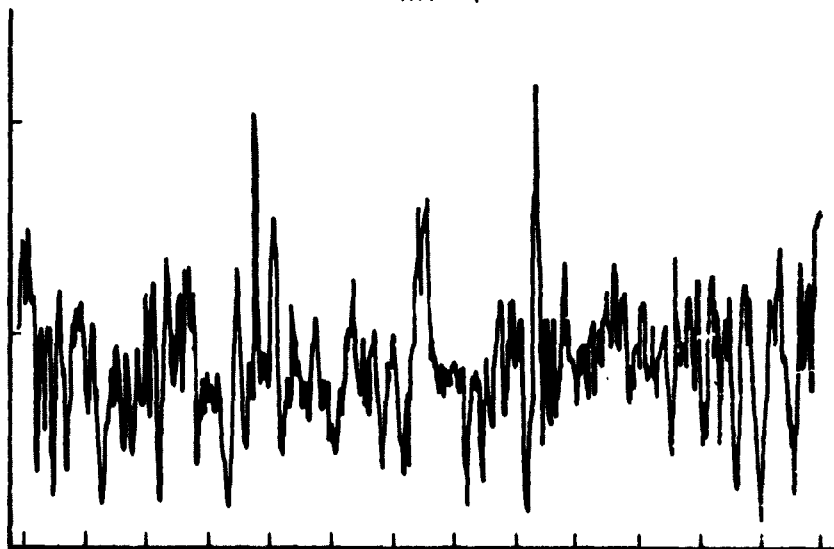
Unit 2

g) Run 213

Figure 3. Continued



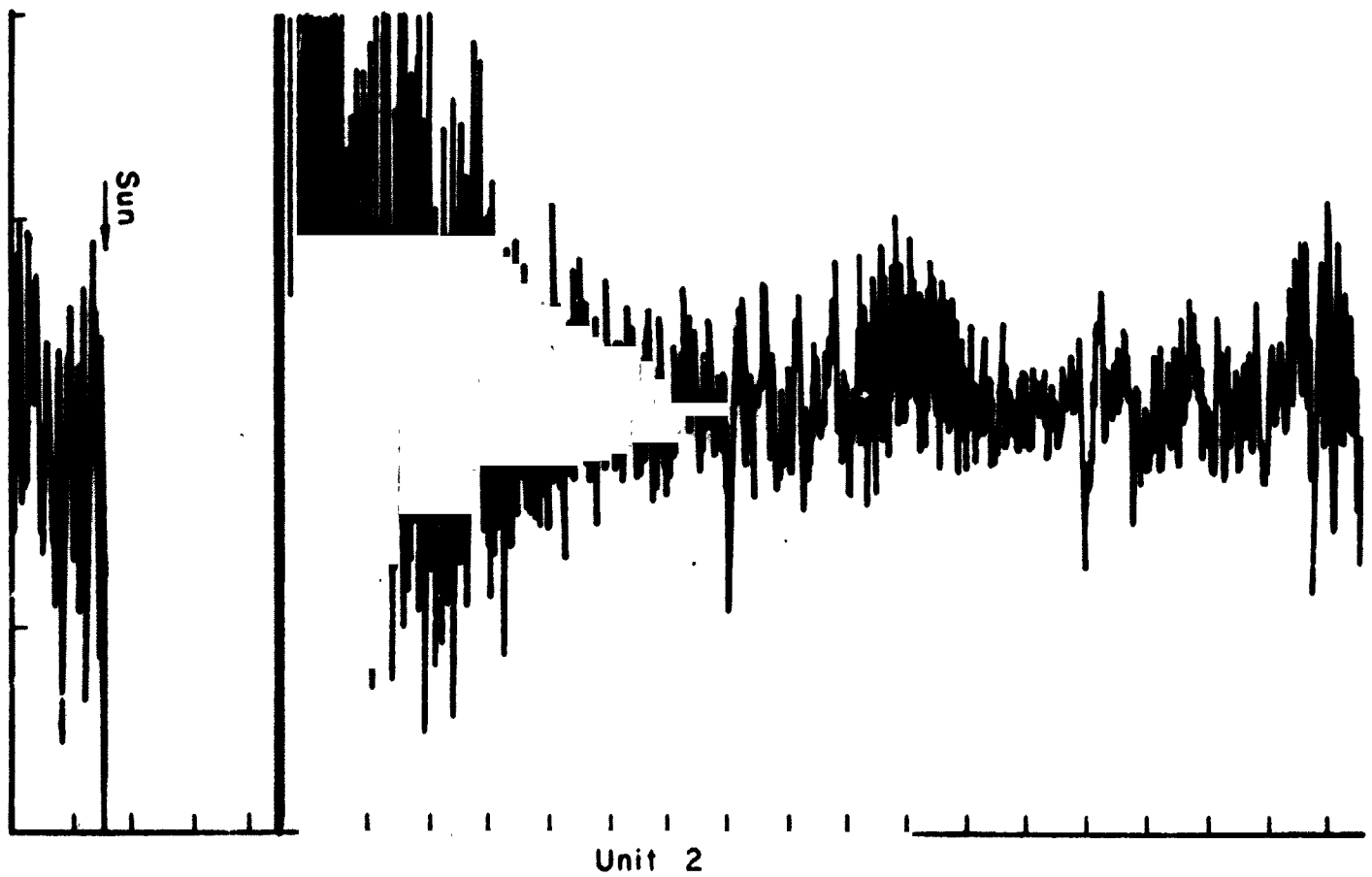
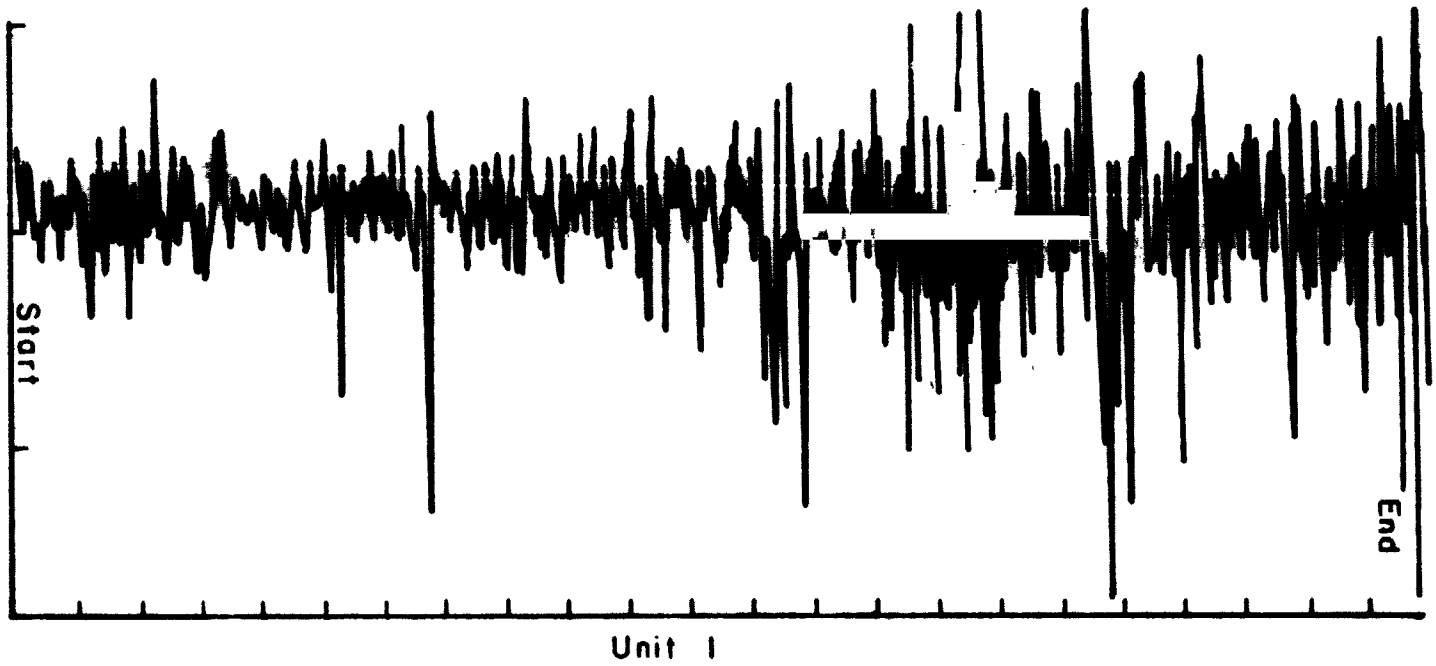
Unit 1



Unit 2

h) Run 214

Figure 3. Continued



i) Run 214

Figure 3. Concluded

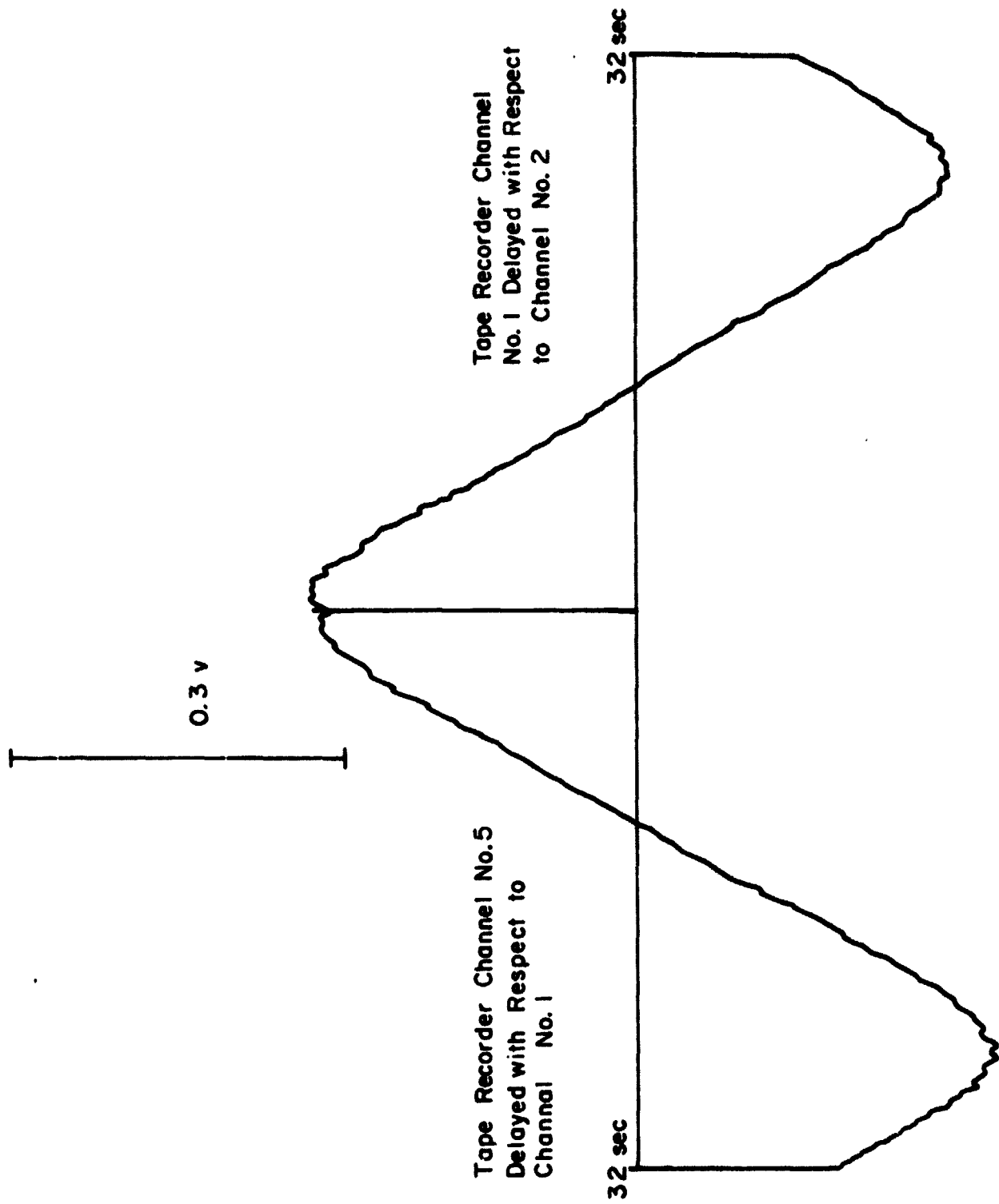
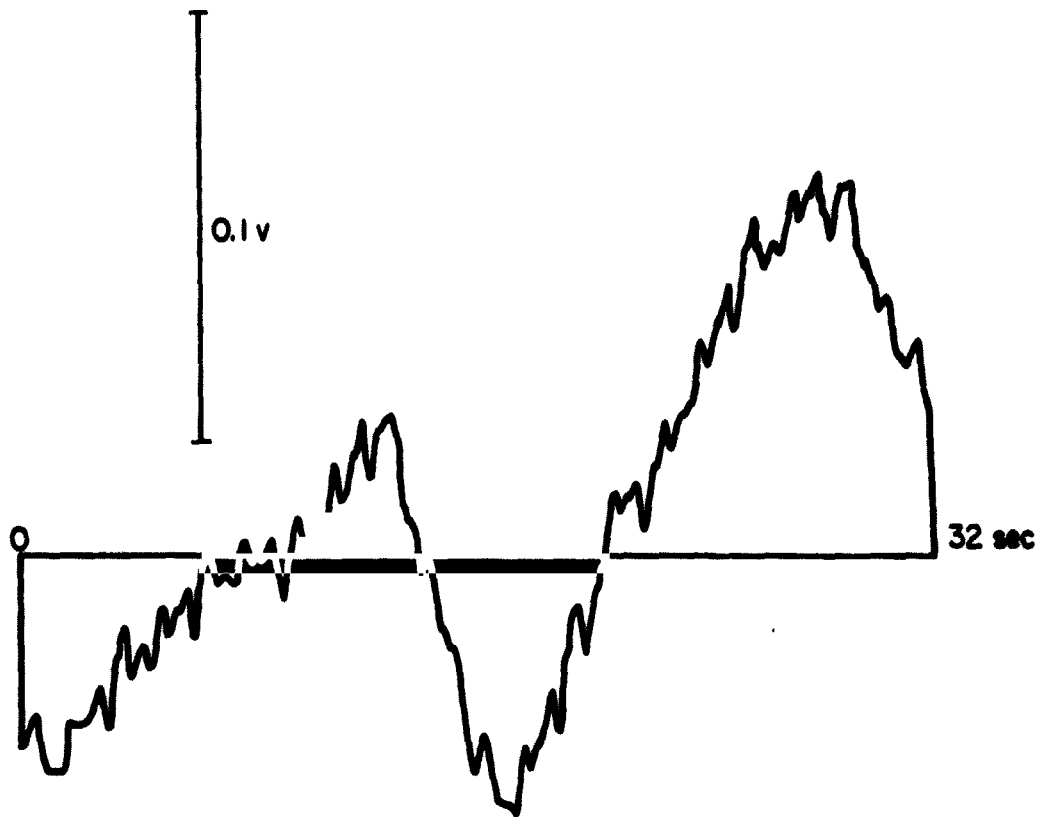
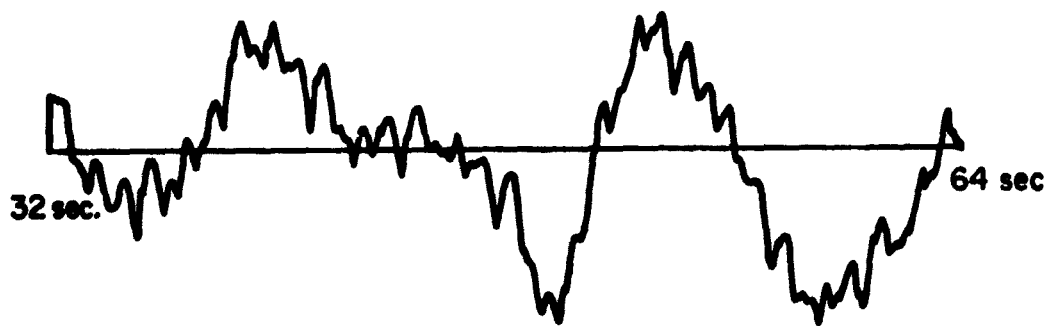


Figure 4. Correlation of Calibration Signal before Run 204



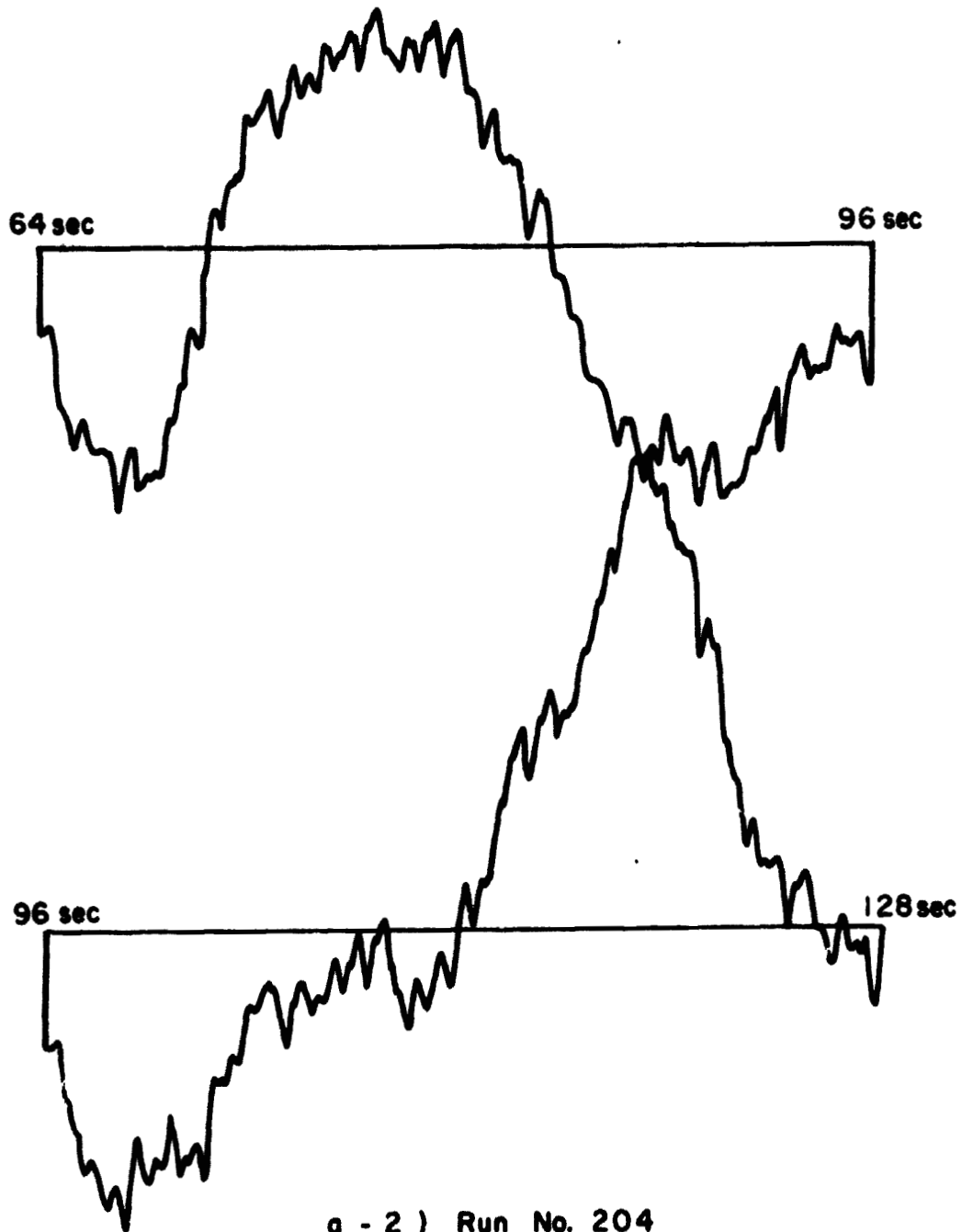
Unit #1 Delayed with Respect to Unit #2



a-1) Run No. 204

Count: 10 - 98

Figure 5. Cross- and Auto- Correlation Measurements



a - 2 ) Run No. 204  
Count : 10 - 98

Figure 5. Continued

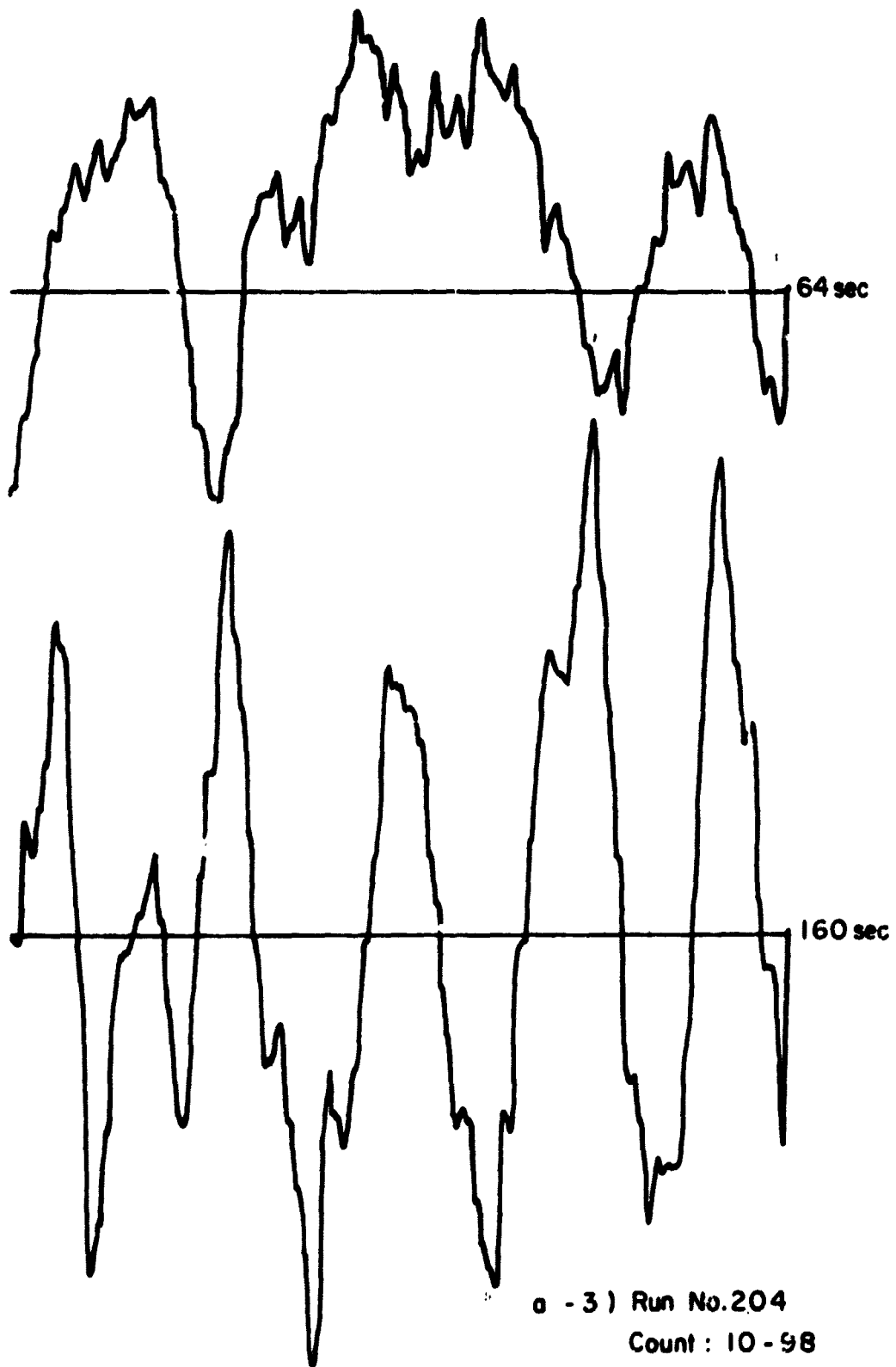
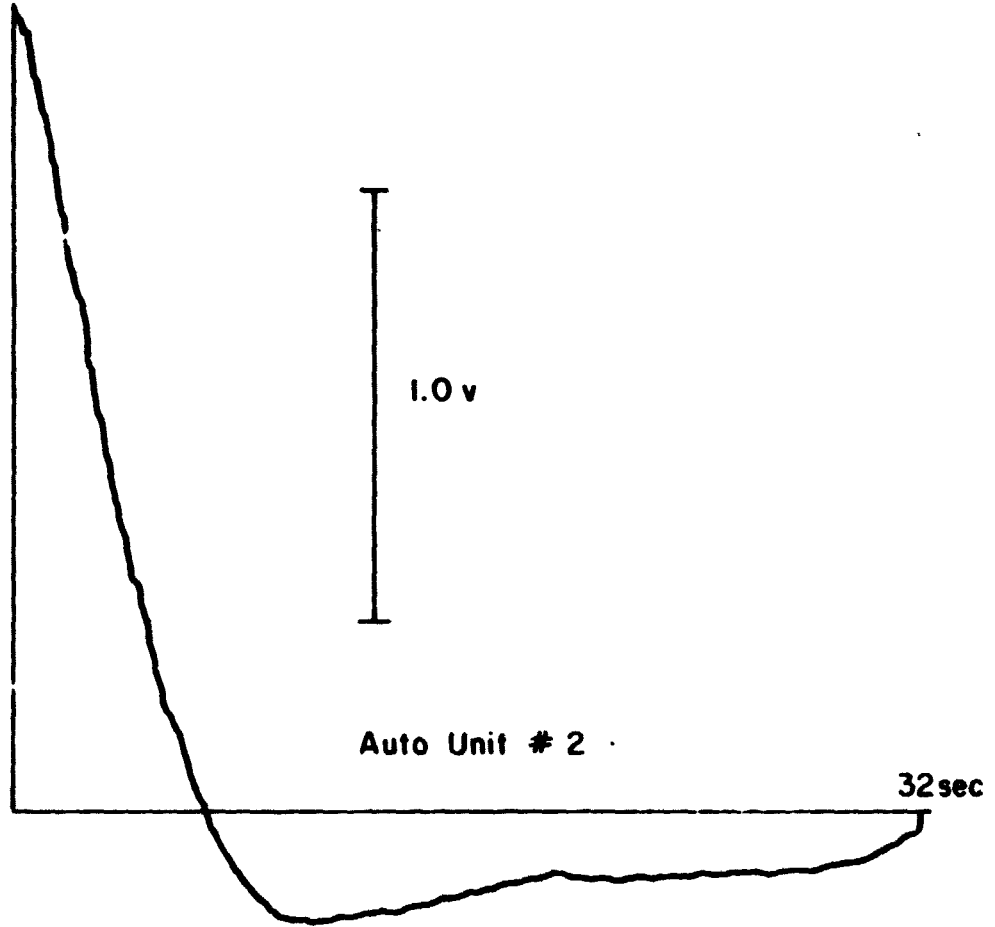
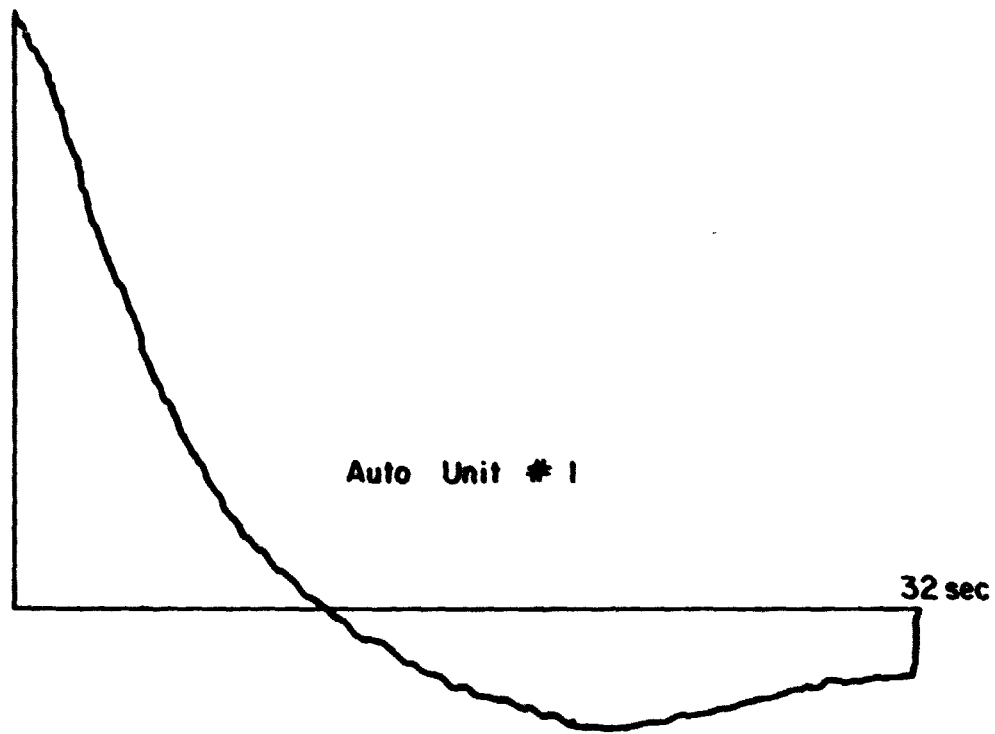
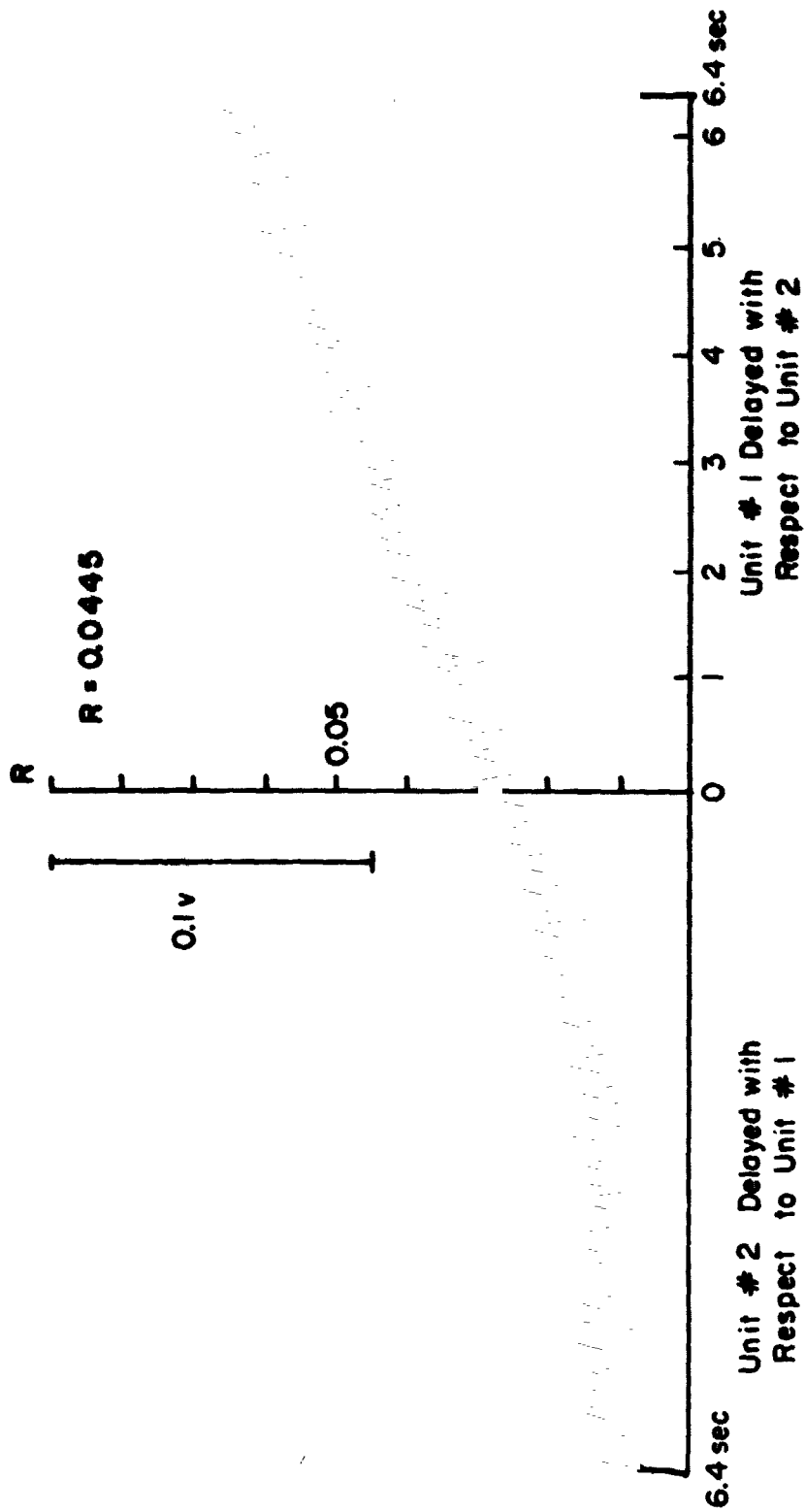


Figure 5. Continued



a) Run No. 204  
Count: 10 - 98

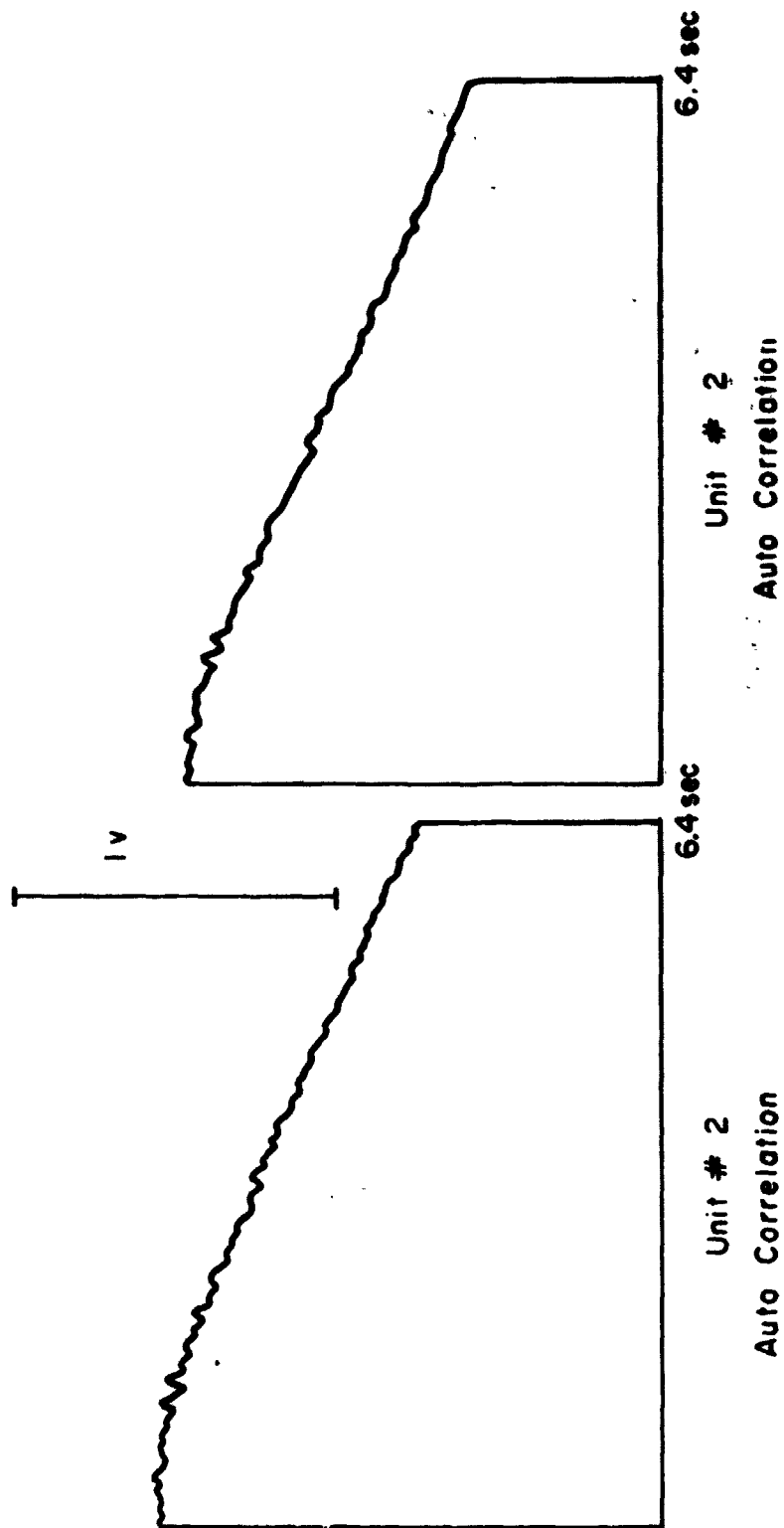
Figure 5. Continued



**Frequency Range**  
 $0.156 \text{ Hz} \leq f \leq 3.9 \text{ Hz}$

**b - 1 ) Run No. 205**

**Figure 5. Continued**



Frequency Range  
0.156 Hz ≤ f ≤ 3.9 Hz

b-1) Run No 205

Figure 5. Continued

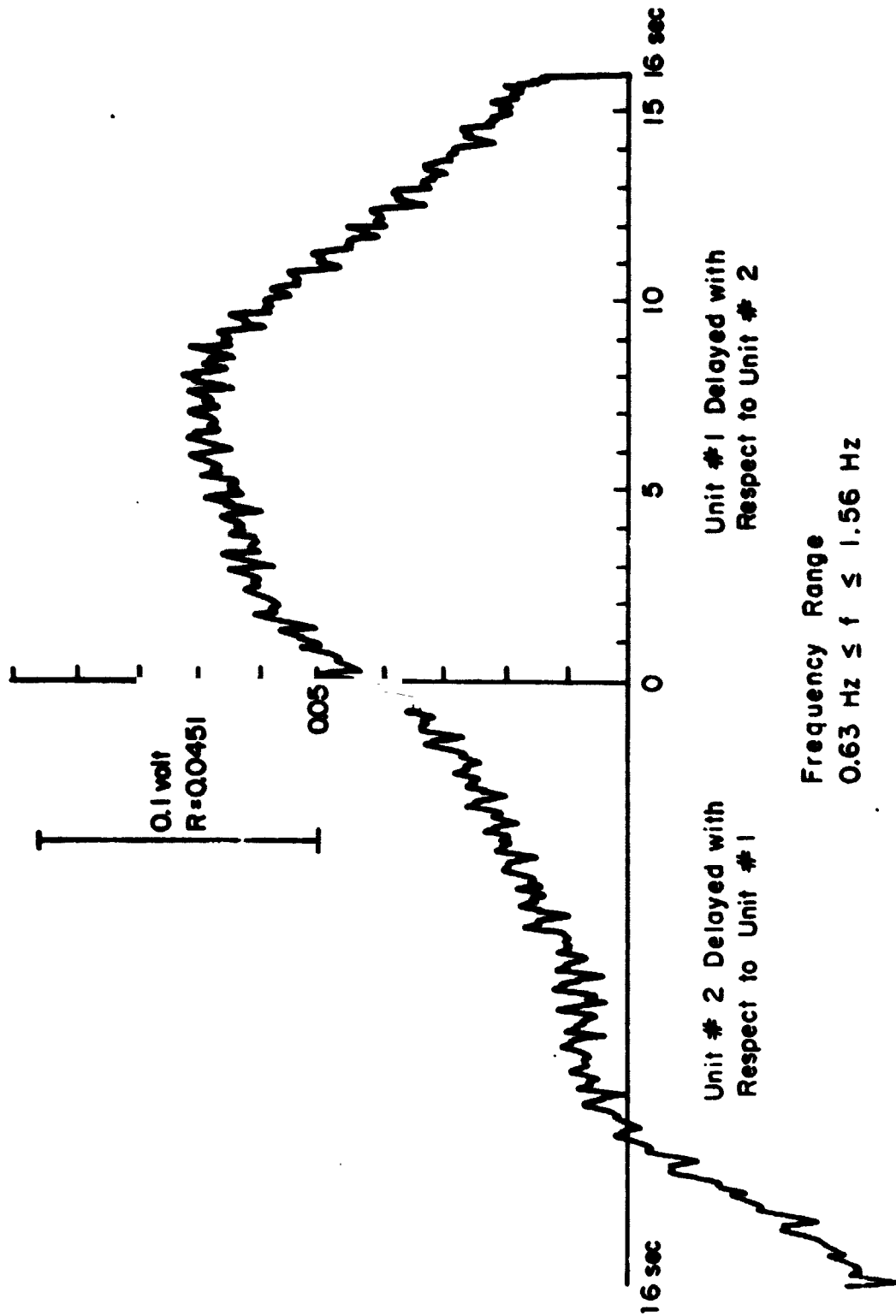
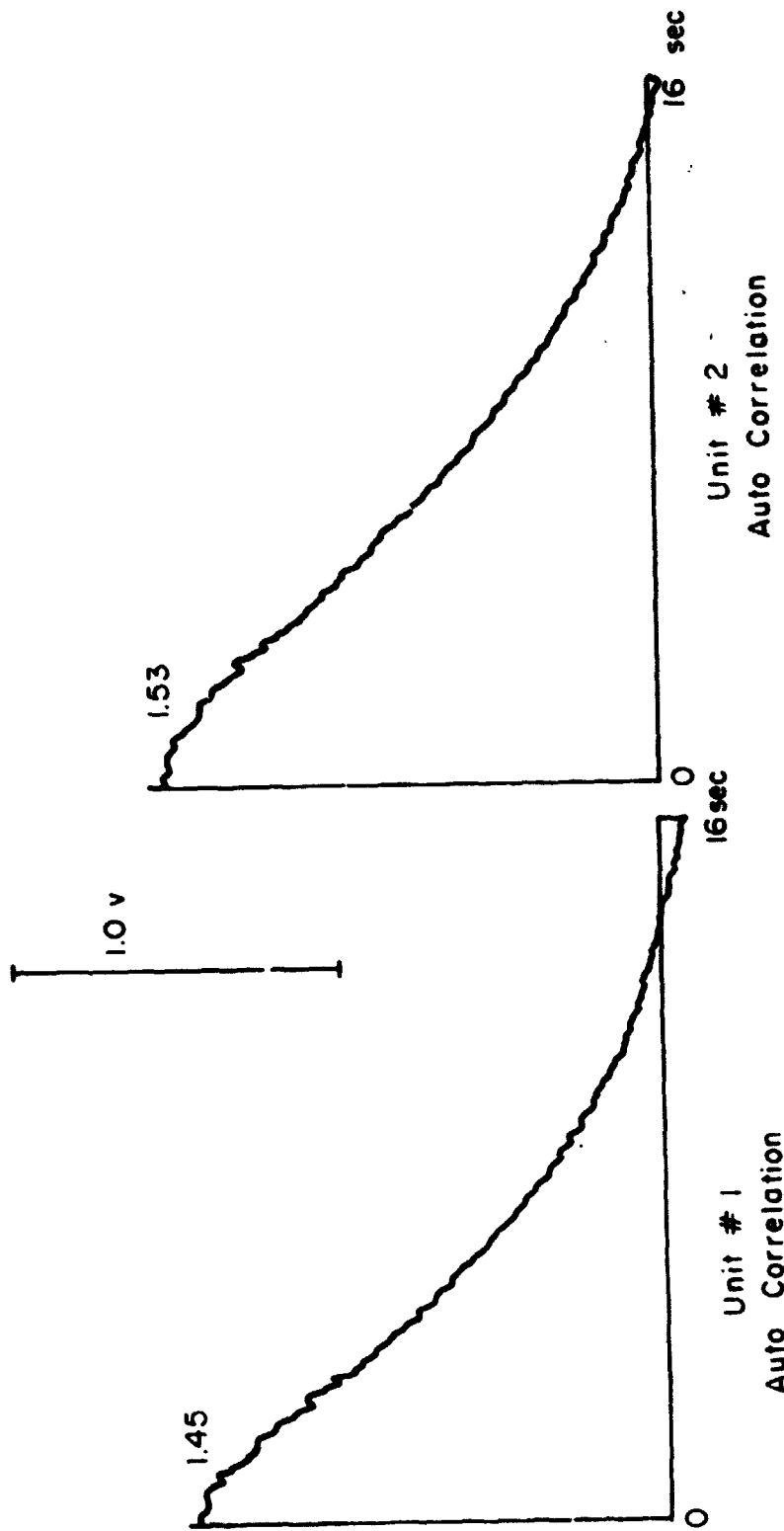
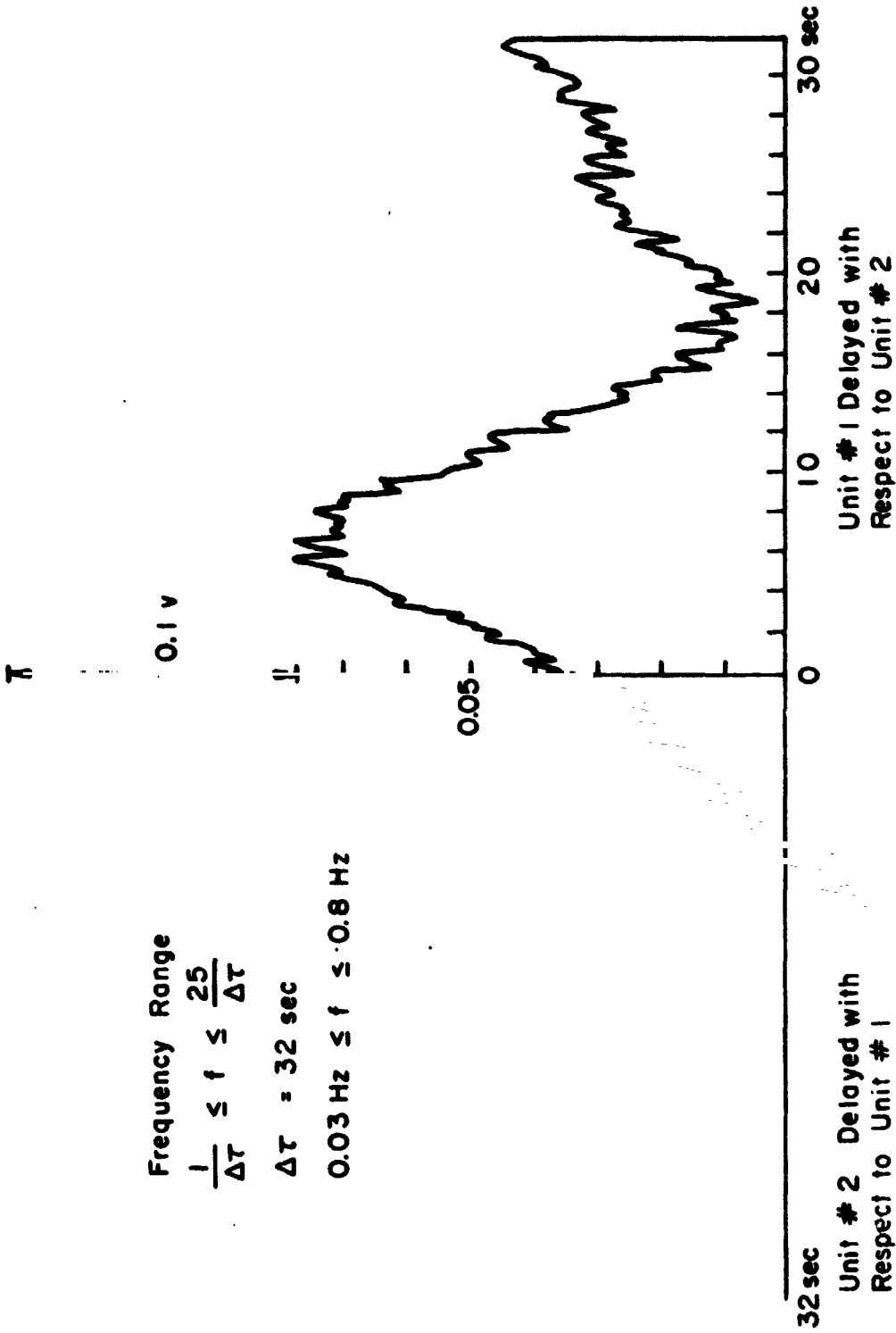


Figure 5. Continued

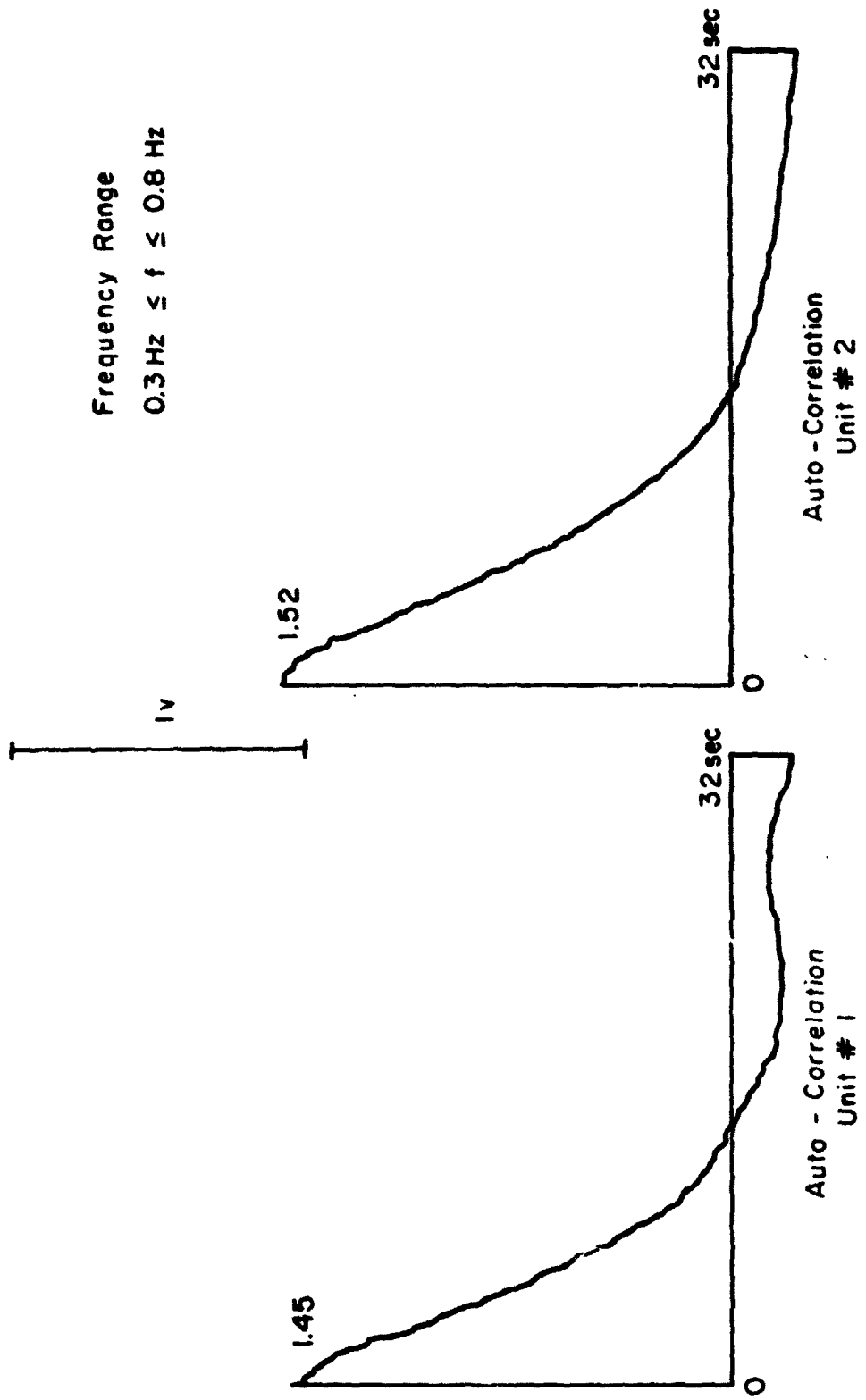


Frequency Range  
 $0.06 \text{ Hz} \leq f \leq 1.56 \text{ Hz}$   
 b - 2 ) Run No. 205

Figure 5. Continued

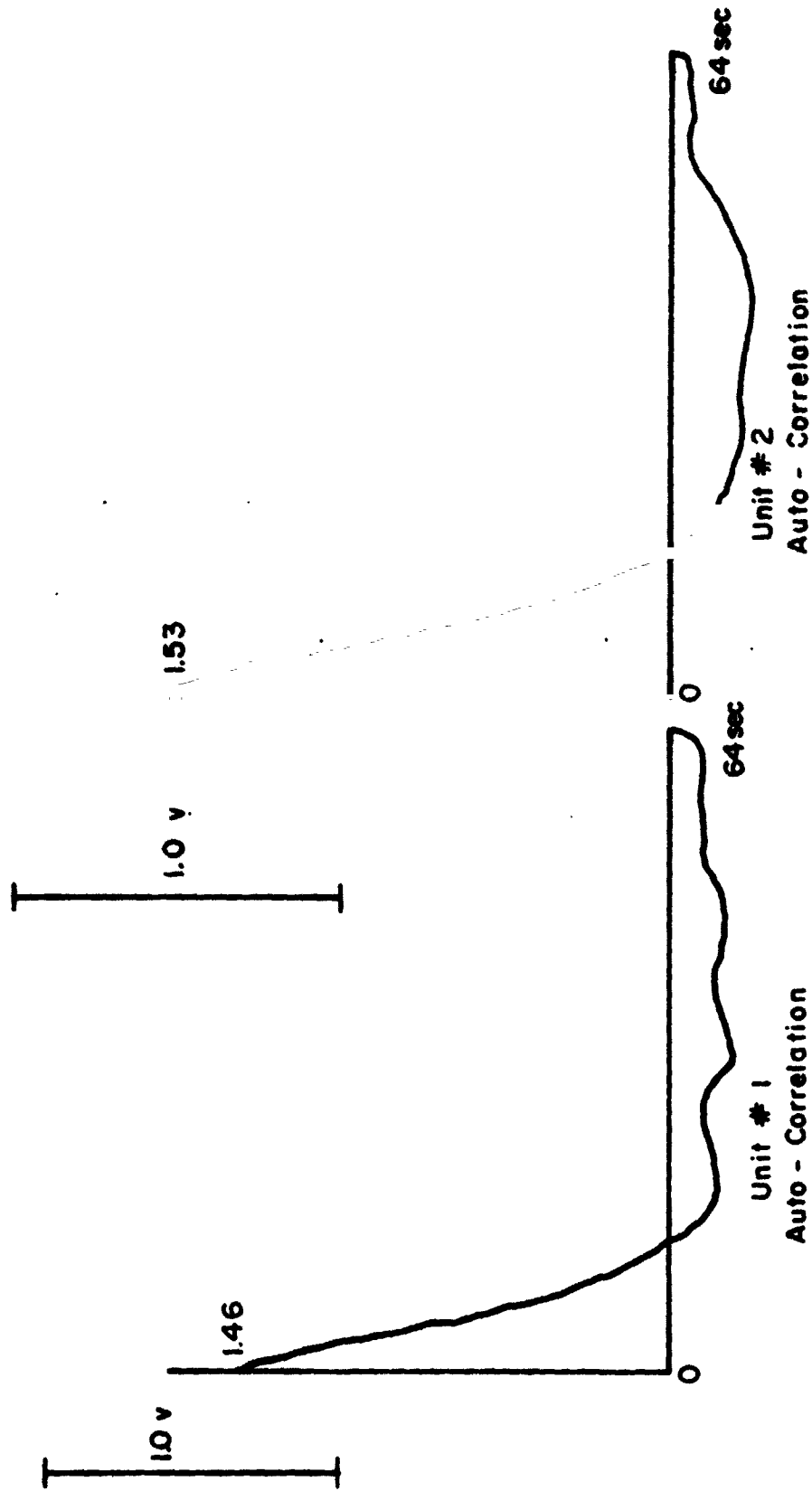


b - 3 ) Run No. 205



b - 3 ) Run No. 205

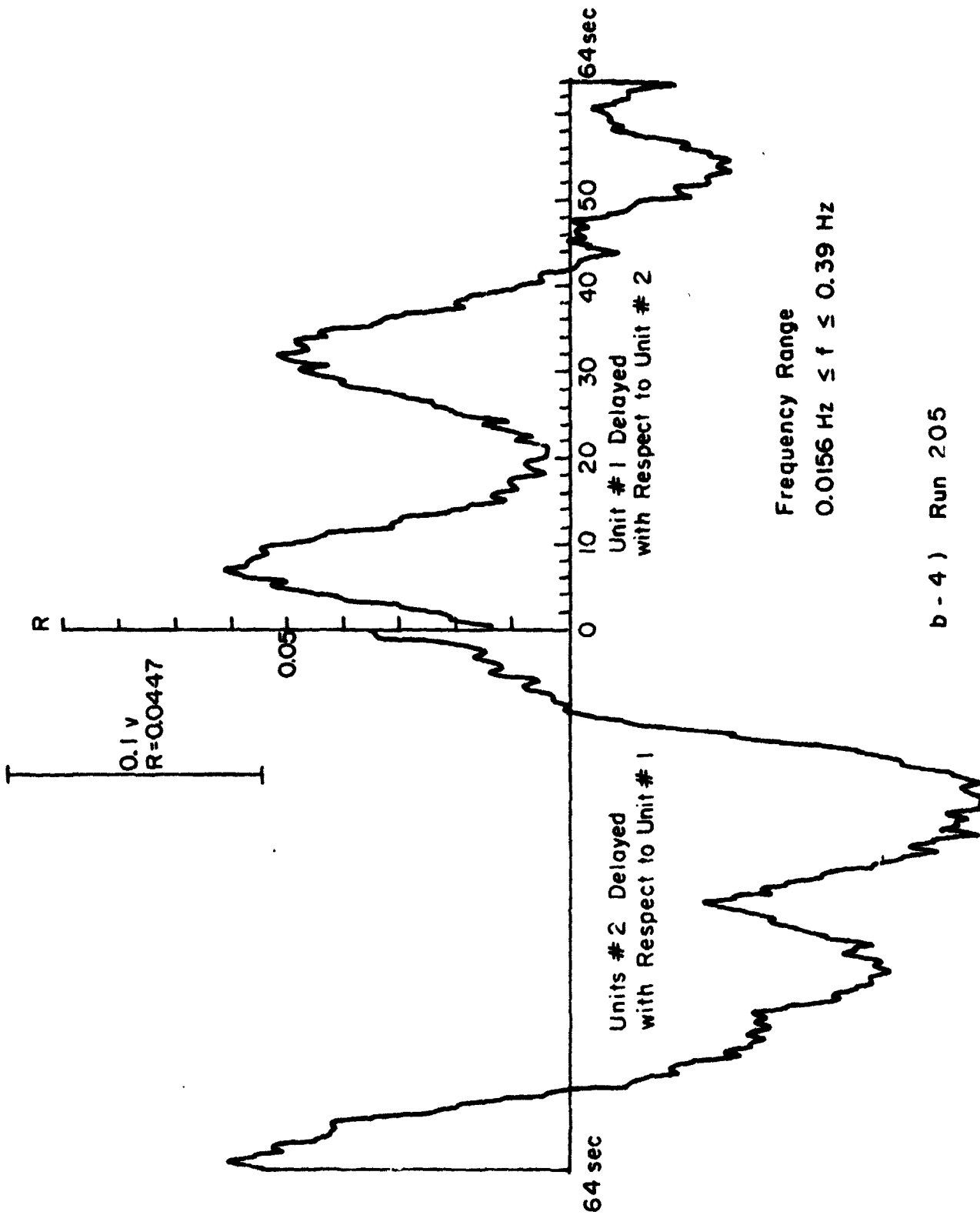
Figure 5. Continued



Frequency Range  
 $0.0156 \leq f \leq 0.39 \text{ Hz}$

b - 4 ) Run No. 205

Figure 5. Continued



b - 4 ) Run 205

Figure 5. Continued

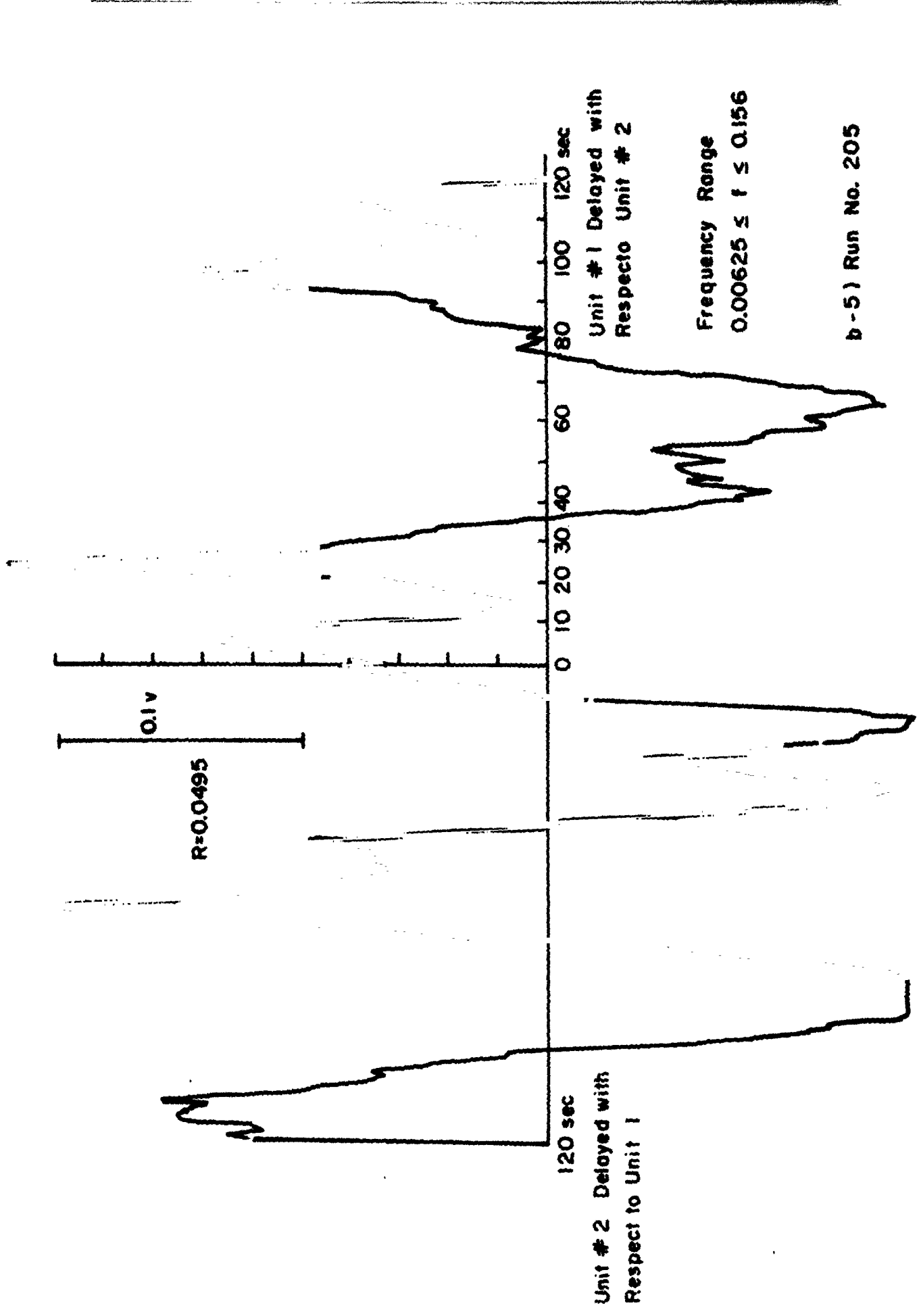
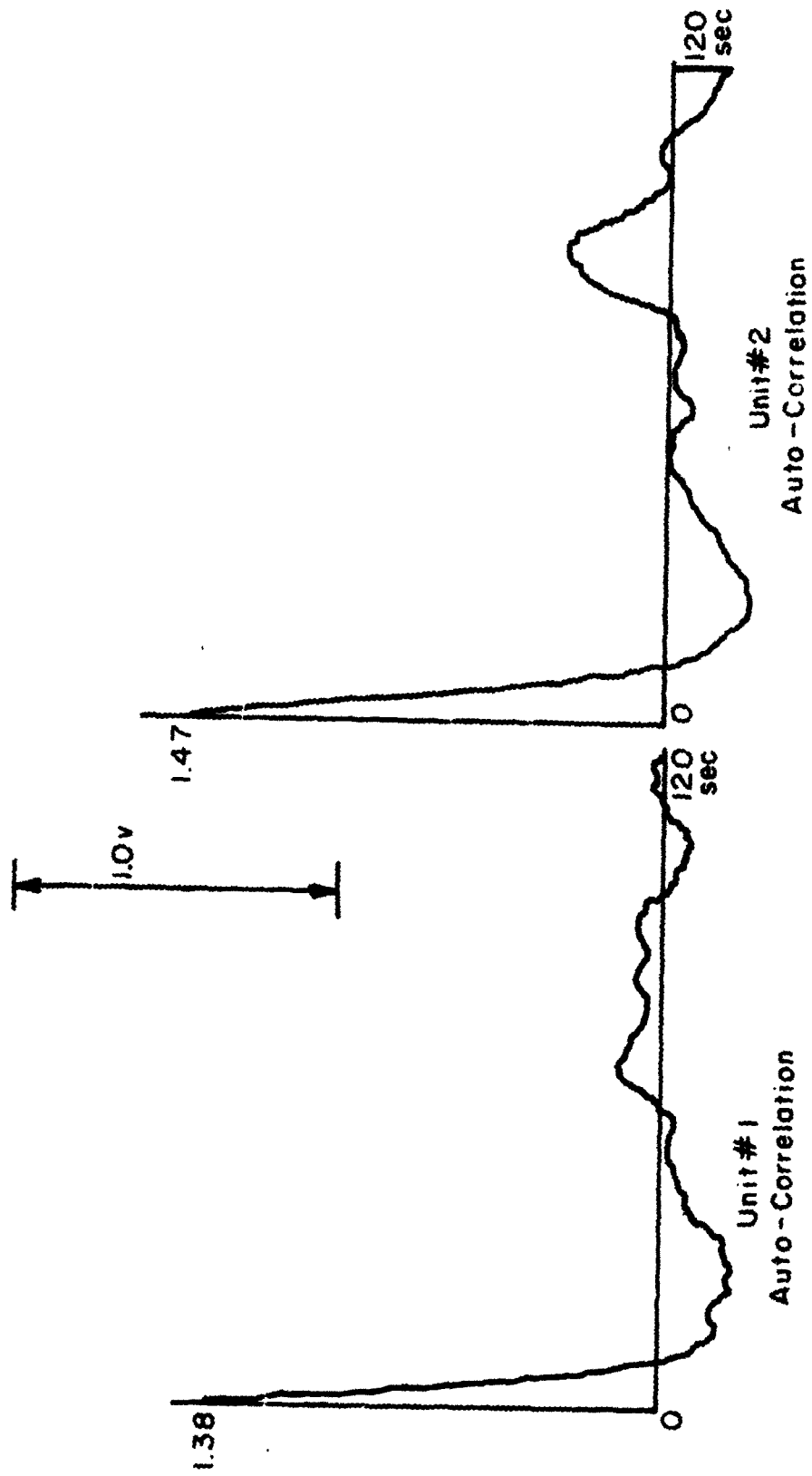


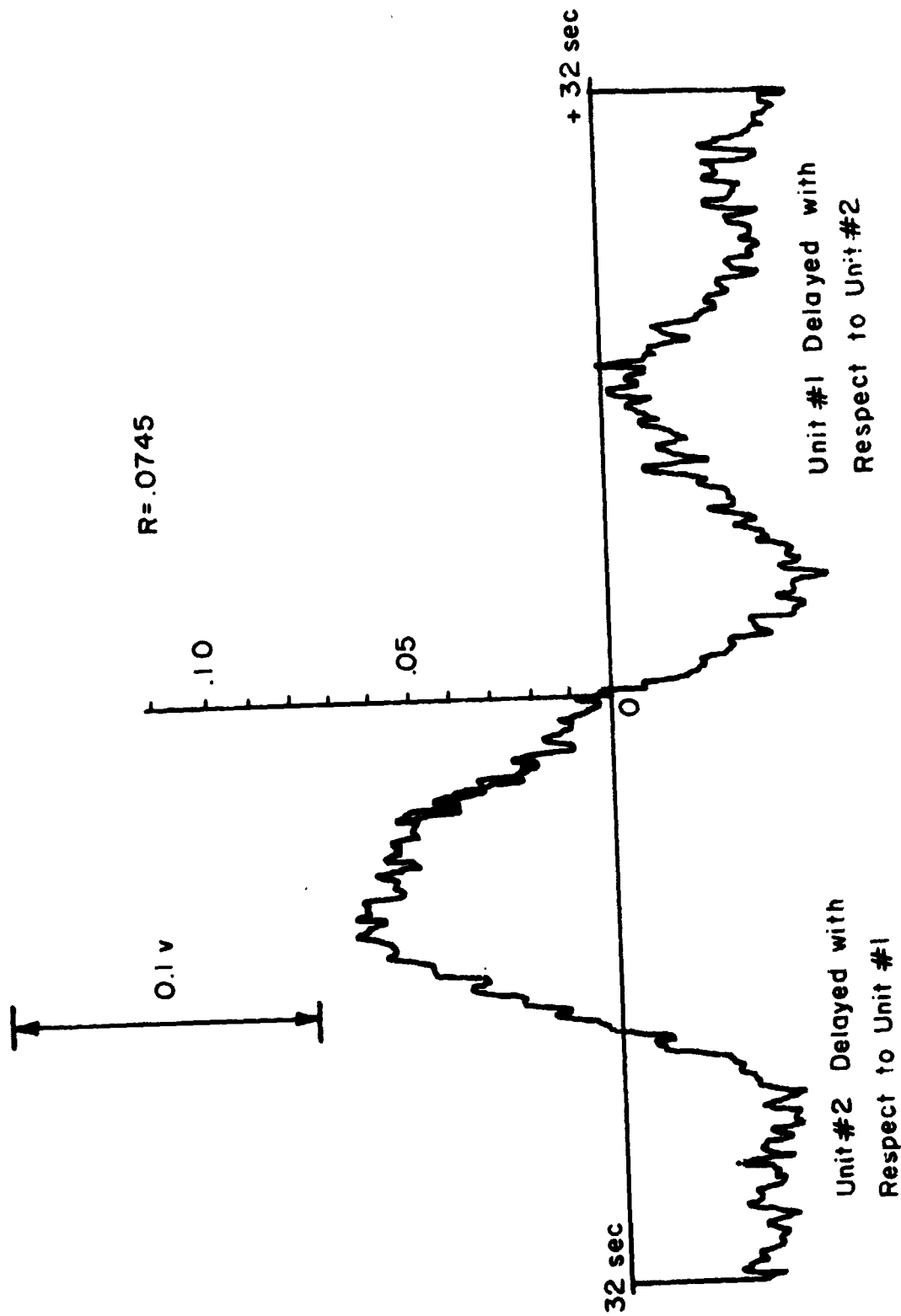
Figure 5. Continued



Frequency Range  
 $0.00625 \leq f \leq 0.156$

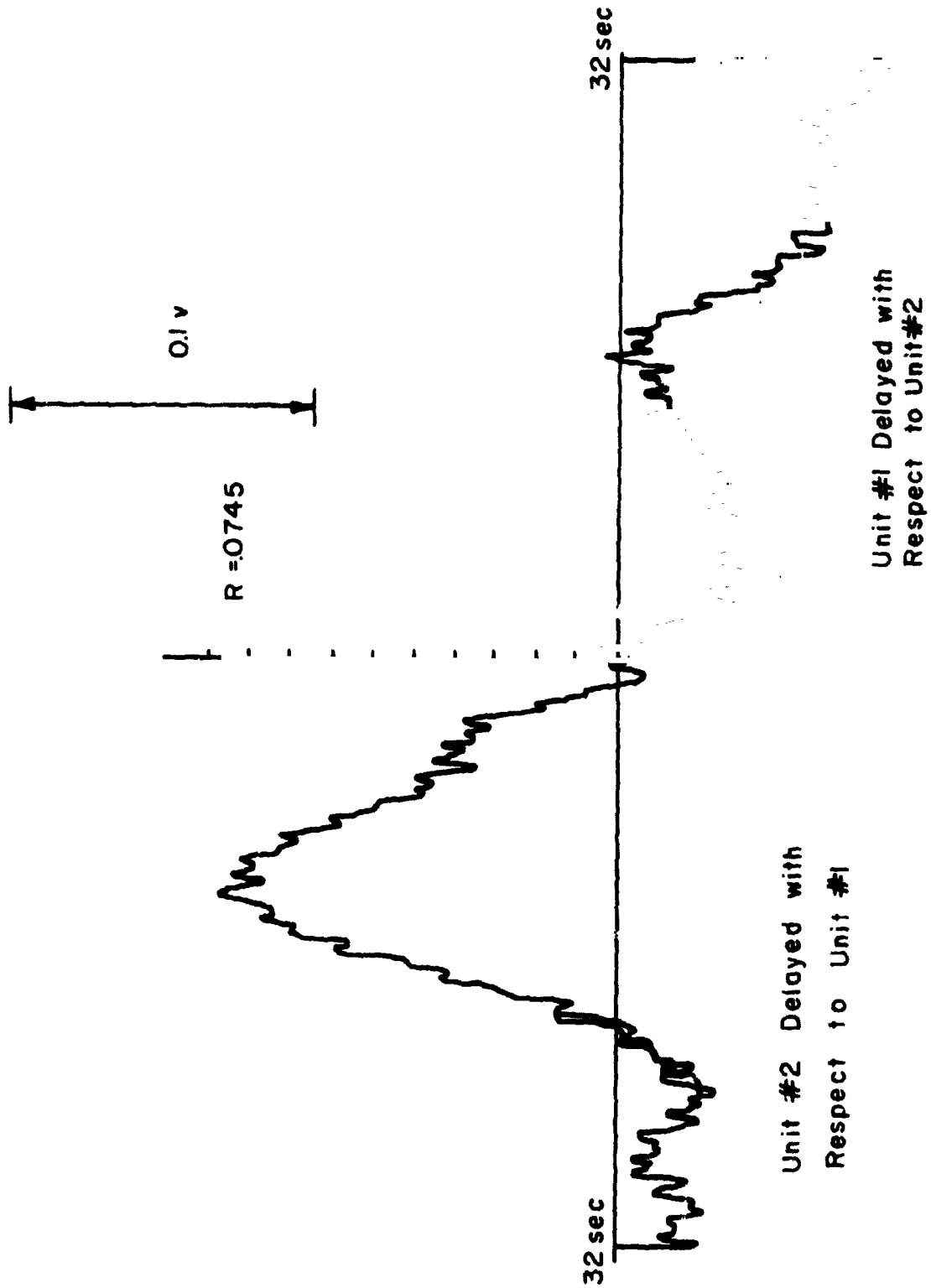
b - 5 ) Run No. 205

Figure 5. Continued



C-1) Run No. 206

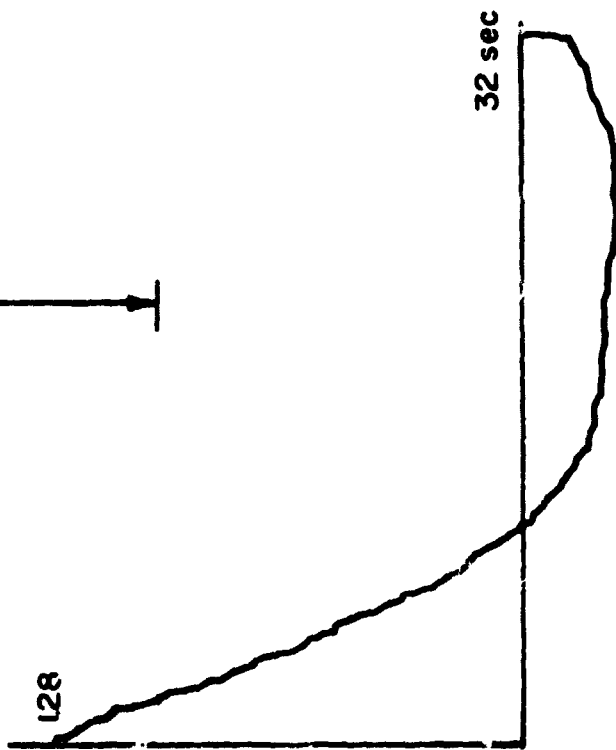
Figure 5. Continued



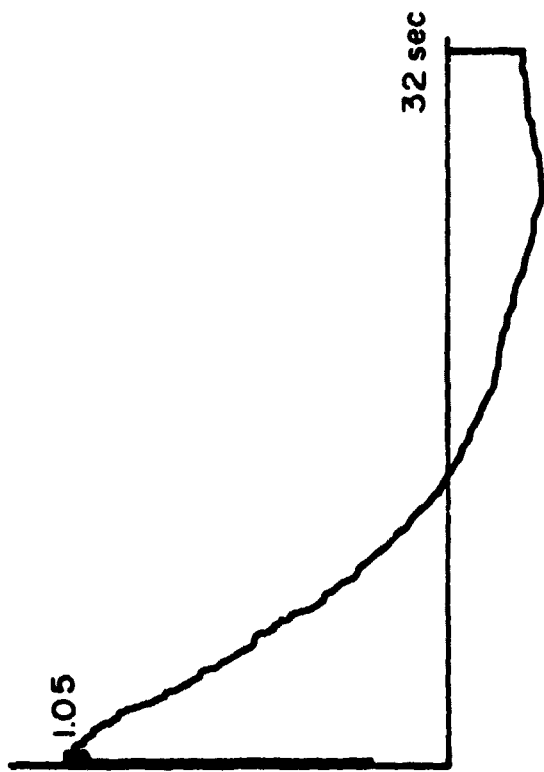
C--2) Run No. 206

Figure 5. Continued

1 v.



Auto - Correlation Unit #1

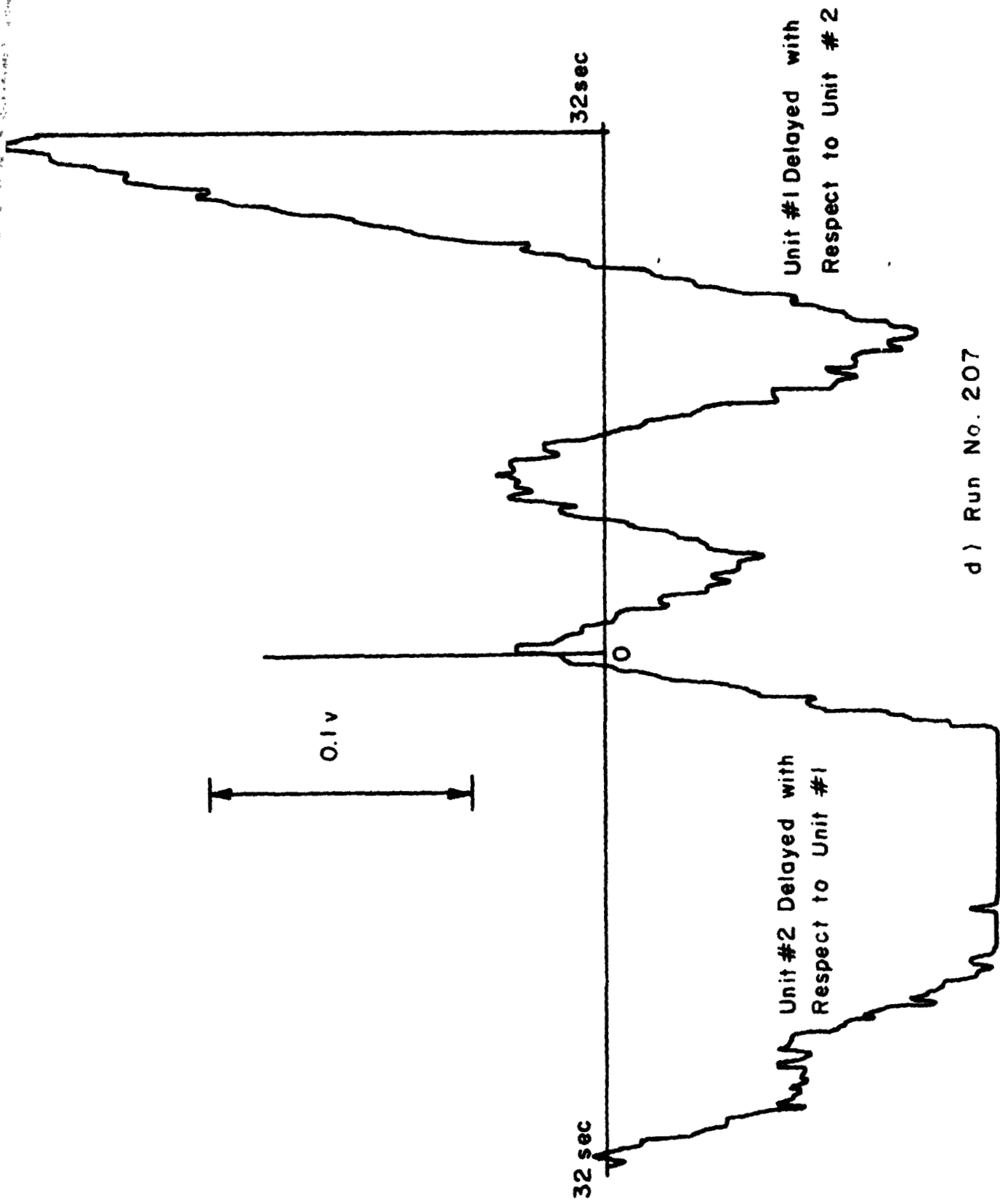


Auto - Correlation Unit #2

c) Run No. 206

Figure 5. Continued

C-2



d) Run No. 207

Figure 5. Continued

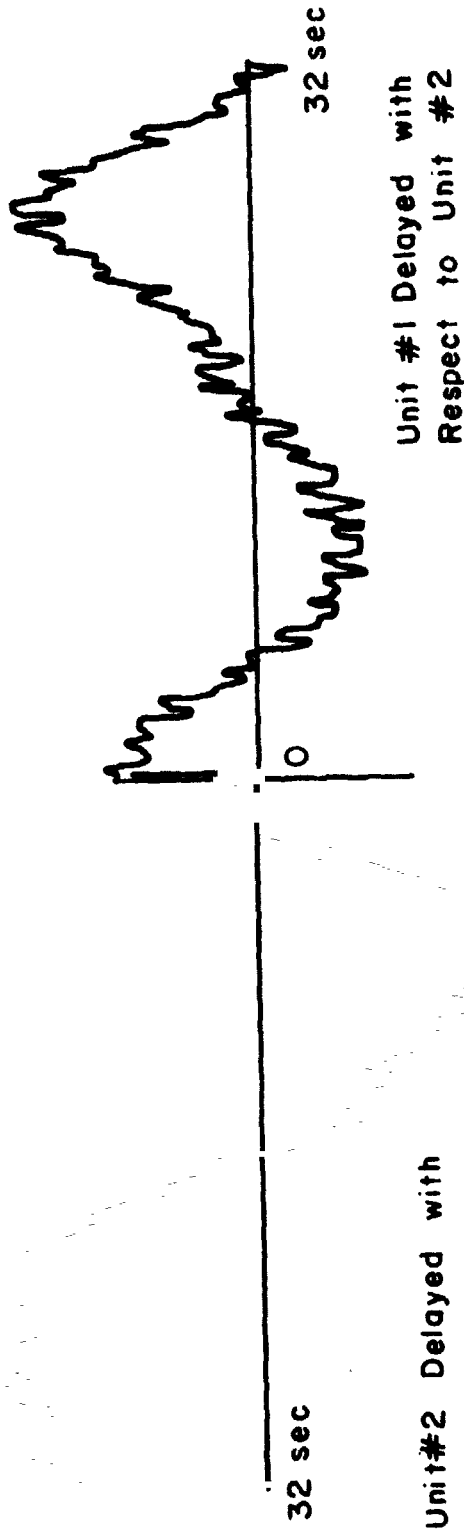


Auto - Correlation Unit #1      Auto - Correlation #2

d) Run No.207

Figure 5. Continued

0.1 v



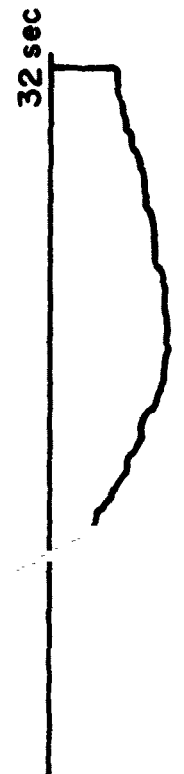
e) Run No. 208

Figure 5. Continued

1. v



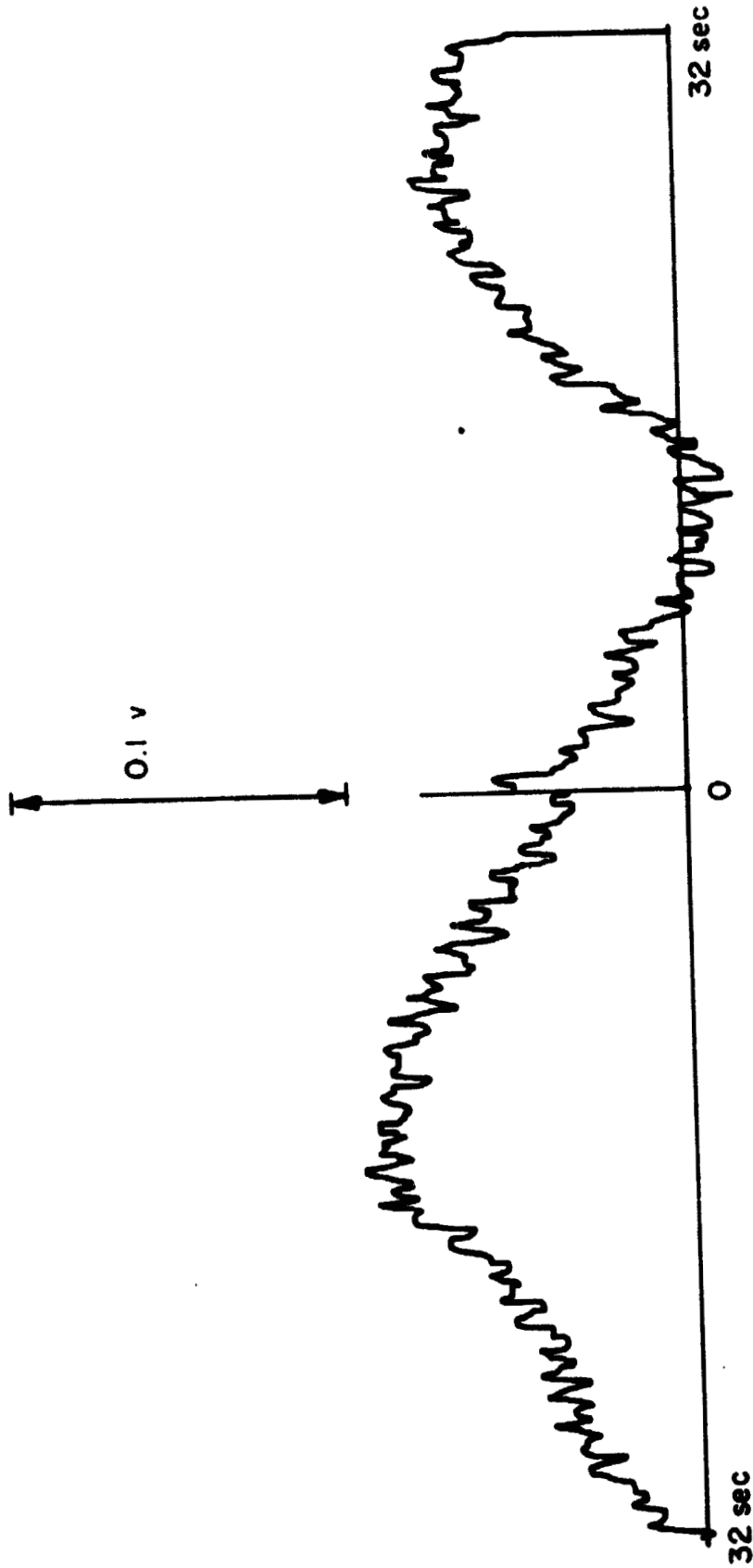
Auto-Correlation Unit #2



Auto-Correlation Unit #1

e) Run No. 208

Figure 5. Continued



Unit #2 Delayed with Respect to Unit #1      Unit #1 Delayed with Respect to Unit #2

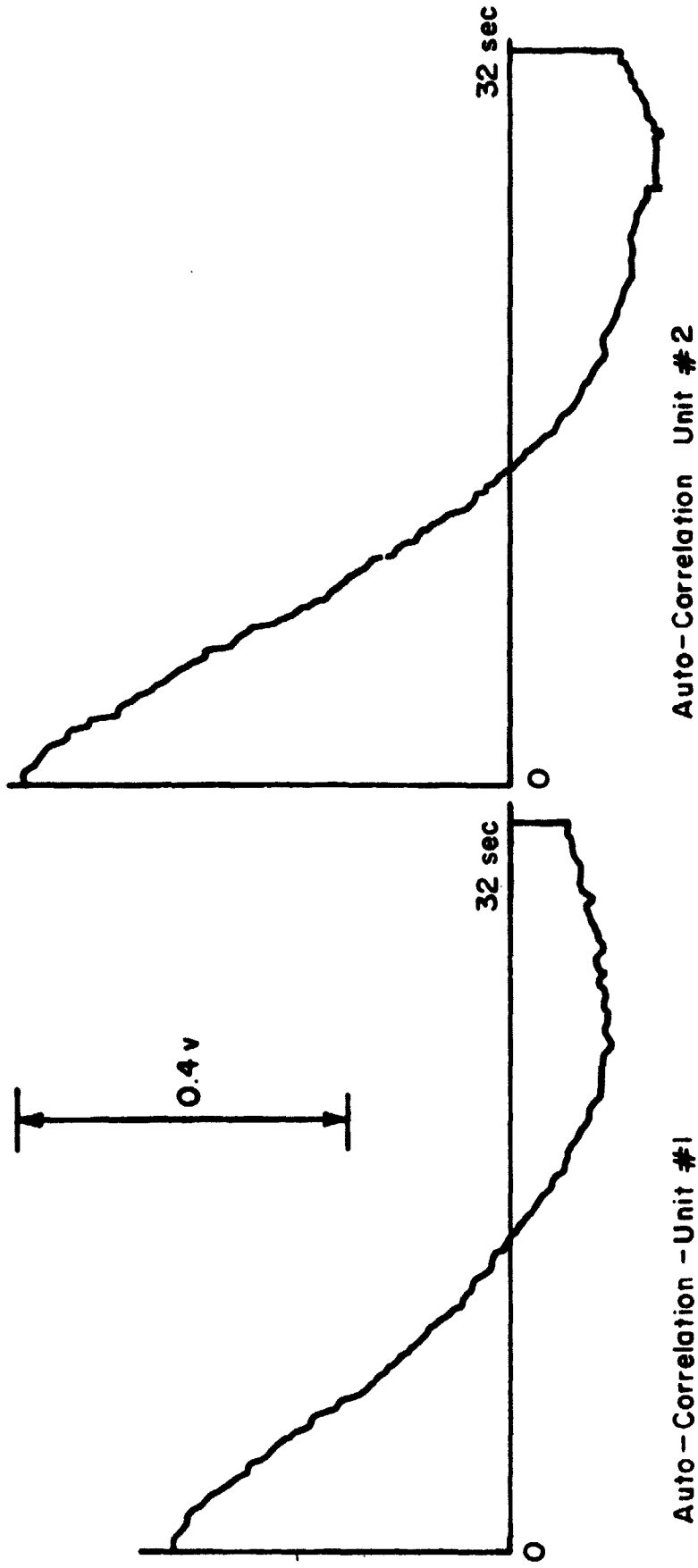
f ) Run No. 212

Count : 10-98

Channels : Unit 1 - #7

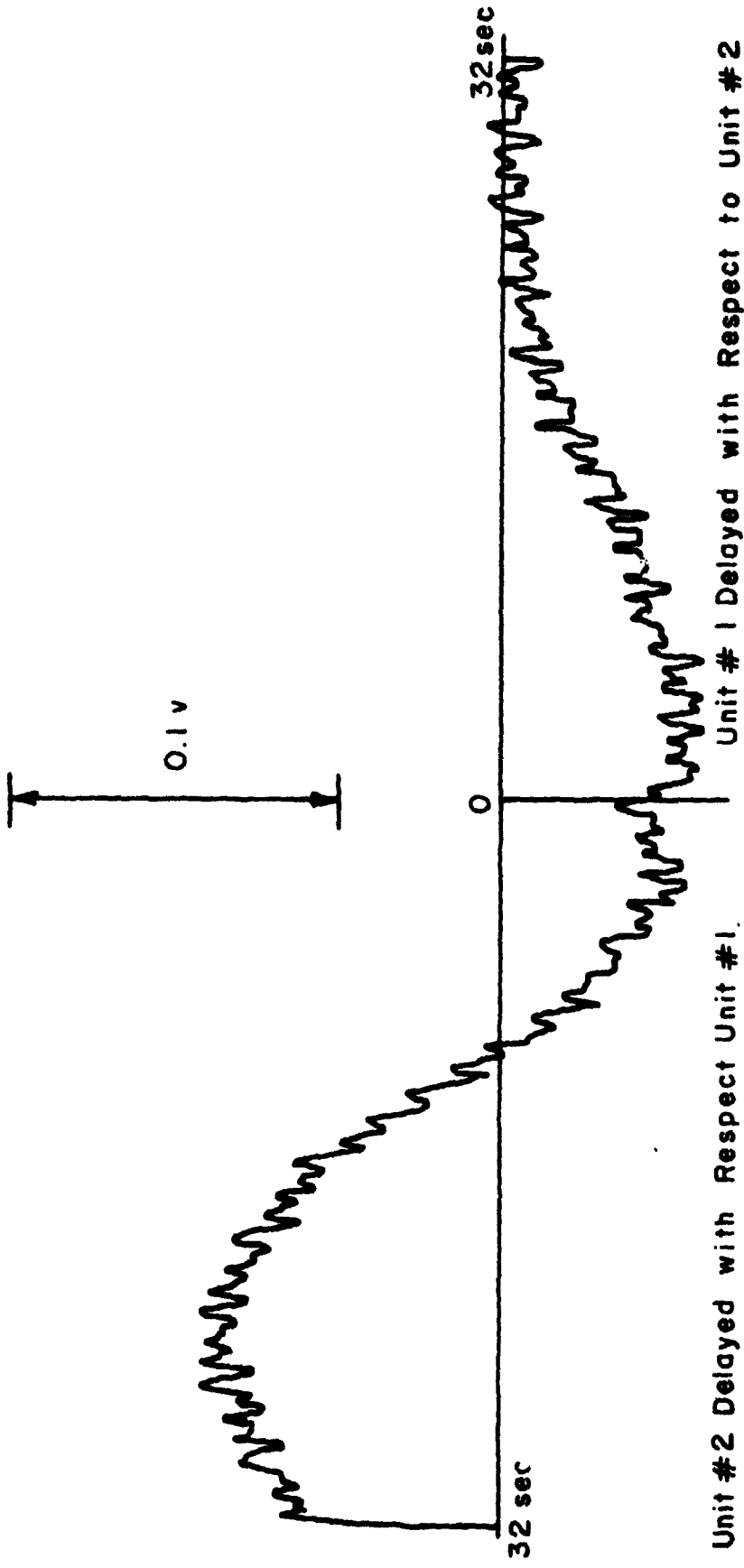
Unit 2 - #11

Figure 5. Continued



f) Run No. 212  
 Count : 10-98  
 Channels : Unit 1 - #7  
 Unit 2 - #11

Figure 5. Continued

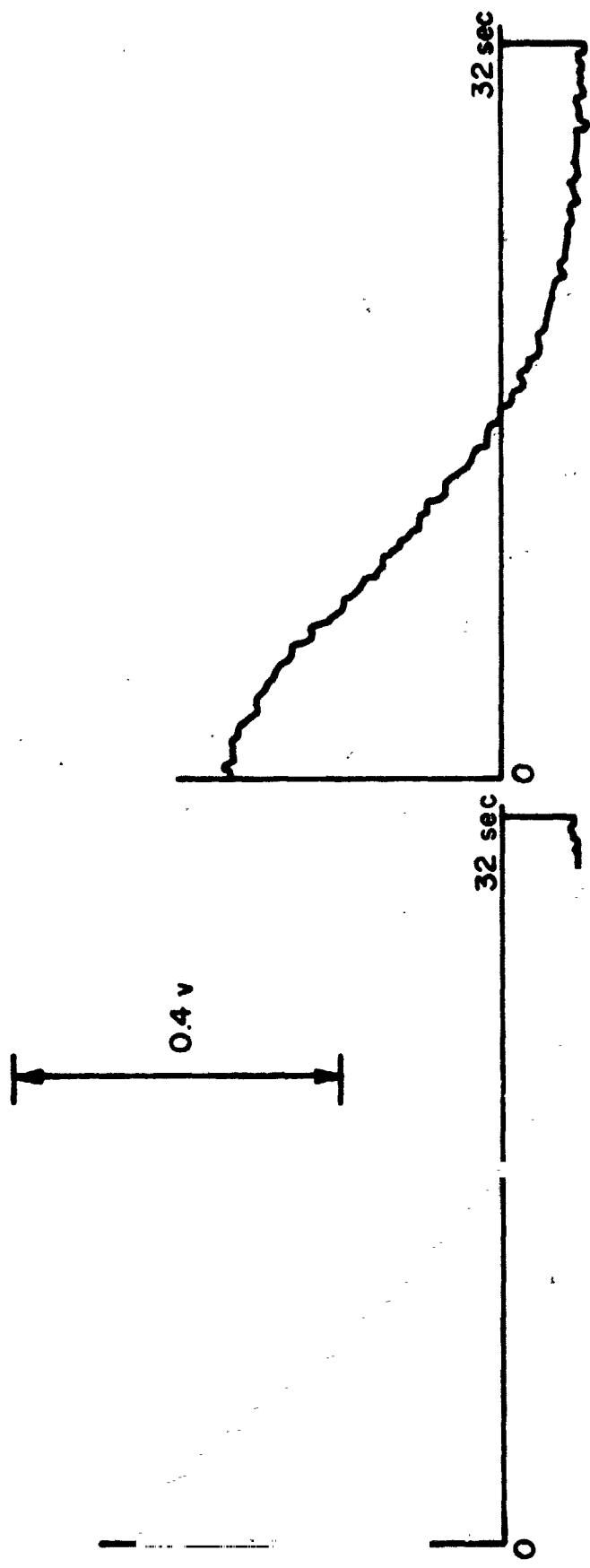


Unit #2 Delayed with Respect to Unit #1

Unit #1 Delayed with Respect to Unit #2

9) Run No. 213  
 Count: 10-98  
 Channels: Unit 1 - #7  
 Unit 2 - #11

Figure 5. Continued

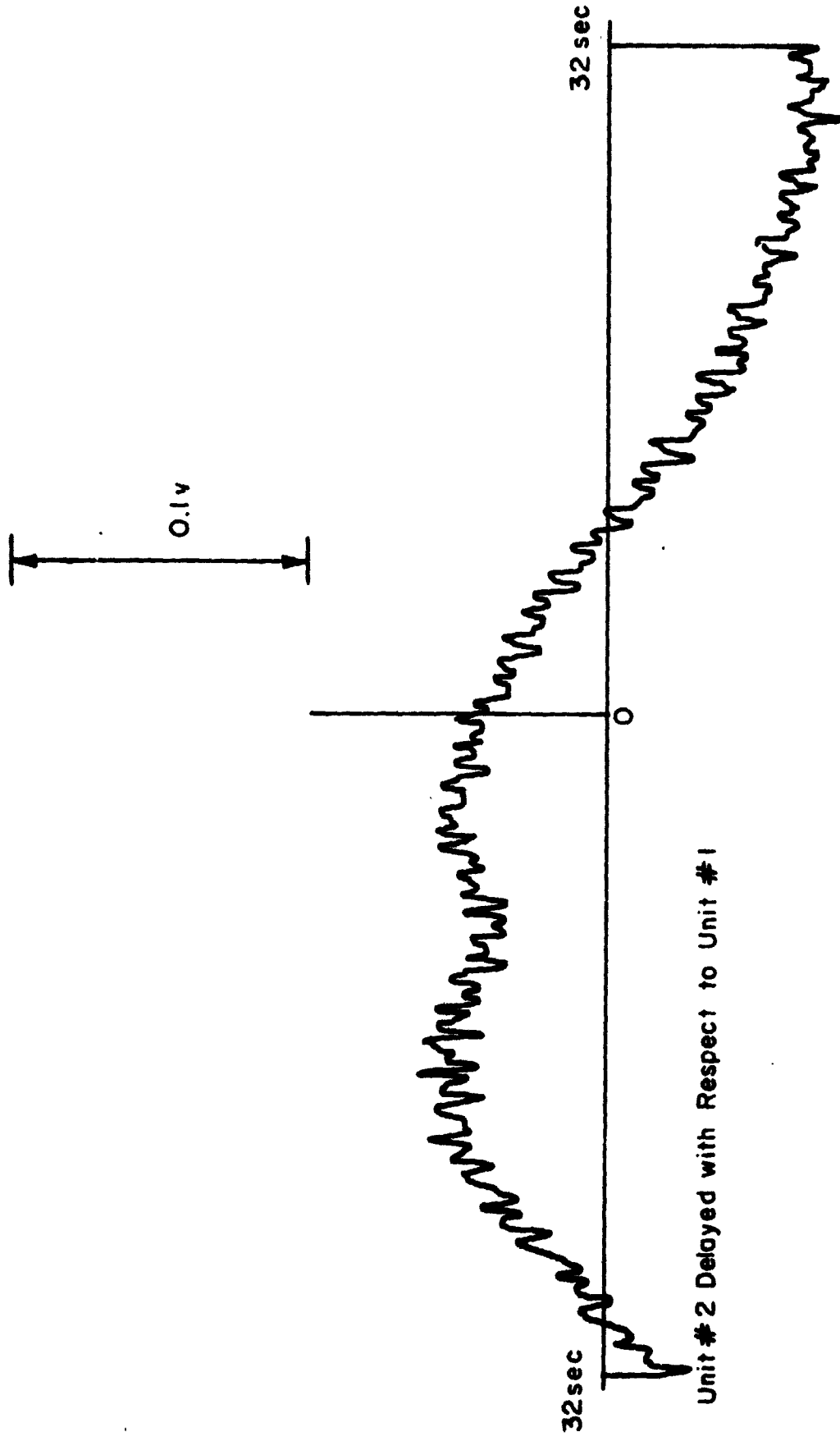


Auto - Correlation Unit #1

Auto - Correlation Unit #2

g) Run No. 213  
 Count : 10 - 98  
 Channels: Unit 1 - #7  
 Unit 2 - #11

Figure 5. Continued



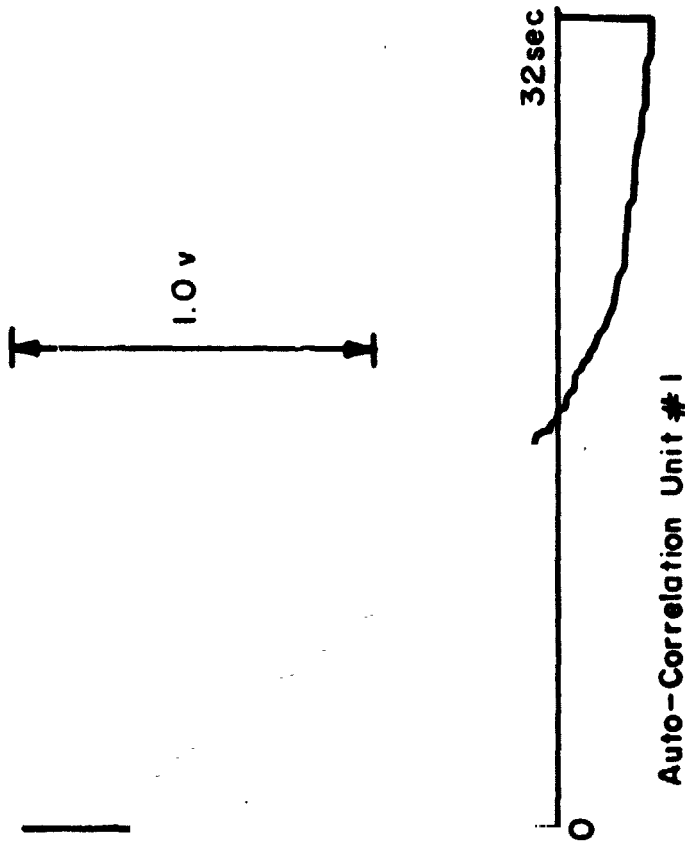
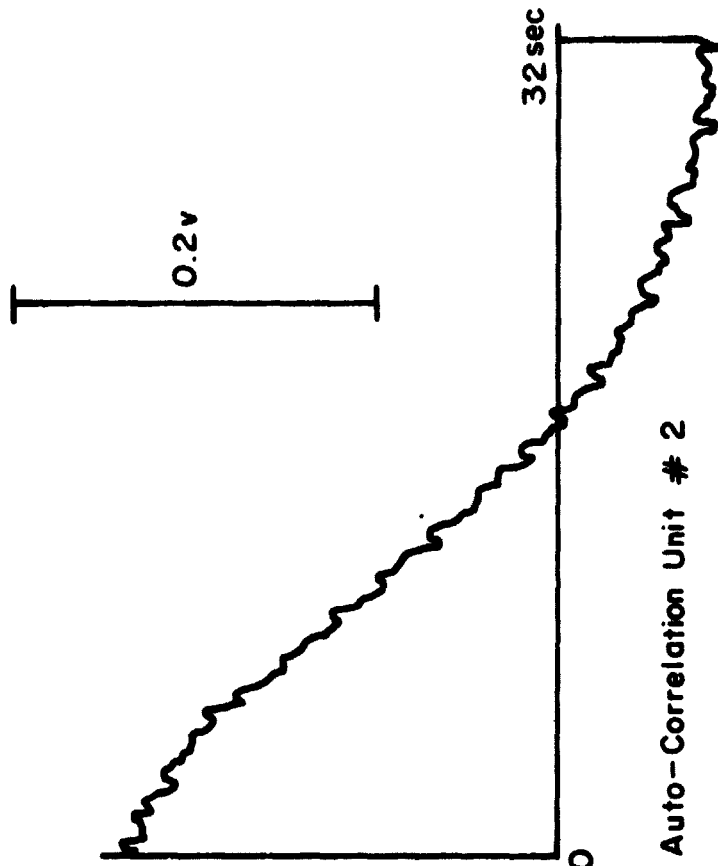
h) Run No. 214

Count: 10-98

Channels: Unit 1 - #7

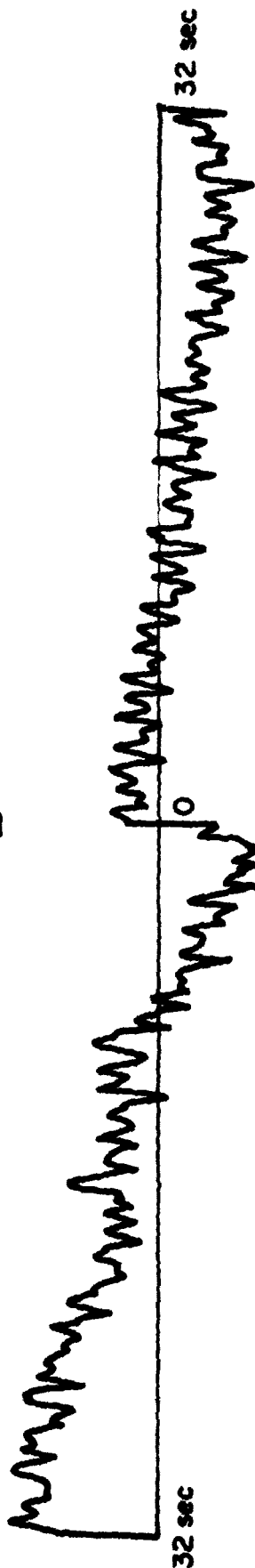
Unit 2 - #11

Figure 5. Continued



h) Run No. 214  
 Count: 10-98  
 Channels: Unit 1 - #7  
 Unit 2 - #11

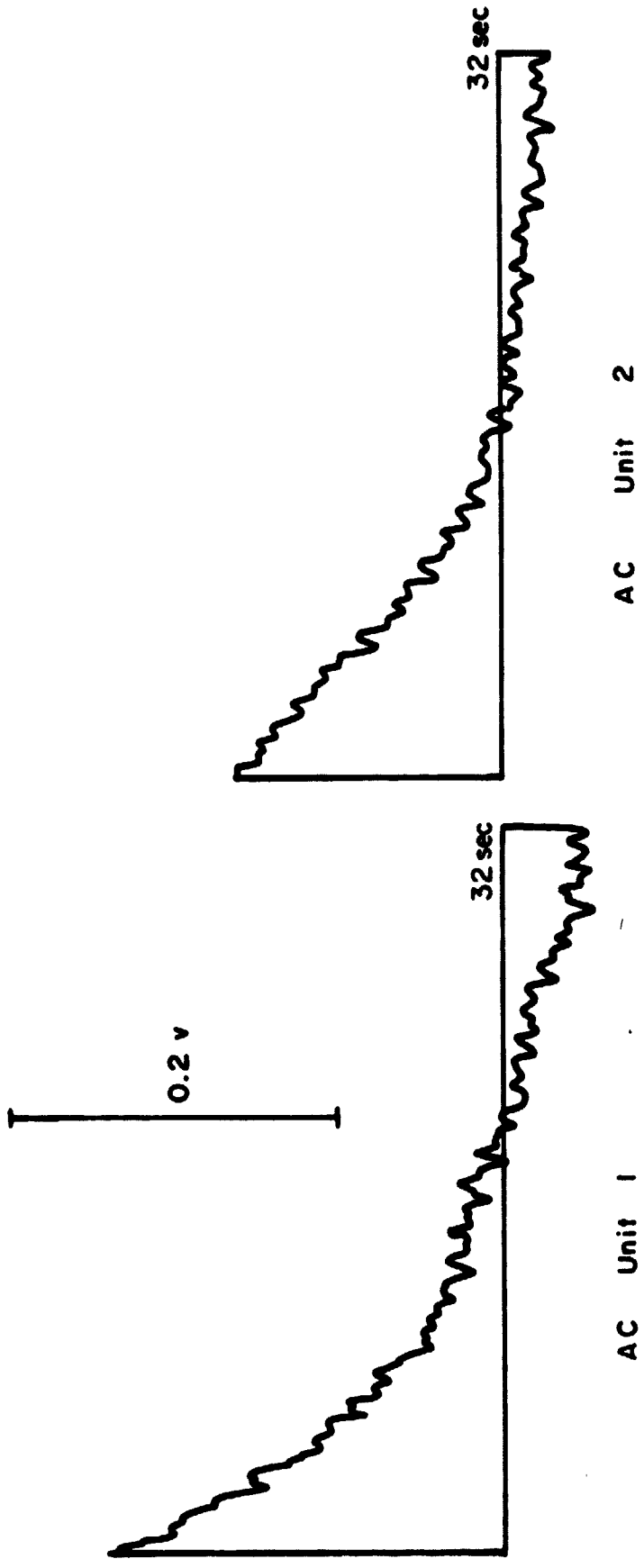
Figure 5. Continued



Unit # 2 Delayed with Respect to Unit 1      Unit 1 Delayed with Respect to Unit 2

i) Run No. 215

Figure 5. Continued



i) Run No. 215

Figure 5. Concluded.

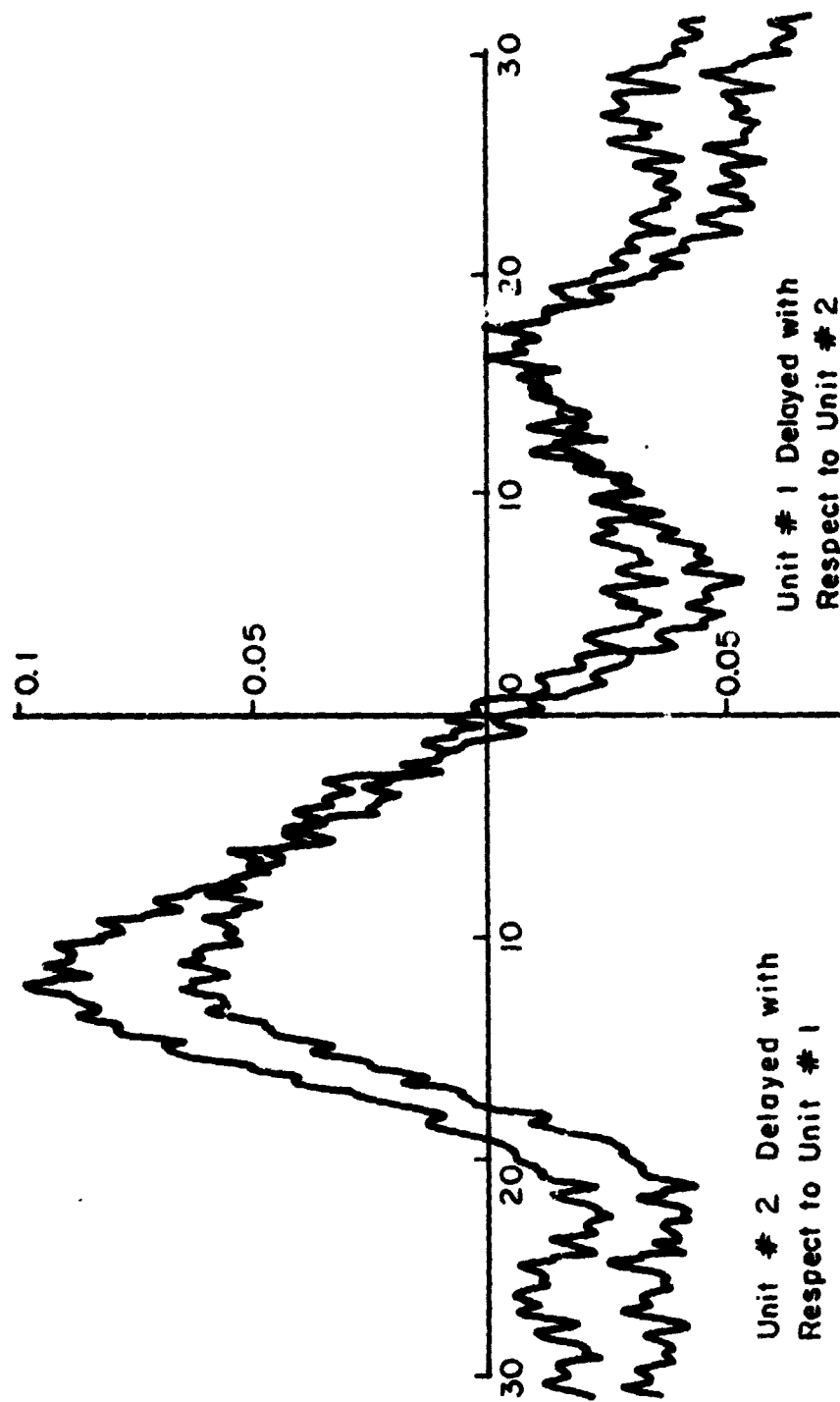


Figure 6. Reproducibility of a Cross-Correlation Curve

$\tau_{max}$	$f_{min}$	$f_{max}$
6.4 sec	0.156 Hz	3.9 Hz
32	0.03	0.8
64	0.00156	0.39
120	0.00625	0.156

Time Delay, seconds

- ..... 32
- 16
- 120
- 64
- ..... 6.4

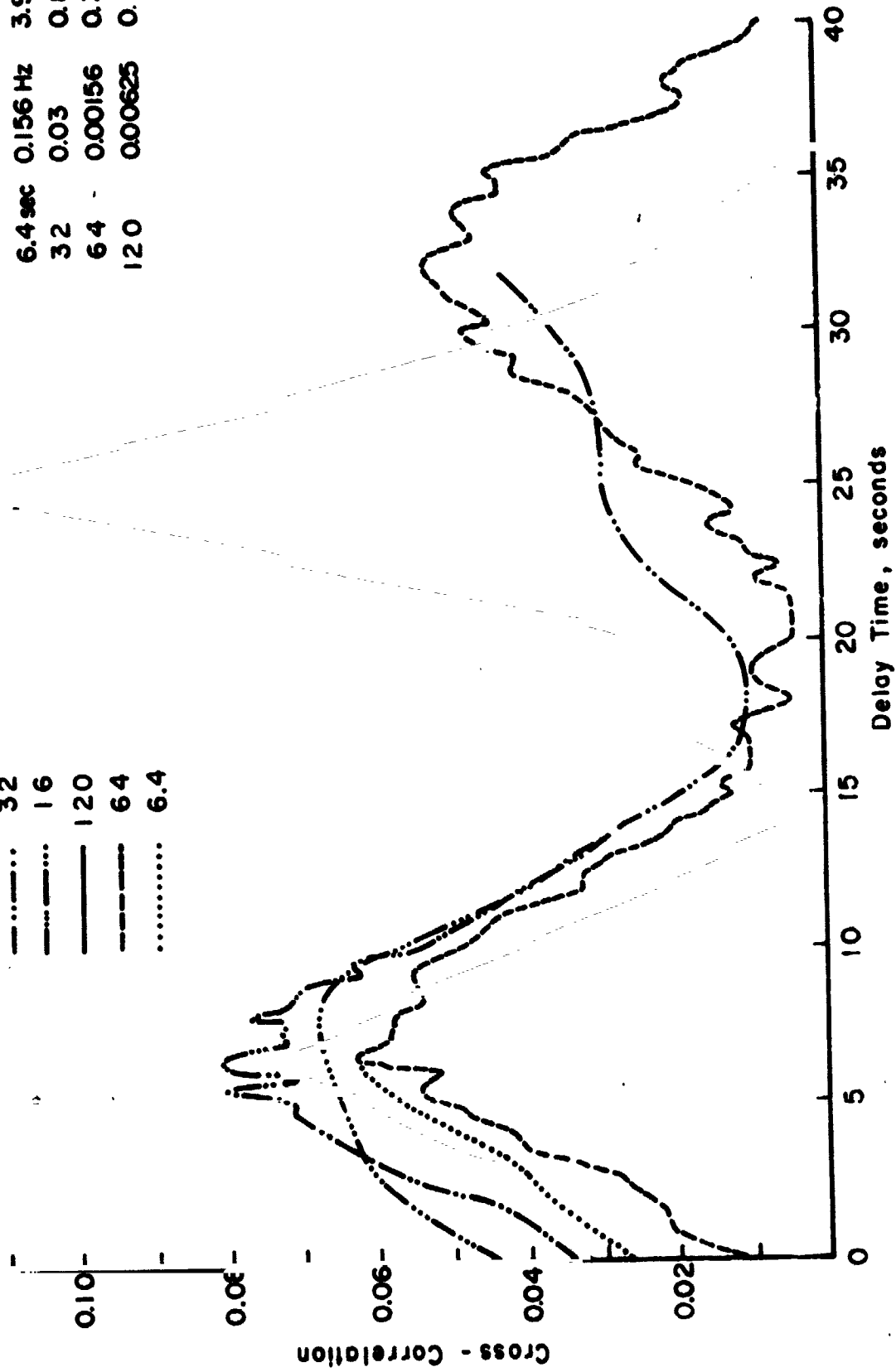
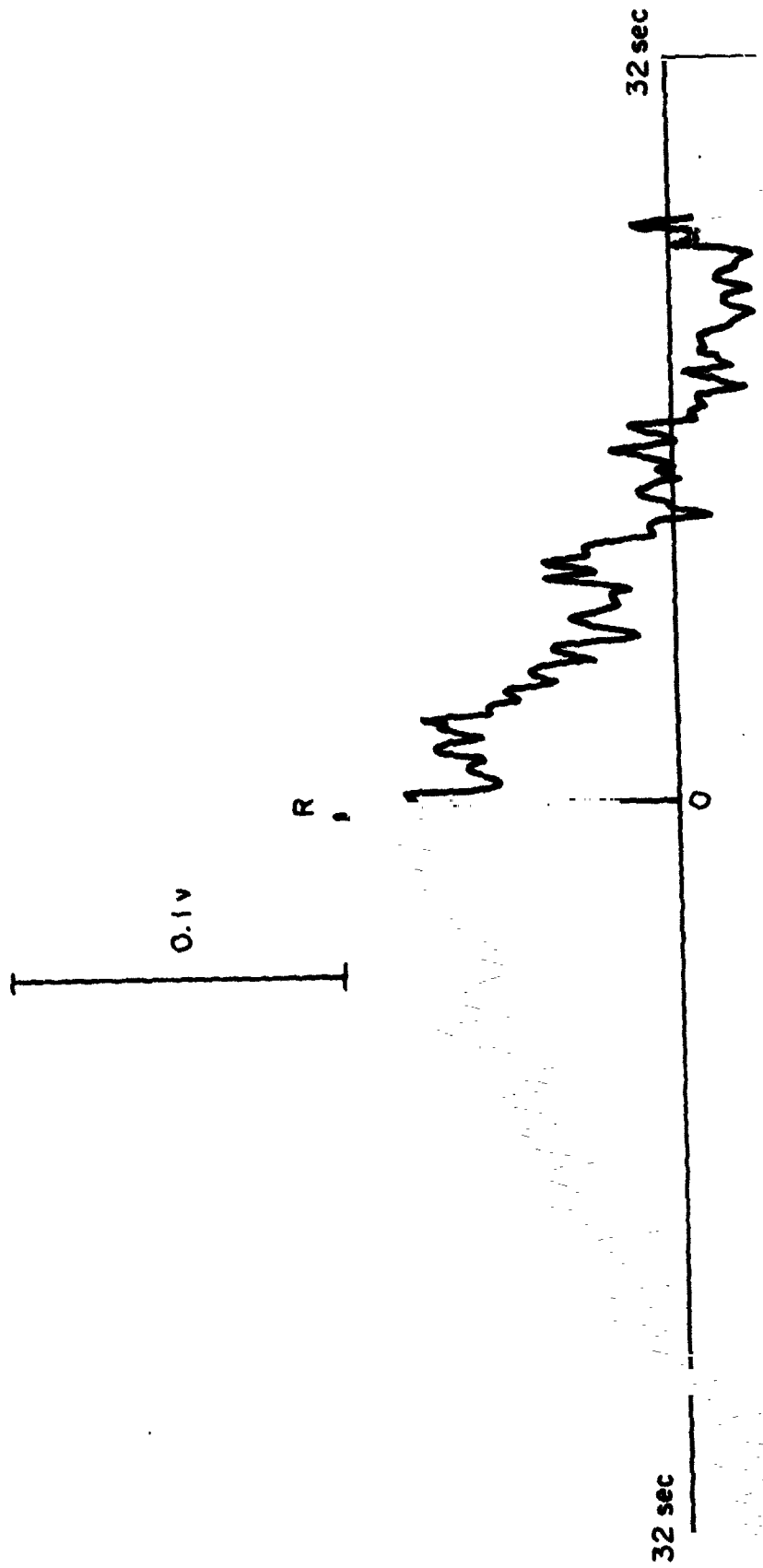


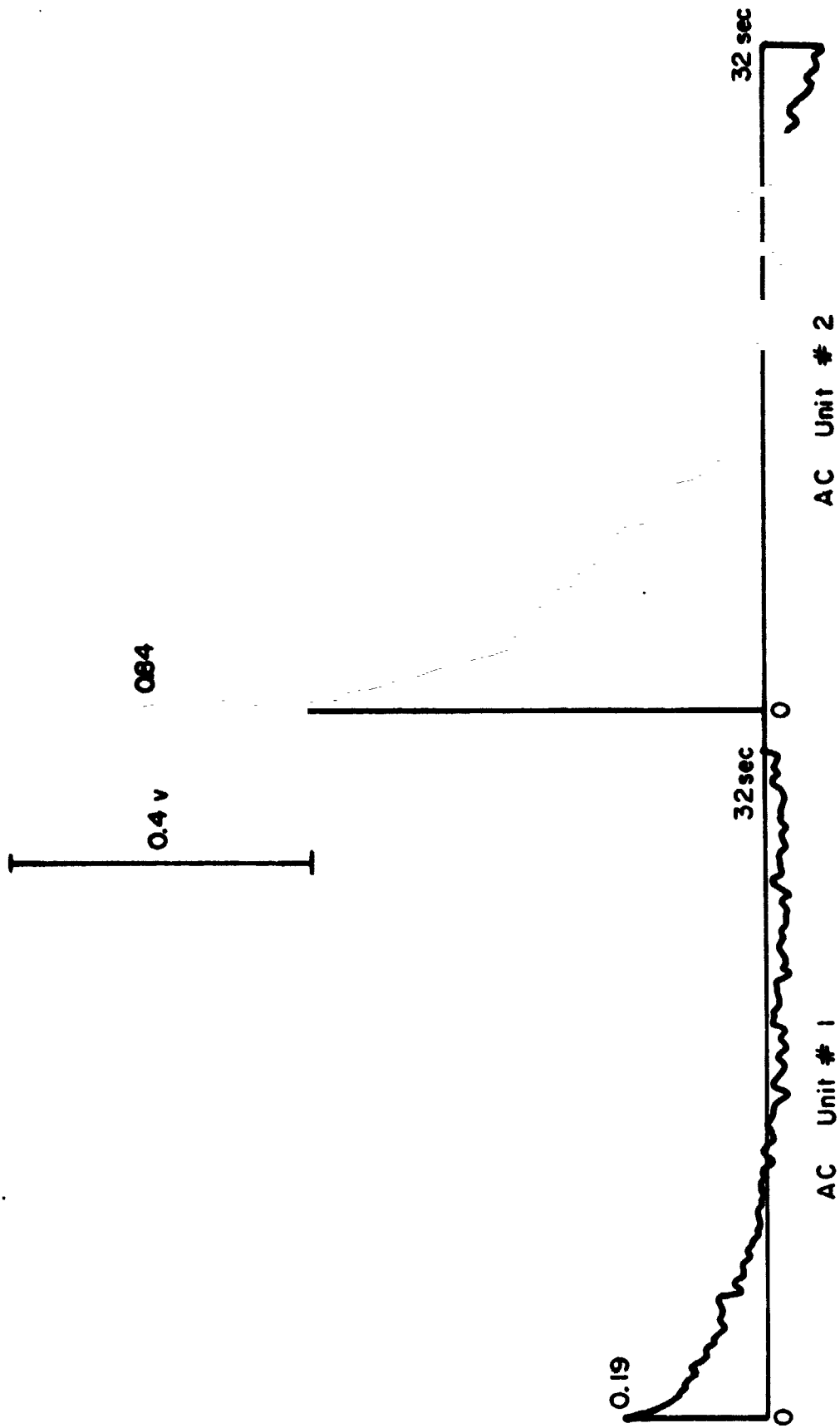
Figure 7. Comparison of a Cross-Correlation for Several Settings of Maximum Time Delay



Unit # 2 Delayed with Respect to Unit # 1  
 Unit # 1 Delayed with Respect to Unit # 2

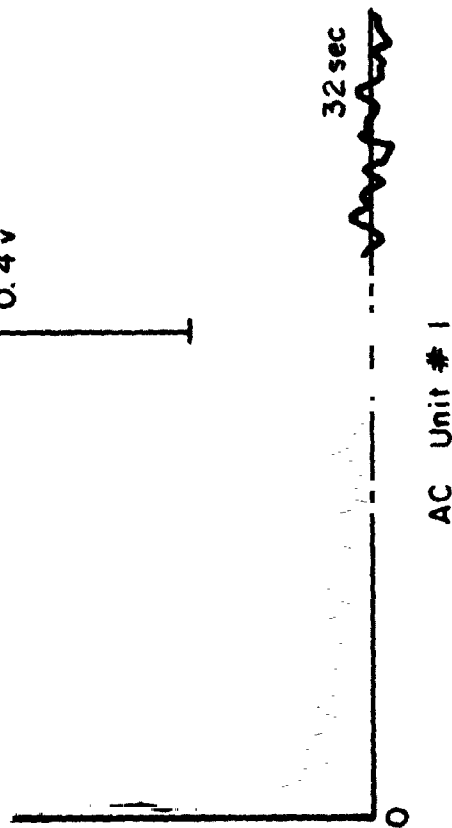
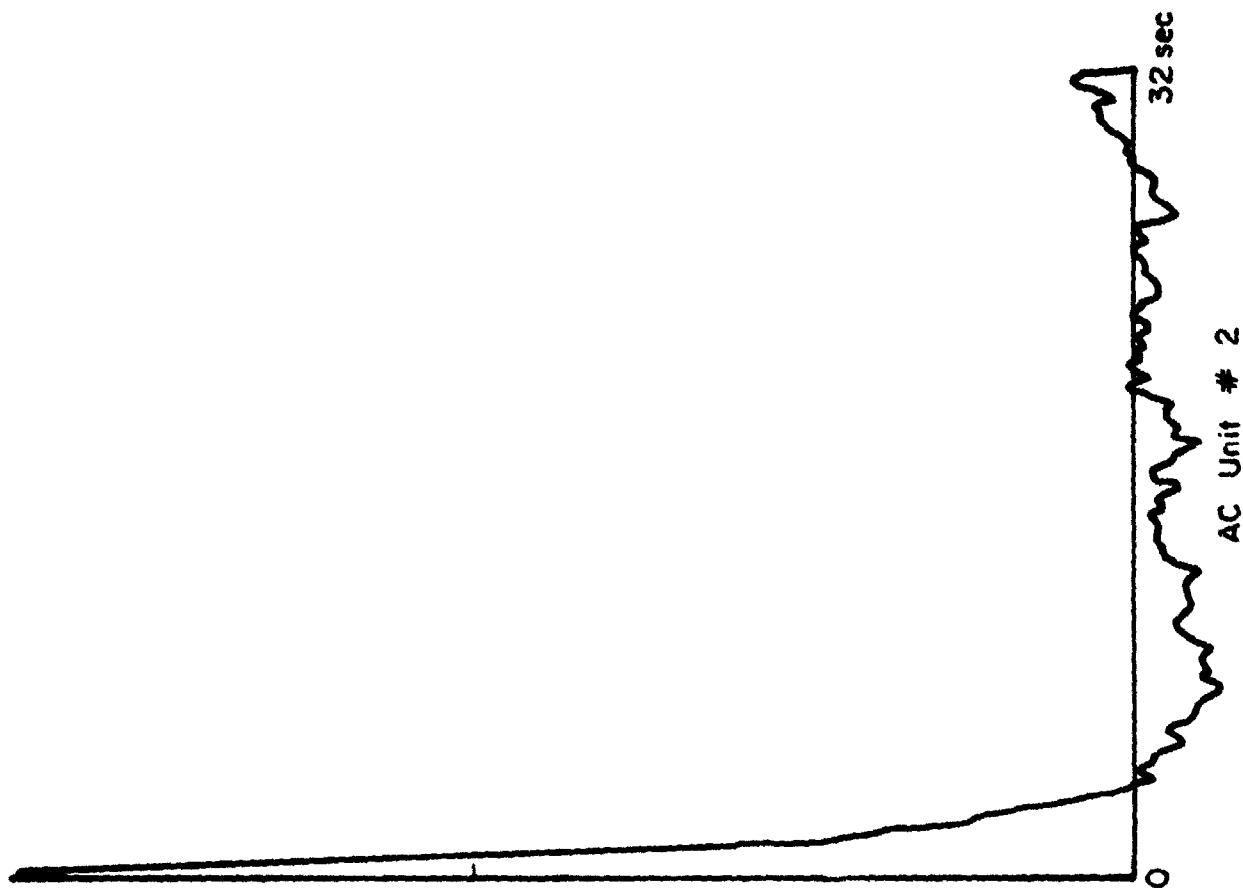
a) Run No. B C 100

Figure 8. Cross- and Auto- Correlation Measurements for Low-Level Intersecting Beams



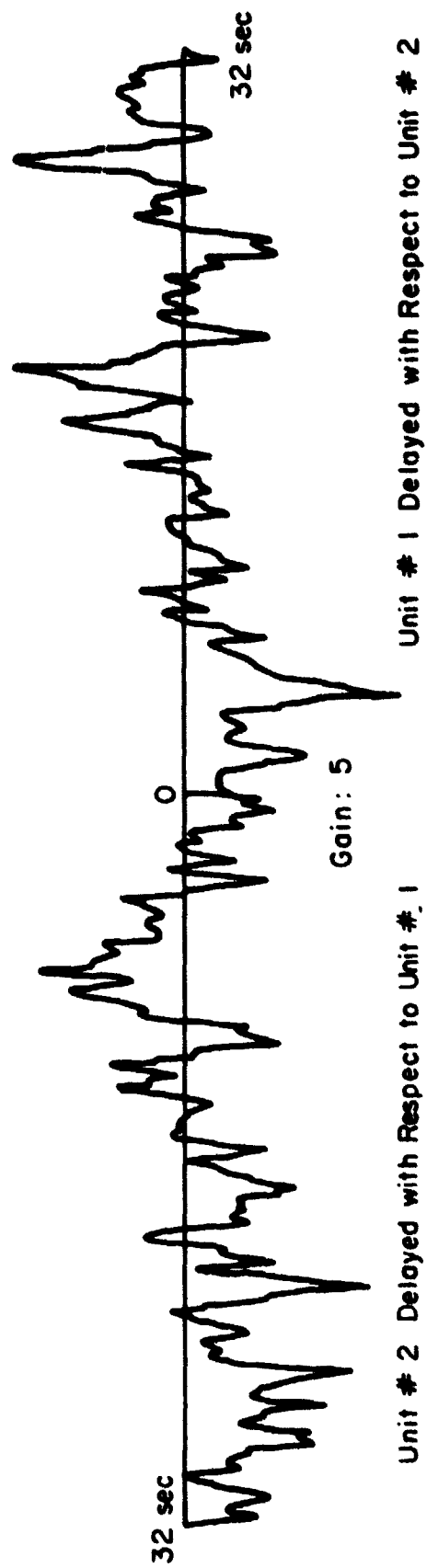
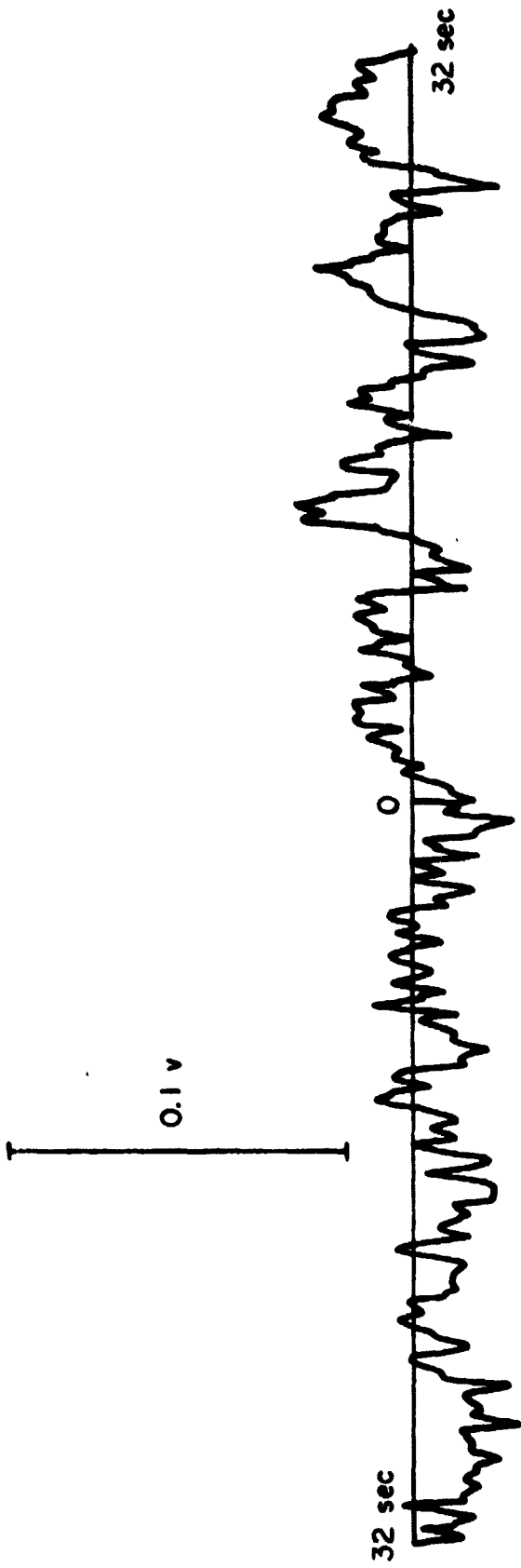
a) Run No. BC 100

Figure 8. Continued



b) Run No. BC 100

Figure 8. Continued



b) Run No. B C 100

Figure 8. Concluded

SECTION V.  
CHECK OUT OF REBUILT OPTICAL CROSS-BEAM UNITS

by

N74-30542

L. I. Huff

V. A. Sandborn

k. E. Cary

5.1 SUMMARY

Preliminary evaluations of limited cross beam data taken with the rebuilt optical cross beam units at the Gun Barrel Hill Test Site of ESSA are presented. The evaluations were made using the analogue Princeton Time Correlator. A study of these evaluations indicates that the rebuilt units are performing satisfactorily. However, there are indications that, in order to obtain useful information from the cross-correlations, it is essential to make judicious choices of computation time and frequency band pass filtering for the analysis of the data.

5.2 INTRODUCTION

Unsuccessful attempts to acquire reliable data with the cross beam optical units during June and July resulted in a decision to have the signal processing electronics rebuilt by IITRI. In August the circuit boards were removed from the units and taken to IITRI for rebuilding. Several components were discovered to be faulty, apparently having failed for unknown reasons. These components were replaced and the signal processing electronics were modified to reflect improvements made possible by increased knowledge of the signal processing requirements. At the same time, IITRI adjusted the circuits for optimum performance. The rebuilt circuit boards were delivered to the Gun Barrel Hill test site and installed in the optical units by IITRI during the first week in September.

### 5.3 EVALUATION OF SIGNALS

Following installation of the rebuilt electronics, several runs (tape numbers X and Y) were recorded to verify operational status of the equipment. Preliminary checks of selected runs indicated that the equipment was operating satisfactorily. Run X-1 was a typical clear sky run with the units looking directly at each other. Run X-2 was a repetition of run X-1 with the low-frequency components of the signal filtered out. Run X-3 was a repetition of run X-1 with a heavy cloud cover. All three of these runs were made with black targets blocking the background. Two of the runs (X-4 and X-5) were recorded at night with both units looking at a high-intensity light bulb located on the line of sight between the units and equidistant from the two units. As anticipated, both units displayed a large 120 Hz component due to the fact that the light bulb was powered by a 60 Hz voltage. On run X-4 relatively large variations in the signal were observed which were apparently due to line voltage variations. Accordingly, on run X-5 the band-pass filters on the units were adjusted for 0.01 Hz to 10 Hz to reduce the 120 Hz component of the signal, and the high-intensity lamp was powered from the output of a voltage regulator to reduce the effects of line voltage variation. The final run (X-6) on tape X was recorded as a simulator run on unit #2. For this run the photo diode was disconnected and a signal generated by a simulator supplied by IITRI was inserted in its place.

Tape Y contains the records of three clear sky runs. The first of these (Y-1) was recorded with the beams intersecting at tower height (48.2 meters). Run Y-2 was recorded with the beams aimed in skewed directions and run Y-3 with the units looking directly at each other. Table I presents a summary of these runs, and Figure 1 shows the location of the units relative to the tower during the runs.

## 5.4 RESULTS

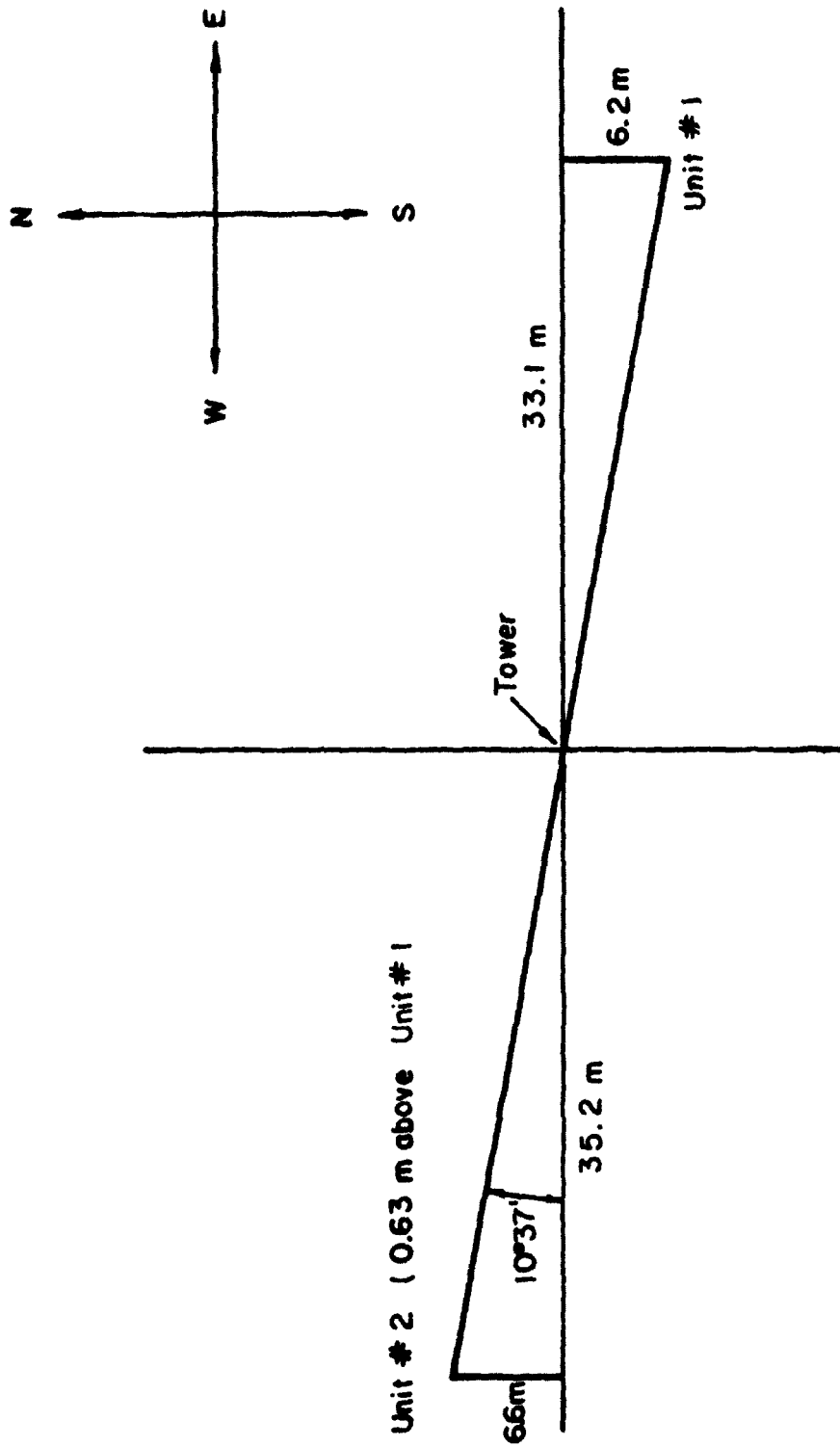
Figures 2 through 9 present the results of preliminary analogue auto-and cross-correlations of the runs described above. These correlations were obtained with the Princeton Time Correlator. Figure 2 shows a definite peak in the cross-correlation curve with a nearly zero time delay and a maximum correlation of almost 40%. Figures 3 a, b and c present the effects of cutting out the low frequency components and using different computation periods. Note that there is still a clear peak at nearly zero time delay but that the maximum correlation has now been reduced to approximately 4%. The effect of a heavy cloud cover is presented in figure 4. It is no longer possible to detect a single clearly defined peak in the cross-correlation curve. Figure 5 presents a preliminary correlation for the first night run (X-4). The cross-correlation curve shows a very definite peak of large magnitude with zero time delay. There is some doubt, however, about the scale for this figure since the maximum cross-correlation is greater than 1. It was not possible to check this correlation because both types X and Y were sent to Marshall Space Flight Center shortly after the preliminary evaluations were completed. Figures 6 a and b show the correlations of run X-5 with two different computation periods. Again, there is a distinct peak in the cross-correlation curve at zero time delay. The maximum correlation of between 20% and 25% is unexpectedly low.

Preliminary correlations for runs Y-1, Y-2 and Y-3 are present in figures 7, 8 and 9. In figure 7 there appears to be a strong positive correlation with a time delay of between 15 and 16 seconds, and there does not seem to be any logical explanation for this phenomenon. There also appears to be a strong negative correlation in figure 8 with a time delay of between -2 and -3 seconds for which no logical explanation can be offered. Figure 9 shows two distinct positive peaks and two distinct negative peaks of about the same magnitude in the cross-correlation curve. Again, no logical interpretation of these peaks is forthcoming. It should be noted here, however, that there was some question as to whether or not the units were aimed directly at each other on run Y-3.

TABLE I

CROSS-BEAM CHECK OUT RUNS AT GUN-BARREL HILL

Tape	Run No.	Sky Cond.	Wind Info.	Beam Separation	Approx. Altitude	Remarks
X	X-1	Clear	?	0	0	Bandwidth 0.1-10HZ Optical Filters Black Targets
	X-2	Clear	?	0	0	Bandwidth 1.0-10HZ Optical Filters Black Targets
	X-3	Heavy cloud cover	?	0	0	Bandwidth 0.01-10 HZ. Black Targets
	X-4	Night run	?	0	0	Bandwidth 0.01-30 HZ
	X-5	Night run	?	0	0	Bandwidth 0.01-10 HZ
	X-6	Simulator run on Unit #2 Simulator rate 2, Modulation 4%				Bandwidth 0.01 -10HZ
Y	Y-1	Clear	Gusts(S.E.)	0	48.2m	Bandwidth 0.01-10HZ
	Y-2	Clear	Light(E.-S.E.)	-	-	Bandwidth 0.01-10HZ Beams not intersecting
	Y-3	Clear	Moderate(E.S.E.)	0	0	Bandwidth 0.01-10HZ Hot wire @ 10 ft.level Recorded on Ch.#7



Unit # 2 ( 0.63 m above Unit # 1

Figure 1. Gun-Barrel Test Site No. 2.

Low-pass : 320 cps  
100 sec Averaging Time  
Playback @ 60ips

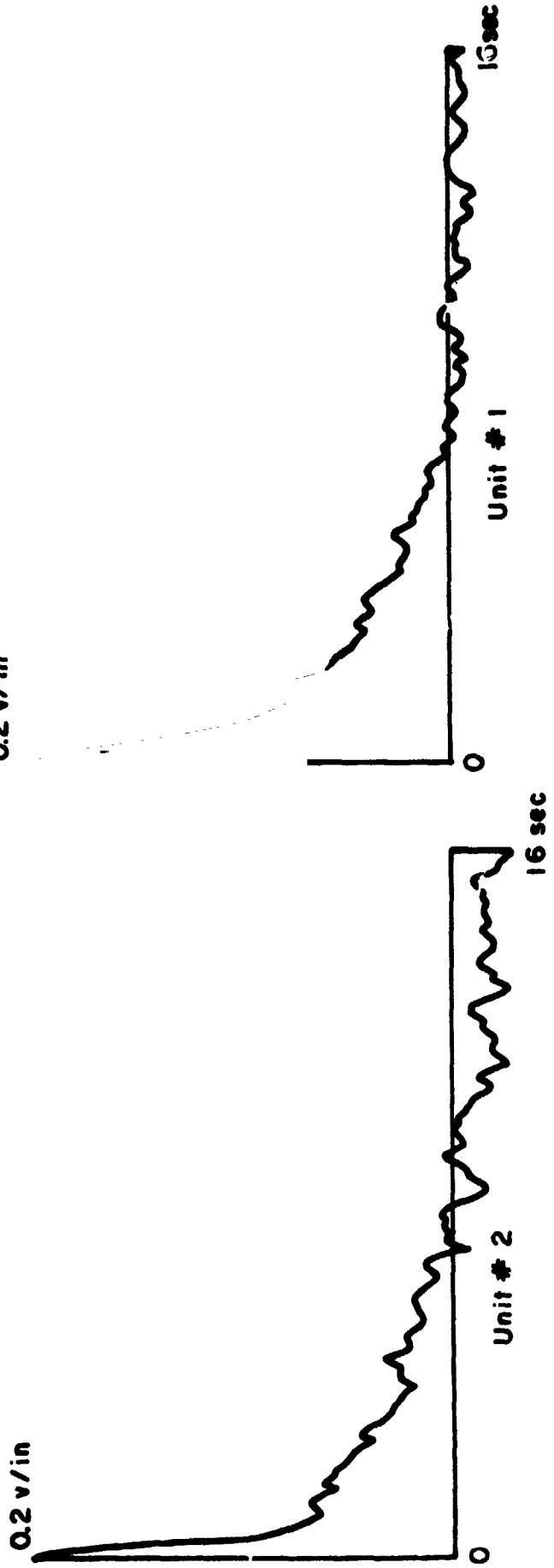
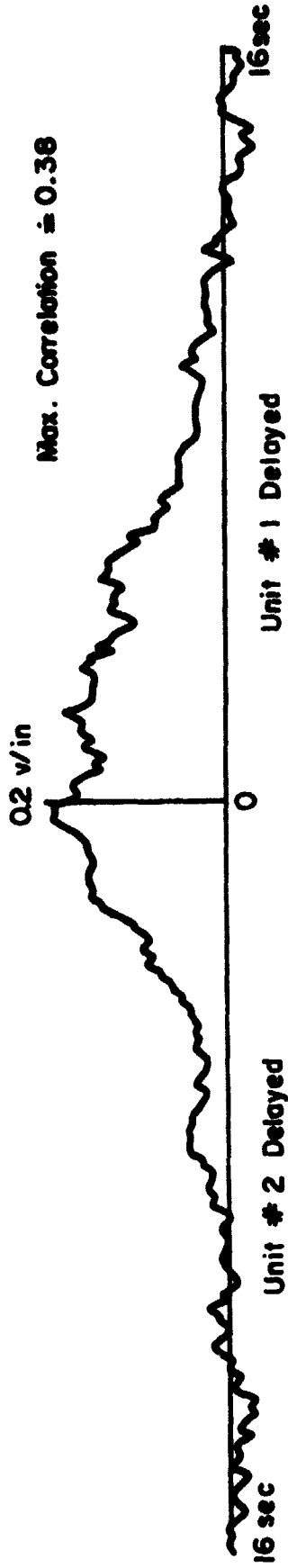
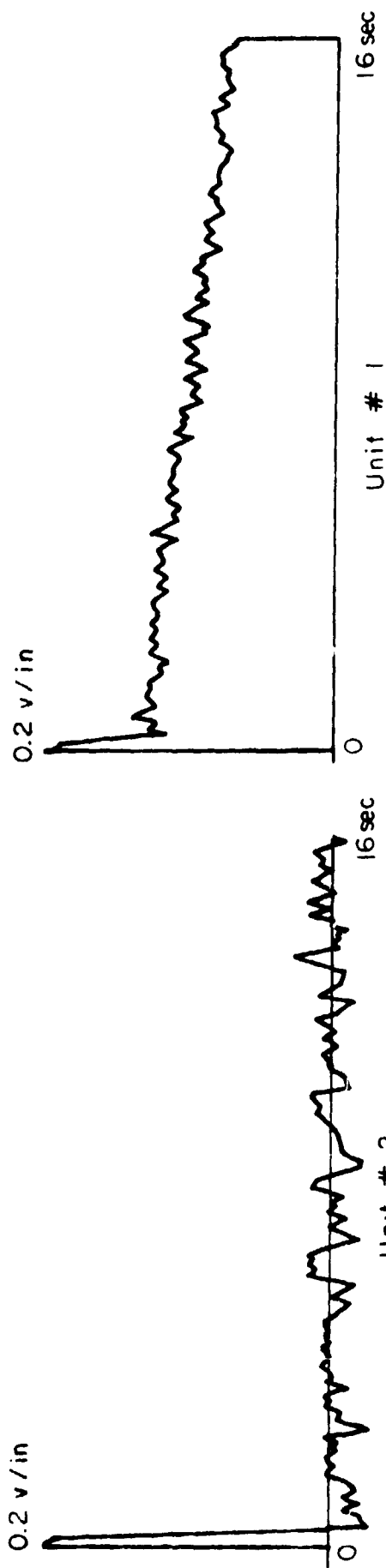
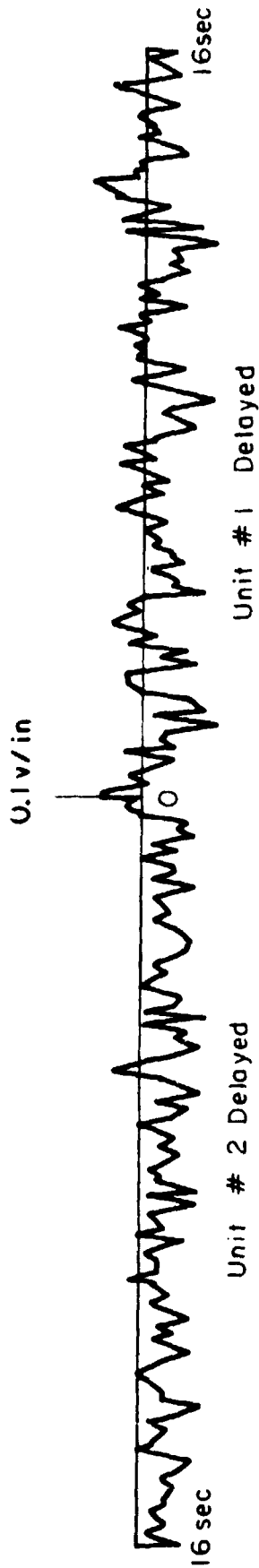


Figure 2. Cross- and Auto-Correlations for Run No. X-1.

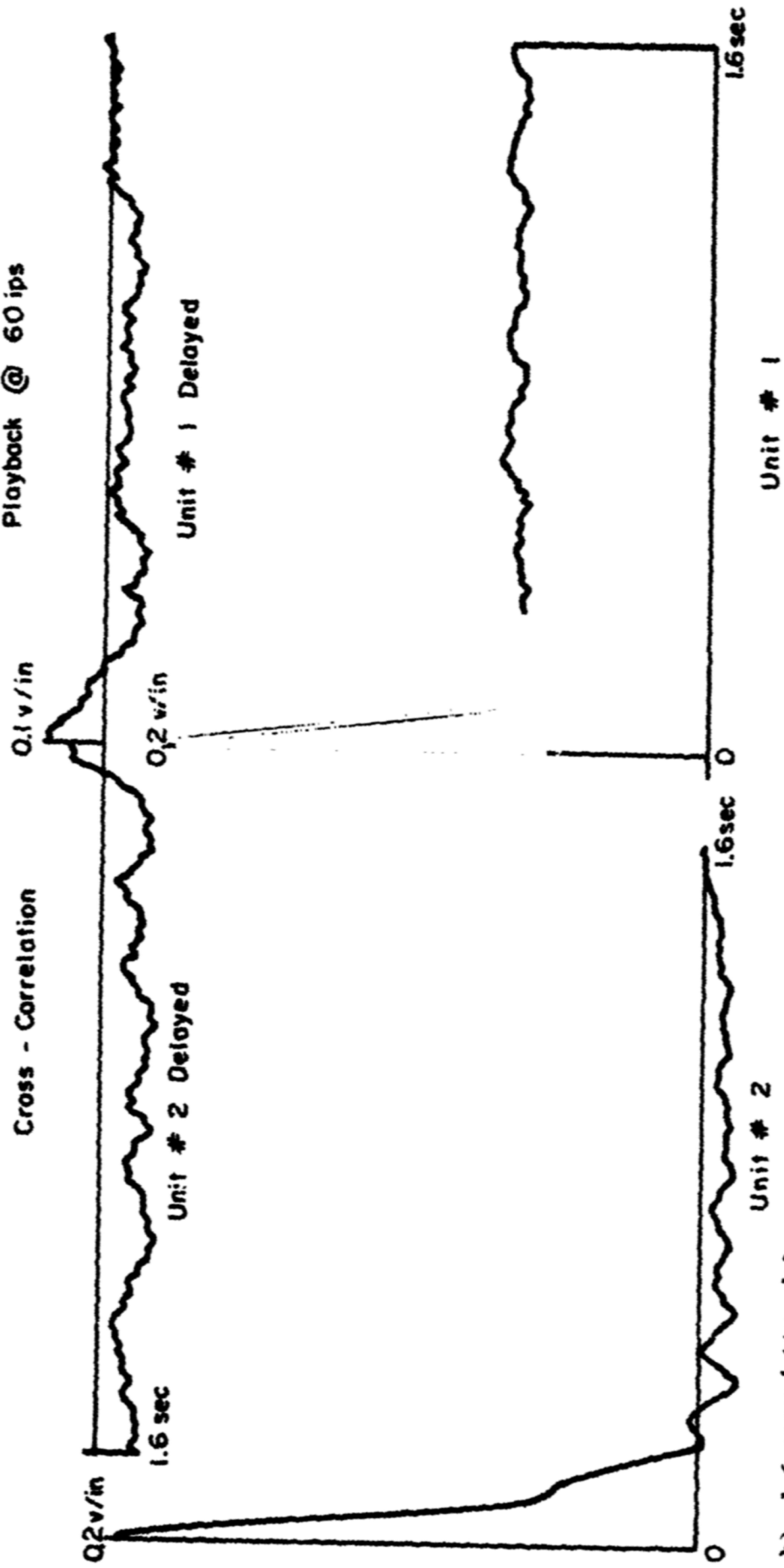
Low-pass: 320 cps  
 100 sec Averaging Time  
 Playback @ 60 ips



a) 16 second time delay

Figure 3. Cross-and Auto-Correlations for Run No. X-2.

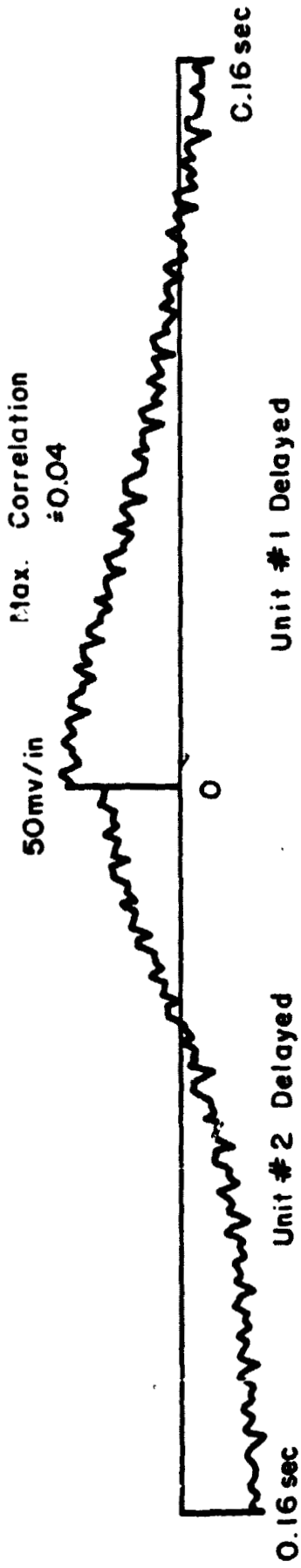
Low-pass : 320 cps  
100 sec Averaging Time  
Playback @ 60 ips



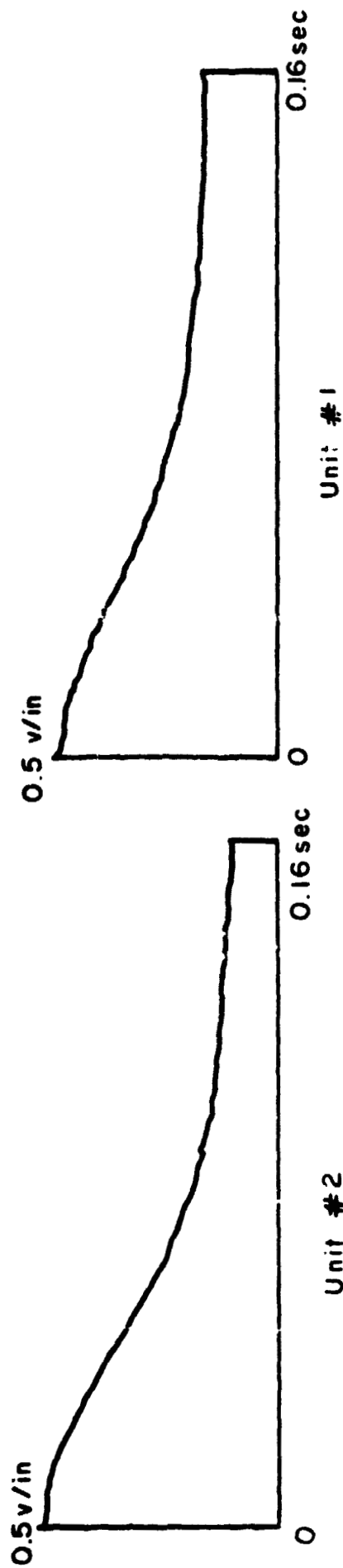
b) 1.6 second time delay

Figure 5 continued.

Low-pass : 320 cps  
 100 sec Averaging Time  
 Playback @ 60 ips



Cross - Correlation

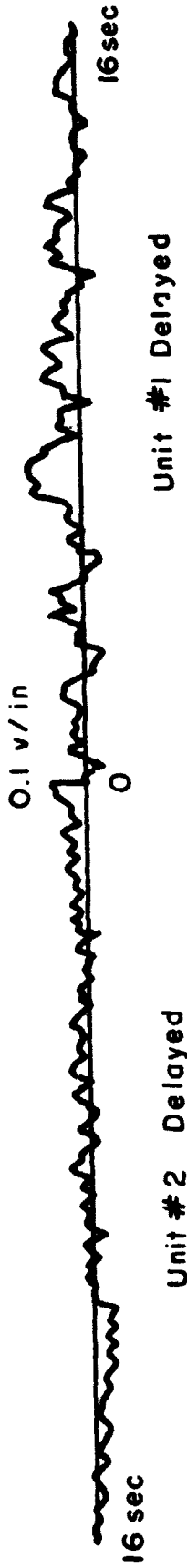


c) 0.16 second time delay

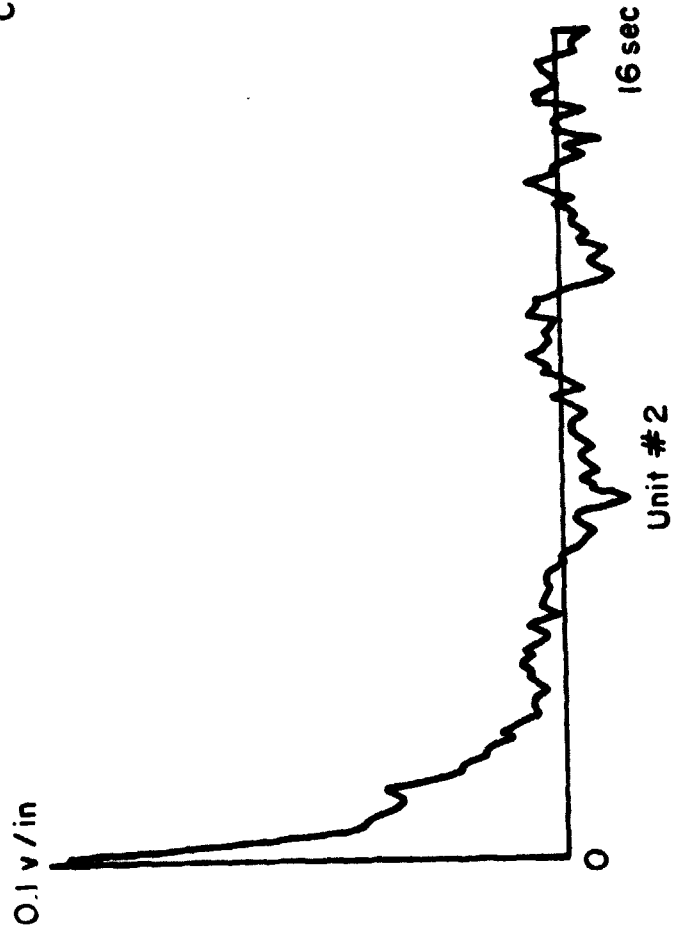
Auto - Correlation

Figure 3 Concluded.

Low-pass: 320 cps  
100 sec Averaging Time  
Playback @ 60 ips



Cross-Correlation



Auto-Correlation

Figure 4. Cross- and Auto-Correlations for Run No. X-3.

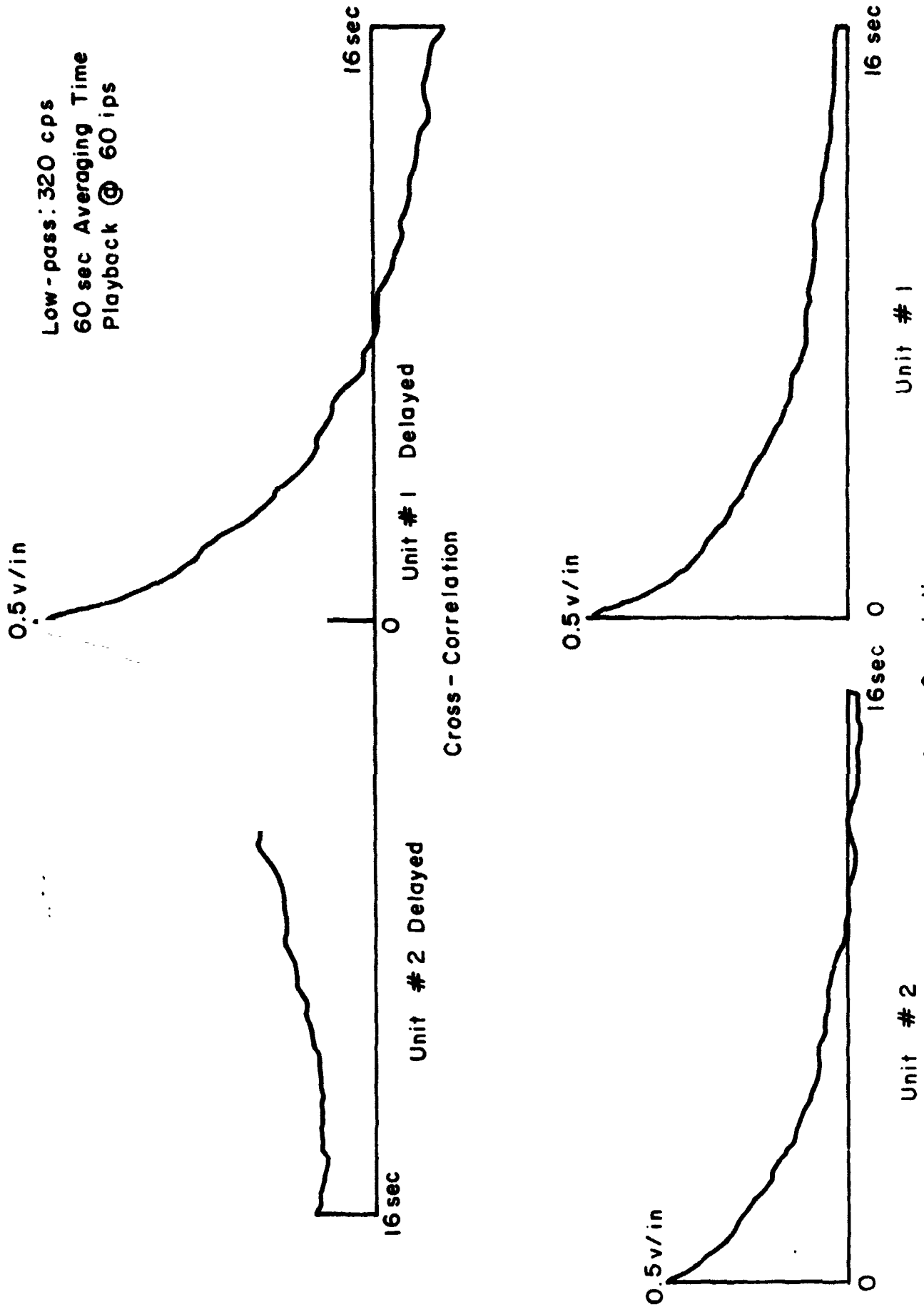
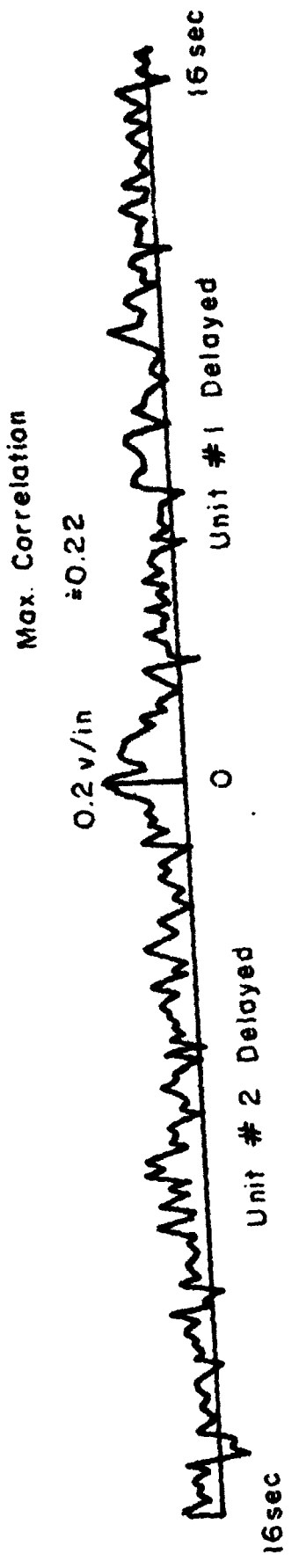
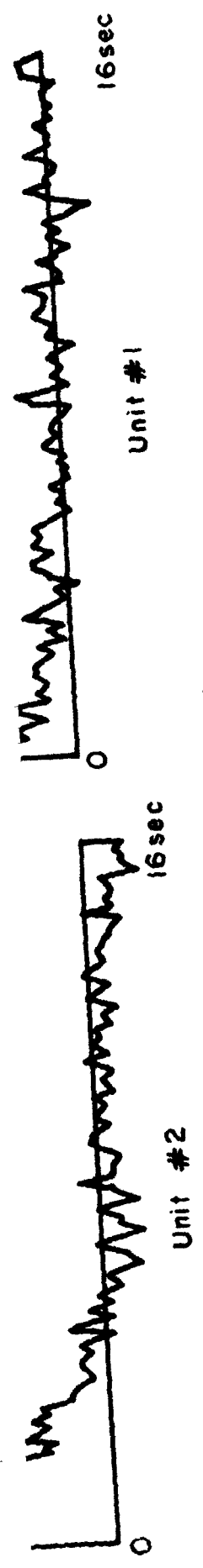


Figure 5. Cross- and Auto-Correlations for Run No. X-4.

Low-pass: 320 cps  
55 sec Averaging Time  
Playback @ 60 ips



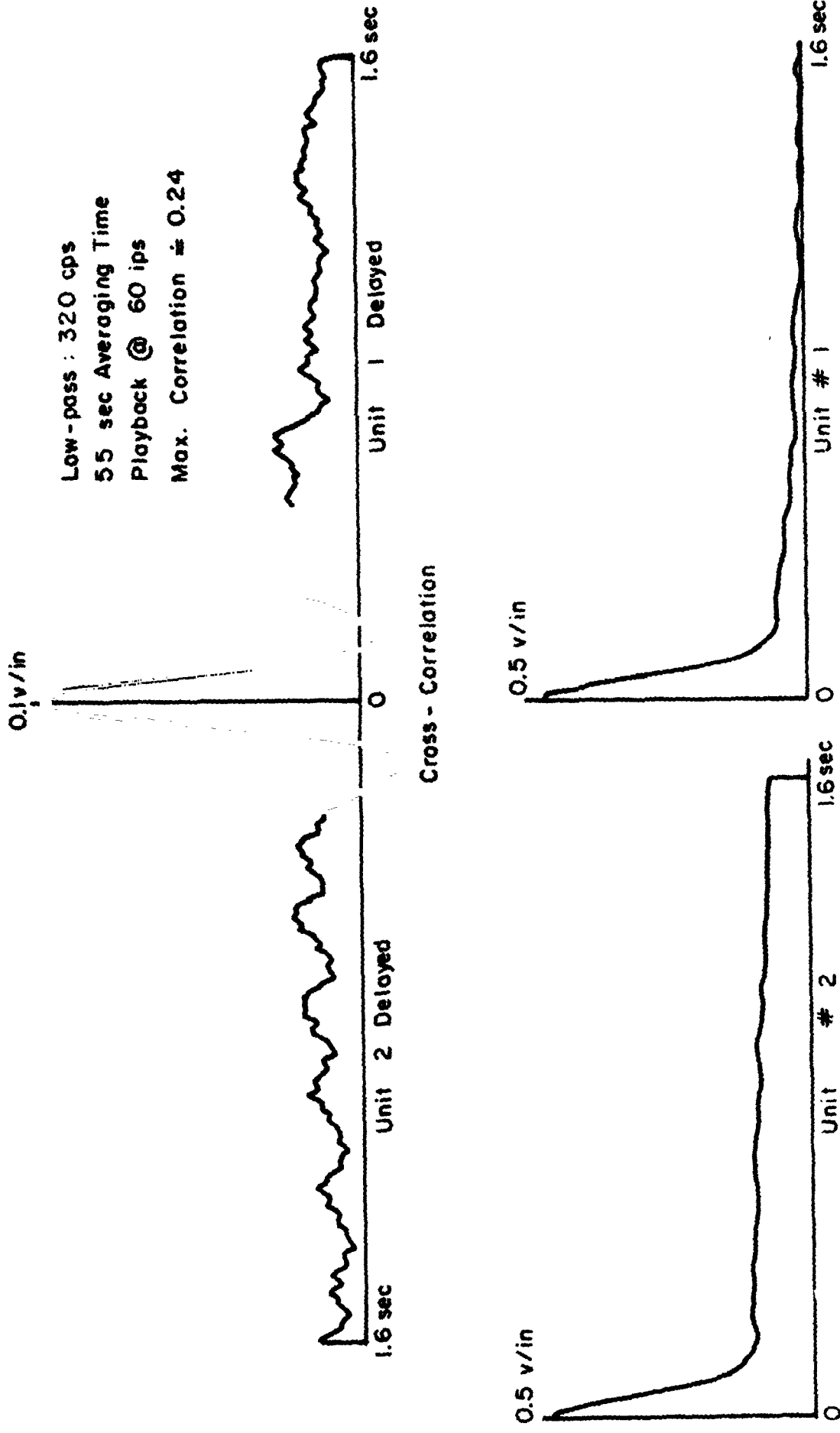
Cross - Correlation



Auto - Correlation

a) 16 second time delay

Figure 6. Cross- and Auto-Correlations for Run No. X-5.



b) 1.6 second time delay

Figure 6 Concluded.

Low-pass : 320 cps  
100 sec Averaging Time

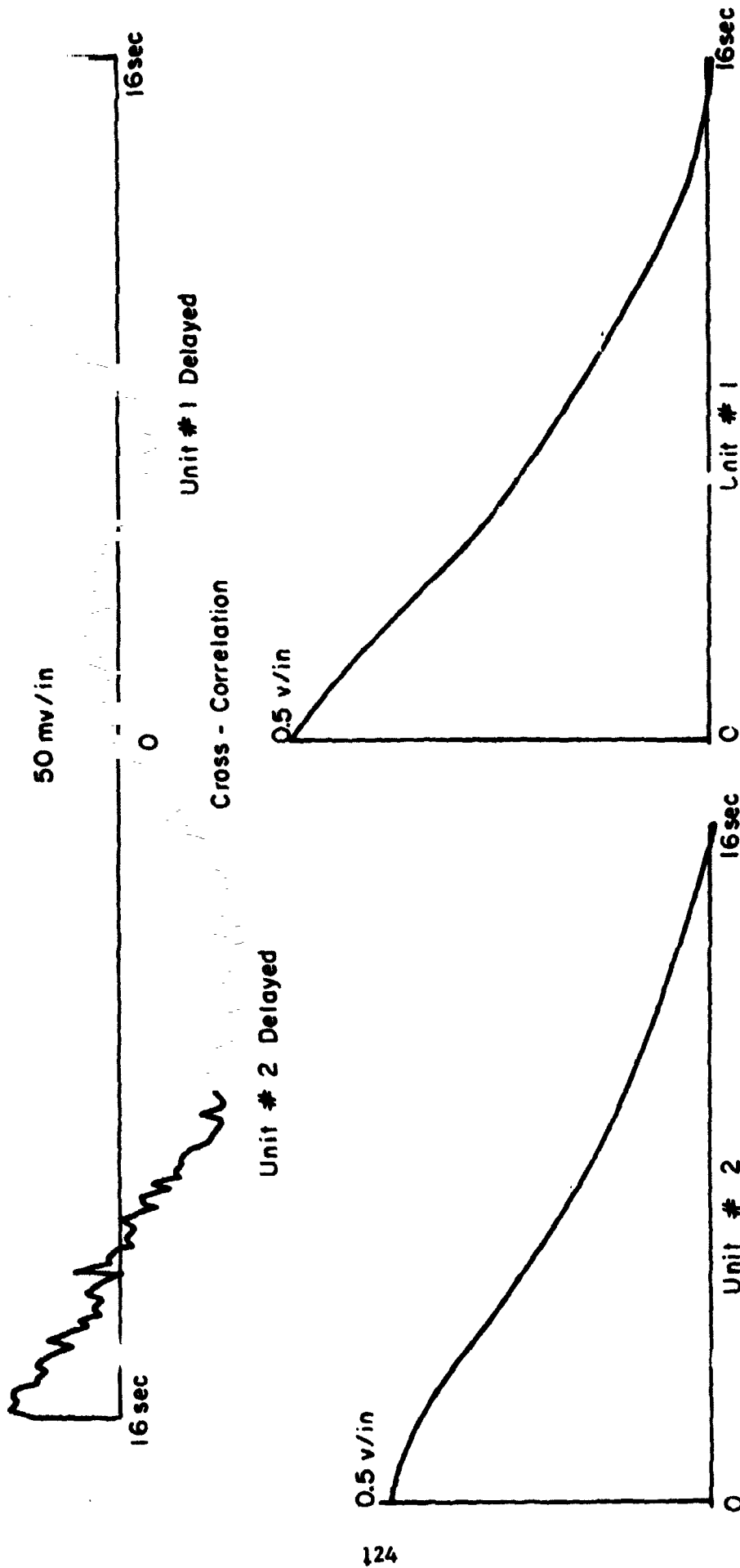
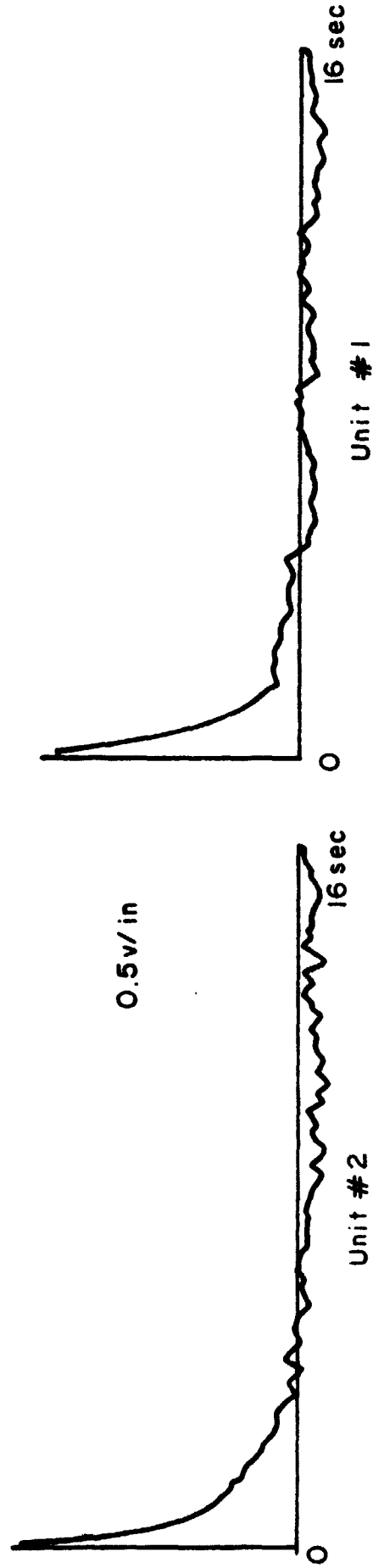


Figure 7. Cross- and Auto-Correlation for Run No. Y-1.

Low-pass : 320 cps  
100 sec Averaging Time



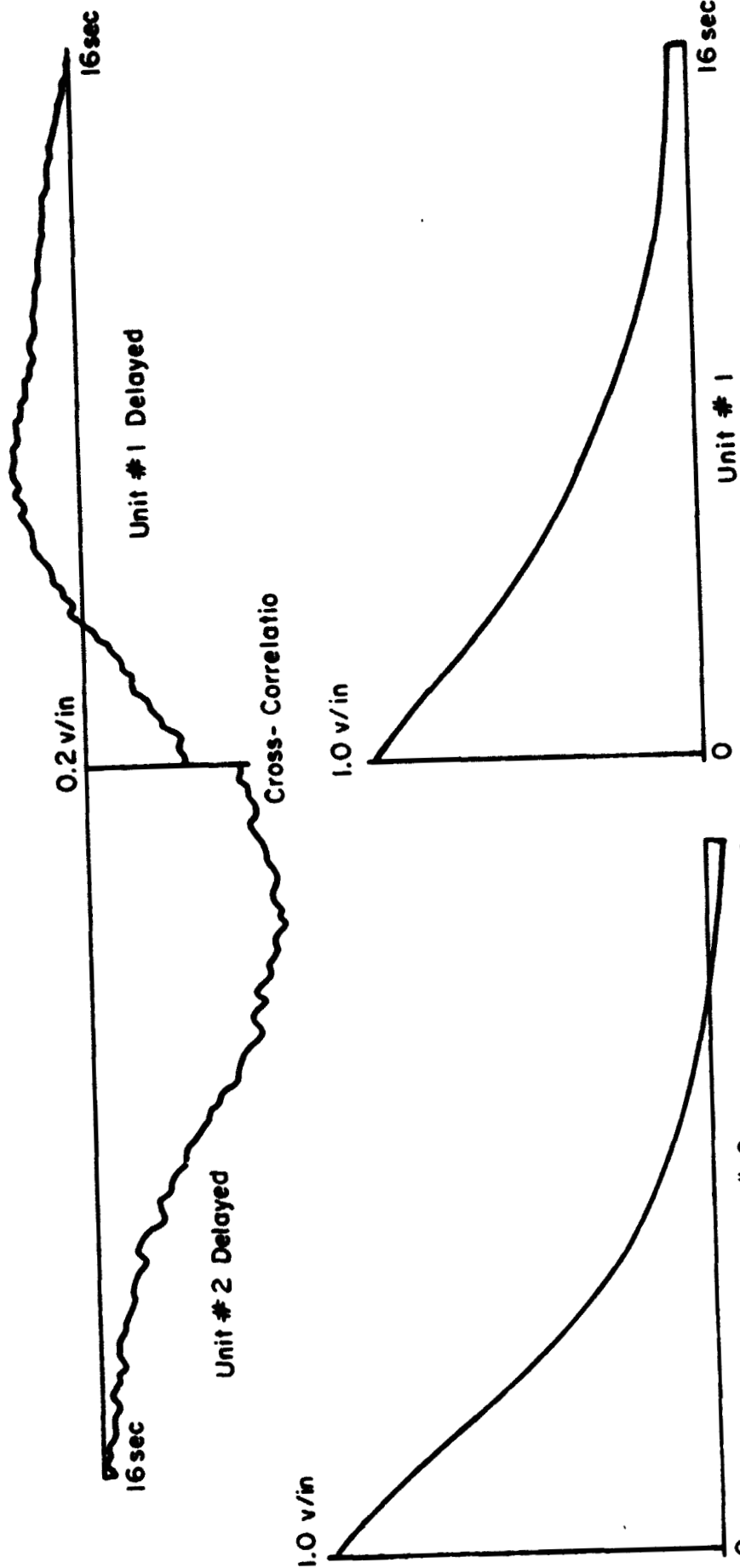
Cross - Correlation



Auto - Correlation

Figure 9. Cross- and Auto-Correlation for Run No. Y-3.

Low-pass : 320 cps  
100 sec Averaging Time



Auto - Correlation

Figure 8. Cross- and Auto-Correlation for Run No. Y-2.

n74-35043

**SECTION VI.**  
**OPTICAL CROSS BEAM FIELD TESTS AT ESSA**  
**HASWELL FIELD SITE, OCTOBER 1969**

by

V. A. Sandborn

**SUMMARY**

A series of tests with both the visible and IR optical cross beam systems was made at the Haswell, Colorado, Field Site of ESSA between October 4 and 8, 1969. This memorandum covers only the details of the test setup and runs. The data obtained from the tests have not as yet been analyzed.

**6.2 INTRODUCTION**

A joint field test program was undertaken by ESSA at a 164 meter (500 foot) meteorological tower located at Haswell, Colorado. The tower was instrumented with wind sensors, temperature sensors, fluctuating wind and temperature sensors and humidity sensors. The sensors were located at three elevations: 42, 192 and 162 meters. A movable elevator was also instrumented and could be positioned at any desired location along the tower height. The main object of the cross beam studies was to compare the visible and IR systems. The instruments were also arranged so that direct comparison with the sensors on the tower can be made.

**6.3 TEST CONDITIONS**

Two physical arrangements of the visible optical units were employed in the tests. Similar arrangements were employed for the IR units. Figure 1 is a diagram of the two test conditions. Figure 1a is the arrangement used for runs H-1 through H-13. Figure 1 b is the arrangement used for runs H-14 through H-20. A log of the visible optical cross beam runs is given in Table I.

The first 10 runs with the exception of runs H-3 and H-4 were taken as a direct comparison between the two cross beam systems. These runs include cases where the beams are looking directly at each other, looking vertical, and intersecting at the 42 meter level. Runs H-3 and H-4 are a special case (under cloudy sky) where the beams are approximately parallel to the ground and intersecting at right angles. Runs H-11 through H-13 are for the visible optical beams intersecting at 102 meters.

The second test setup shown in figure 1 b placed the visible optical unit number 1 directly below the tower looking approximately straight up. The signal from the number 1 unit will be compared with the sensors mounted on the tower. The number 2 unit was 53 meters approximately due east of the number 1 unit. Tests number H-14 through H-19 were zero separation runs at different heights for the two beams. Observation of the data, while the recording was being made, appeared to indicate a possible higher degree of correlation for the high level intersections than the low level.

Run number H-20 was the only beam separation test attempted. Unfortunately, the separation runs were not feasible for most of the test time due to the absence of well defined winds. The winds began October 8 but they also were accompanied by clouds. A storm system moved into the area on October 8 and terminated any hope of further runs.

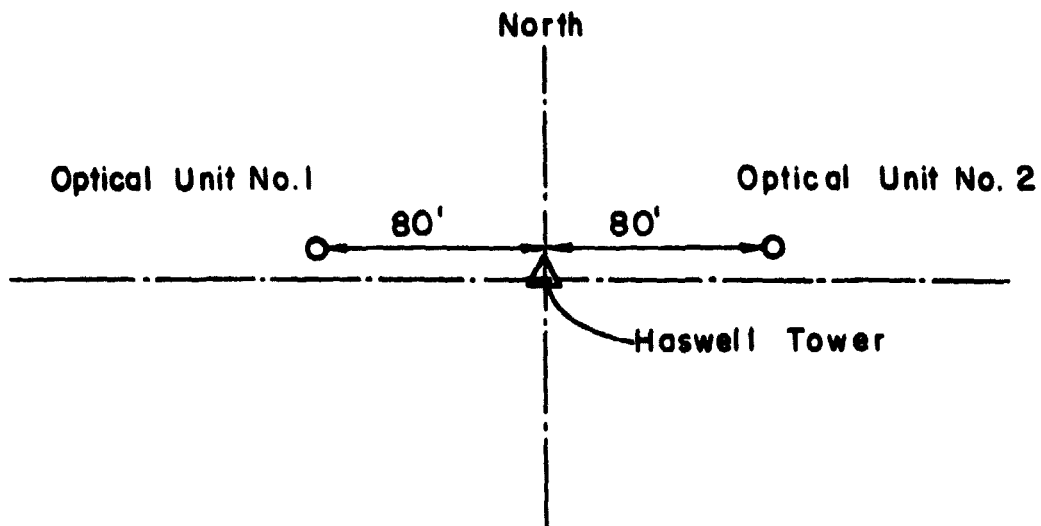
Reduced size copies of the data sheets for the runs are attached. The data sheets contain a time history of the DC voltage level from the two units. The AC output of the units was recorded on channels 5 and 11 of tape transport 100. The AC signals were amplified to maximum level short of saturation at the units. These high level signals were attenuated before entering the tape recorder. The calibration signals (1 VRMS, 1VDC, and 0.5 VDC ) were fed into the attenuator at the same place as the optical signals. Thus, the calibration signals can be used to calibrate the voltage fluctuations of the optical units, but they do not serve as a calibration of the tape recorder. The fluctuating optical signal will, in general, be greater than the calibration signal.

TABLE I  
LOG OF HASWELL RUNS

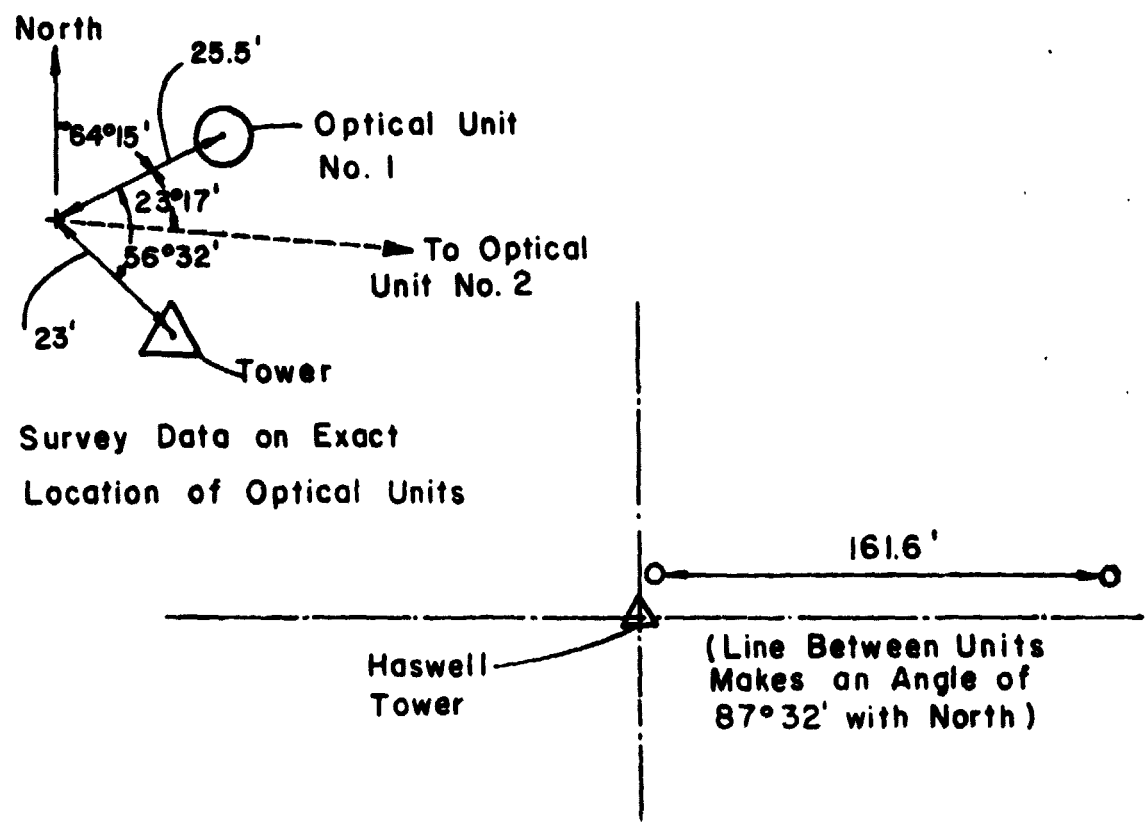
RECORDED ON TAPE TRANSPORT No. 100

Day	Time Clock	Run Number	Tape Number	IR Run Number	Remarks
277	14:03	Cal	29		
"	14:19	H-1 start	29	6-14:24	side by side
"	15:25	H-1 stop	29	6-15:24	comparison
"	15:51	Cal	29		.1-10 cps open
"	16:07	H-2 start	29	7-16:08	
"	17:08	H-2 stop	29	7-17:08	comparison
278	8:56	Cal	30		Beams looking at each other
"	9:10	H-3 start	"	9-9:33	
"	10:17	H-3 stop	"	9-11:30	comparison
"	10:41	Cal	"		.1-10 cps. 0.6-1.1u
"	10:54	H-4 start	"		90° Intersection
"	11:53	H-4 stop	"		.1-3 cps 0.6-1.1u
"	12:28	Cal	"		90° Intersection
"	13:18	H-5 start	"	10-13:17	
"	14:21	H-5 stop	"	10-14 27	comparison
"	14:43	Cal	31		.1-3 cps 0.6-1.1u
"	14:58	H-6 start	"	11-14:58	
"	16:00	H-6 stop	"	11-16:00	comparison
"	16:14	Cal	"		.1-3 cps open
"	16:28	H-7 start	"	12-16:28	
"	17:30	H-7 stop	"	12-17:30	comparison
"	17:42	Cal	"		Intersection at 128 feet
"	17:47	H-8 start	"	13-17:49	
"	18:30	H-8 stop	"	13-18:50	crossed 128 ft.
279	7:19	Cal	33		.1-3cps open
"	7:34	H-9 start	"	23-7:49	
"	9:52	H-9 stop	"	23-8:39	vertical
"	10:41	Cal	"	24-8:54 to 9:52	vertical
"	11:04	H-10 start	34	25-10:59 to 11:45	Horz.
"	13:22	H-10 stop	"	26-12:24 to 13:22	Horz.
"	13:25	Cal	"	27-13:56 to 14:52	128ft. crossing.
"	14:05	H-11 start	"	28-15:10 to 16:10	" " "
"	16:00	H-11 stop	"		0.01-3 cps. open
"	16:02	Cal	"		
"	16:17	H-12 start	"		Intersection at 311 ft.
"	17:23	H-12 stop	"		0.01 -3cps 0.6-1.1u
"	17:27	Cal	"		
"	17:34	H-13 start	"		Intersection at 311 ft.
"	17:54	H-13 stop	"		0.1 - 3cps 0.6-1.1u
POSITIONS OF UNITS CHANGED					
280	8:39	Cal	36		
"	9:08	H-14 start	"		#1 vertical #2 Intersect 128ft.
"	11:02	H-14 stop	"		0.1- 3cps open
"	11:03	Cal	"		
"	11:25	H-15 start	"		#1 vert. #2 Intersect 50 ft.
"	13:07	H-15	"		0.01- 3cps open
"	13:11	Cal	37		
"	13:37	H-15	"		
"	14:27	H-15 stop	"		
"	14:27	Cal	"		
"	14:50	H-16 start	"		#1 vertical #2 Intersect.495 ft.
"	16:18	H-16 stop	"		0.01 - 3 cps open
"	16:19	Cal	"		
"	16:38	H-17 start	"		#1 vert #2 Intersect 495 ft.
"	17:20	H-17 stop	"		0.01-3cps open
"	17:22	Cal	"		
"	17:43	H-18 start	"		#1 vert. #2 intersect 900 ft.
"	18:29	H-18 stop	"		0.01-3 cps open
281	8:20	Cal	39		
"	8:36	H-19 start	"		#1 vert. #2 intersect 900 ft.
"	9:36	H-19 stop	"		0.01-3cps open
"	9:36	Cal.	"		
"	10:05	H-20 start	"		#1 vert. #2 Intersect 128 ft.
"	11:06	H-20 stop	"		0.01 -3 cps open
"	11:07	Cal	"		
"	11:30	H-21 start	"	Clouds moved in and caused	# 1 vert. #2 Intersect 128 ft.
"	13:03	H-21 stop	"	much loss of signal.	0.01 -3cps .6-1.1u
"	19:32	Cal.	40	Looking at light. Blinking	
"	19:47	H-22 start	"	red light at 300 ft. level	#1 vert. #2 Intersect 128ft.
"	21:10	H-22 stop	"	can be seen by beam warts	0.01- 30 cps. open

REPRODUCIBILITY OF THE ORIGINAL PAGE IS POOR.



a) Locations for Runs H-1 through H-13

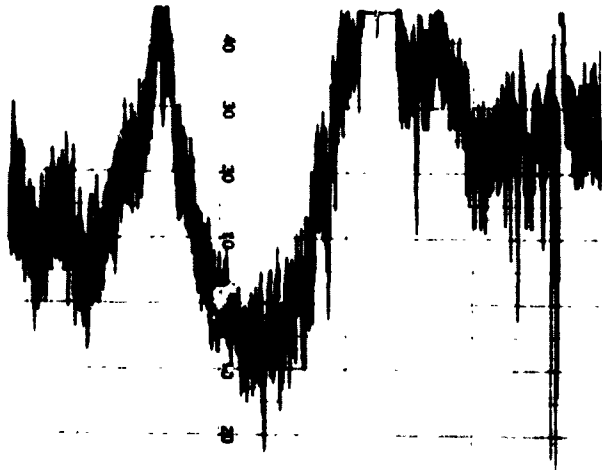


b) Location for Runs H-14 through H-22

FIG. 1. Location of optical units for Haswell field tests.

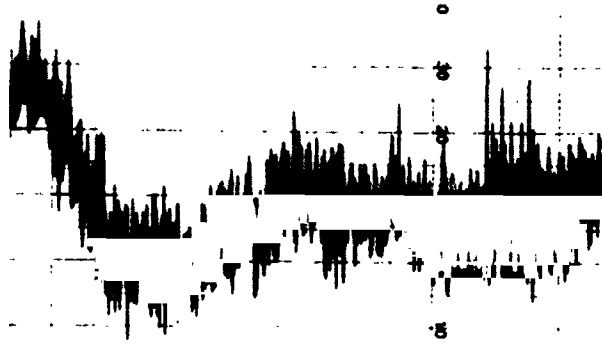
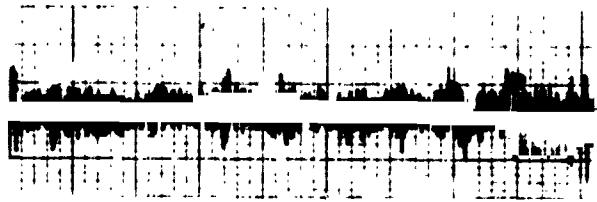
**FIGURE 1- SAMPLE OF OPTICAL SIGNALS**

UNIT No. 1

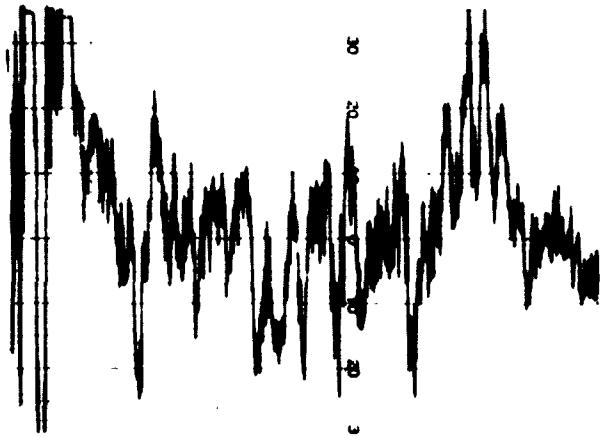
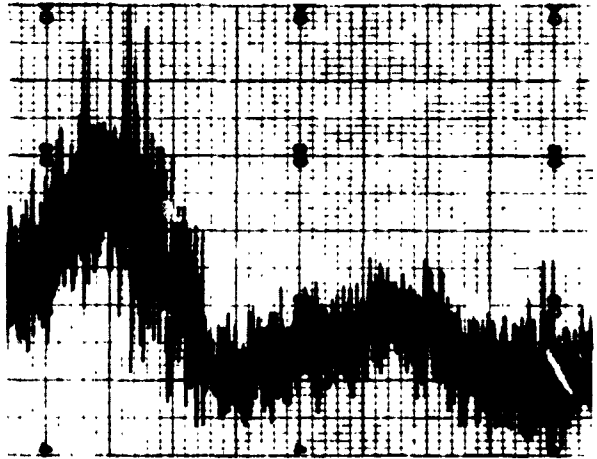


RUN N-1

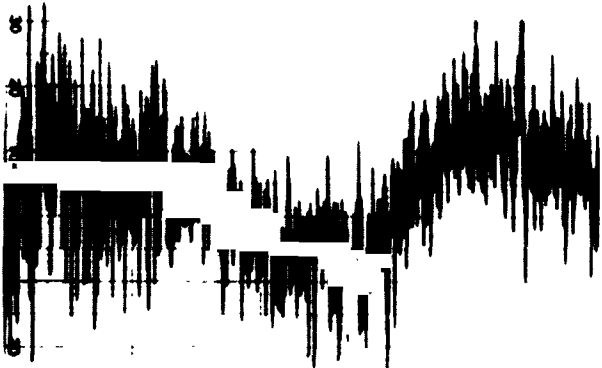
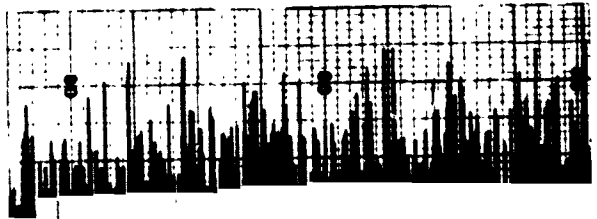
UNIT No. 2



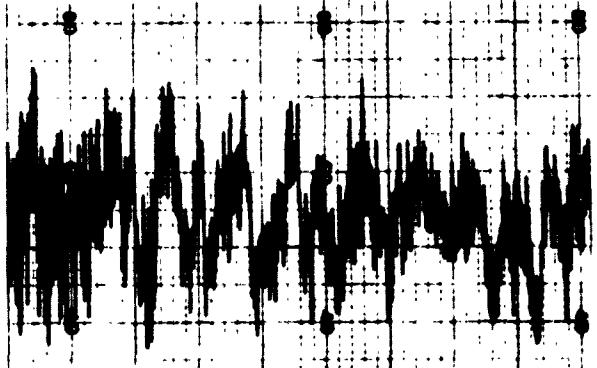
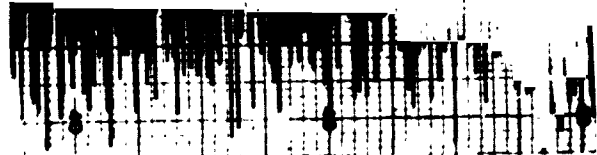
RUN N-2



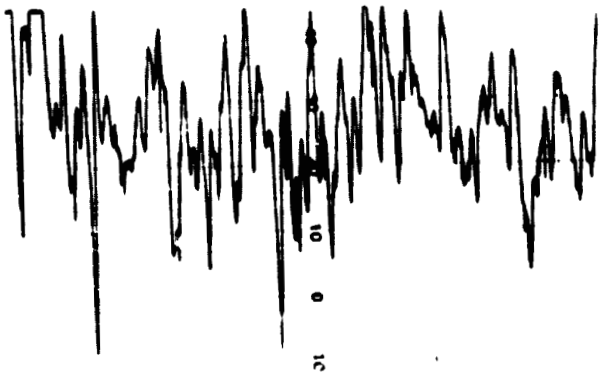
RUN N-3



RUN N-4

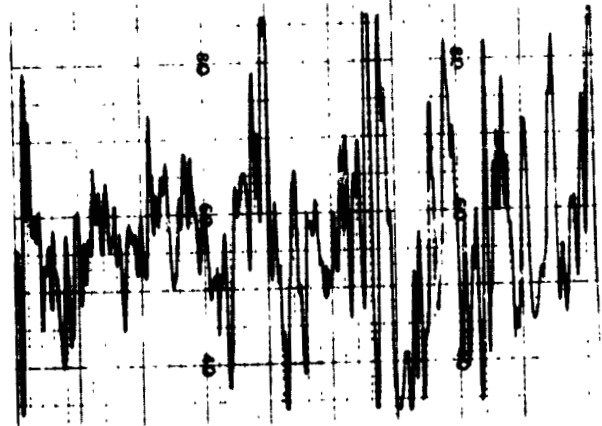


UNIT No. 1

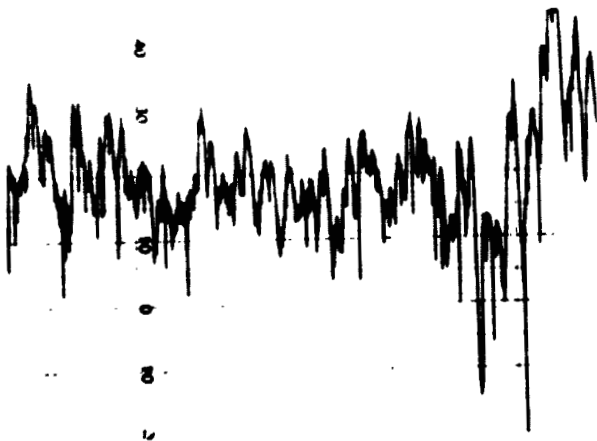


RUN H-5

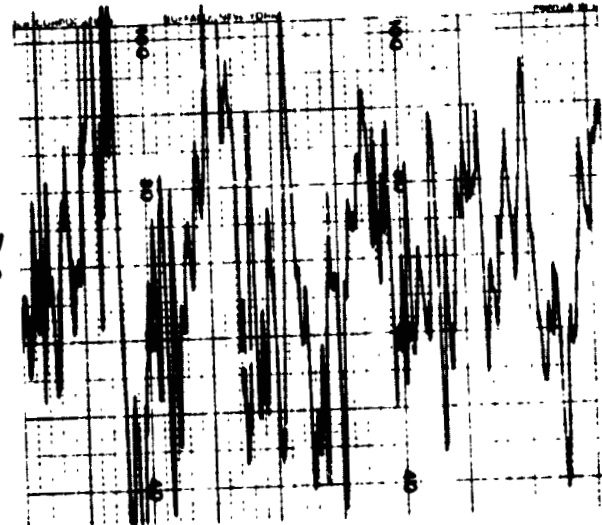
UNIT No. 2



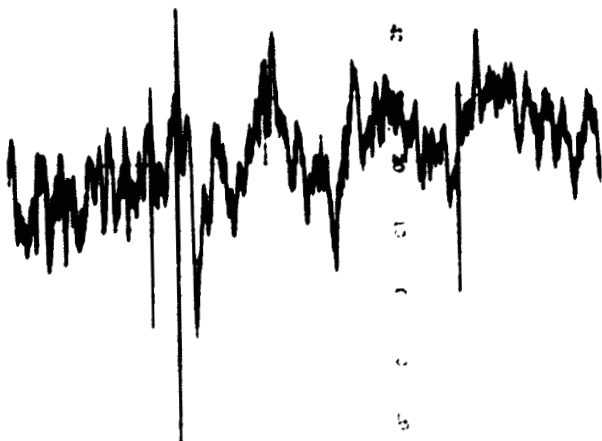
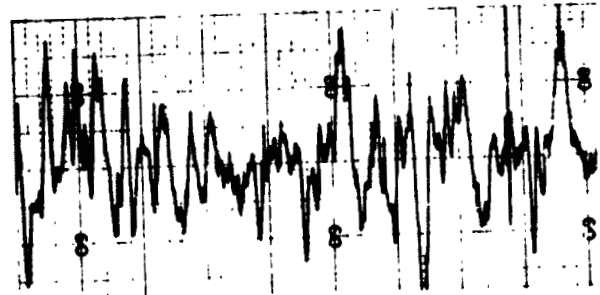
0  
20  
10  
0  
0  
0  
0  
0



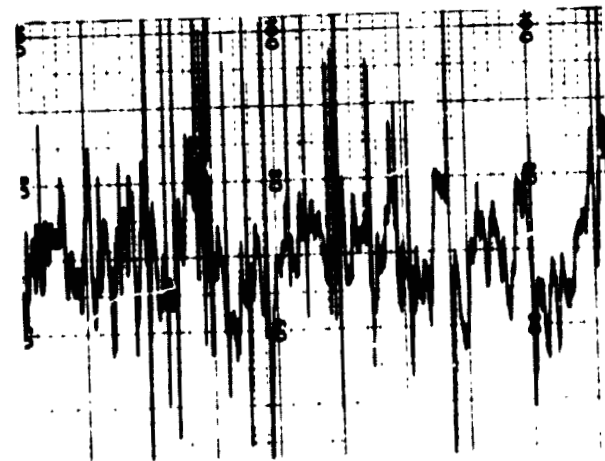
RUN H-6



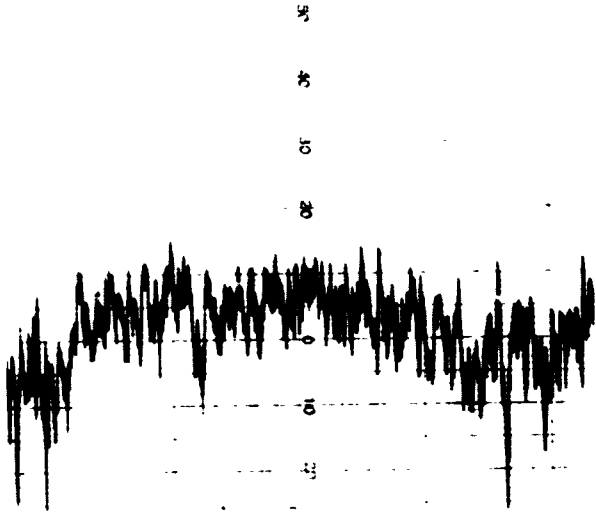
RUN H-7



RUN H-8

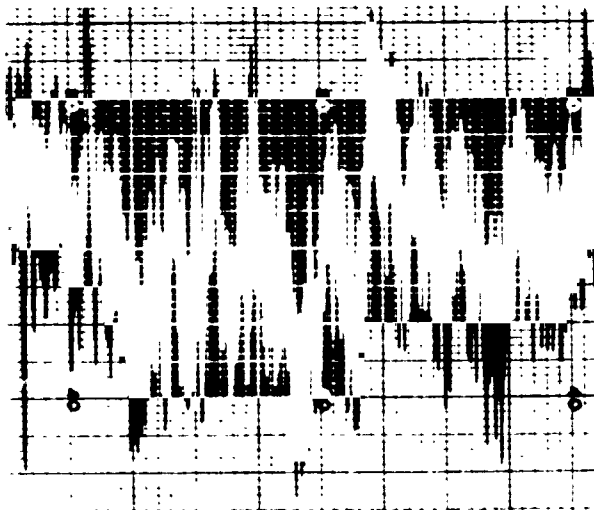
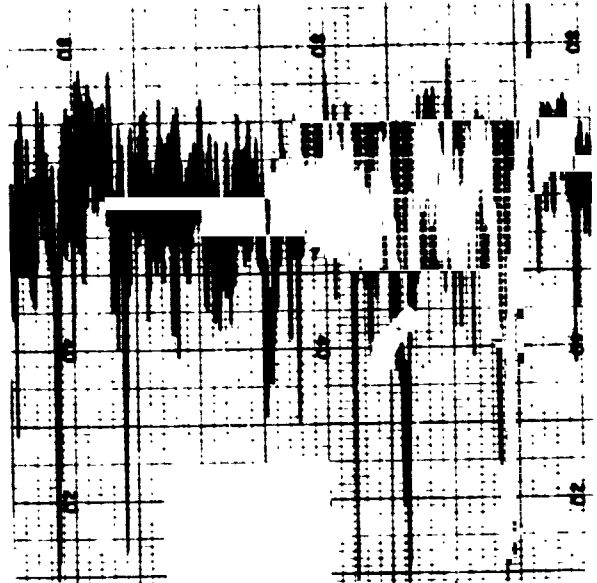


UNIT No. 1

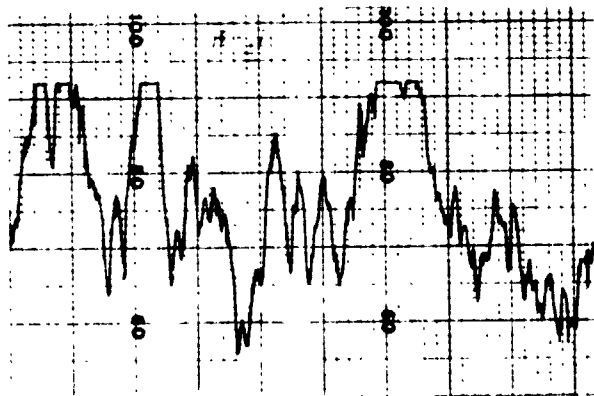
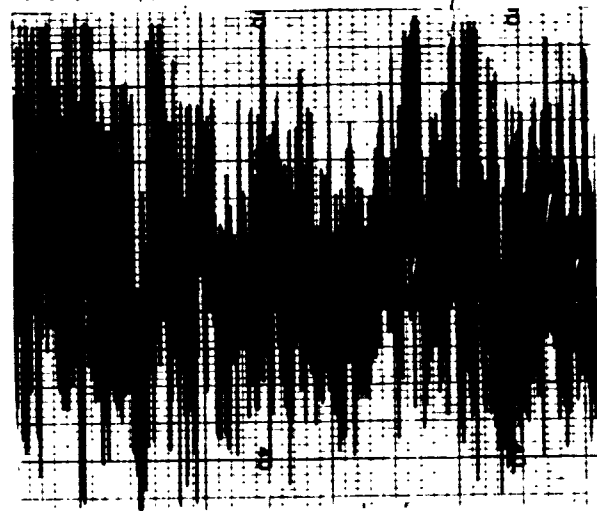


RUN  
H-9

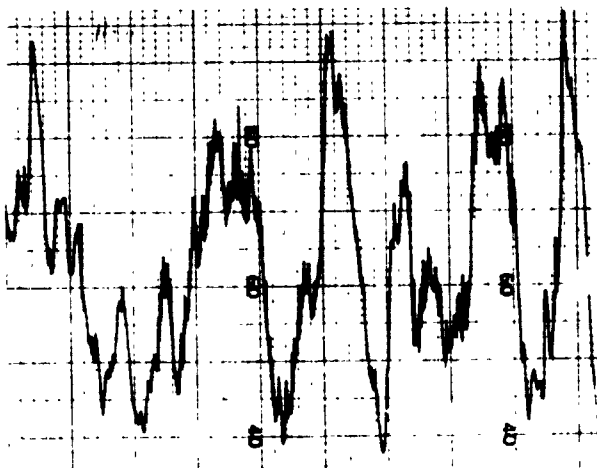
UNIT No. 2



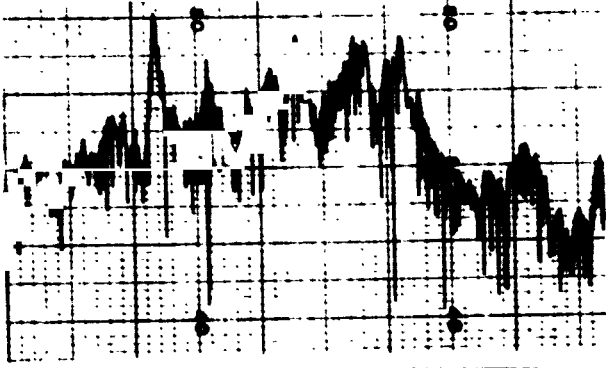
RUN  
H-10



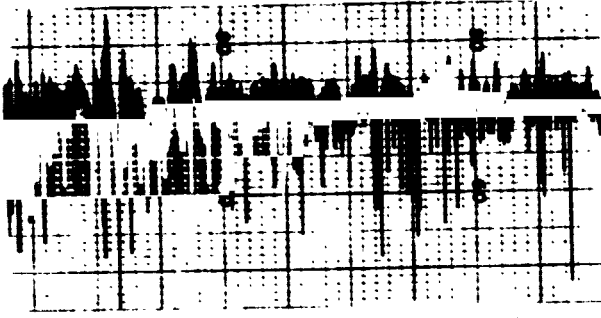
RUN  
H-11



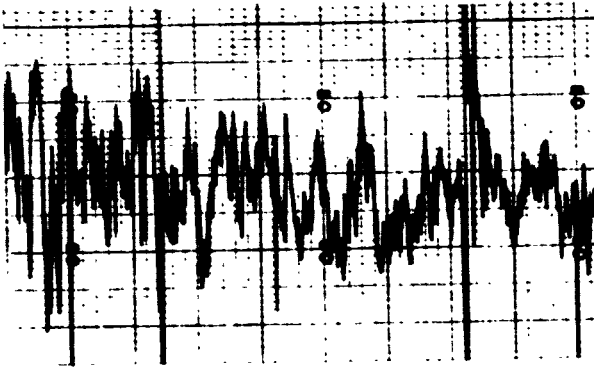
UNIT No. 1



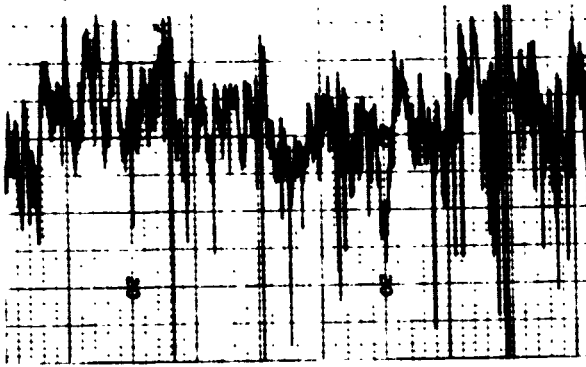
RUN  
H-12



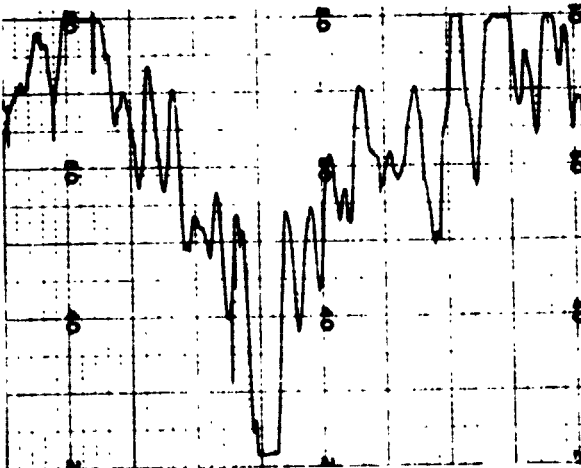
RUN  
H-13



RUN  
H-14

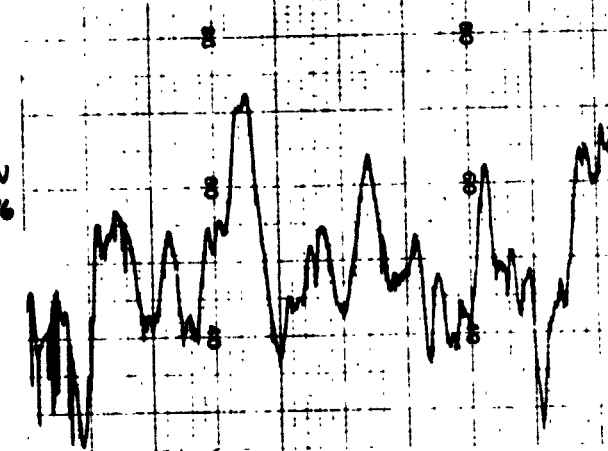
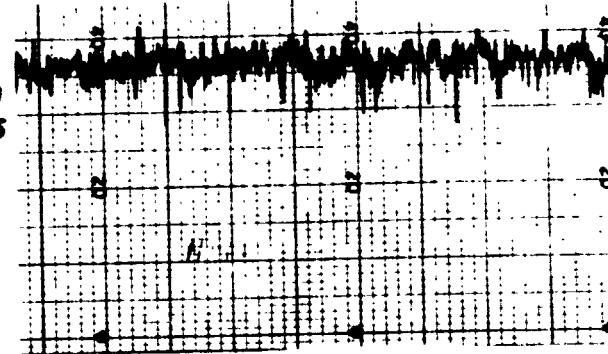
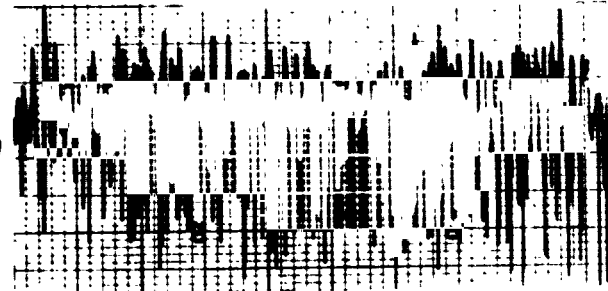
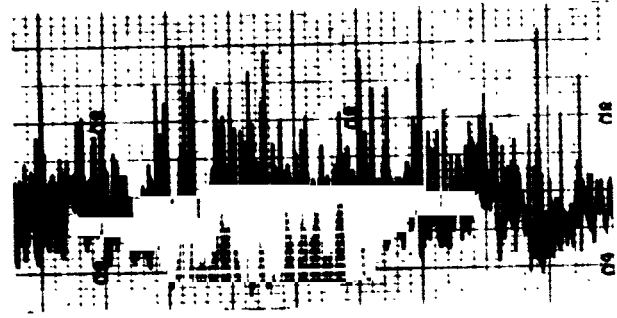
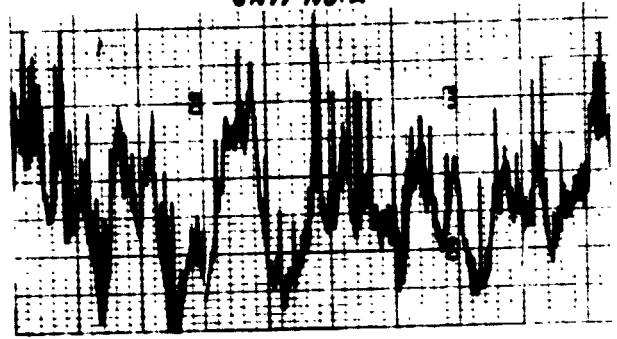


RUN  
H-15

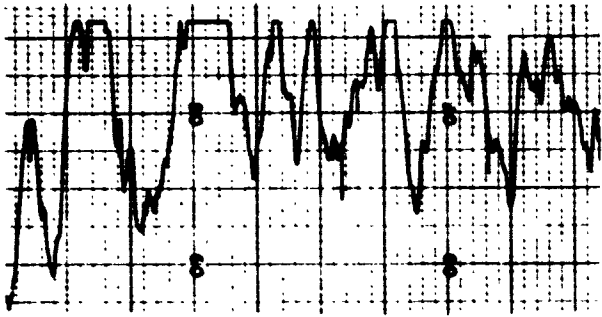


RUN  
H-16

UNIT No. 2

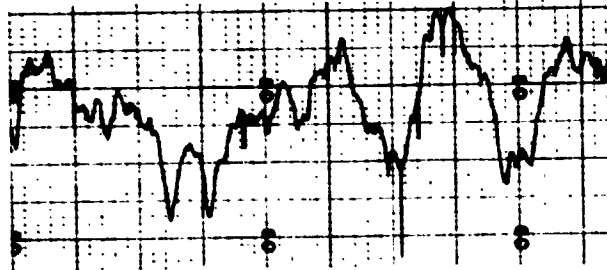
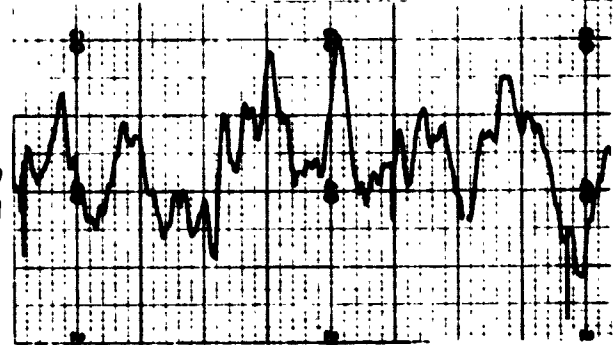


UNIT No. 1

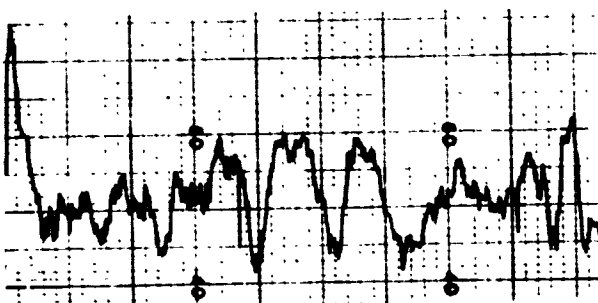
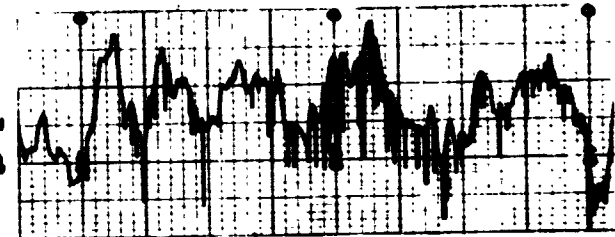


RUN H-17

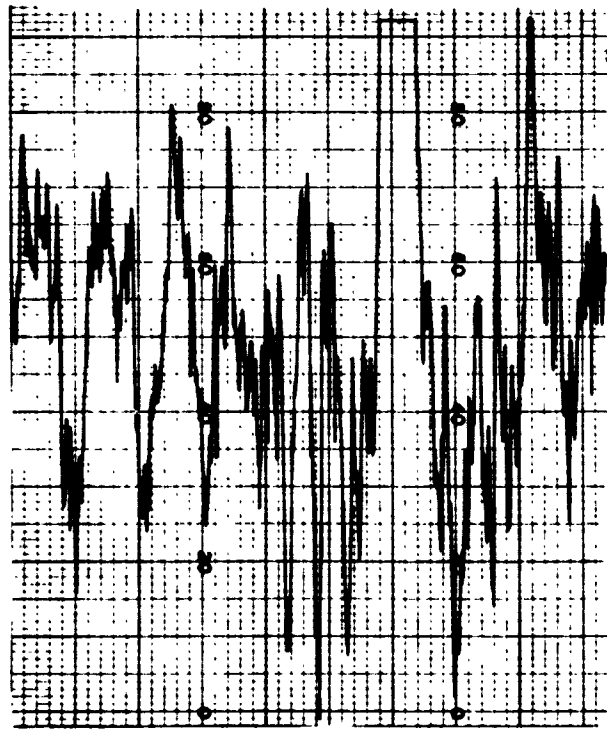
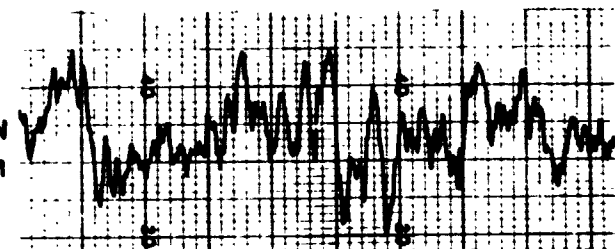
UNIT No. 2



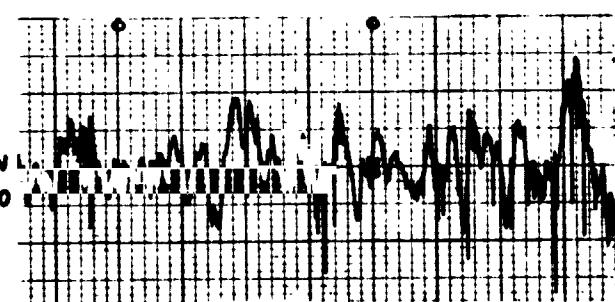
RUN H-18



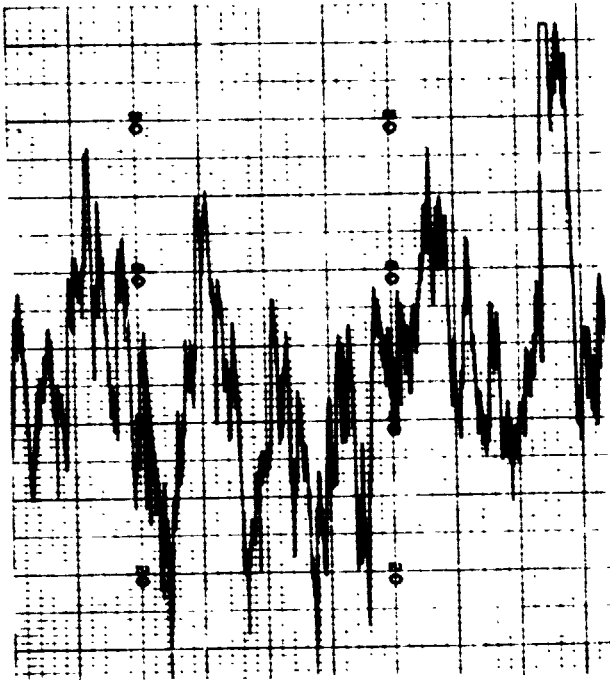
RUN H-19



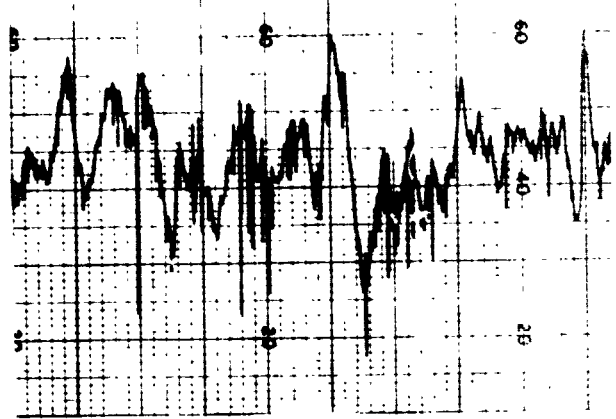
RUN H-20



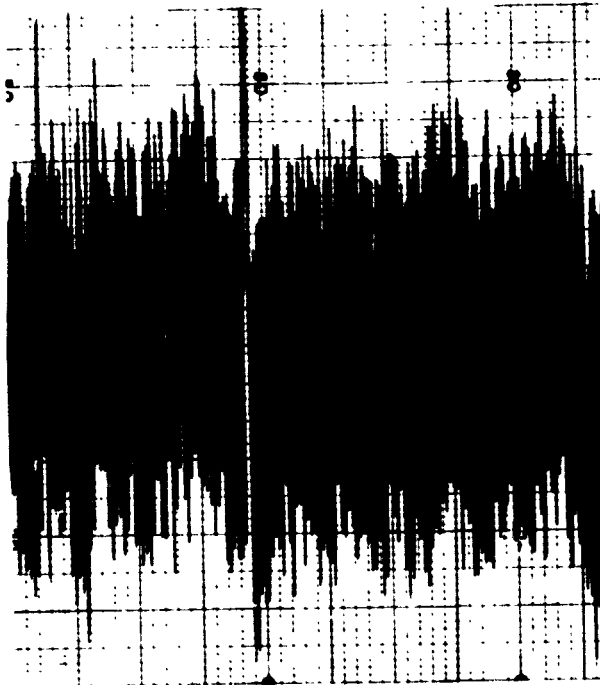
UNIT No. 1



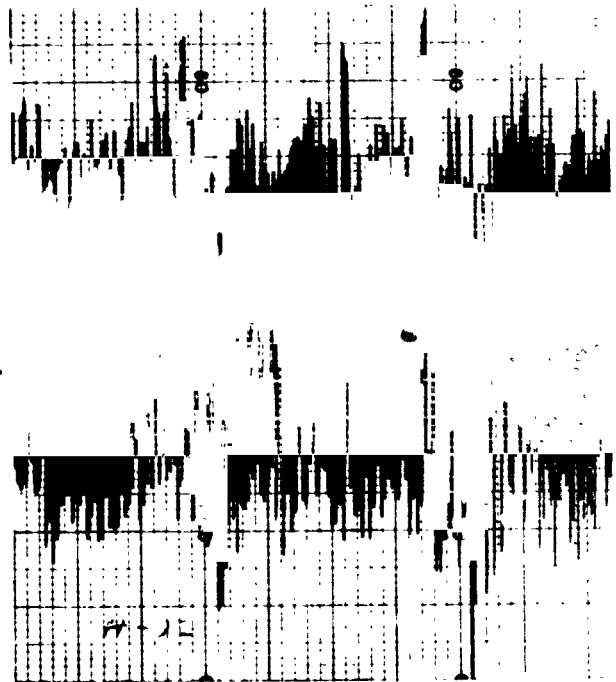
UNIT No. 2



RUN  
H-21



RUN  
H-22



174-35044

SECTION VII.  
ANALYSIS OF CROSS BEAM RUNS TAKEN AT  
HASWELL FIELD SITE, OCTOBER 1969

by  
L. L. Huff  
and  
V. A. Sandborn

7.1 SUMMARY

Auto and cross-correlations of the optical cross beam signals have been computed for the Haswell experiments. A limited number of the infrared cross beam signals has also been computed. The correlations are presented as plots.

7.2 INTRODUCTION

A series of cross beam experiments was conducted at the ESSA field site at Haswell, Colorado, in October 1969. Both the optical visual and infrared units were operated on a comparison basis. The test configuration and experiment identification were given in reference 1. The present memorandum is a data report of the initial auto-and cross-correlation evaluation of these tests. The data reported is in its original form, and no detailed analysis of the results has, as yet, been made.

7.3 EVALUATION OF THE CORRELATIONS

The original test data from the Haswell tests were recorded on F M magnetic tape. A copy of the original tapes was made and employed for the present analysis. The tapes were played back at 60 inches per second for analysis. Some of the infrared units runs ( Run Nos. 8,25,40,41,42,43,44,45) were played back at 30 inches per second in order to gain sufficient averaging time. The averaging time was nominally 3200 seconds real time at 60 inches per second and 1600 seconds real time at 30 inches per second. These averaging times correspond to 100 seconds of averaging time of the correlator.

All correlations were computed with the Princeton Applied Research Model 101 Correlation Function Computer. The time delay for each correlation presented was set according to the relation

$$\text{MAX. Time delay} = \frac{25}{f_{\text{max}}}$$

where  $f_{\text{max}}$  corresponds to the maximum frequency limit of the original recorded

data, ref. 1. Only the original recorded frequency range has been employed in the present analysis.

A limited number of "scatter diagrams" was also obtained by putting one of the optical signals on the y-axis of an oscilloscope and the second signal on the x-axis of the oscilloscope.

Figure 1 shows a short sample of the actual optical units output for the runs. The vertical scale corresponds to light intensity and the horizontal scale is time.

Figure 2 shows the cross-and auto-correlations for the runs evaluated. Runs Nos. H-12, H-13, H-18 and H-21 could not be evaluated from the tapes. Runs No. H-12 and H-18 were cut off in the reproducing process and may be recovered from the original tapes. Run No. H-13 was too short to be analyzed with the present setup. Run No. H-21 was taken during cloudy sky conditions, and as noted on the original data sheet, ref. 1, it does not contain useable data.

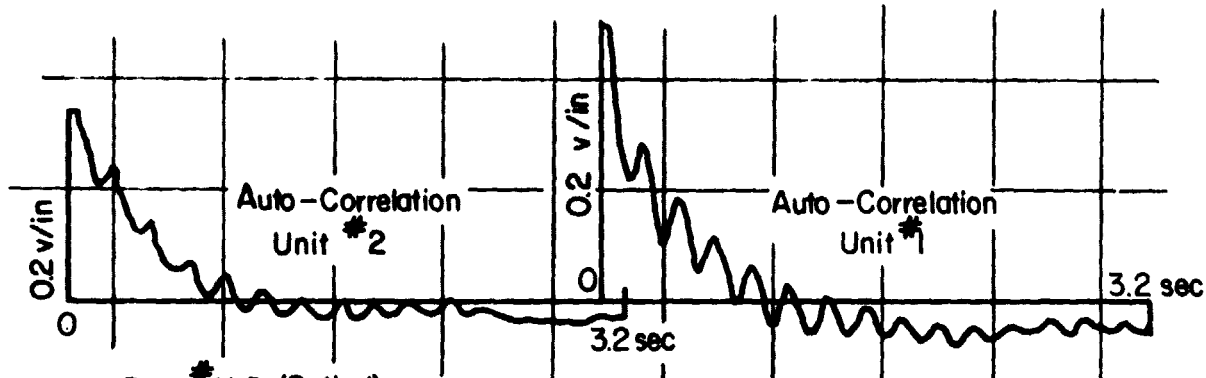
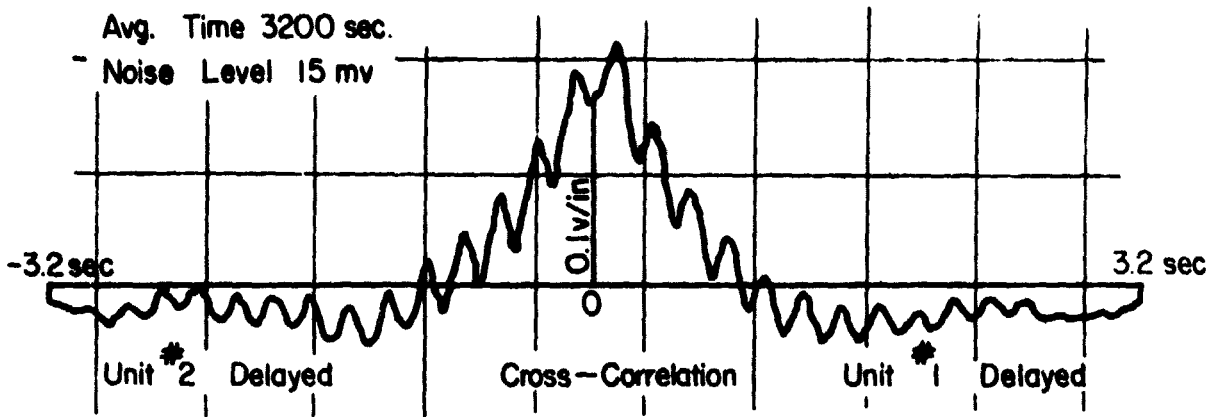
Figure 3 shows the cross-and auto-correlations for the infrared runs analyzed.

#### 7.4 REFERENCE

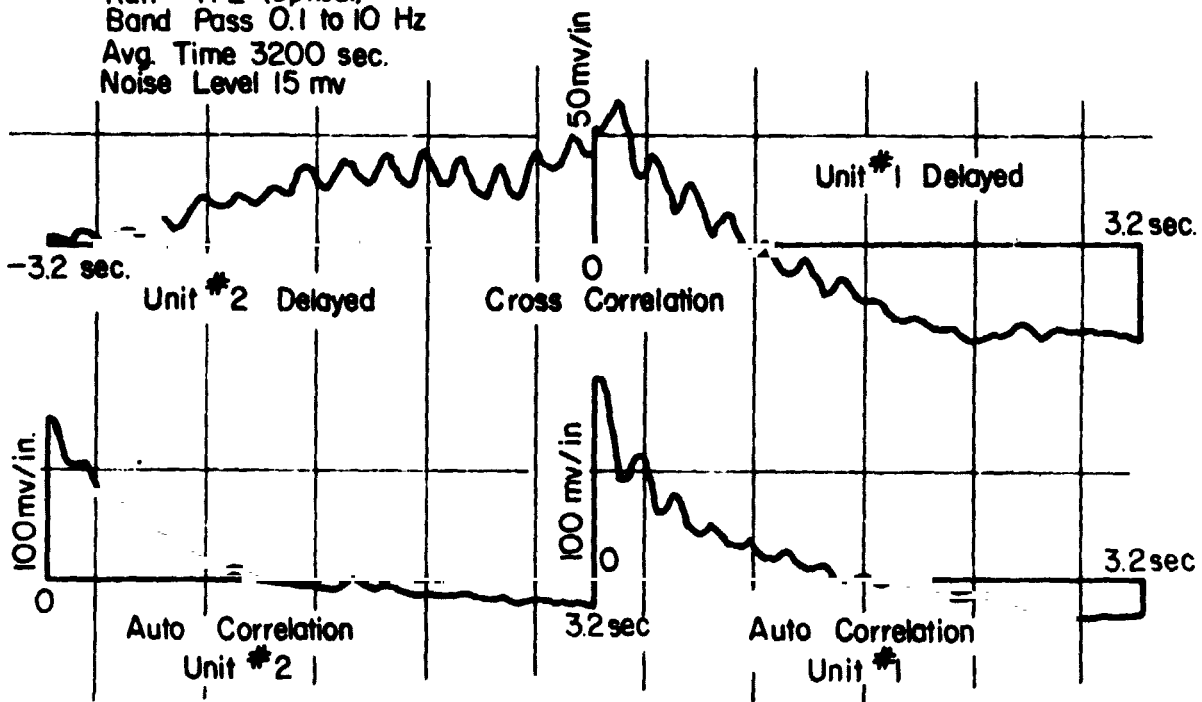
1. Sandborn, V. A., Optical Cross Beam Field Tests at ESSA, Haswell Field Site, October 1969. Colorado State University, College of Engineering, Research Memorandum No. 18, 1969.

**FIGURE 2- CORRELATIONS OF OPTICAL CROSS BEAM SYSTEMS**

Run # H-1 (Optical)  
 Band Pass 0.1 to 10 Hz  
 Avg. Time 3200 sec.  
 Noise Level 15 mv

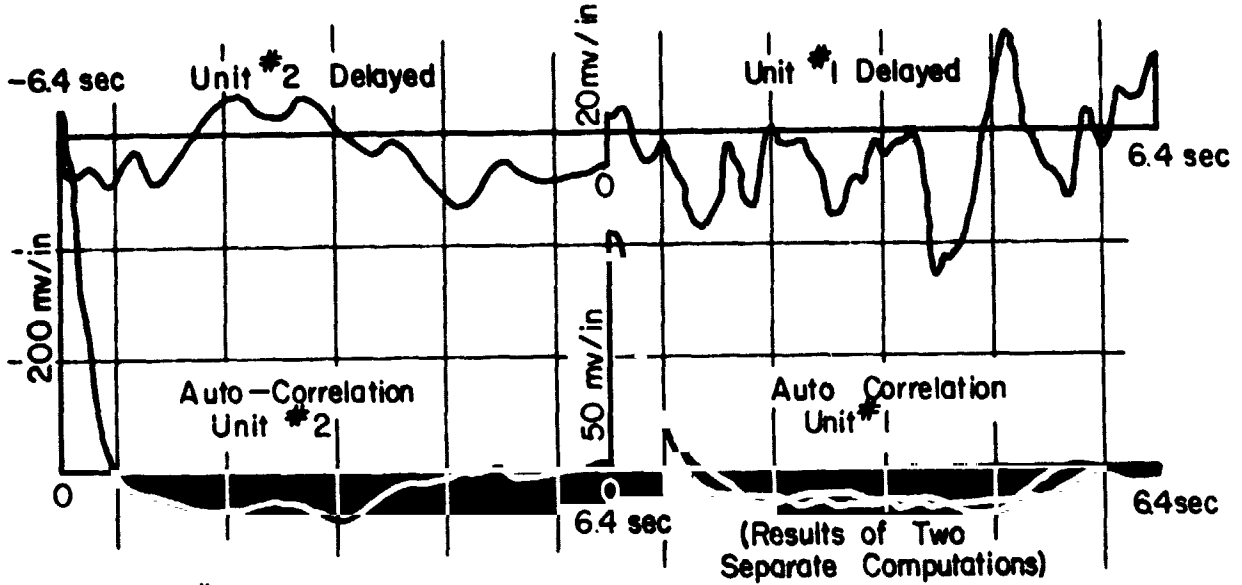


Run # H-2 (Optical)  
 Band Pass 0.1 to 10 Hz  
 Avg. Time 3200 sec.  
 Noise Level 15 mv

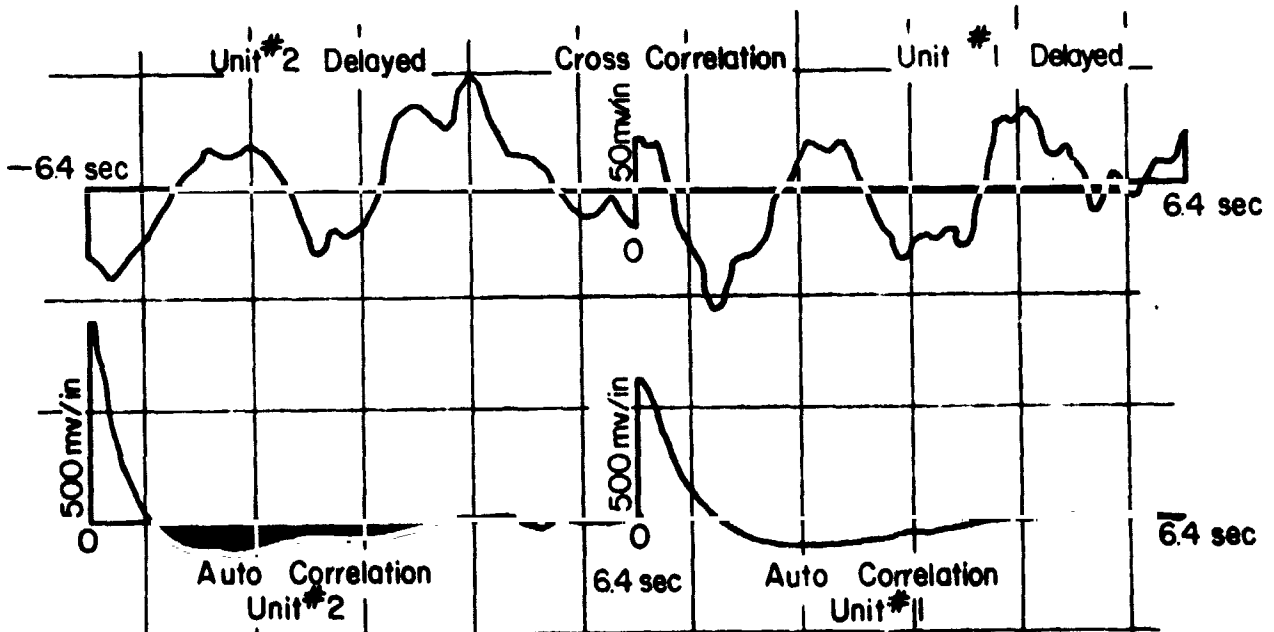


Run \*H-3 (Optical)  
 Band Pass 0.1 to 3.0 Hz  
 Avg. Time 3200 sec  
 Noise Level 22 mv

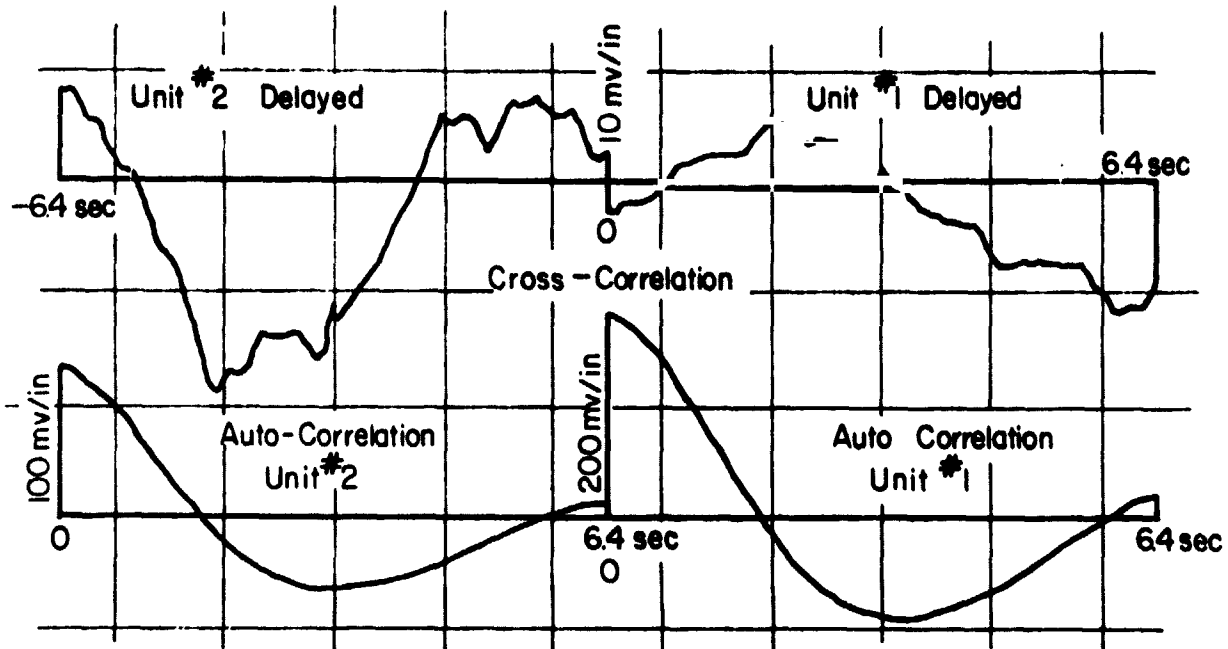
Cross - Correlation



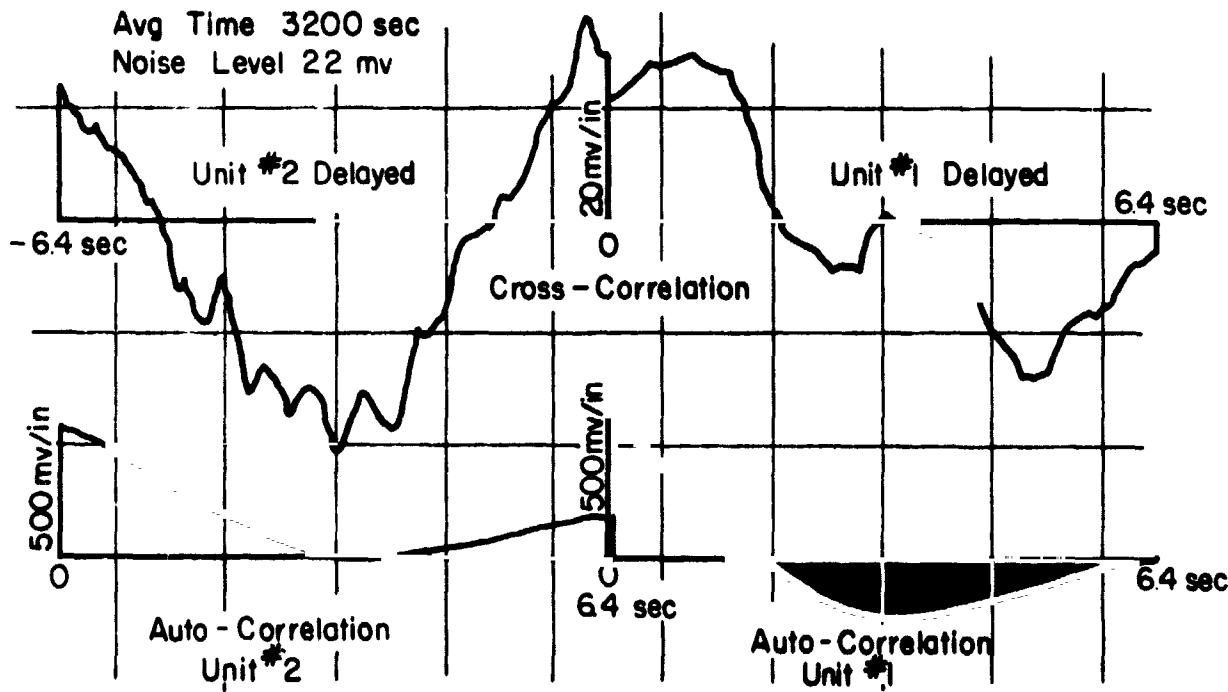
Run \*H-4 (Optical)  
 Band Pass 0.1 to 3.0 Hz  
 Avg. Time 3200 sec  
 Noise Level 22 mv



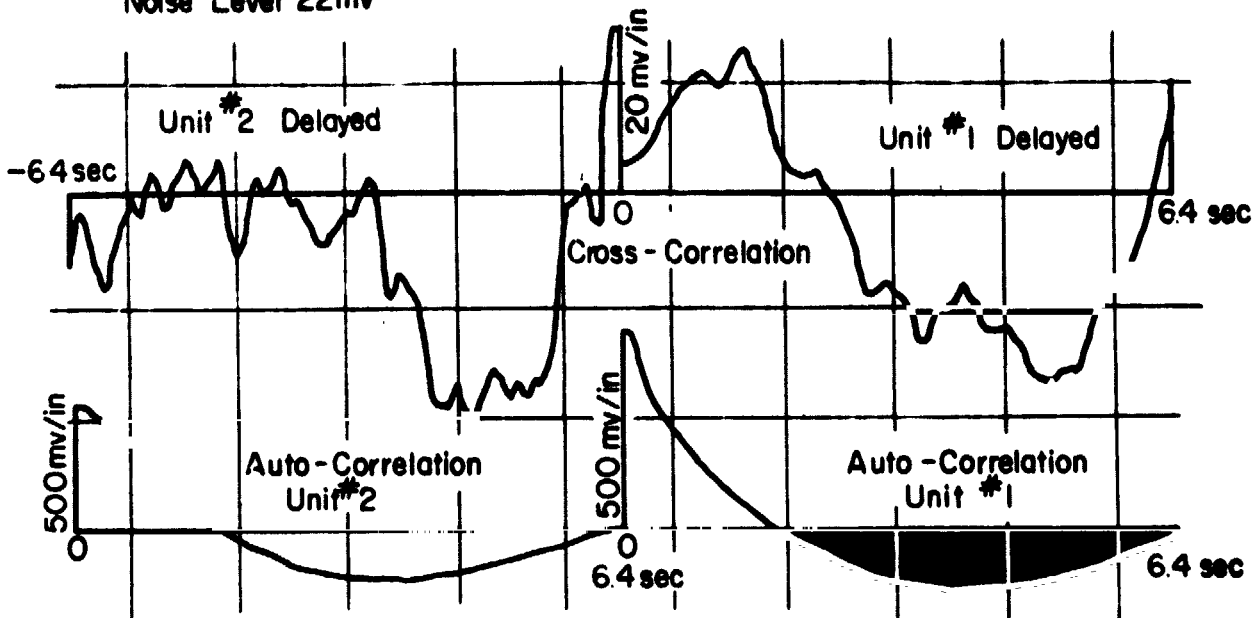
Run #H-5 (Optical)  
 Band Pass 0.1 to 3.0 Hz  
 Avg. Time 3200 sec  
 Noise Level 22mv



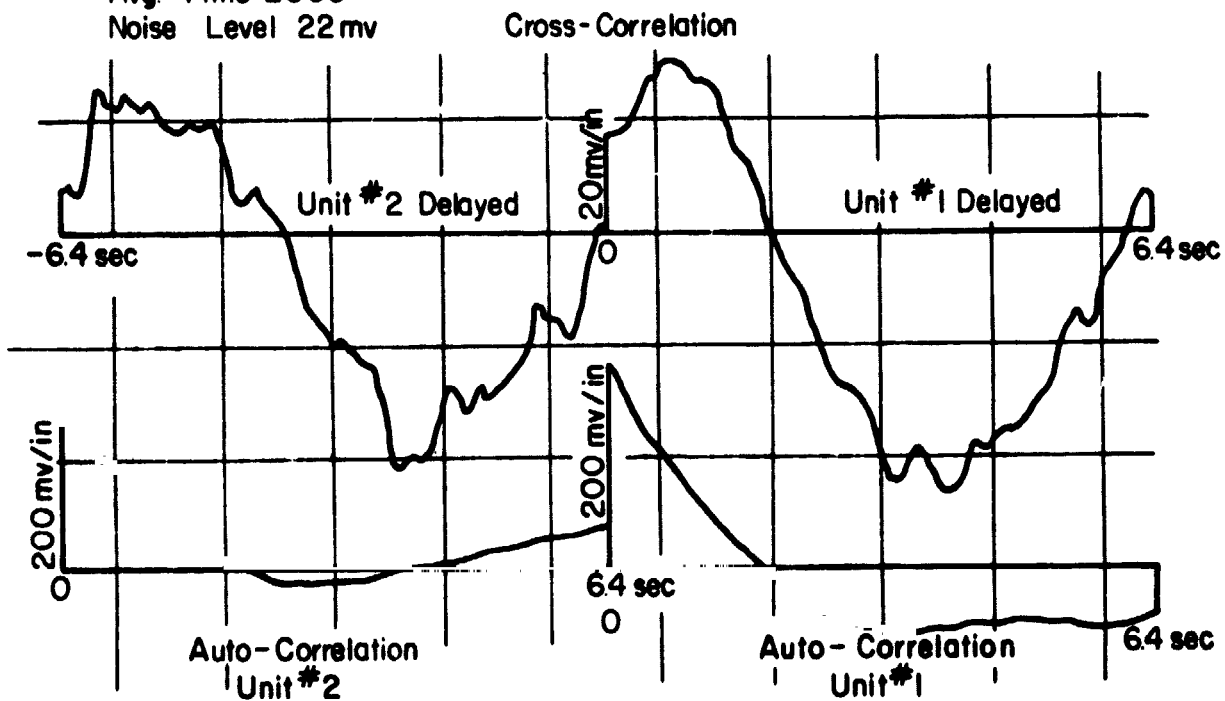
Run #H-6 (Optical)  
 Band Pass 0.1 to 3.0 Hz  
 Avg Time 3200 sec  
 Noise Level 22 mv



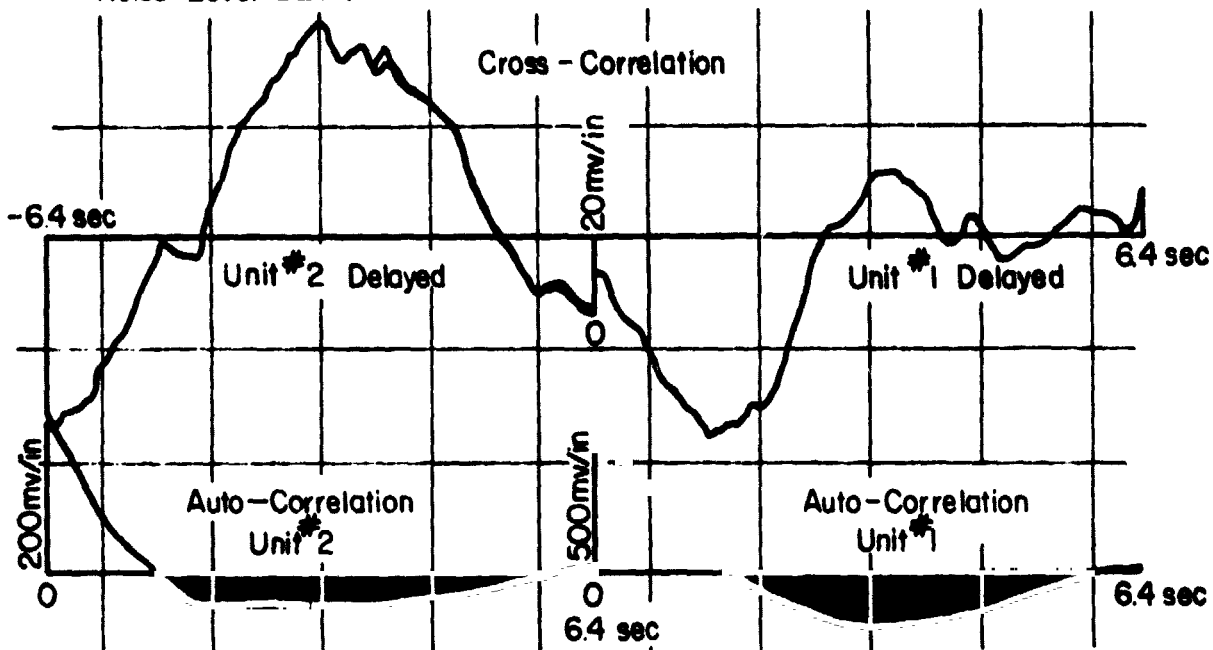
Run #H-7 (Optical)  
 Band Pass 0.1 to 30 Hz  
 Avg Time 3200 sec  
 Noise Level 22mv



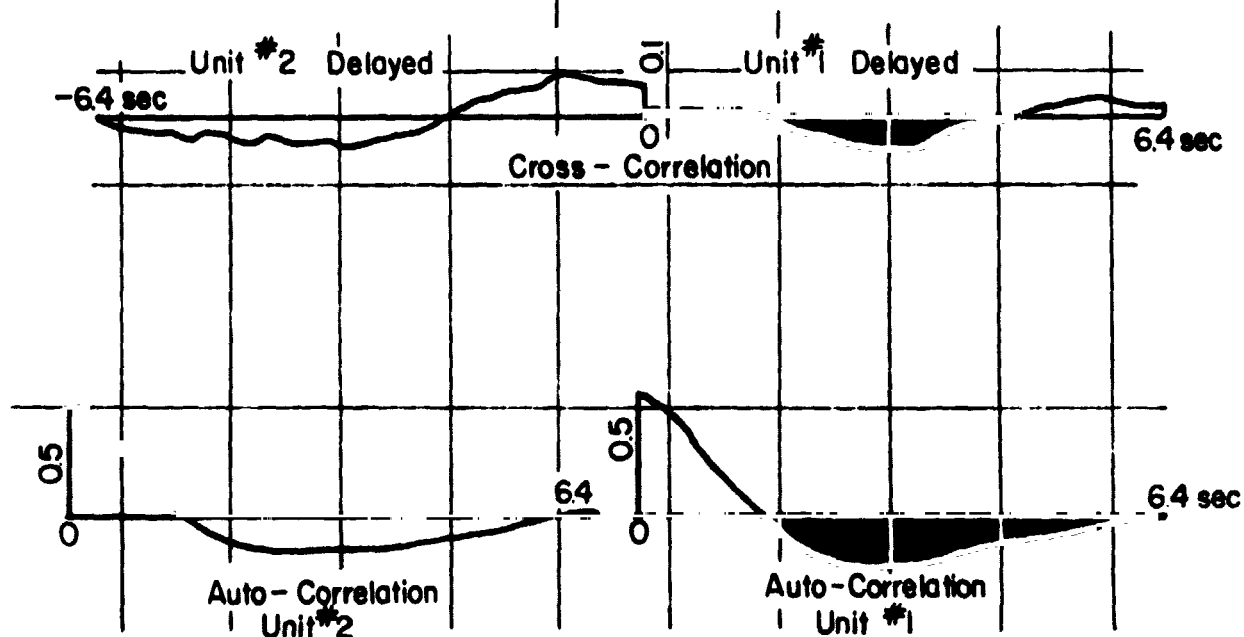
Run #H 8 (Optical)  
 Band Pass 0.1 to 30 Hz  
 Avg Time 2560 sec  
 Noise Level 22mv



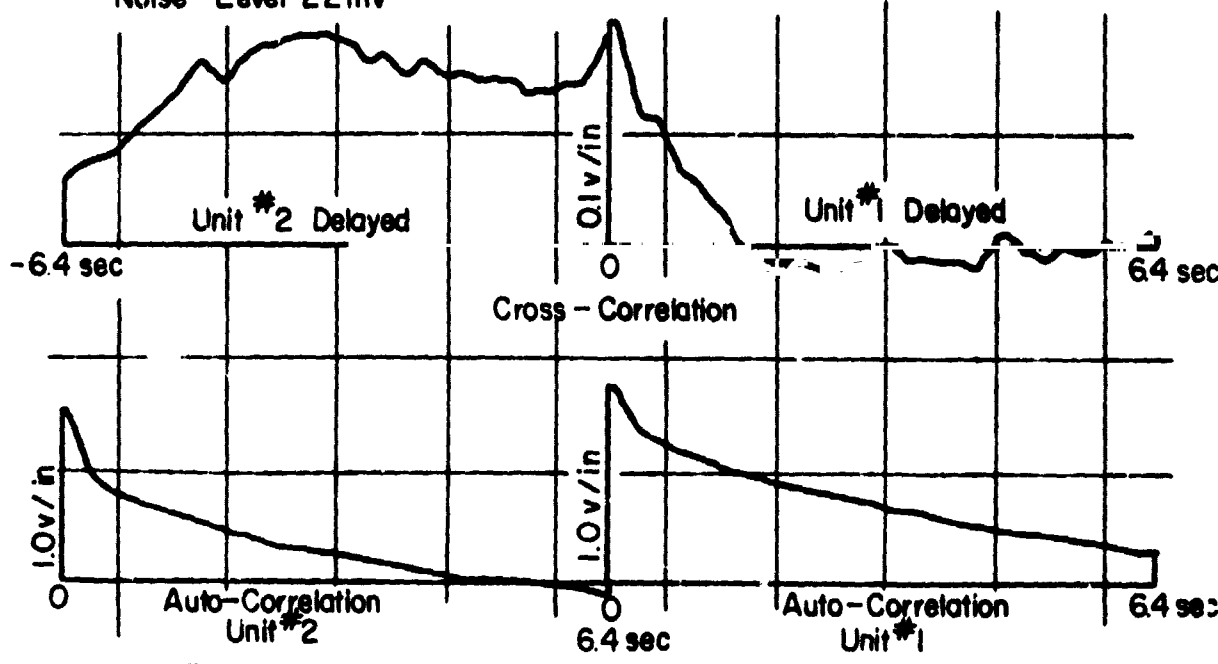
Run # H-9 1<sup>st</sup> Hour  
 Band Pass 0.1 to 30  
 Avg. Time 3200 sec  
 Noise Level 22 mv



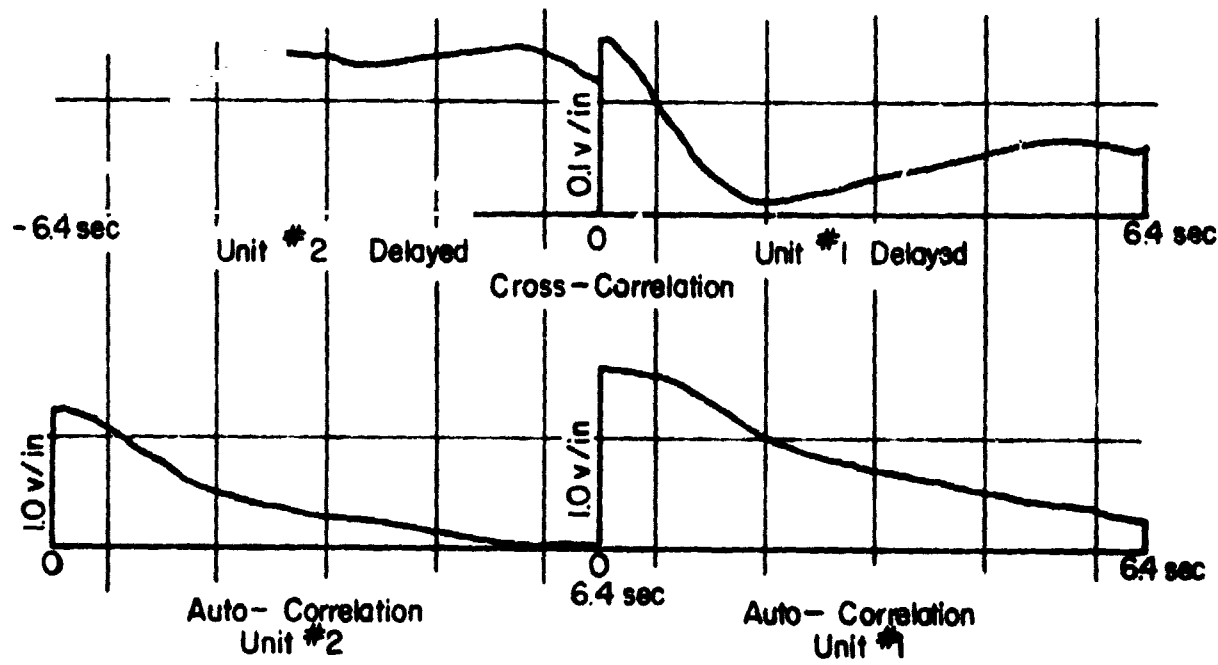
Run # H-9 2<sup>nd</sup> Hour  
 Band Pass 1-3 CPS  
 Avg. Time 3200sec  
 Noise Level 22 mv



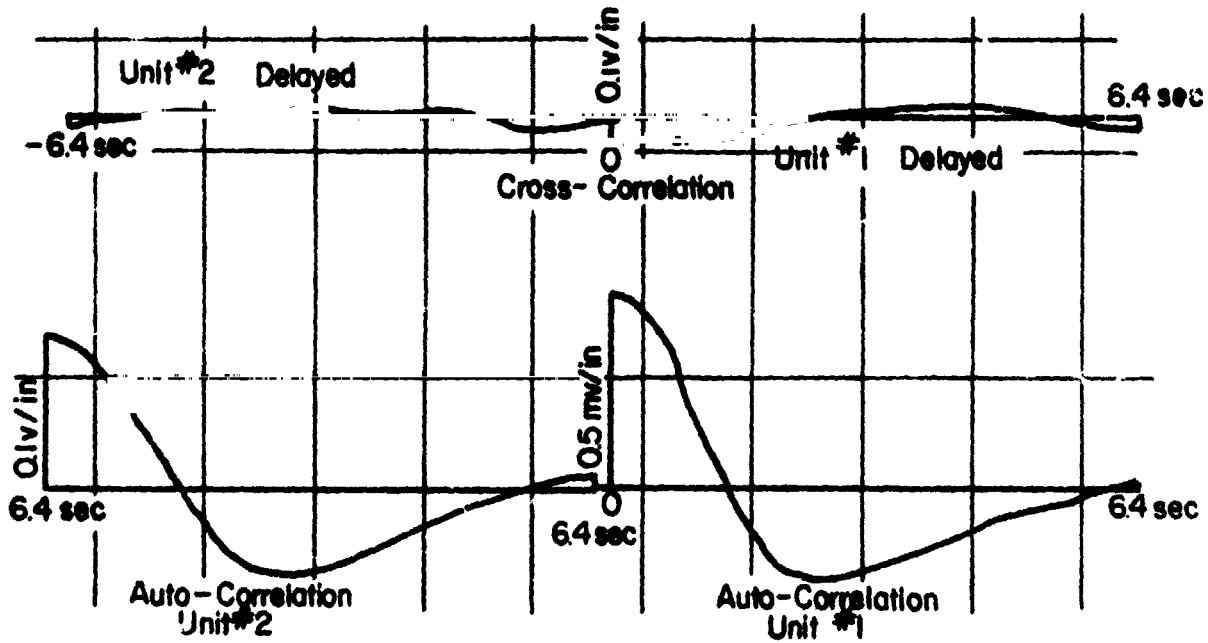
Run #H-10 (Optical) 1<sup>st</sup> Hour  
 Band Pass 0.01 to 3.0 Hz  
 Avg. Time 3200 sec  
 Noise Level 22 mv



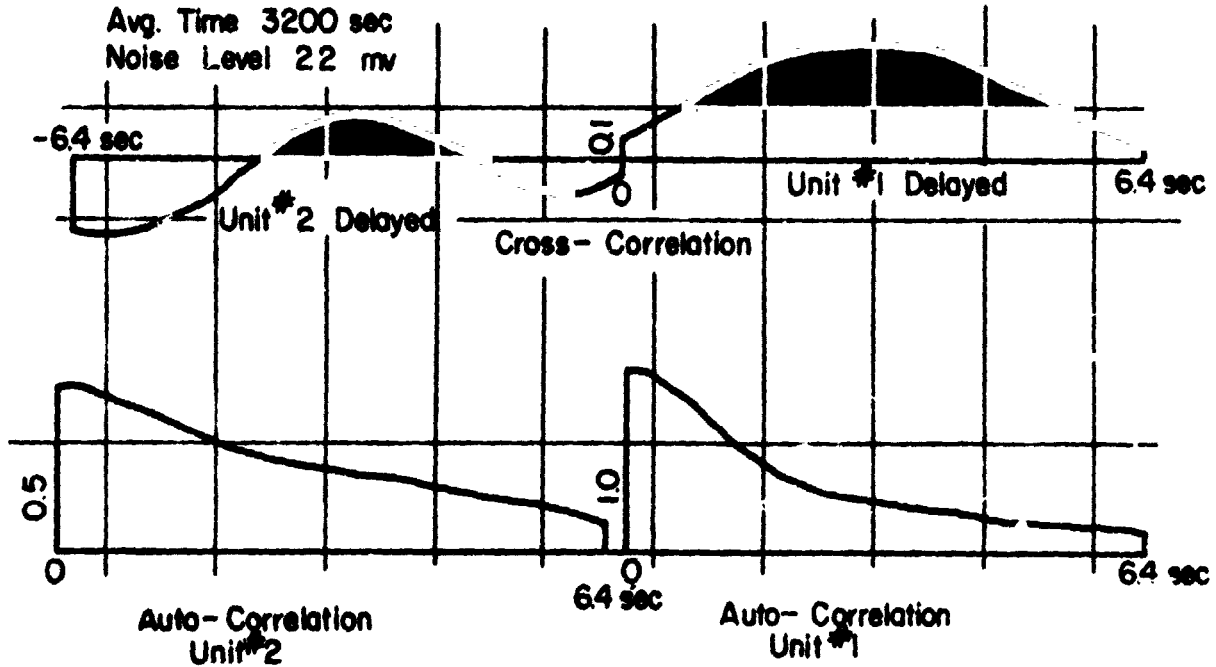
Run #H-10 (Optical) 1<sup>st</sup> Hour  
 Band Pass 0.01 to 0.3 mv  
 Avg. Time 3200 sec  
 Noise Level 22 mv



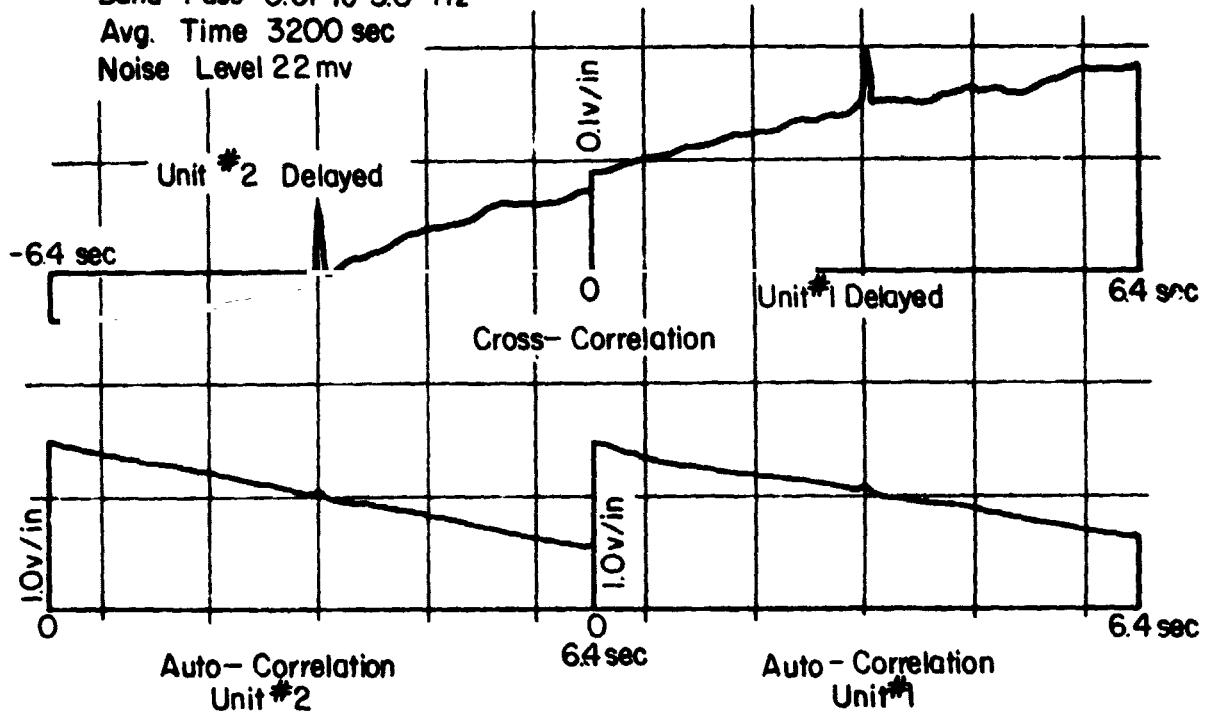
Run # H-10 (Optical) 2<sup>nd</sup> Hour  
 Band Pass 0.01-3 CPS  
 Avg. Time 3200 sec  
 Noise Level 22 mv



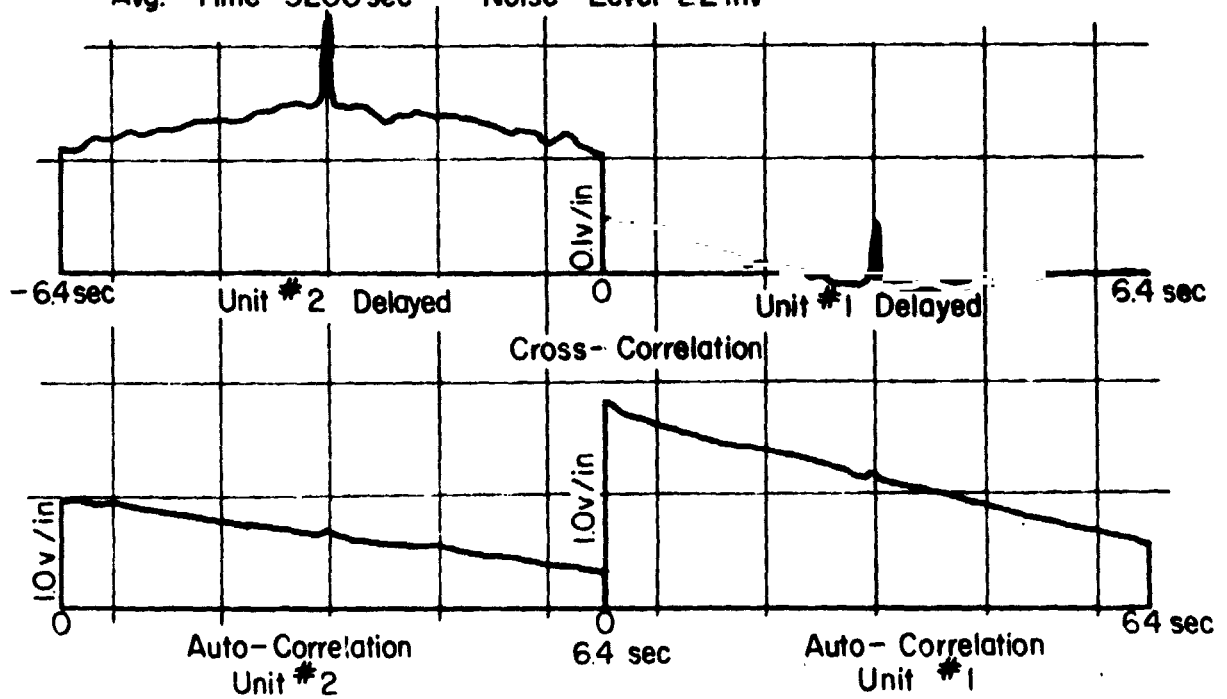
Band Pass 0.01-0.3 CPS  
 Avg. Time 3200 sec  
 Noise Level 22 mv



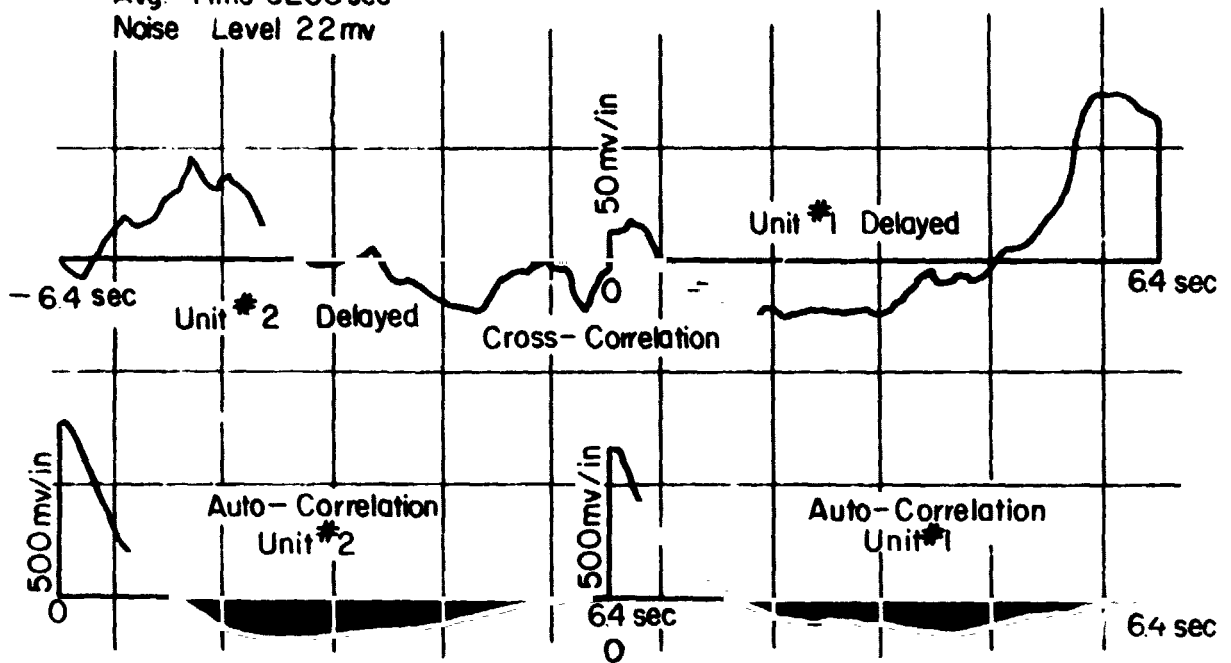
Run #H-11 (Optical) 1<sup>st</sup> Hour  
 Band Pass 0.01 to 3.0 Hz  
 Avg. Time 3200 sec  
 Noise Level 22 mv



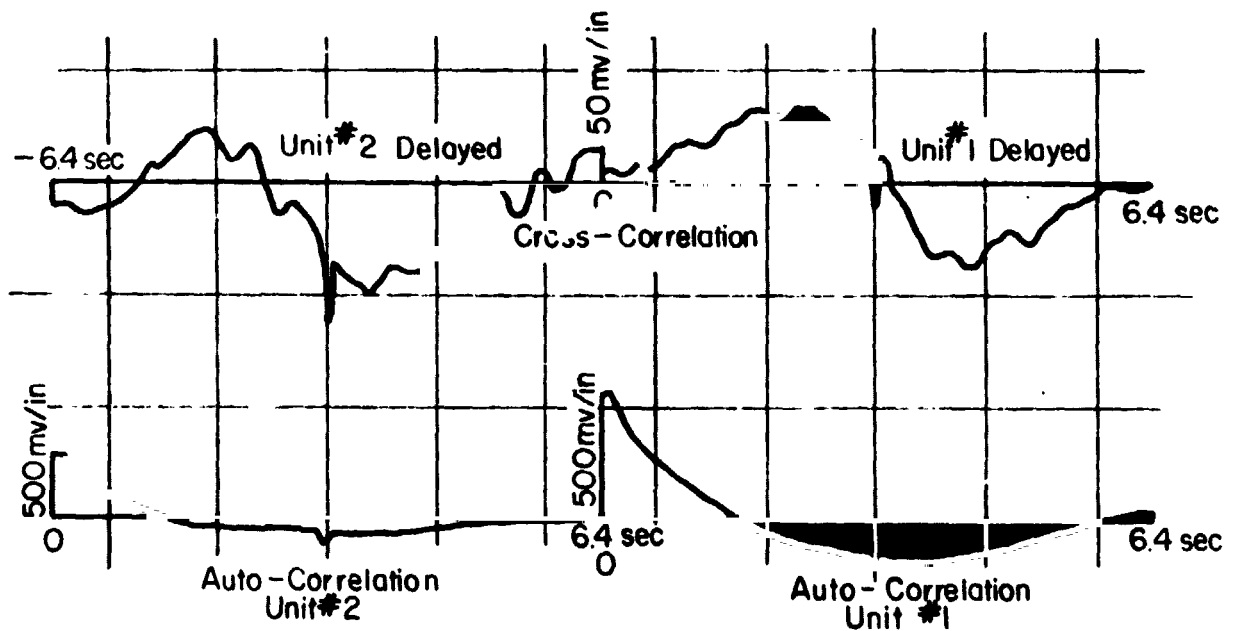
Run #H-11 (Optical) 2<sup>nd</sup> Hour Band Pass 0.01 to 3.0 Hz  
 Avg. Time 3200 sec Noise Level 22 mv



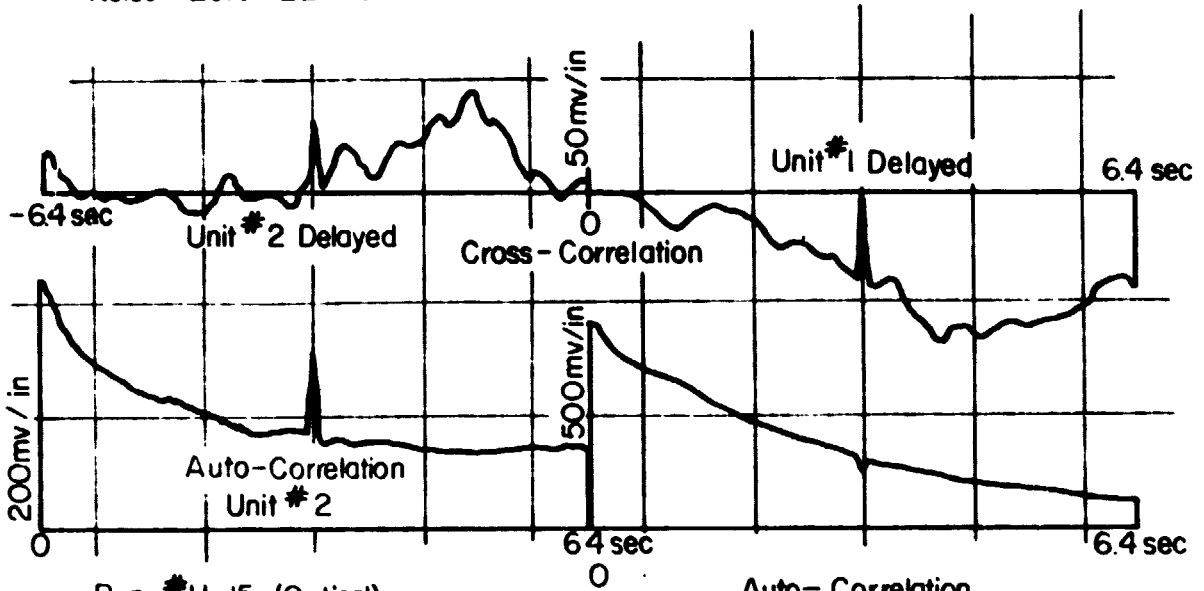
Run # H-14 (Optical) 1<sup>st</sup> Hour  
 Band Pass 01 to 30 Hz  
 Avg. Time 3200sec  
 Noise Level 22mv



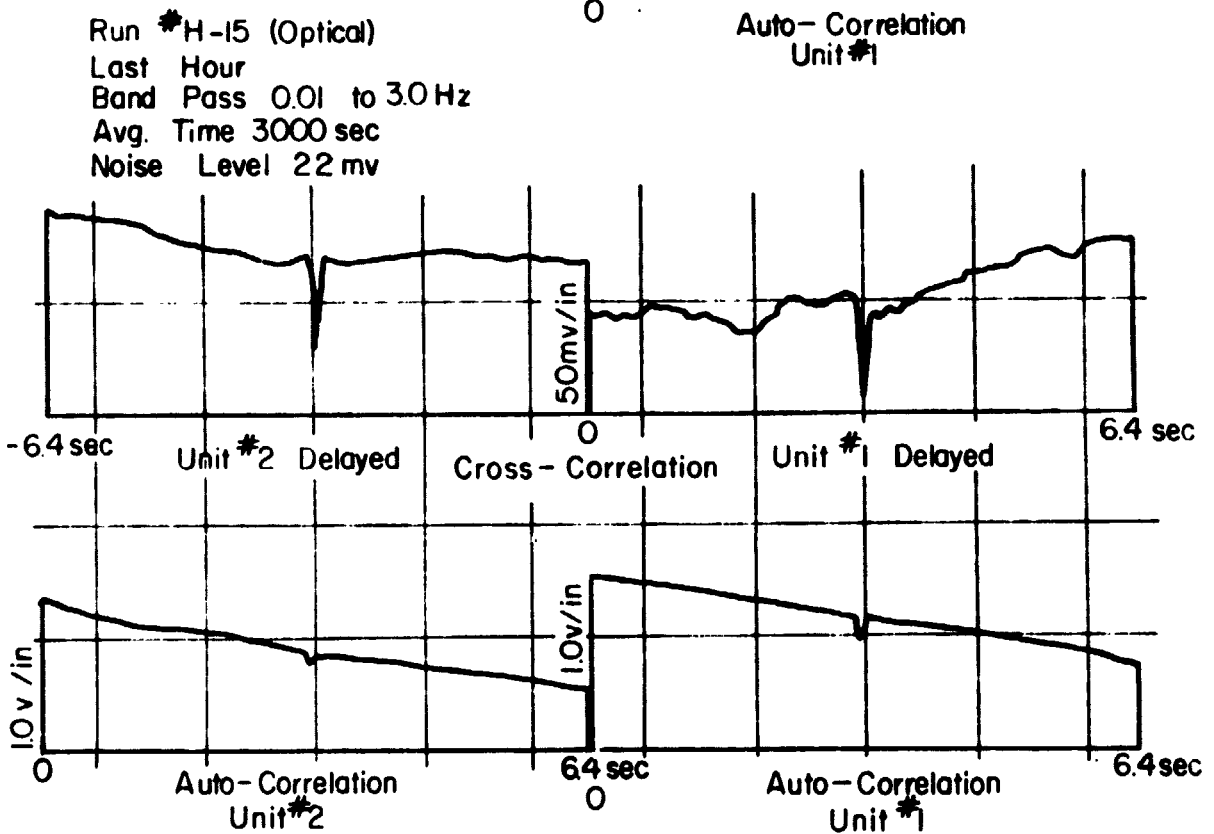
Run # H-14 (Optical) 2<sup>nd</sup> Hour  
 Band Pass 01 to 30 Hz  
 Avg. Time 3200mv  
 Noise Level 22 mv



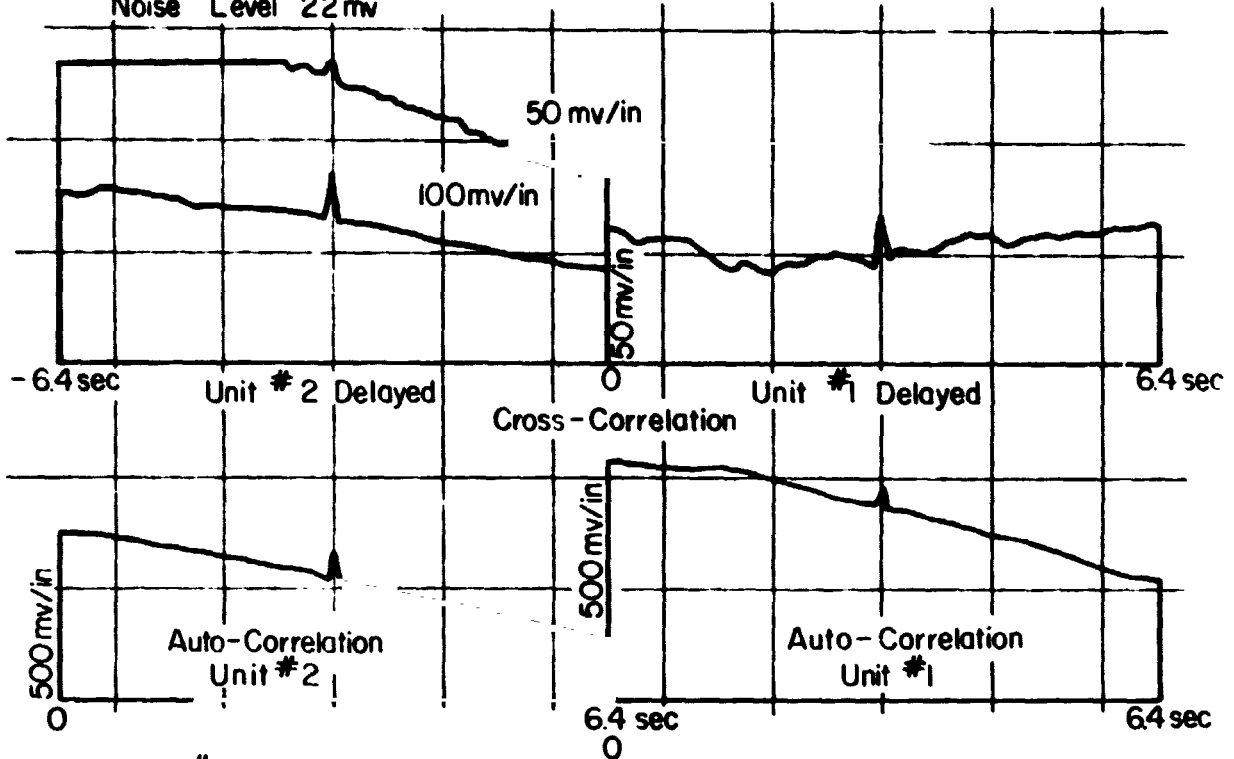
Run #H-15 (Optical) 1 Hours  
 Band Pass 0.01 to 3.0 Hz  
 Avg Time 3200 sec  
 Noise Level 22 mv



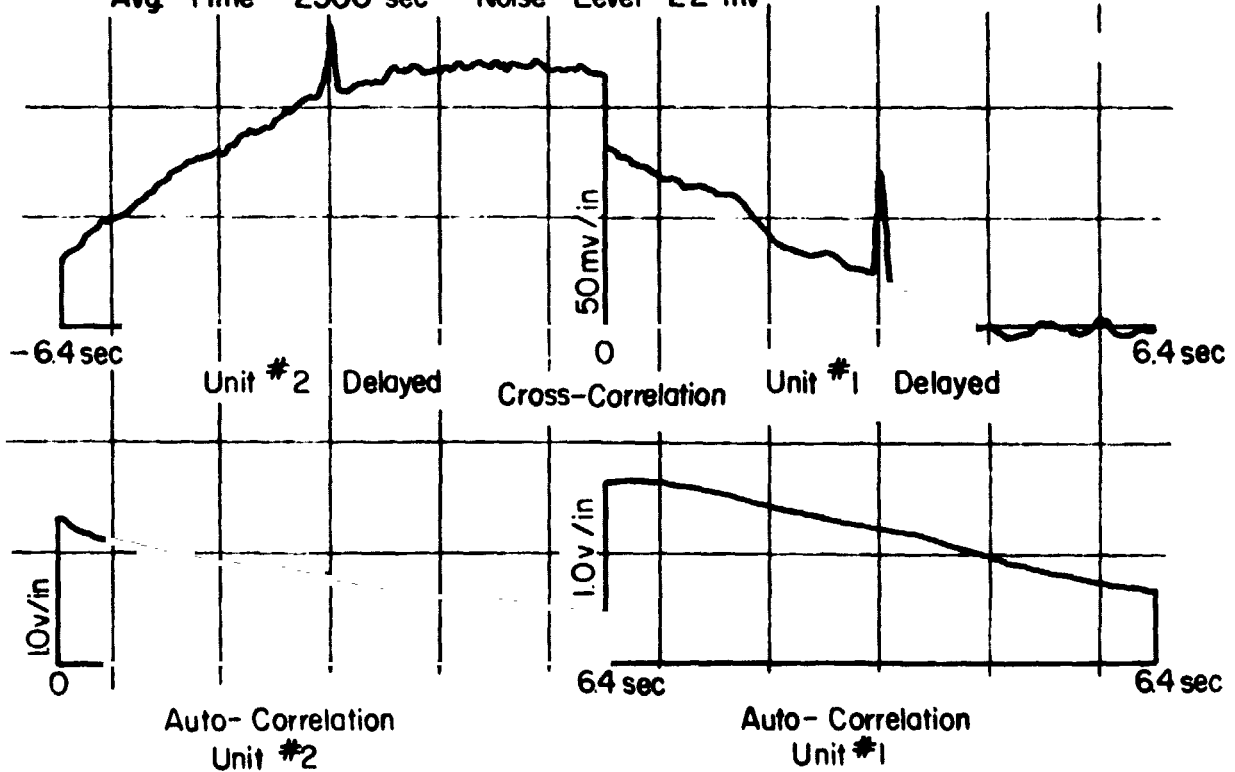
Run #H-15 (Optical)  
 Last Hour  
 Band Pass 0.01 to 3.0 Hz  
 Avg. Time 3000 sec  
 Noise Level 22 mv



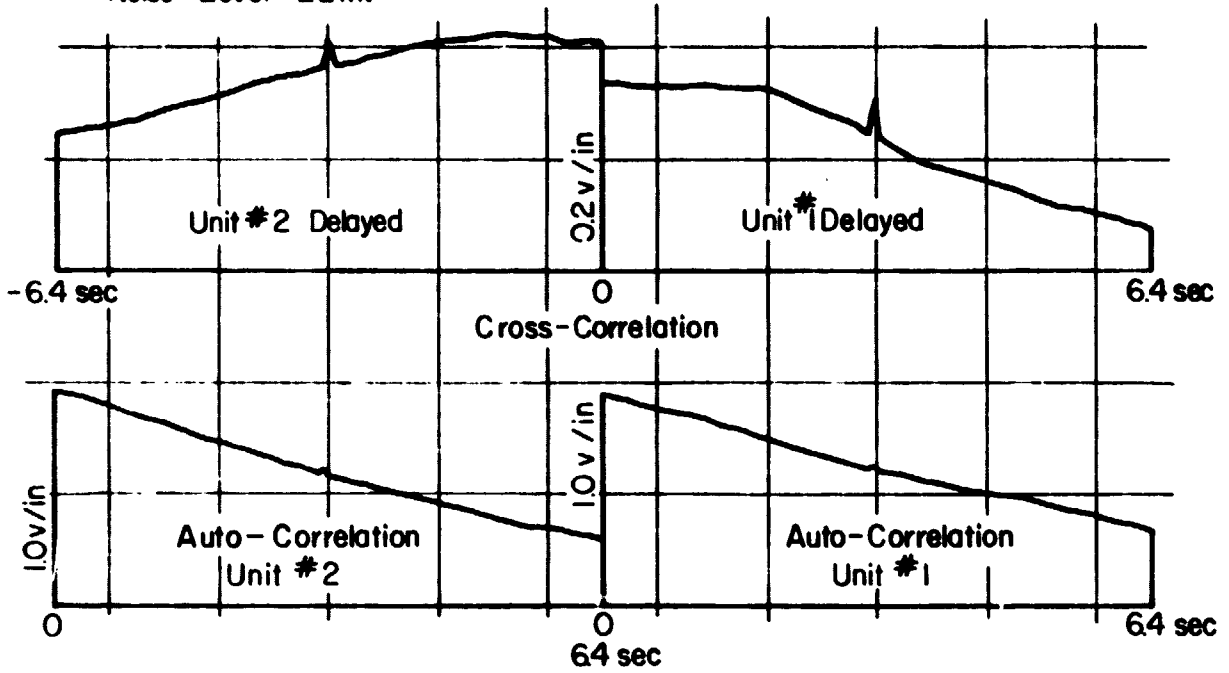
Run # H-16 (Optical)  
 Avg Time 3200 sec  
 Band Pass 0.01 to 30 Hz  
 Noise Level 22 mv



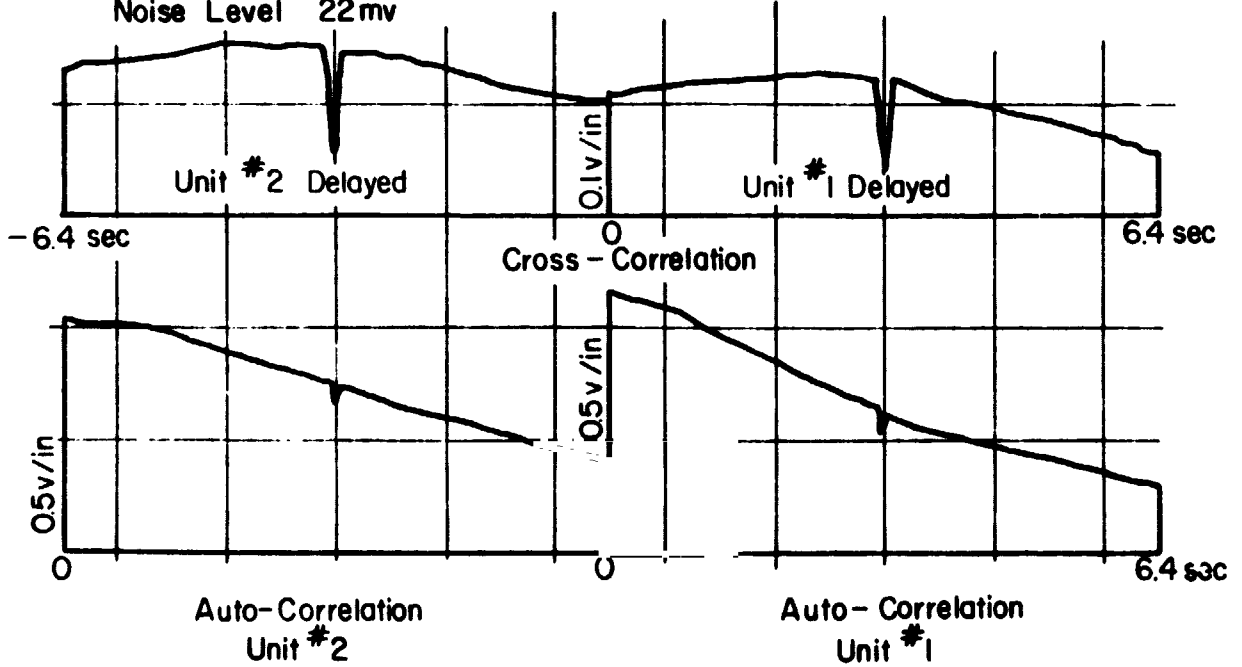
Run # H 17 (Optical) Band Pass 0.01 to 3.0 sec  
 Avg Time 2500 sec Noise Level 22 mv



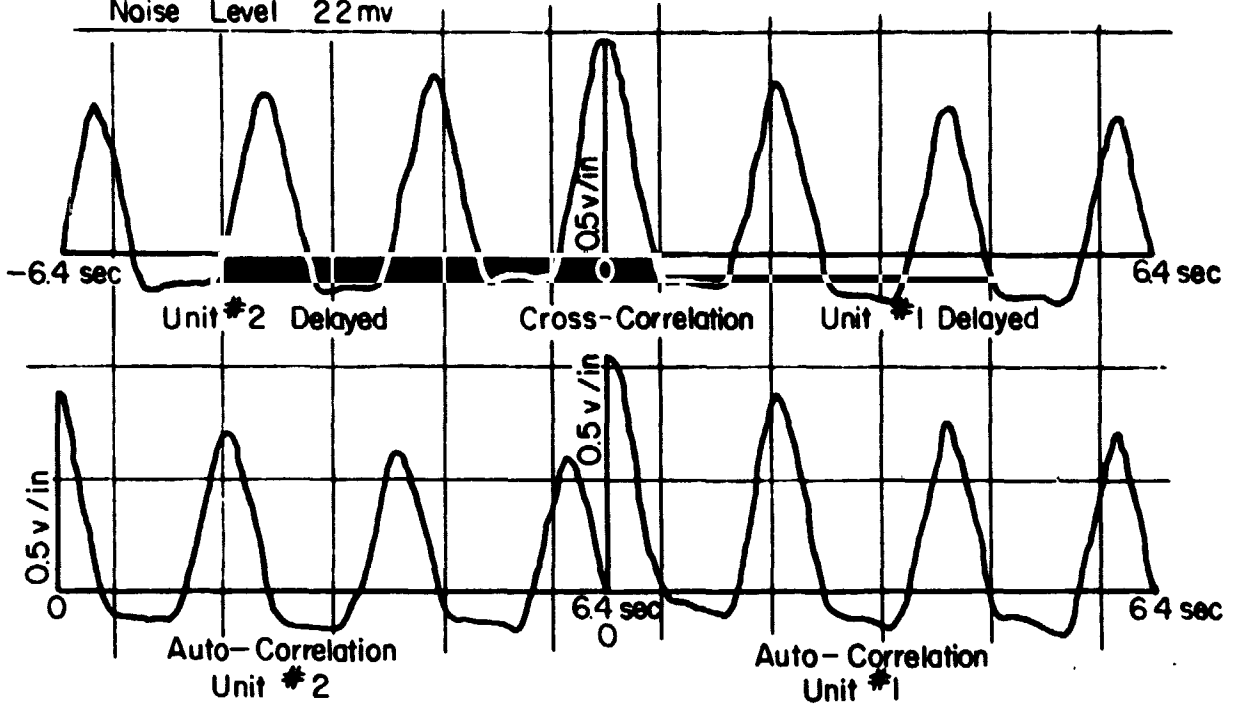
Run # H-19 (Optical)  
 Band Pass 0.01 to 30 Hz  
 Avg. Time 3200 sec  
 Noise Level 22mv



Run # H-20 (Optical)  
 Band Pass 0.01 to 3.0 Hz  
 Avg. Time 3200 sec  
 Noise Level 22mv



Run # H-22 (Optical)  
 Band Pass 0.01 to 3.0 Hz  
 Avg. Time 3200 sec  
 Noise Level 22 mv



Run # H-22 (Optical)  
 Band Pass 0.01 to 300 Hz  
 Avg. Time 3200 sec  
 Noise Level 6.9 mv

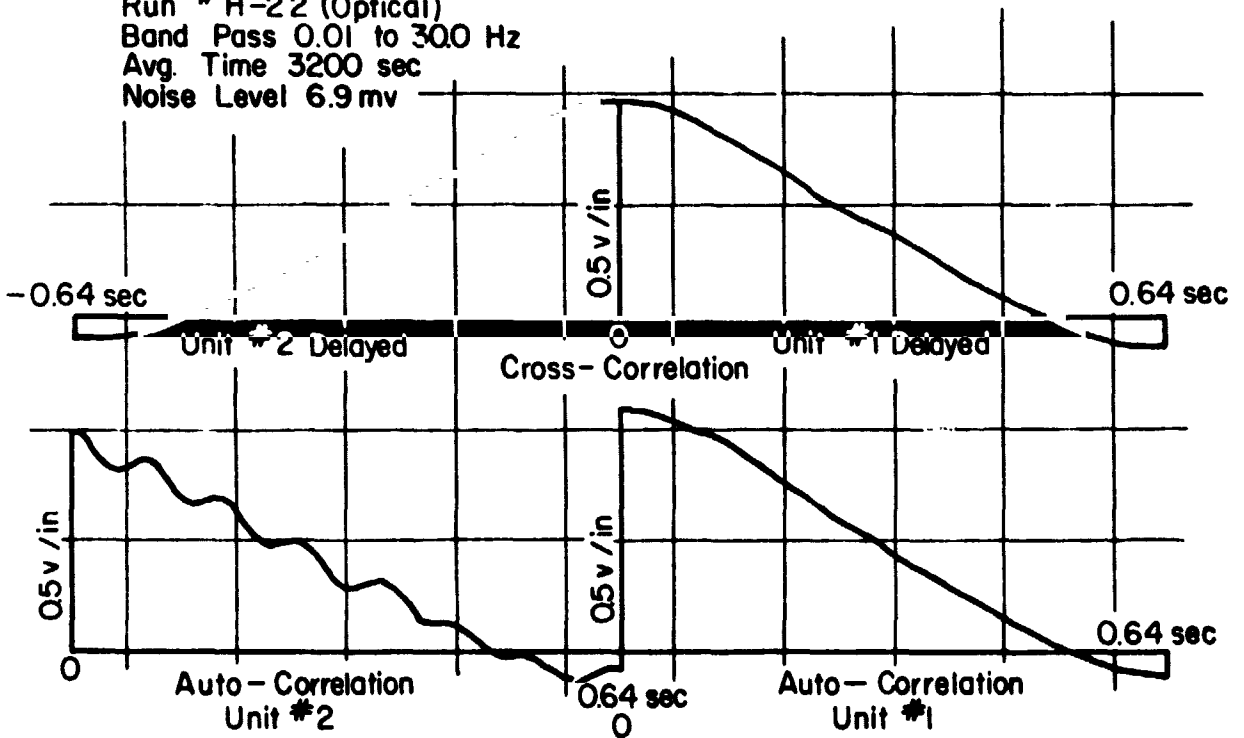
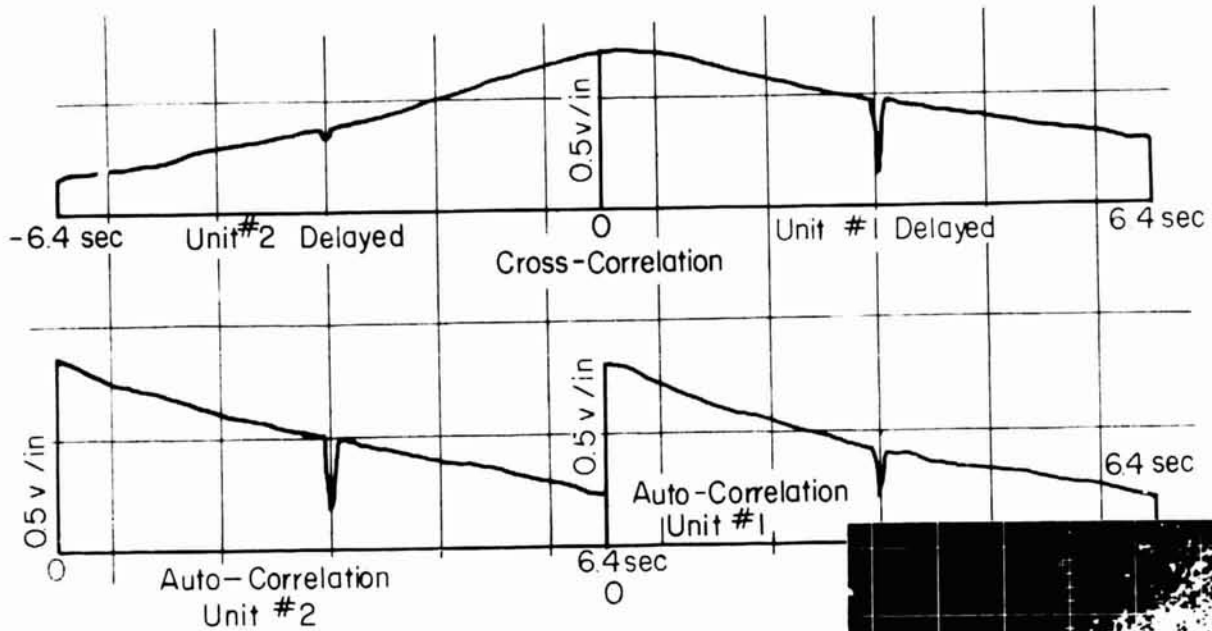
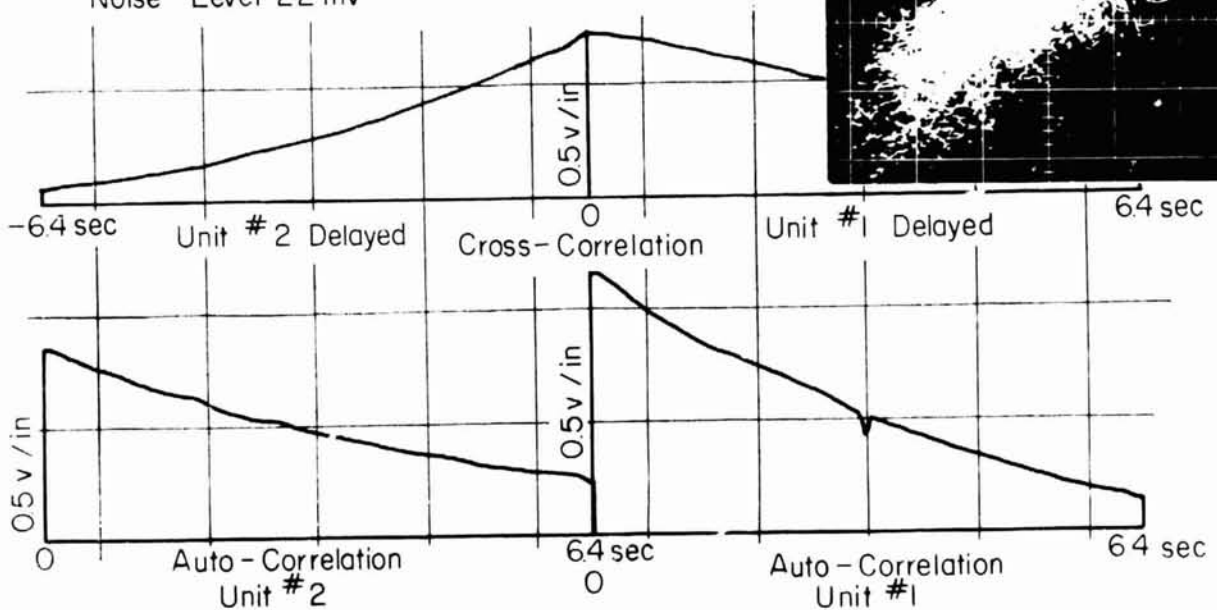


FIGURE 3- CORRELATIONS OF INFRARED CROSS BEAM SYSTEMS

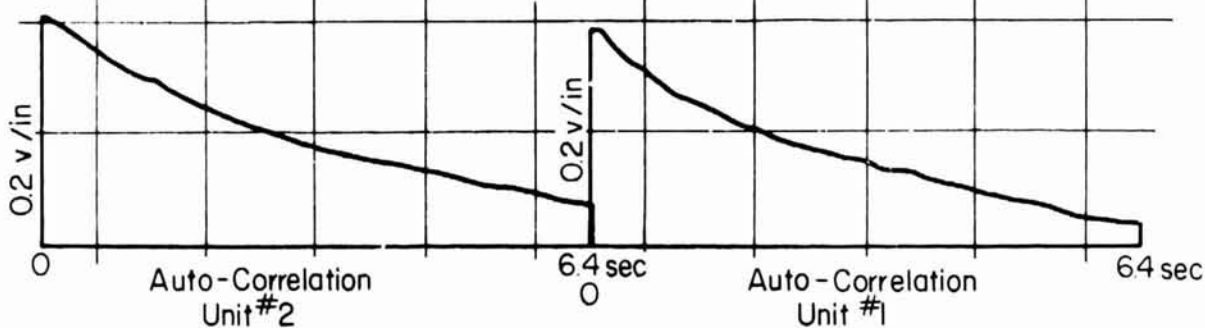
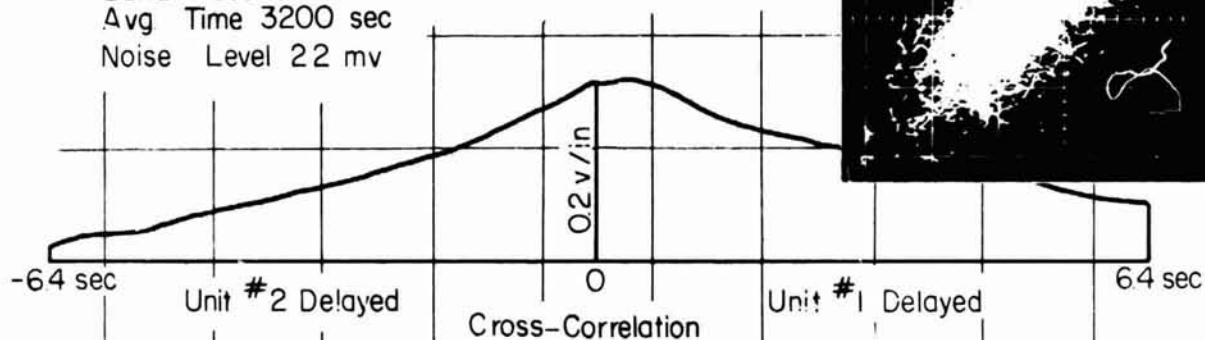
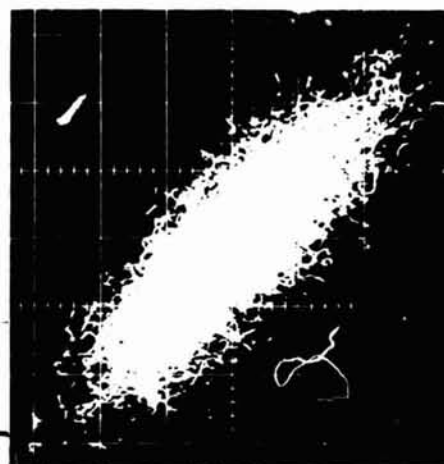
Run #1 (IR)  
 Band Pass 0.01 to 3.0 Hz  
 Avg Time 3200sec  
 Noise Level 22mv



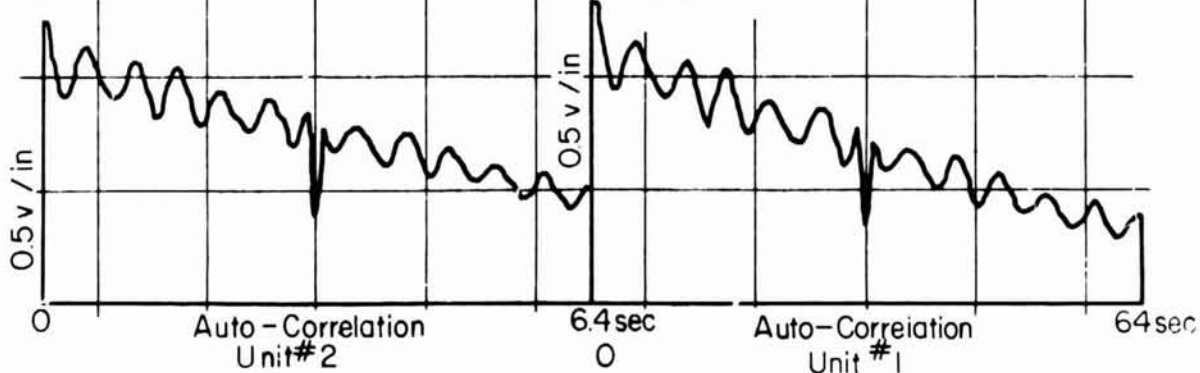
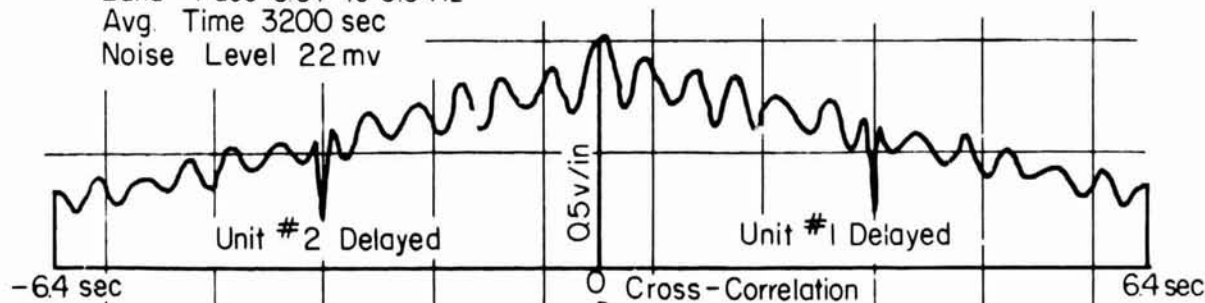
Run #2 (IR)  
 Band Pass 0.01 to 3.0 Hz  
 Avg Time 3200 sec  
 Noise Level 22mv

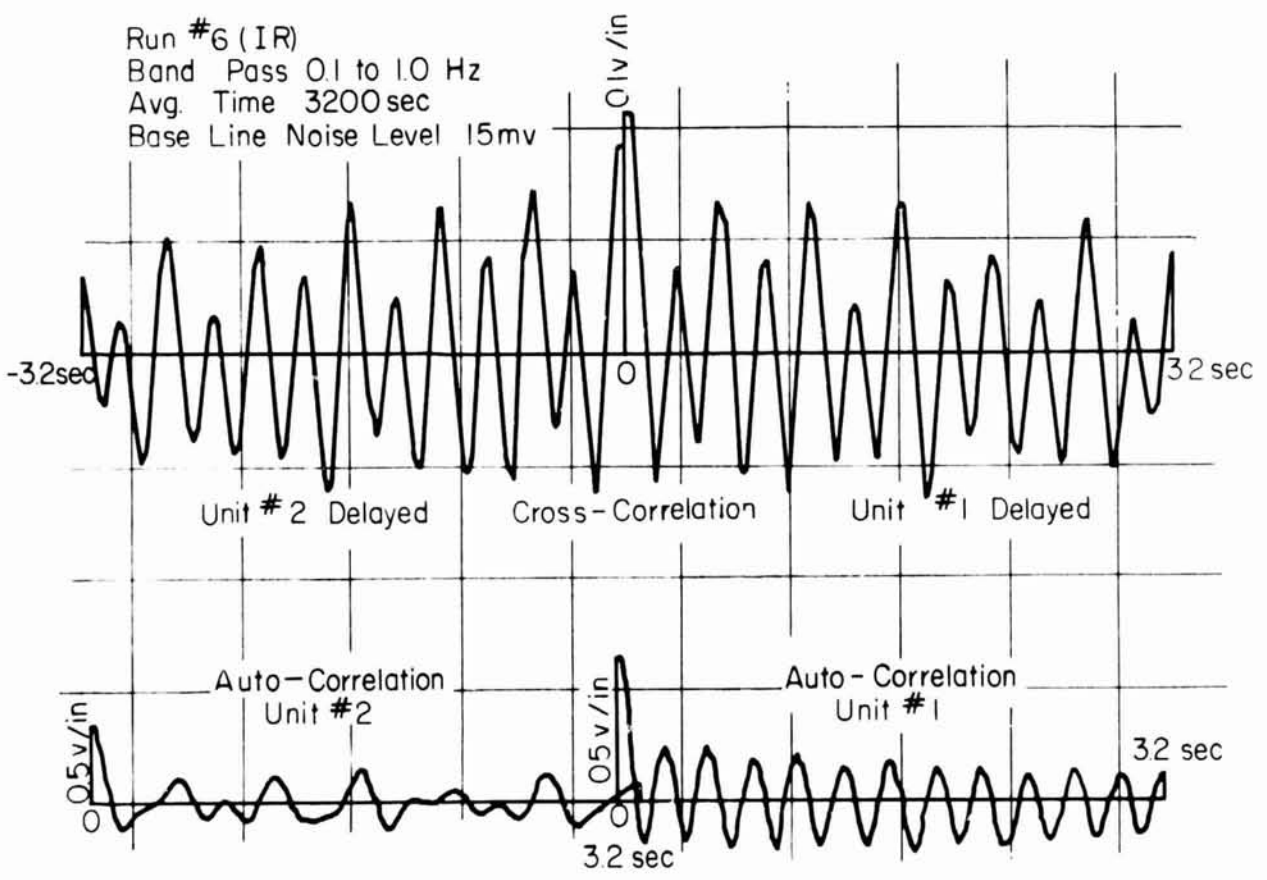
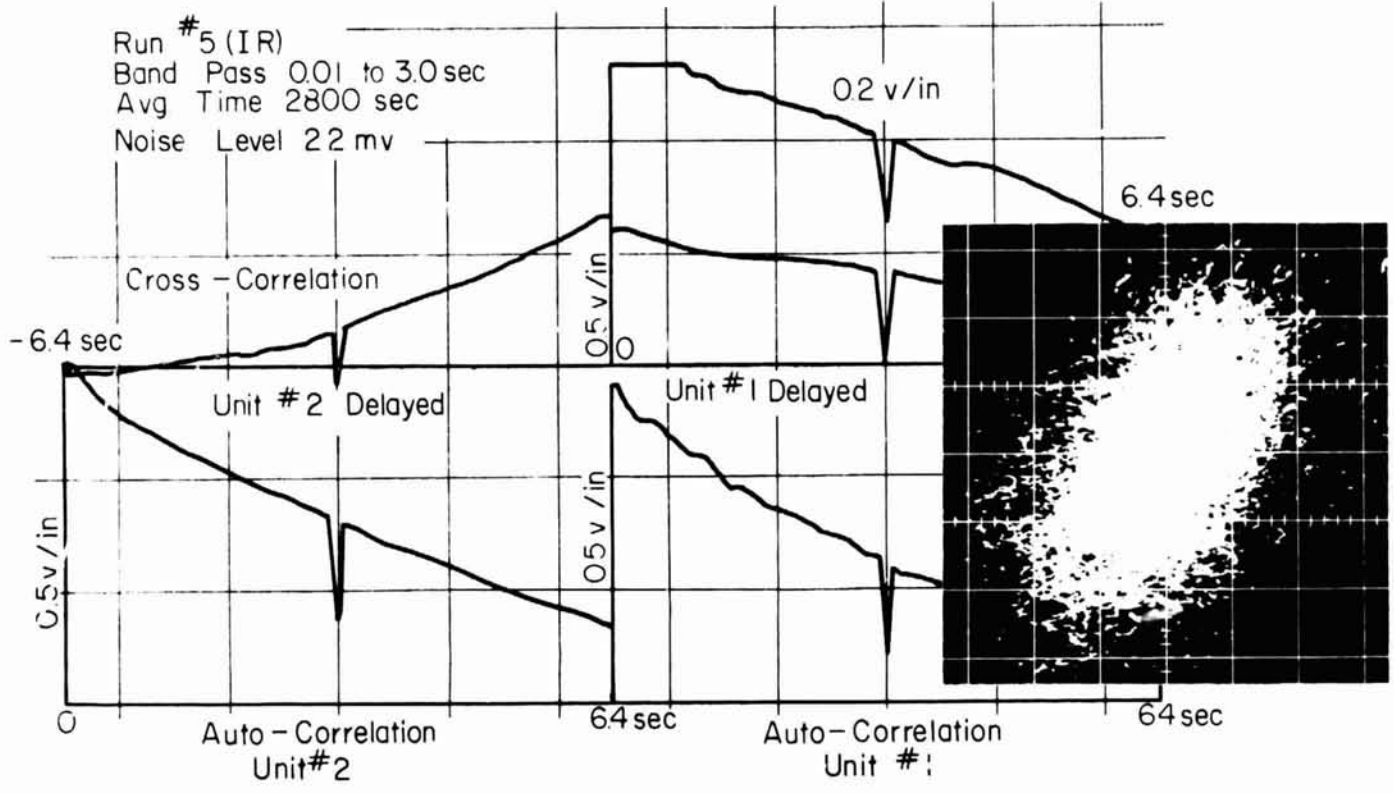


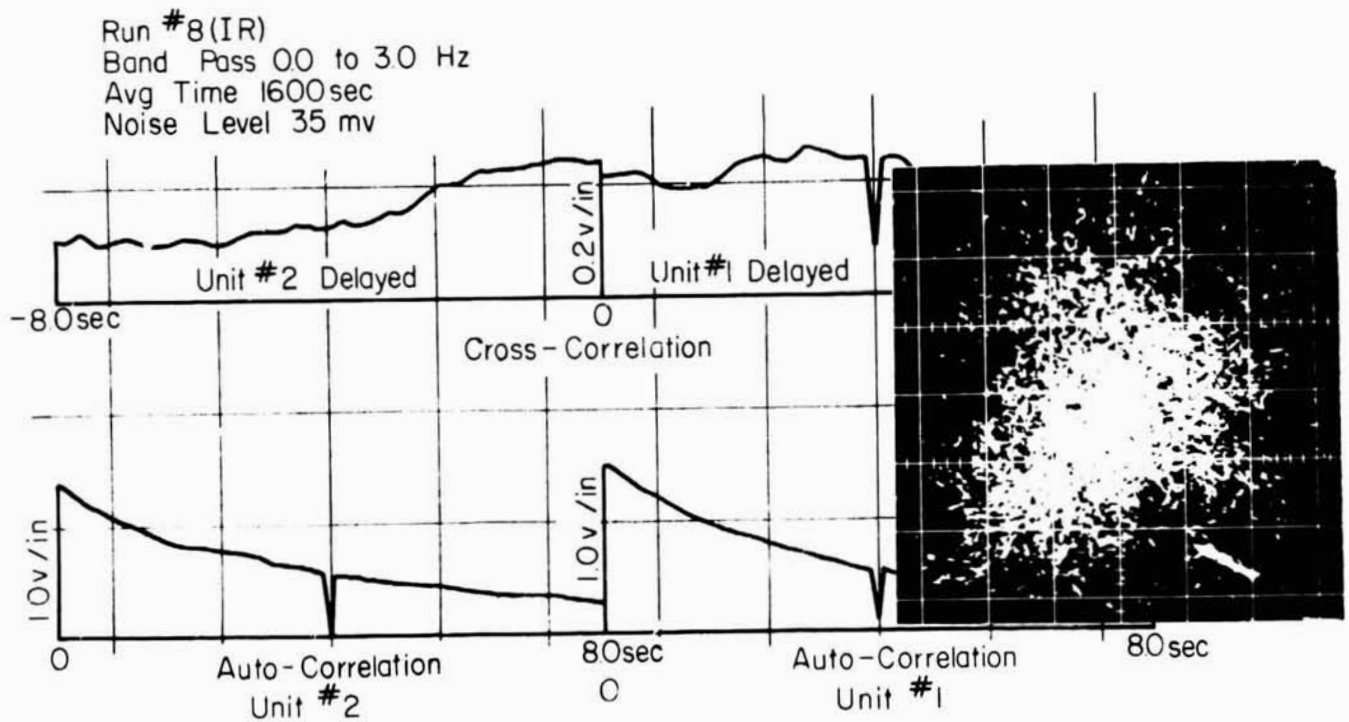
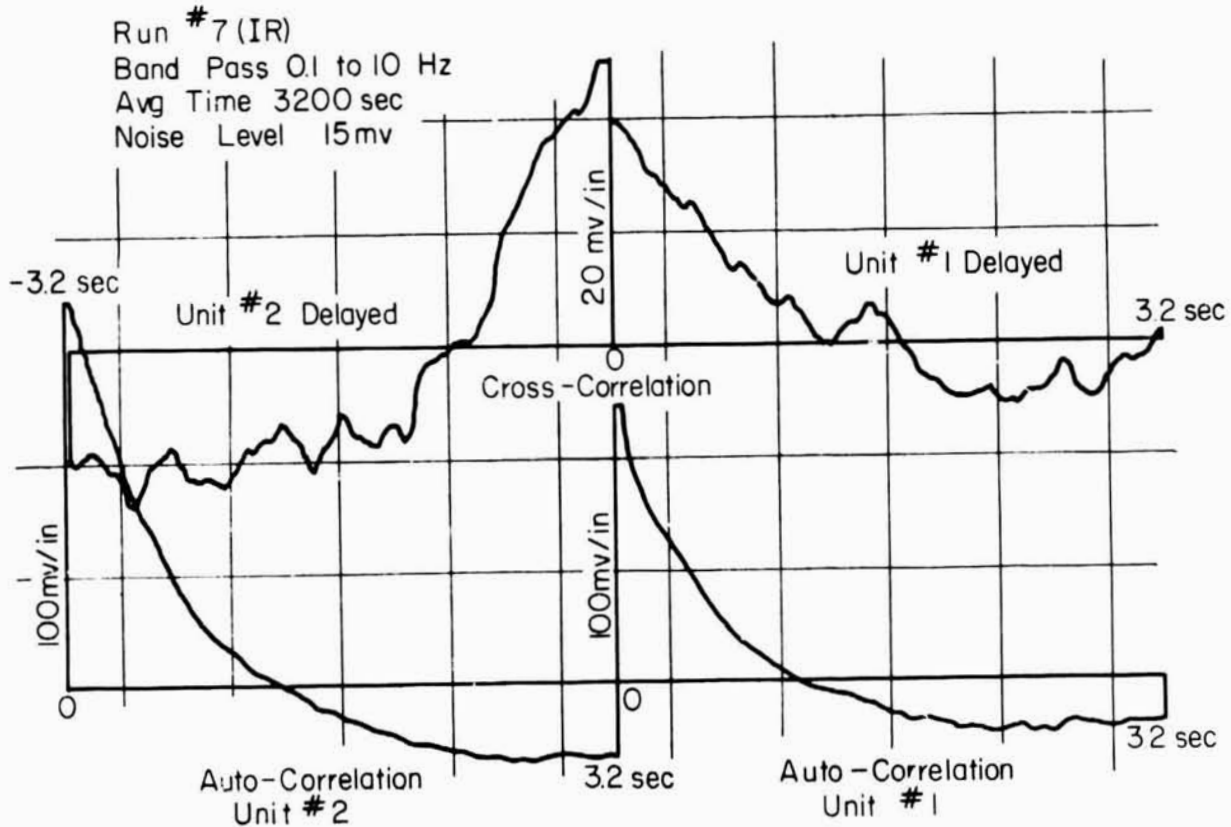
Run #3 (IR)  
 Band Pass 0.01 to 3.0 Hz  
 Avg Time 3200 sec  
 Noise Level 22 mv



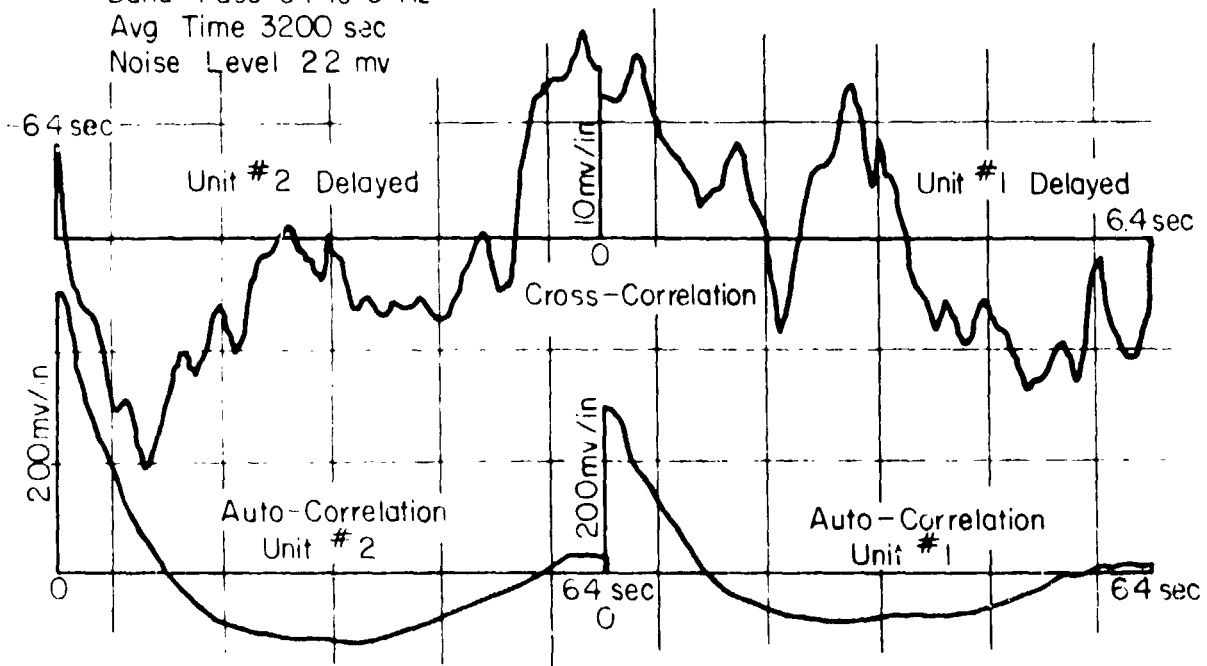
Run #4 (IR)  
 Band Pass 0.01 to 3.0 Hz  
 Avg Time 3200 sec  
 Noise Level 22 mv



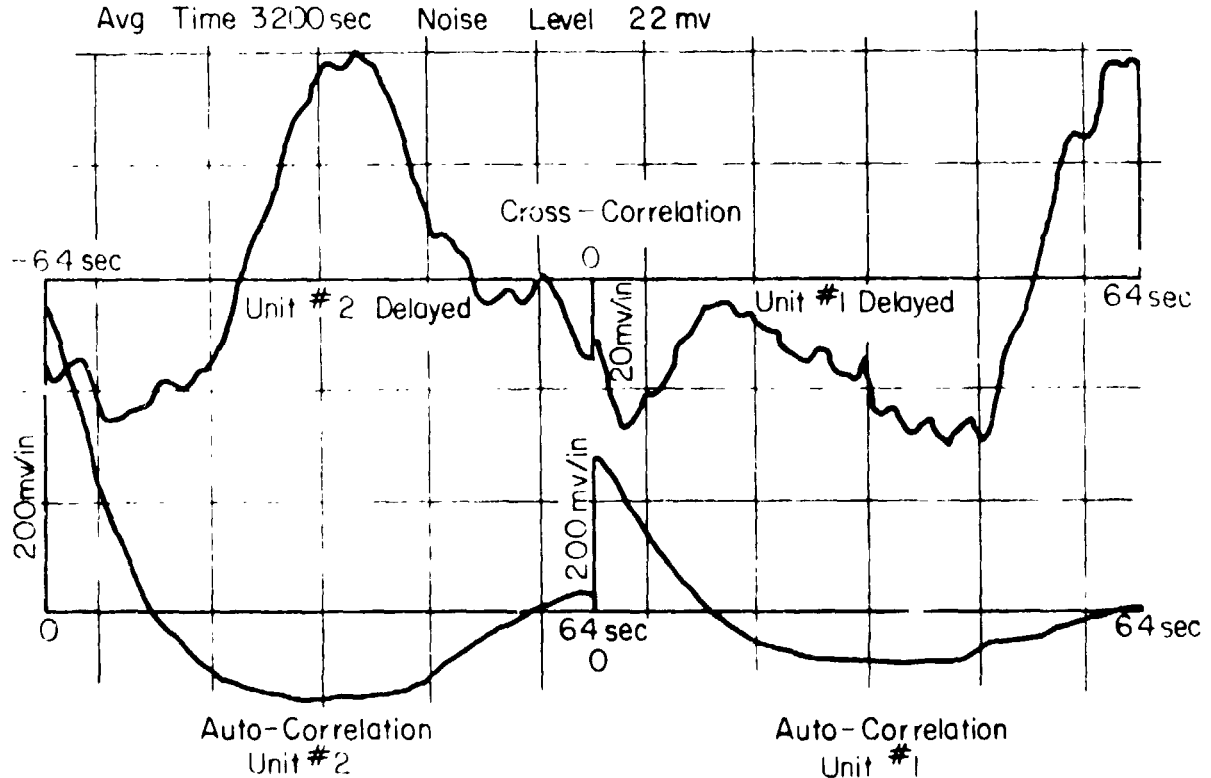




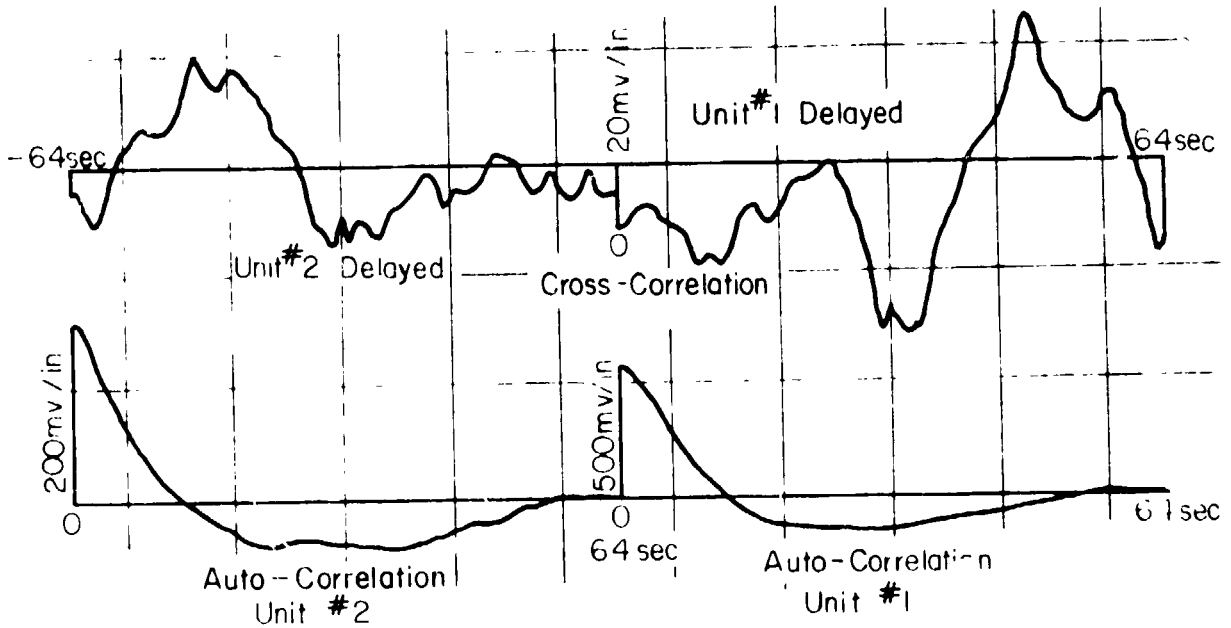
Run #9(IR) 1<sup>st</sup> Hour  
Band Pass 0.1 to 3 Hz  
Avg Time 3200 sec  
Noise Level 22 mv



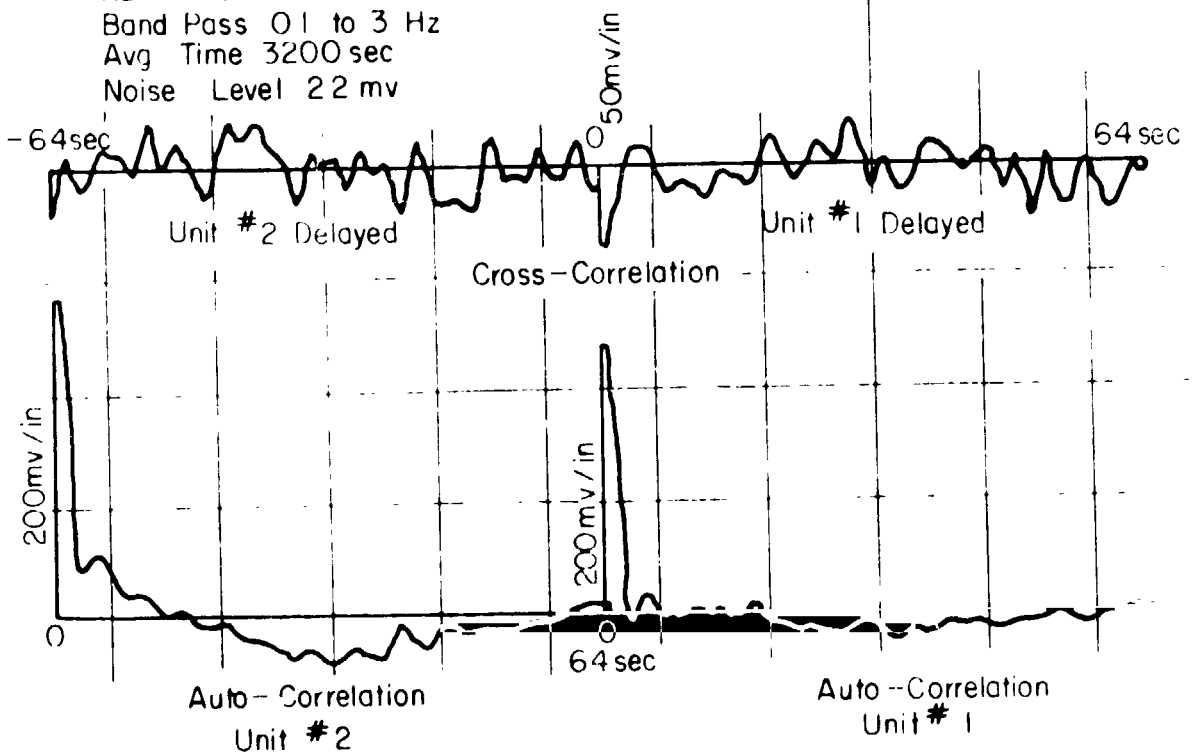
Run #9(IR) 2<sup>nd</sup> Hour Band Pass 0.1 to 30 Hz  
Avg Time 3200sec Noise Level 22 mv

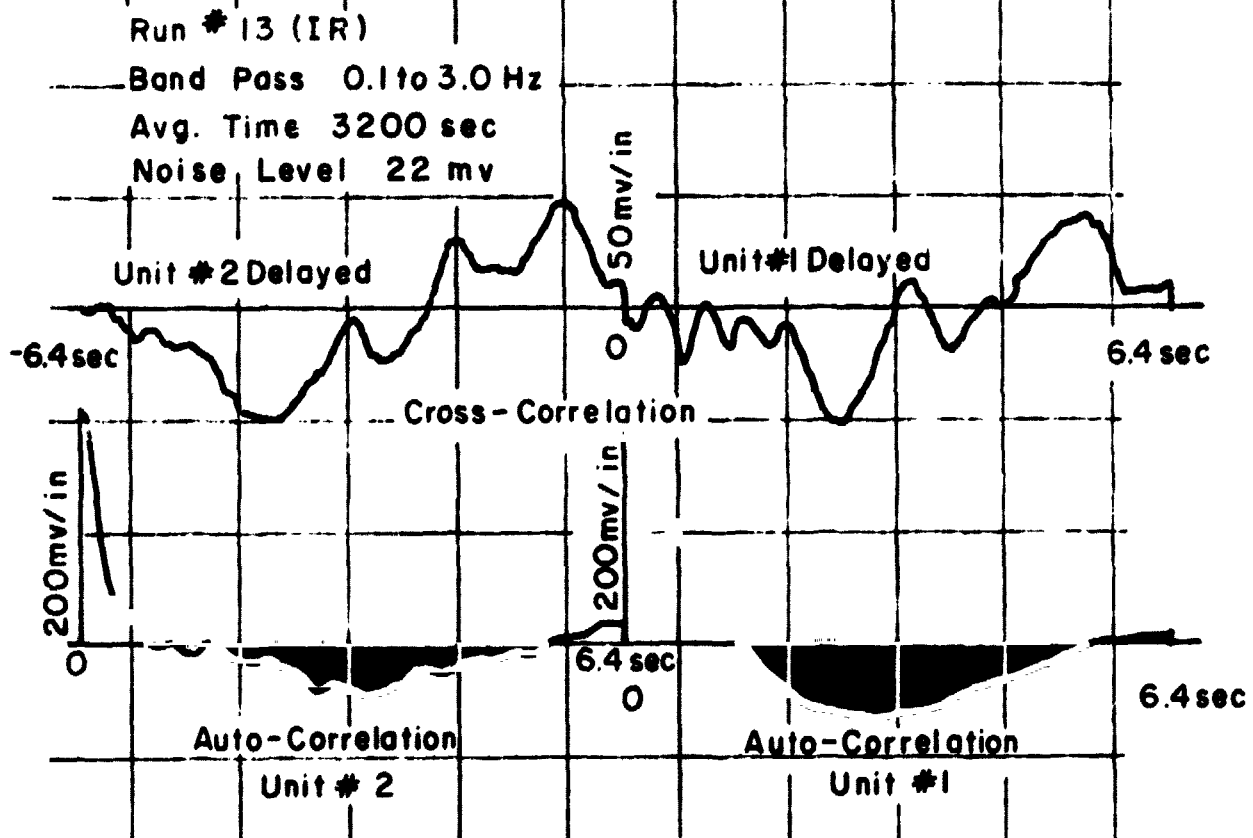
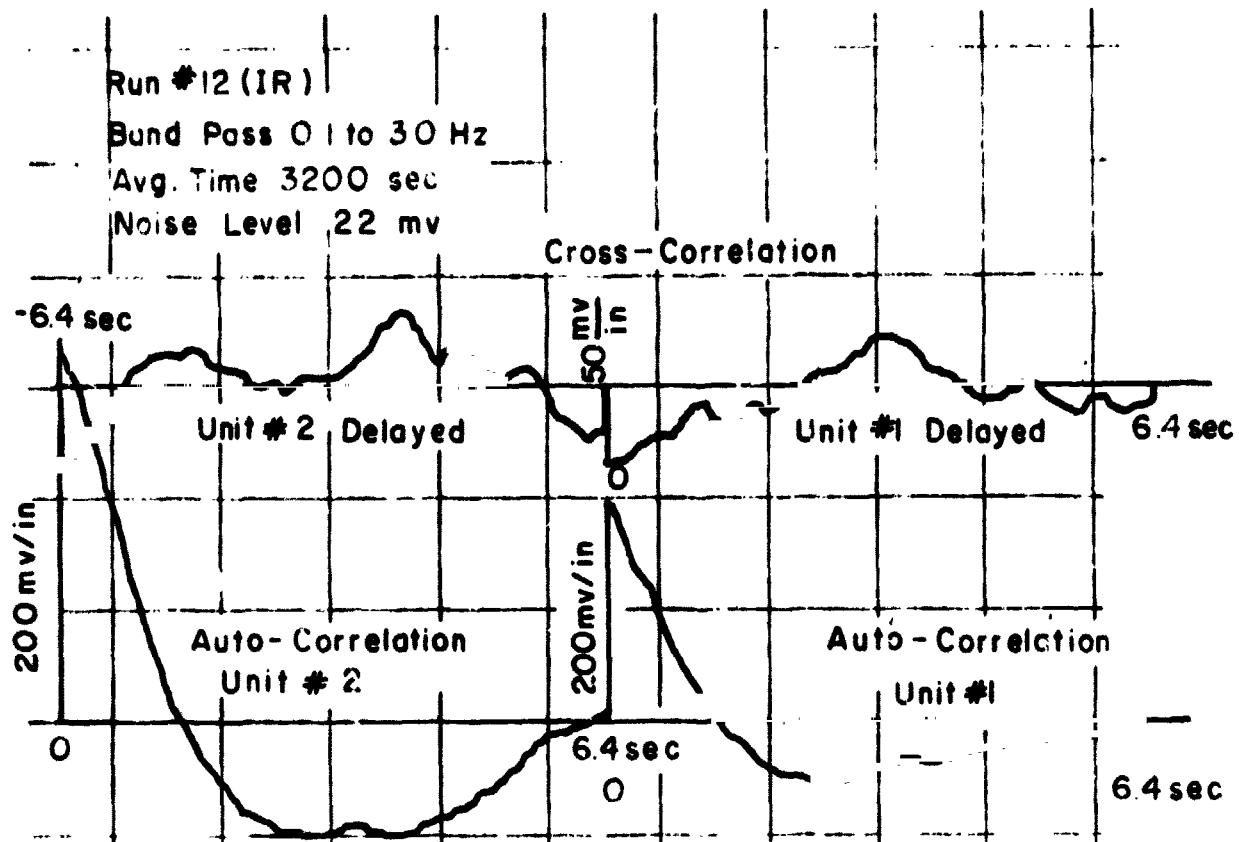


Run #10 (IR)  
 Band Pass 0.1 to 30 Hz  
 Avg Time 3200 sec  
 Noise Level 22mv

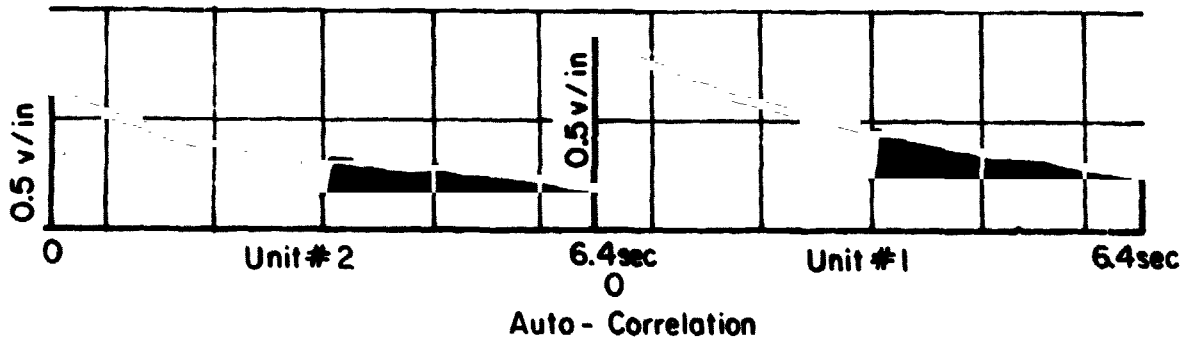
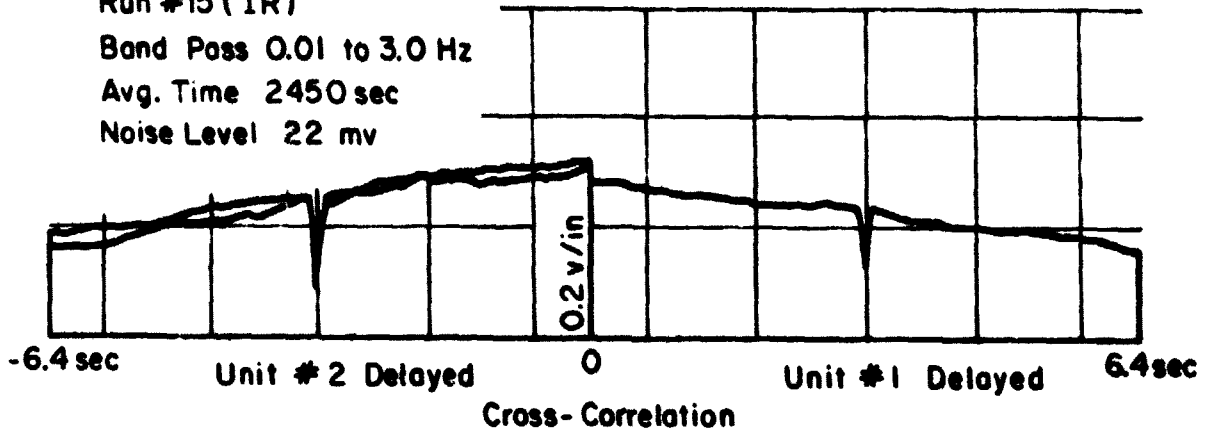


Run #11 (IR)  
 Band Pass 0.1 to 3 Hz  
 Avg Time 3200 sec  
 Noise Level 22 mv

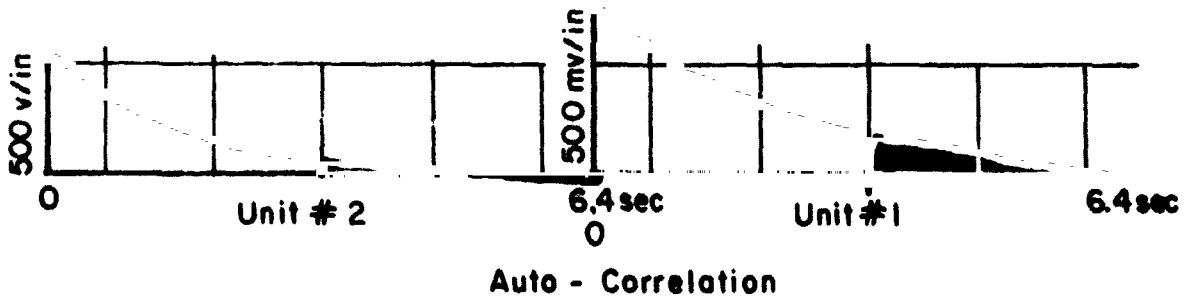
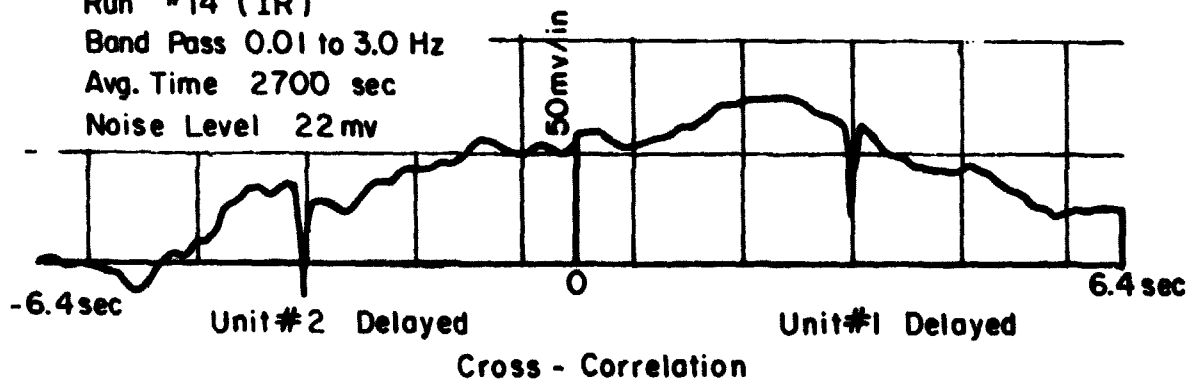




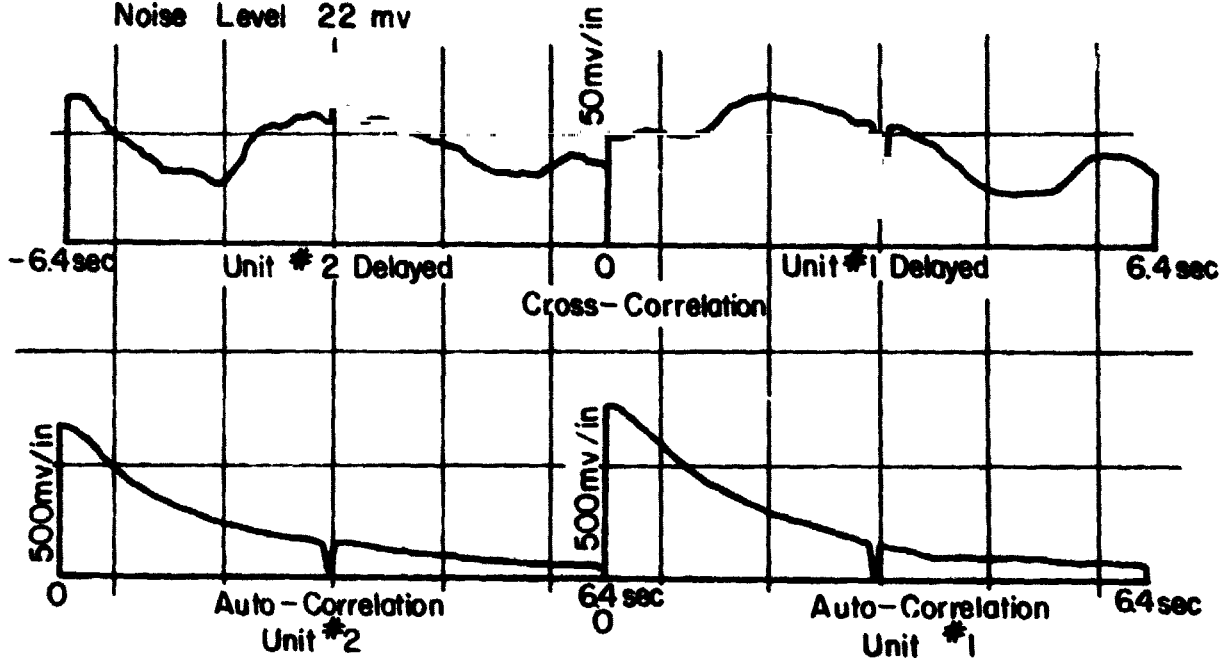
Run #15 (IR)  
 Band Pass 0.01 to 3.0 Hz  
 Avg. Time 2450 sec  
 Noise Level 22 mv



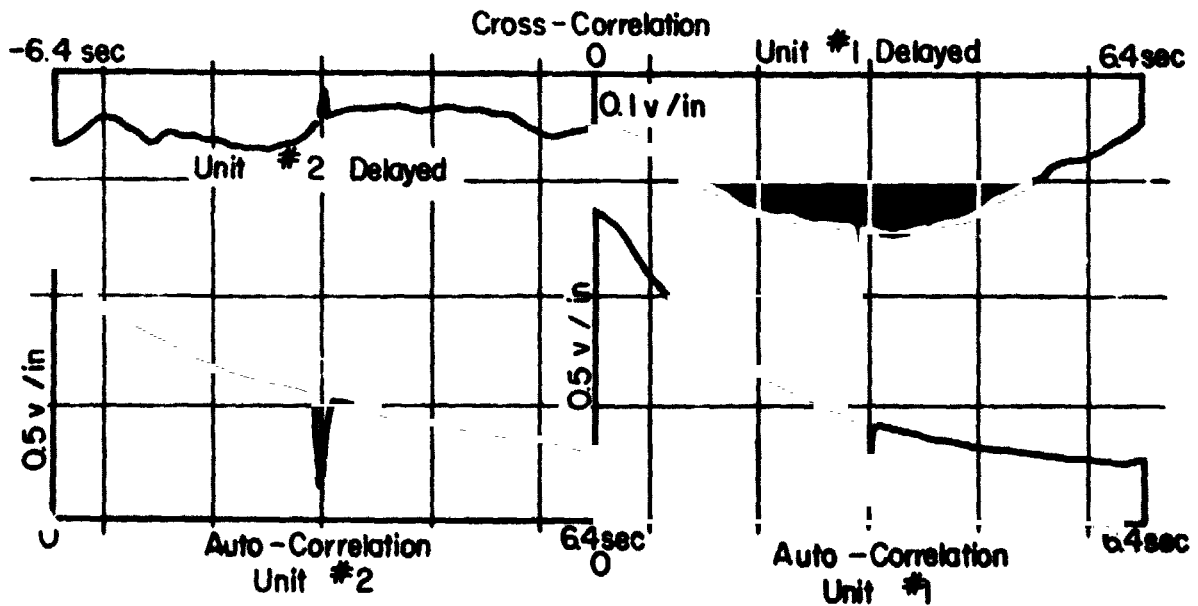
Run #14 (IR)  
 Band Pass 0.01 to 3.0 Hz  
 Avg. Time 2700 sec  
 Noise Level 22 mv



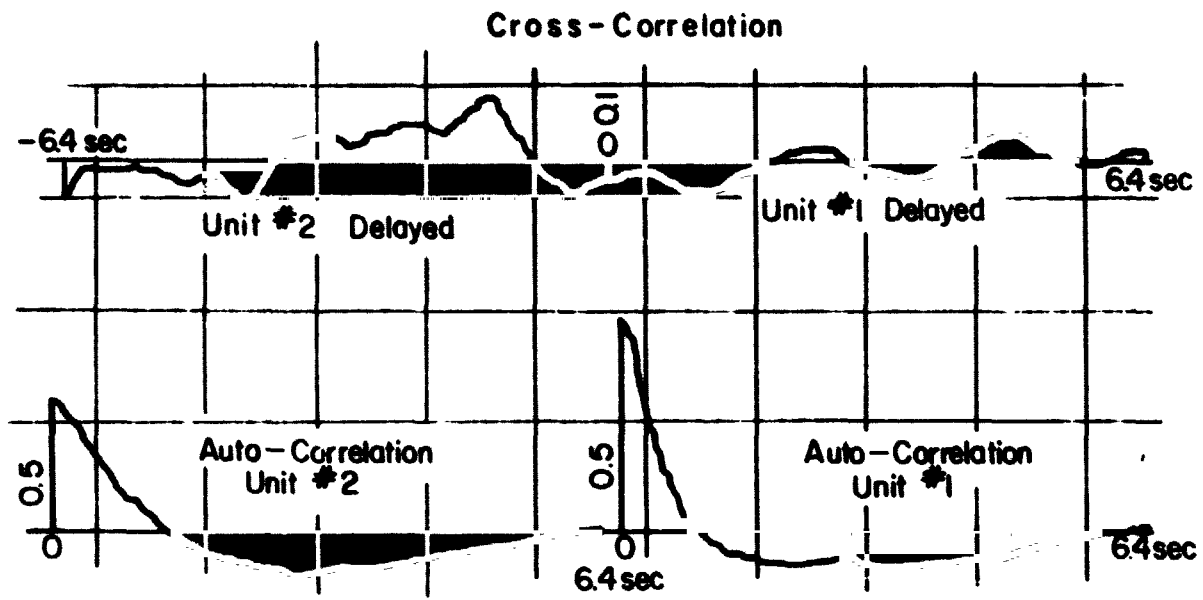
Run #20 (IR)  
 Band Pass 0.01 to 30 Hz  
 Avg Time 3200 sec  
 Noise Level 22 mv



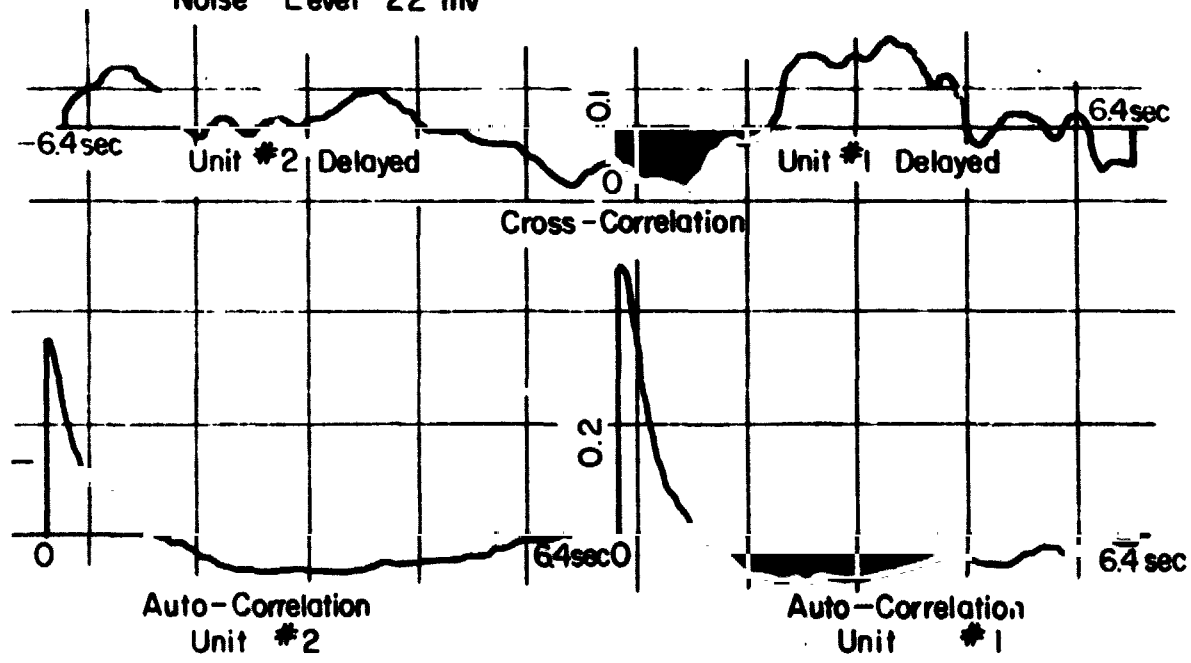
Run #22 (IR)  
 Band Pass 0.01 to 30 Hz  
 Avg. Time 3200 sec  
 Noise Level 22 mv



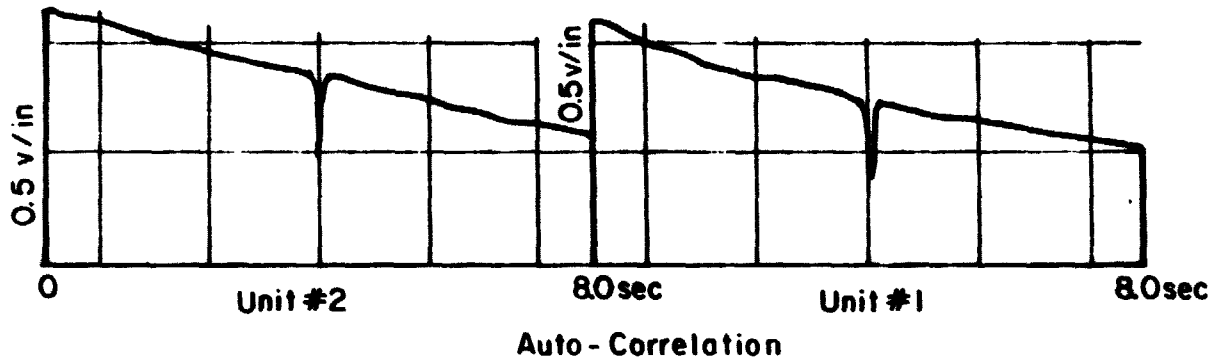
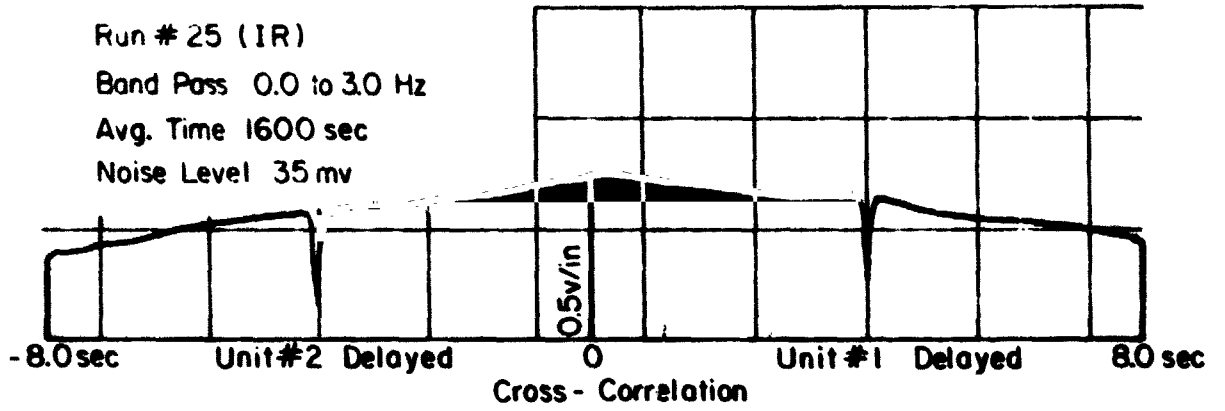
Run # 23 (IR)  
 Band Pass .1-3 cps  
 Avg. Time 3200 sec  
 Noise Level 22 mv



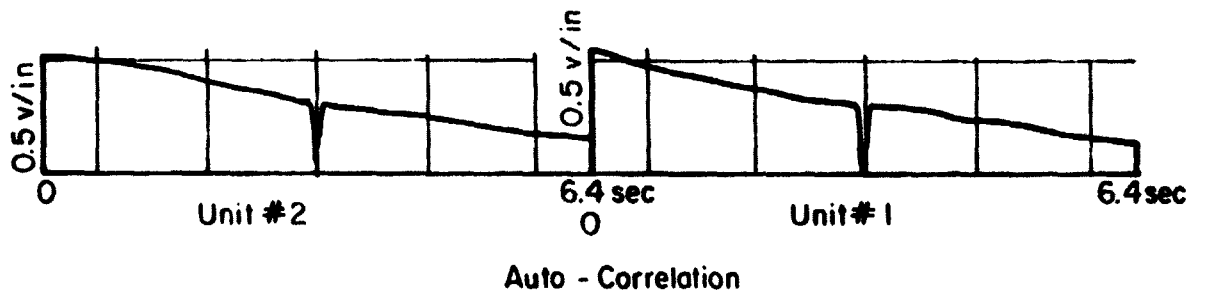
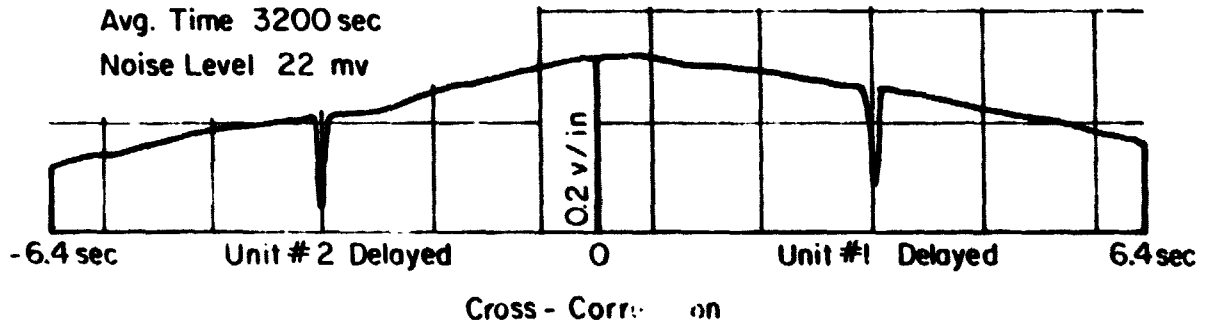
Run #24 (IR)  
 Band Pass 0.1-3 CPS  
 Avg. Time 3200 sec  
 Noise Level 22 mv

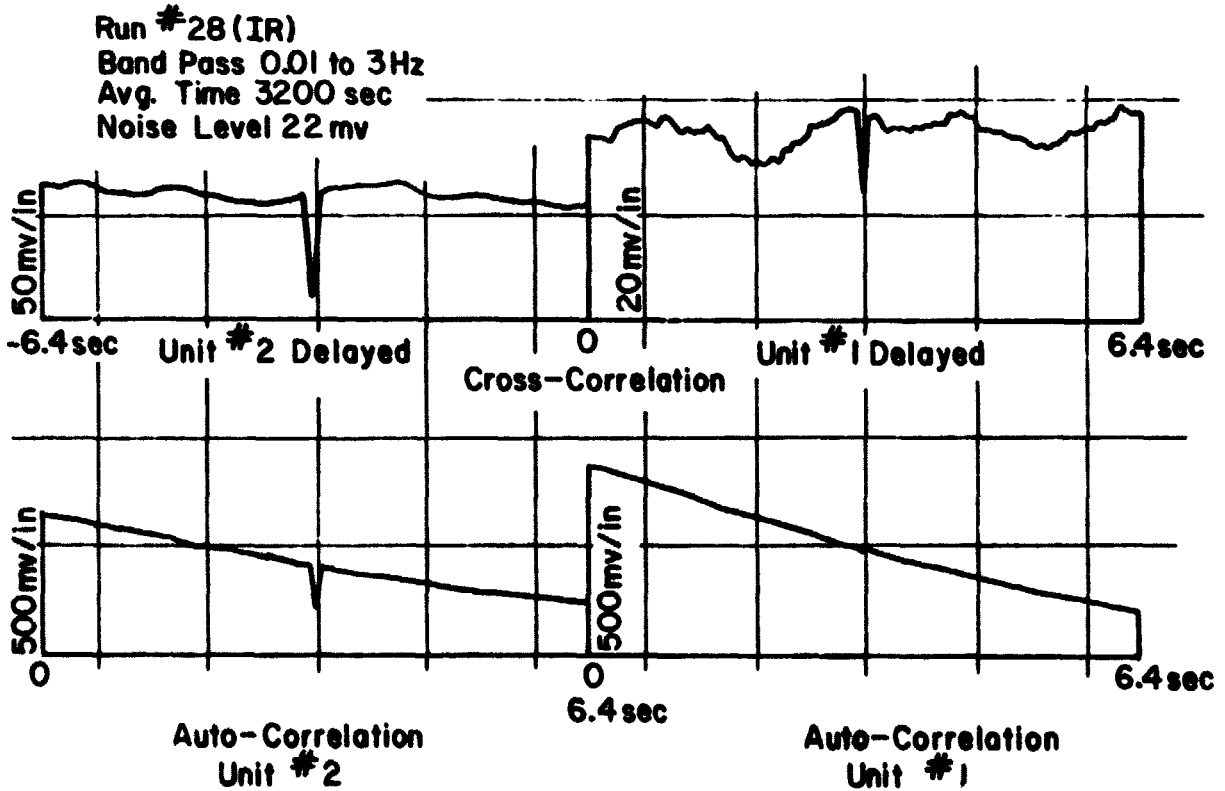
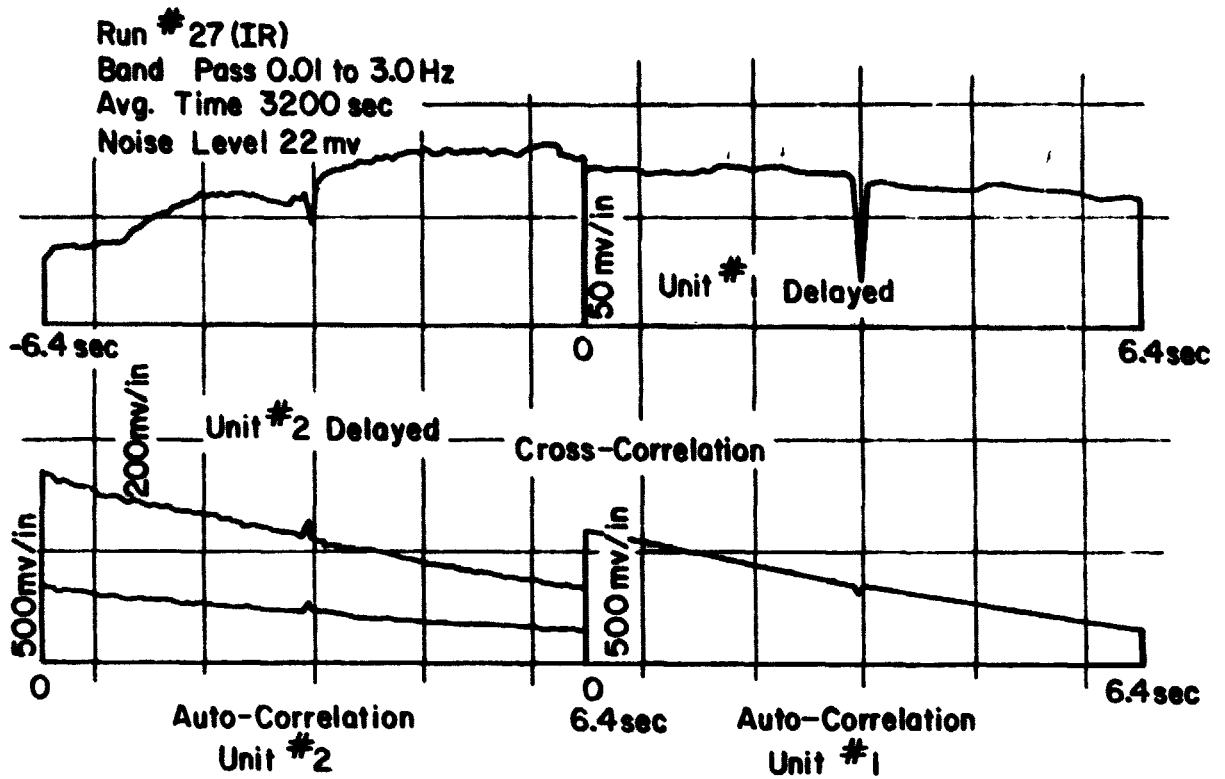


Run # 25 (IR)  
 Band Pass 0.0 to 3.0 Hz  
 Avg. Time 1600 sec  
 Noise Level 35 mv

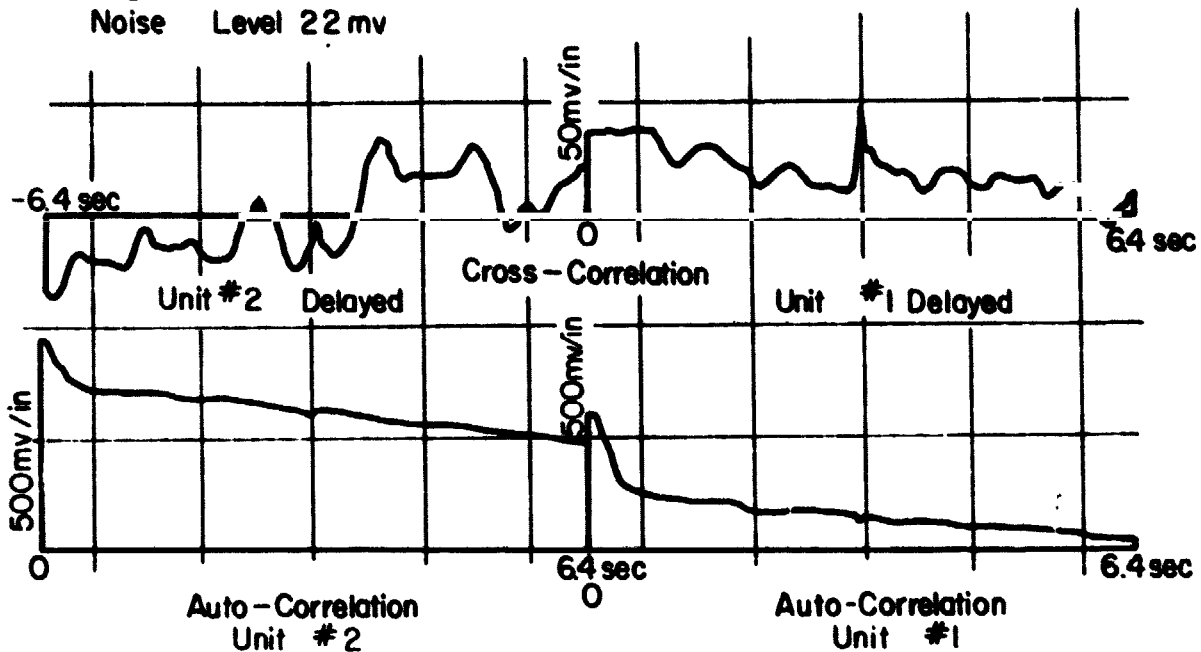


Run # 26 (IR)  
 Band Pass 0.01 to 3.0 Hz  
 Avg. Time 3200 sec  
 Noise Level 22 mv

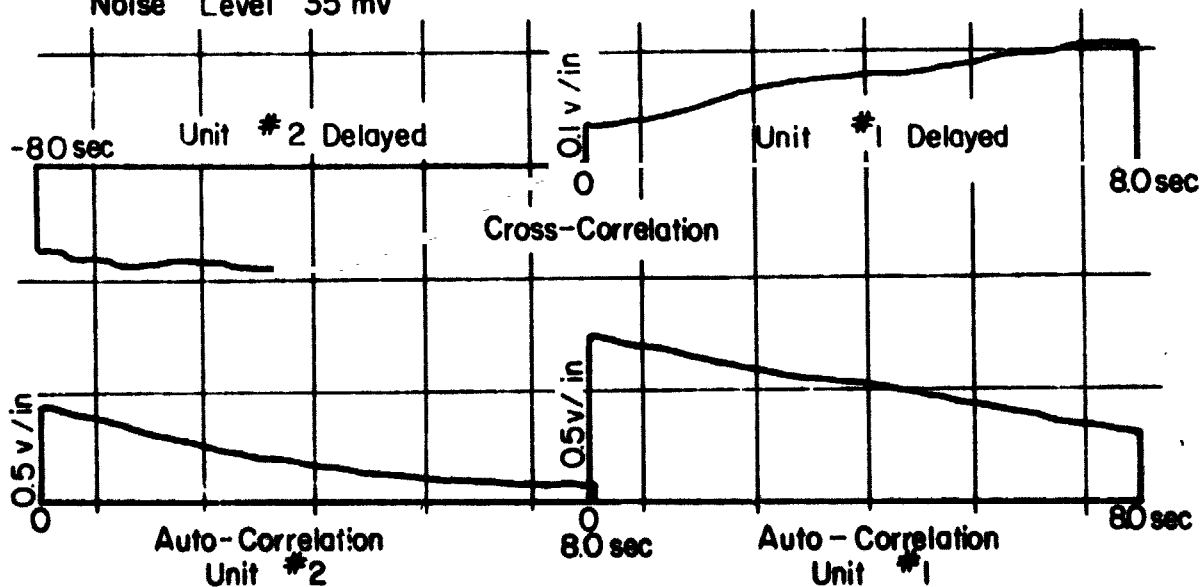




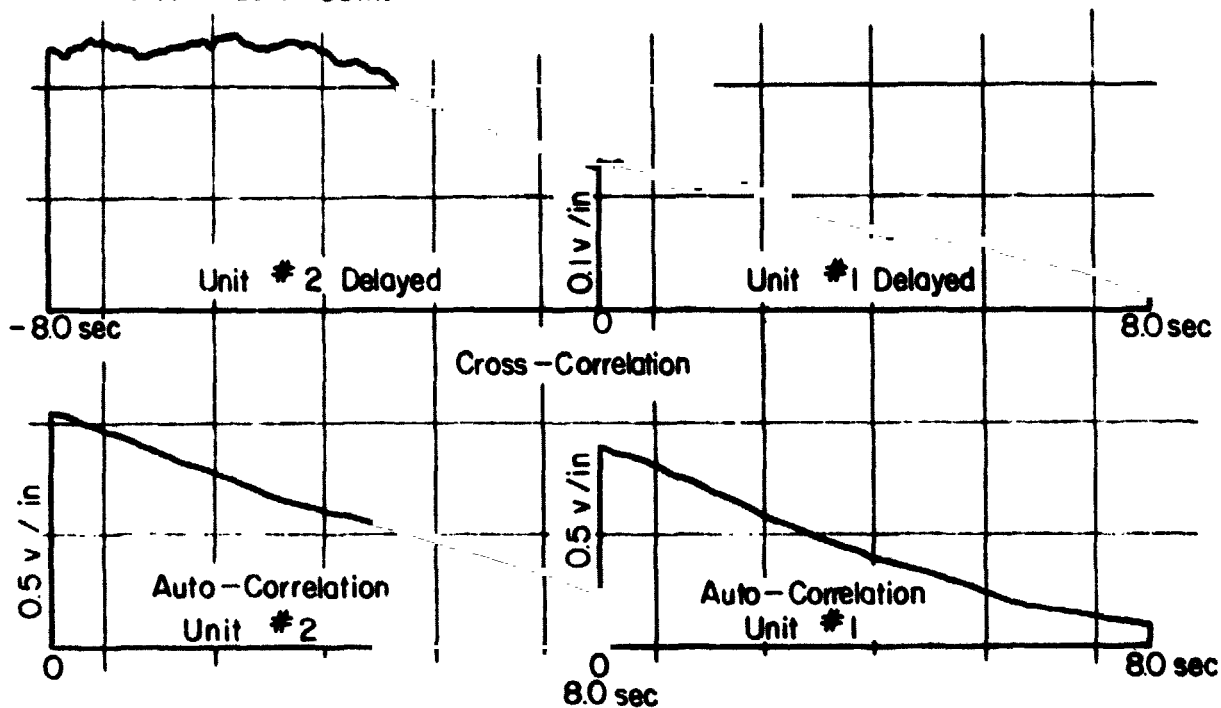
Run #34 (IR)  
 Band Pass 001 to 3.0 Hz  
 Avg. Time 3200 sec  
 Noise Level 22 mv



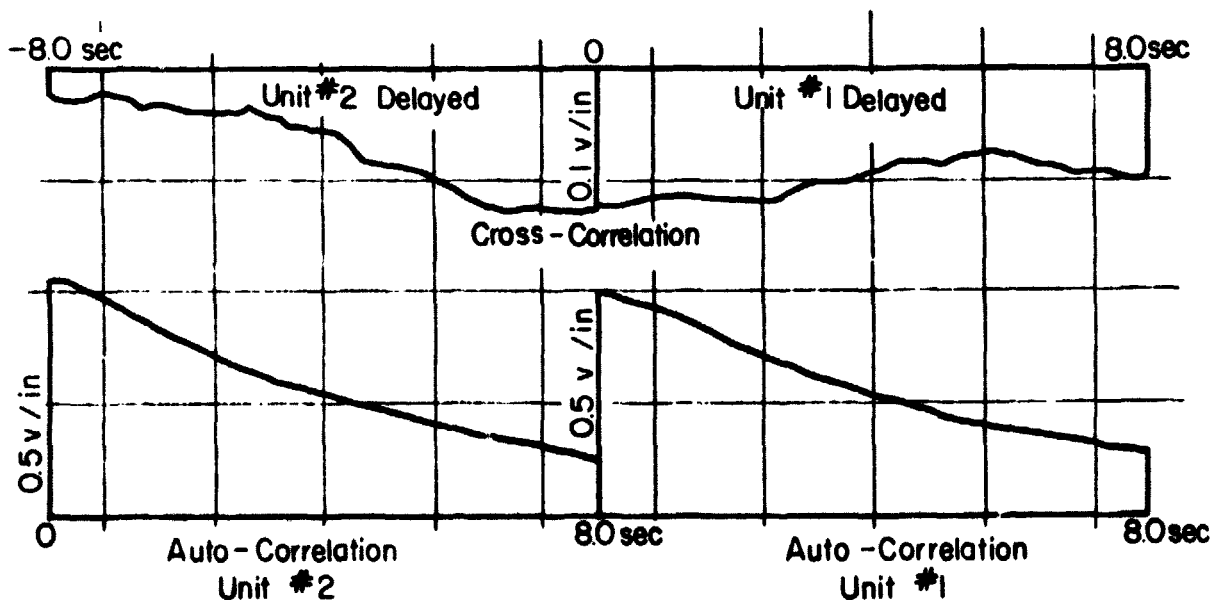
Run #40 (IR)  
 Band Pass 0.0 to 3.0  
 Avg. Time 1600 sec  
 Noise Level 35 mv



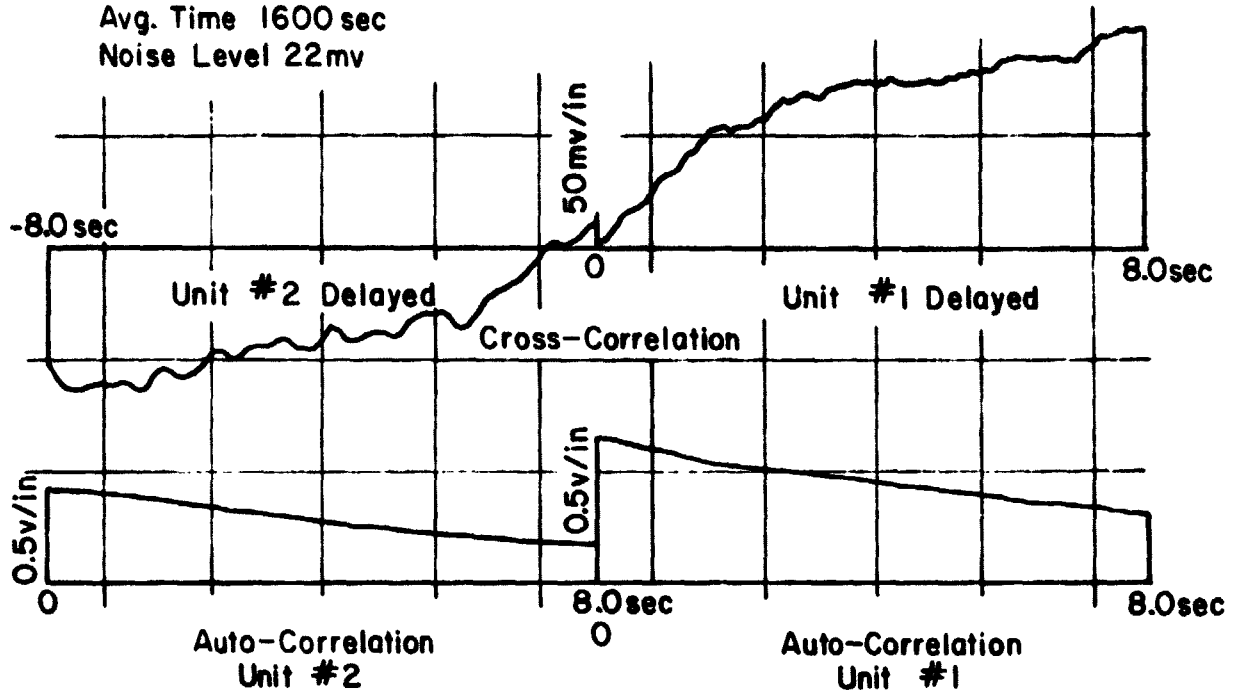
Run #41 (IR) 1<sup>st</sup> Half Hour  
 Band Pass 00 to 3.0 Hz  
 Avg Time 1600 sec  
 Noise Level 35mv



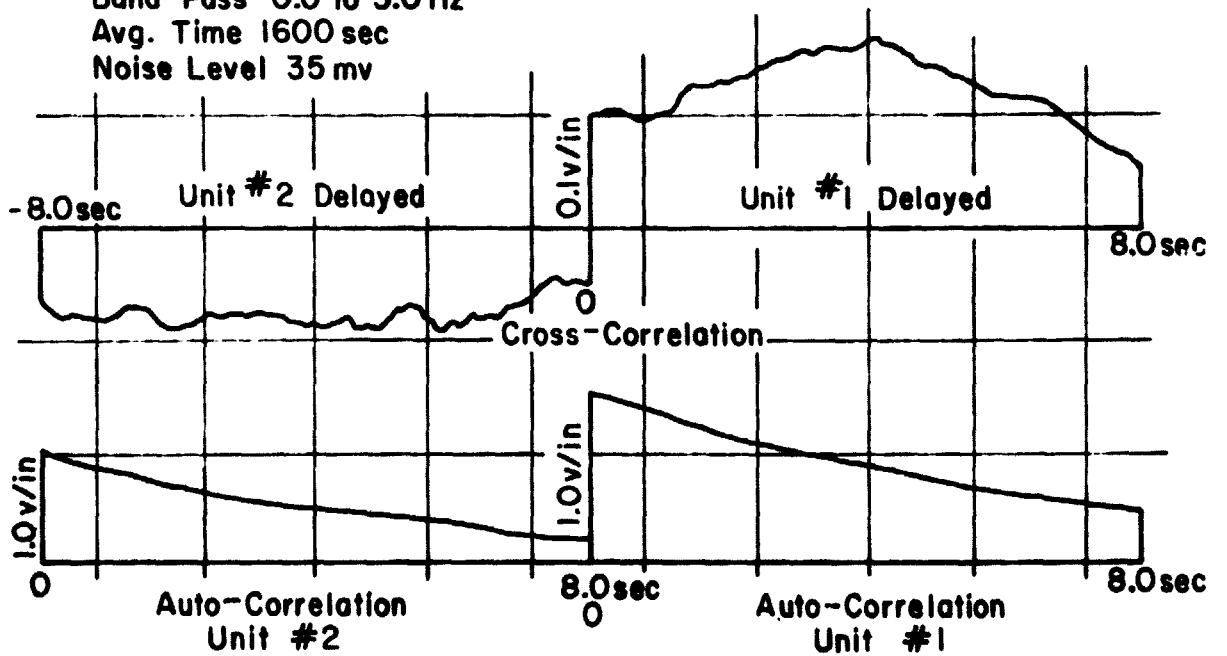
Run #41 (IR) 2<sup>nd</sup> Half Hour  
 Band Pass 00 to 3.0 Hz  
 Avg Time 1600 sec  
 Noise Level 35mv



Run #42 (IR) 1<sup>st</sup> Half Hour  
 Band Pass 0.0 to 3.0 Hz  
 Avg. Time 1600 sec  
 Noise Level 22mv



Run #42 (IR) 2<sup>nd</sup> Half Hour  
 Band Pass 0.0 to 3.0 Hz  
 Avg. Time 1600 sec  
 Noise Level 35mv

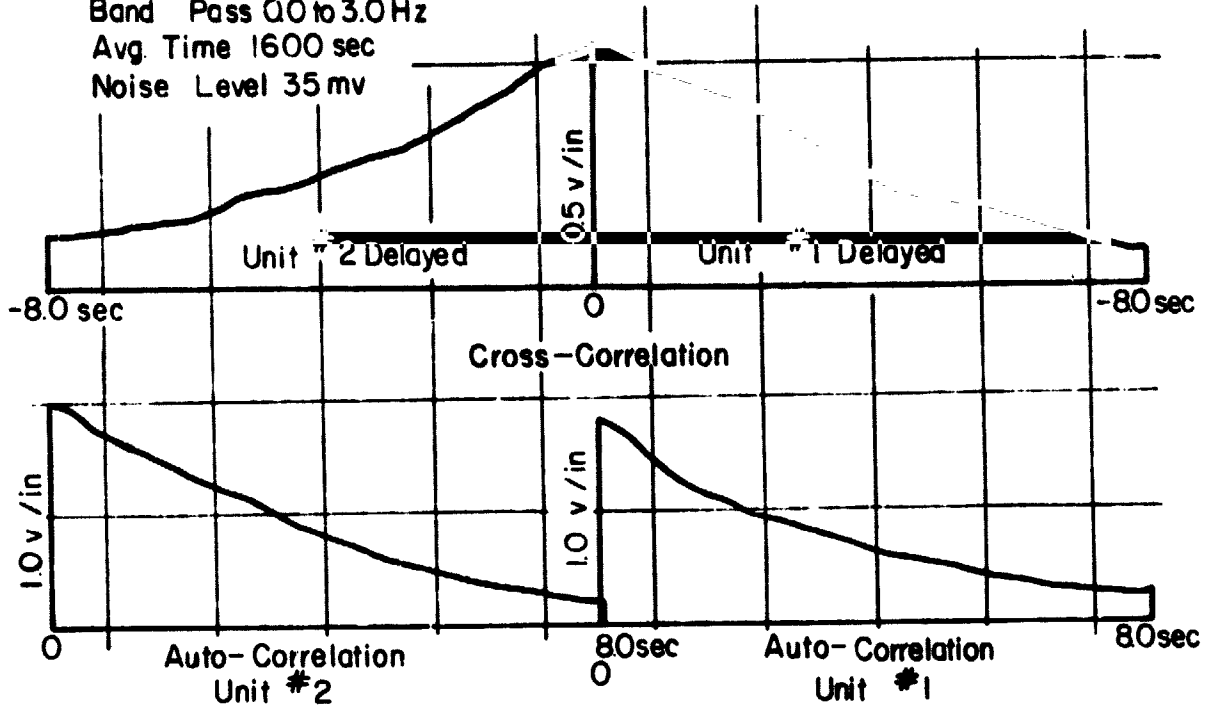


Run #43 (I R)

Band Pass 0.0 to 3.0 Hz

Avg. Time 1600 sec

Noise Level 35 mv

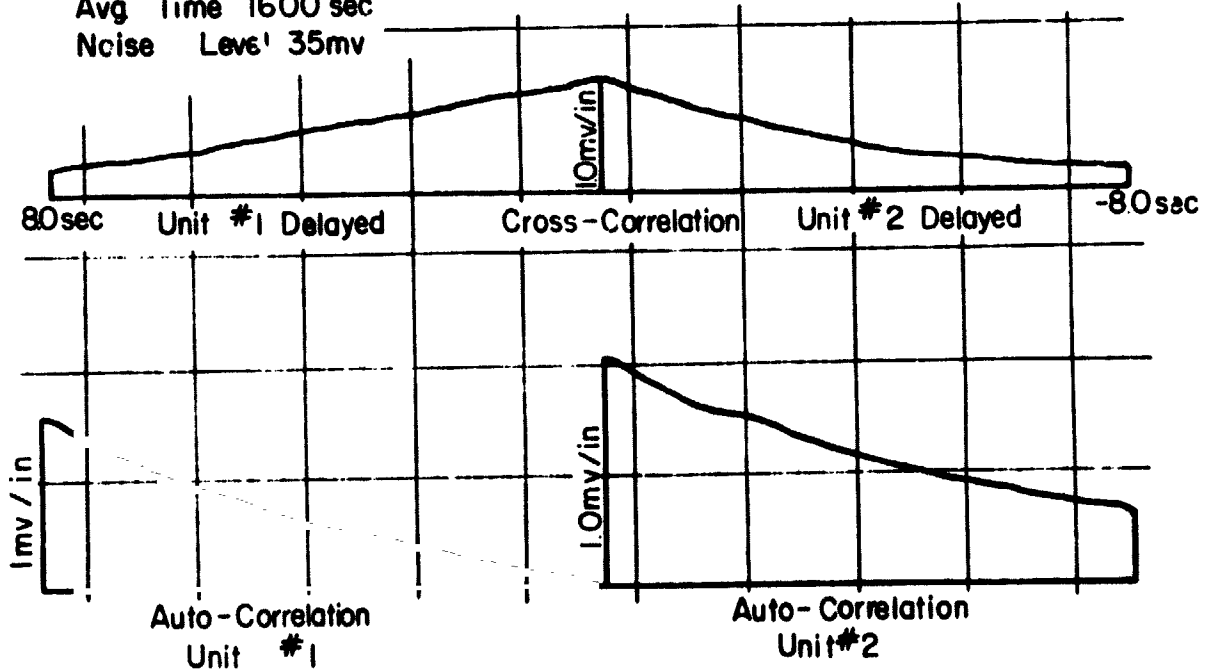


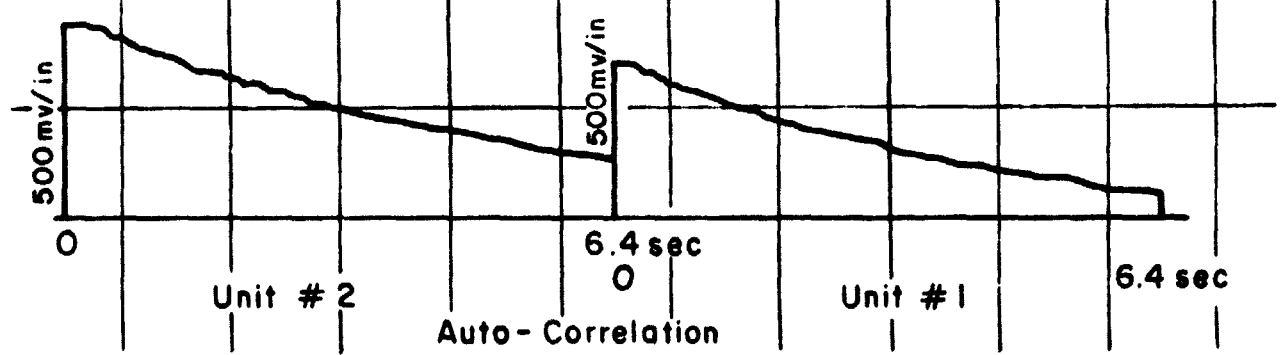
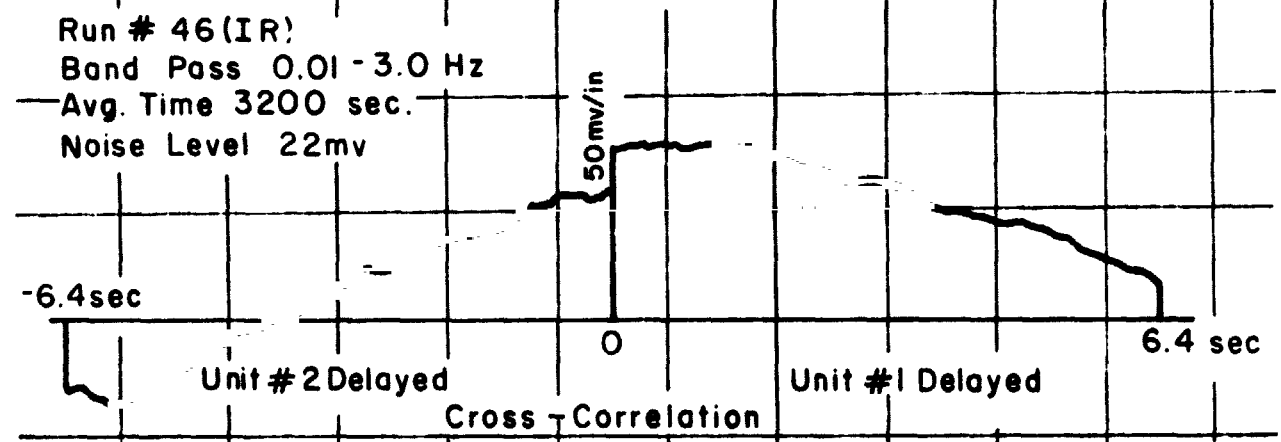
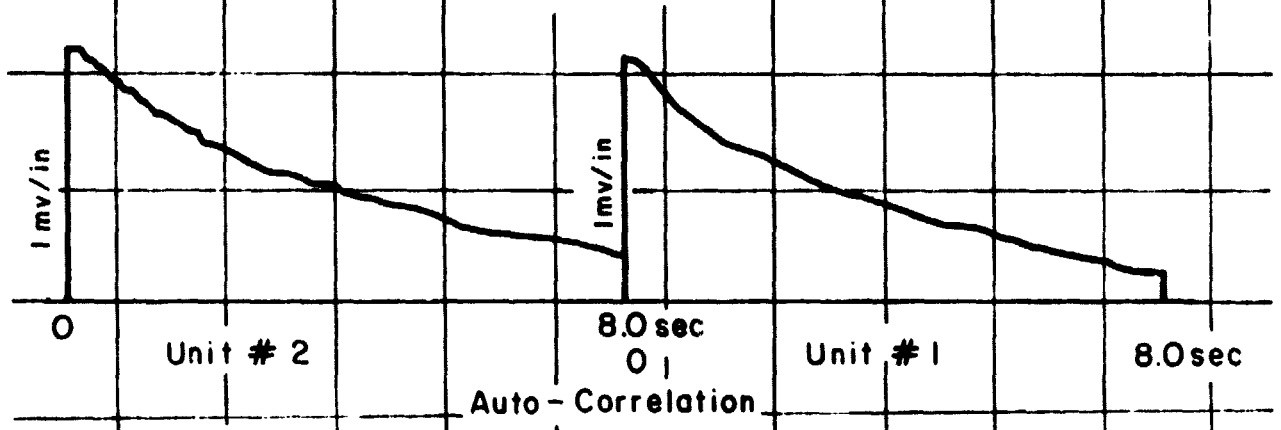
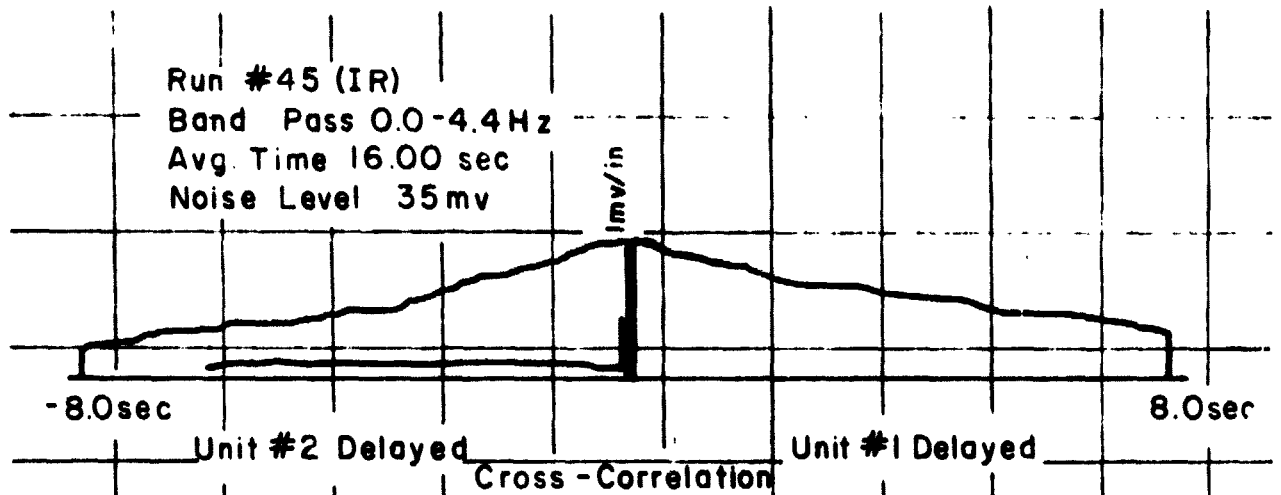
Run #44 (IR)

Band Pass 0.0- 4.4 Hz

Avg Time 1600 sec

Noise Level 35mv





**APPROVAL**

**WEATHER WATCH STUDIES BY MEANS OF**

**AN OPTICAL TECHNIQUE**

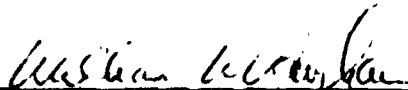
**Robert E. Turner, Editor**

The information in this report has been reviewed for security classification. Review of any information concerning Department of Defense or Atomic Energy Commission programs has been made by the MSFC Security Classification Officer. This report, in its entirety, has been determined to be unclassified.

This document has also been reviewed and approved for technical accuracy.



**Robert E. Smith**  
Chief, Orbital & Space Environment Branch



**William W. Vaughan**  
Chief, Aerospace Environment Division



**Charles A. Lundquist**  
Director, Space Sciences Laboratory